UNITED STATES
NUCLEAR REGULATORY COMMISSION
WASHINGTON, D. C. 20555

AUG 8 1985

MEMORANDUM FOR: Raymond F. Fraley
Executive Director, ACRS

FROM: Guy A. Arlotto, Director
Division of Engineering Technology
Office of Nuclear Regulatory Research

SUBJECT: DRAFT 3, PROPOSED REV. 1, REGULATORY GUIDE 1.82 "WATER SOURCES FOR LONG TERM RECIRCULATION COOLING FOLLOWING A LOSS OF COOLANT ACCIDENT"

Enclosed for the use of the Subcommittee on ECCS are twenty copies of Draft 3, Proposed Rev. 1 of the regulatory guide, "Water Sources for Long Term Recirculation Following a Loss of Coolant Accident."

Technical findings on Unresolved Safety Issue (USI) A-43, "Containment Emergency Sump Performance" are in NUREG-0897, Rev. 1B. The value/impact analysis, comments received on the "for comment" version of the regulatory guide and the comment resolution are in NUREG-0869, Rev. 1B.

Twenty copies of each NUREG are enclosed. The regulatory guide has been forwarded to the Committee to Review Generic Requirements as part of the USI A-43 submittal for their consideration with the resolution of USI A-43.

ACRS concurrence in the technical aspects of the regulatory guide is requested.

Guy A. Arlotto, Director
Division of Engineering Technology
Office of Nuclear Regulatory Research

Enclosures:
1. Draft 3, Proposed Rev. 1, R.G. 1.82 dated July 24, 1985 (20)
2. NUREG-0869 Rev. 1B draft dated June 1985 (20)
3. NUREG-0897 Rev. 1B draft dated June 1985 (20)

CONTACT: W. E. Campbell, Jr.
Telephone: 443-7856

Advance Copy
NUREG-0897

Revision 1B

DRAFT

June 5, 1985

CONTAINMENT EMERGENCY SUMP PERFORMANCE

Technical Findings Related to Unresolved Safety Issue A-43

FOR COMMENT PUBLICATION DATE: April 1983
REVISION NO. 1A COMPLETED: March 1985
DATE PUBLISHED:

A. W. Serkiz, Task Manager

Division of Safety Technology
Office of Nuclear Reactor Regulation
U. S. Nuclear Regulatory Commission
Washington, D. C. 20555

ABSTRACT

This report summarizes key technical findings related to the Unresolved Safety Issue (USI) A-43, Containment Emergency Sump Performance. Although this issue was formulated considering pressurized water reactor (PWR) sumps, the generic safety questions apply to both boiling water reactors (BWRs) and PWRs.

Emergency core cooling systems require a clean and reliable water source to maintain long-term recirculation following a loss of coolant accident (LOCA). PWRs rely on the containment emergency sump to provide such a water supply to residual heat removal pumps and containment spray pumps. BWRs rely on pump suction intakes located in the suppression pool, or wet well, to provide a water source to residual heat removal systems and core spray systems. Thus, pumping performance under post-LOCA conditions must be evaluated.

The key safety questions relate to: (1) PWR sump or BWR suction intake hydraulic performance (i.e., air ingestion potential); (2) potential sump screen or suction strainer blockage as a result of LOCA damage to insulation materials; and (3) pump performance under post-LOCA conditions where ingestion of air and debris particulates could occur.

The technical findings presented in this report provide information relevant to assessing these safety concerns. These findings have been derived from extensive experimental studies, generic plant studies, and assessment of pumps utilized for long-term cooling. Hydraulic results have revealed a less severe potential for air ingestion than previously hypothesized. Debris blockage effects on NPSH margin should be dealt with on a plant-specific basis because of the large uncertainty in quantifying the extent of debris blockage. Therefore, these findings have been used to develop revisions to Regulatory Guide 1.82 and Standard Review Plan Section 6.2.2 (NUREG-0800).

TABLE OF CONTENTS

LIST OF FIGURES

LIST OF TABLES

FOREWORD

This report has been prepared to provide a concise and self-contained reference that summarizes technical findings relevant to Unresolved Safety Issue A-43, Containment Emergency Sump Performance. This report was originally issued for public comment in May 1983; comments received were reviewed, and those of substantive technical or informational content have been incorporated into this Revision 1. It should also be clearly noted that this report is not a substitute for requirements set forth in General Design Criteria 16, 35, 36, 38, 40, and 50 in Appendix A of Title 10 of the Code of Federal Regulations Part 50, nor is it a substitute for guidelines set forth in NRC's Standard Review Plan (SRP, NUREG-0800), Regulatory Guides, or other regulatory directives. The information contained herein is of a technical nature and can be used as reference material relevant to the revised SRP Section 6.2.2, Revision 4, and Regulatory Guide 1.82, Revision 1.

ACKNOWLEDGEMENTS

The technical findings relevant to Unresolved Safety Issue A-43, Containment Emergency Sump Performance, set forth in this report are the result of the combined efforts of the staff of the Nuclear Regulatory Commission (NRC), the Department of Energy (DOE), Sandia National Laboratories (SNL), Alden Research Laboratory (ARL), Burns & Roe (B&R), Inc., and Creare, Inc. The following persons deserve special mention for their participation and contributions:

W. Butler, NRC/DSI
W. Durgin, ARL
G. Hecker, ARL
D. Jaffee, NRC/DL
J. Kudrick, NRC/DSI
A. Mullunzi, DOE
P. Norian, NRC/DST
F. Orr, NRC/DSI
G. Otey, SNL
M. Padmanabhan, ARL
P. Strom, SNL
W. Switt, Creare
G. Weigand, SNL
F. Wind, HDR Project
J. Wysocki, B&R

In addition, acknowledgement is given to persons whose efforts are referenced herein, and to those persons who participated in peer reviews of the results obtained and the application of such results. Particular acknowledgement is given to Gilbert Weigand (SNL), who played a major role in developing investigative approaches and maintaining technical quality and continuity in those early efforts, and to G. Hecker (ARL) for his keen insight and questioning regarding the application of the results obtained, particularly in the concluding phases of this USI. In addition, acknowledgement is given to the Diamond Power Speciality Company and Owens Corning Fiberglass, Inc. for providing the technical data and other product line information that have been included in this report. Acknowledgement is also given to S. Khalid Shaukat (NRC/DST), who made valuable contribution to various sections of this report. Final thanks are given to Cindy Barnes (NRC/DST), who persevered with me through all the concluding revisions to this document.

A. W. Serkiz
Task Manager

1 INTRODUCTION

1.1 Safety Significance

After a loss-of-coolant accident (LOCA) in a pressurized water reactor (PWR), water discharged from the break will collect on the containment floor and within the containment emergency sump. PWR emergency core cooling systems (ECCS) and containment spray systems (CSS) initially draw water from the refueling water storage tank (RWST); long-term cooling is implemented by realignment of these ECCS pumps to the containment emergency sump. In boiling water reactors (BWRs), the break flow collects in the suppression pool (or torus), and the residual heat removal (RHR) and core spray (CS) systems take suction from intakes located in the suppression pool. Thus successful long-term recirculation depends on the PWR sump design--or BWR suction intake design--to provide adequate, debris-free water to the RHR recirculation pumps for extended periods of time.

The primary areas of safety concern addressed in this report are as follows:

(1) post-LOCA hydraulic effects (i e., air ingestion potential)

(2) generation of insulation debris as a result of a LOCA, with subsequent transport to PWR sump screens (or BWR suction strainers) and blockage thereof

(3) the combined effects of (1) and (2) on the required recirculation pumping capacity (i.e., impact on net positive suction head (NPSH) of the recirculation pumps)

1.2 Background

The importance of the ECCS sump and the safety considerations associated with its design were early considerations in PWR containment design. NPSH

requirements, operational verification, and sump design requirements are issues that have evolved and are currently addressed in the following Nuclear Regulatory Commission (NRC) Regulatory Guides (RGs):

RG 1.1	Net Positive Suction Head for Emergency Core Cooling and Containment Heat Removal Systems Pumps, 1970
RG 1.79	Preoperational Testing of Emergency Core Cooling Systems for PWRs, 1974
RG 1.82	Sumps for Emergency Cooling and Containment Sprays Systems, 1974

Review of these Regulatory Guides reveals that the concerns of the NRC staff regarding emergency sump performance evolved over time. Initially, in-plant tests were called for in RG 1.79. Then, there was a transition to containment and PWR sump model tests in the mid-1970s. At that time, considerable emphasis was placed on "adequate" sump hydraulic performance during these model tests, and vortex formation was identified as the key determinant. The staff's main concern was that formation of an air-core vortex would result in unacceptable levels of air ingestion and severely degraded pump performance. There was also concern about sump damage or blockage of the flow as a result of insulation debris generated by LOCAs, missiles, and break jet loads. These concerns led to the formulation of some of the guidelines set forth in RG 1.82 (those relating to cover plates, debris screen, and a 50% screen blockage criterion).

In 1979, as a result of continued staff concern about the safe operation of ECCS sumps, the Commission designated the issue as Unresolved Safety Issue (USI) A-43, Containment Emergency Sump Performance. To assist in the resolution of this issue, the Department of Energy (DOE) provided funding for construction of a full-scale sump hydraulic test facility at the Alden Research Laboratory (ARL) of Worcester Polytechnic Institute (WPI) (Durgin,

Padmanabhan, and Janik, 1980). At about the same time an NRC Task Action Plan (TAP) A-43 was developed to address all aspects of this safety issue. Potential debris effects were investigated through plant insulation surveys, sample plant calculations, and supplemental experiments conducted at ARL to determine the transport characteristics of various types of insulation debris and attendant screen blockage head losses.

1.3 Technical Issues

The principal concern is summarized in the following question:

> In the recirculation mode following a LOCA, will the pumps receive water sufficiently free of debris and air and at sufficient inlet pressure to satisfy NPSH requirements so that pump performance is not degraded to the point that long-term recirculation requirements cannot be met?

This concern can be divided into three areas for technical consideration: sump (or suction intake) hydraulic design, insulation debris effects, and pump performance. The three areas are not independent, and certain combinations of effects must be considered as well.

This report presents the technical findings derived from extensive, full-scale experimental measurements, generic plant surveys, sample plant calculations, assessment of the performance of residual heat removal pumps, and public comments received. Public Comments received and staff response to them are contained in Appendix A. These technical findings provide a basis for technically resolving USI A-43 and for developing revisions to RG 1.82 and Section 6.2.2, of the NRC Standard Review Plan (SRP, NUREG-0800).

1.4 Summary of Technical Findings

The following key determinations are derived from the technical findings presented in Section 3 below:

(1) Visual observations of vortex formation cannot be used to quantify levels of air ingestion. Full-scale PWR sump experiments and BWR suction inlet experiments have shown that levels of measured air ingestion were generally less than 2% under a wide range of simulated post-LOCA conditions. On the other hand, the absence of air-entraining vortices can be used to infer zero air ingestion.

(2) Air ingestion levels have been correlated with the Froude number (Fr) that embodies suction submergence level and suction inlet flow velocity. Full-scale experiments have shown zero air ingestion in PWR sumps for $Fr \leq 0.2$ and zero air ingestion for BWR suction inlet designs up to $Fr \leq 0.8$. Envelope, or bounding, plots for estimating air ingestion levels as a function of Froude number are presented in Section 3.4.

(3) Excessive air ingestion levels (i.e., > 2 to 4 volume %) can lead to degradation of pumping capacity (see Section 3.2). Use of vortex suppressors (fabricated from floor grating materials) can effectively reduce air ingestion to 0% (see Section 3.4). For BWR suction inlets, the inlet strainer appears to act as a vortex suppressor and retardant to air ingestion.

(4) RHR recirculation pump operation can be assessed using the findings and methods provided in Section 3.2. As noted above, low levels of air ingestion can be tolerated. However, pumping performance should be based on calculated pump inlet conditions for the postulated LOCA including adjustment of the net positive suction head requirements (NPSHR) for low levels of air ingestion (see Section 3.2).

(5) Ingestion of small particulates does not appear to pose a pumping problem as a result of erosion for the post-LOCA circulating pumps in either PWR or BWR plants because of the materials of construction used in the impellers and casings. Pump seal systems should be reviewed from

the viewpoint of possible clogging. Catastrophic failure of shaft seals (as a result of debris generation) is unlikely because of the safety bushings built into pump seal assemblies. If water-lubricated bearings are specified or used in any of the post-LOCA circulating pumps (e.g., in multistage RHR, reactor core isolation cooling (RCIC), high pressure coolant injection (HPCI) or high pressure core spray (HPCS) pumps in some BWRs), the seal system should be carefully reviewed. Particulate ingestion may be sufficient to cause seal failure and/or bearing seizure in these cases.

(6) Surveys of plant insulation materials have shown a wide variability in the types and quantities of insulations employed in nuclear power plants (see Section 3.3). Furthermore, feedback received during the "for comment" period on USI A-43 has shown that the types and quantities of insulation have changed over time and with replacement changes made in operating plants. Thus, because of the nature and quantities of insulation materials used, debris blockage assessments become very plant specific and time dependent.

(7) Estimating the effects of debris blockage requires an estimation of (a) the quantity of debris that might be generated by a LOCA, (b) the transport of such insulation debris to the PWR sump screen (or BWR suction strainer), and (c) the potential blockage as a result of flow entrainment of debris to the screen (or strainer) surface. Plant-specific studies have shown that there is a strong dependance on plant layout (which affects migration of debris) and on PWR sump design features (or BWR suction intake design). Appendix B provides illustrative sump designs and containment layout.

(8) The destructive power of a LOCA jet has been demonstrated in HDR* blowdown experiments, particularly from the viewpoint of destruction of

---

*The Heissdampfreaktor or superheated steam reactor, in the Federal Republic of Germany; see Appendix C.

fibrous insulation materials. Because finely shredded insulation can be transported at low recirculation flow velocities (i.e., 0.2 ft/sec) and distribute uniformly over debris screens, or suction strainers, such insulations warrent a close review for estimating post-LOCA blockage effects on pump NPSH margin. Experiments have also shown that reflective metallic insulations can suffer severe damage from LOCA jets (see Appendix E) and that undeformed thin foils (such as those used internally in reflective metallic assemblies) can be transported at low velocities (e.g., 0.2 to 0.4 ft/sec). Information on the transport characteristics of simulated insulation debris and debris generation is contained in Section 3.3.

(9) Sample plant analyses and experiments have shown that the uniform 50% blockage criterion in RG 1.82 is not adequate for the reasons noted above. Sump screen blockage (or suction strainer blockage) should be evaluated on a plant-specific basis on the basis of the insulation materials employed, and a plant-specific assessment of potential debris transport and debris screen blockage should be made. Therefore, RG 1.82 has been revised accordingly.

(10) The technical findings in Section 3 have been further refined to develop PWR sump and BWR suction inlet evaluation guidelines. These guidelines are in Section 5.

(11) Methods for estimation of debris generation and transport developed in NUREG/CR-2791 (published in September 1982) are superseded by those outlined in Sections 3.3 and 5.3 of this NUREG.

NUREG/CR-2791 (published in September 1982) should be reviewed from the viewpoint of later information (such as those contained in Section 3.3 and 5.3 of this NUREG). Certain assumptions previously made in NUREG/CR-2791 (i.e., insulation damage effects extending outward to a stagnation pressure level of 0.5 psi) are not supported by more recent evaluations.

2 SUMMARY OF KEY FINDINGS

2.1 Pump Performance

Sustained operation of PWR RHR and CSS pumps, or BWR RHR pumps, in the recirculating mode presents two principal areas of concern:

(1) possible degradation of the hydraulic performance of the pump (inability of the pump to maintain sufficient recirculation flow as a result of sump screen blockage, cavitation or air ingestion effects)

(2) possible degradation of pump performance over the long- or short-term because of mechanical problems (material erosion due to particulates or severe cavitation, shaft or bearing failure due to unbalanced loads, and shaft or impeller seizure due to particulates)

Pumps used in RHR and CSS systems in PWRs are primarily single-stage centrifugal designs of low specific speed. PWR CSS pumps are generally rated at flows of about 1500 gpm, with heads of 400 feet, and require about 20 feet of NPSH at their inlet; PWR RHR pumps are generally rated at about 3000 gpm, with heads of 300 feet, and require about 20 feet NPSH at maximum flow. Rating points and submergence requirements for the pumps are plant specific. Pump impeller materials are generally highly resistant to erosion, corrosion, and cavitation damage.

Experimental results show that under normal flow conditions and in the absence of cavitation effects, pumping performance is only slightly degraded when air ingestion is less than 2%. This value would be a conservative estimate for acceptable performance and is dependent on many variables. However, air ingestion greater than 15% almost completely degrades the performance of pumps of this type.

Submergence or NPSHR for RHR and CSS pumps (routinely determined by manufacturers' tests) are established by percent of degradation in pump output pressure. Individual pump specifications determine that NPSH required be set according to a 1% or 3% degradation criterion. No industry standard exists for the percent degradation criterion, nor for the margin between available NPSH and that required in setting RHR and CSS pump submergence criteria. Air ingestion affects NPSHR for pumps. Test data on the combined effects of air ingestion and cavitation are limited, but the combined effects of both increase the NPSH required. A value of 3% degradation in pump output pressure for the combined effects of air ingestion and cavitation appears to be realistic for assessing recirculation pump performance.

The types and quantities of debris small enough to pass through screens (or suction strainers) and reach the pump impeller should not impair long-term hydraulic performance. In pumps with mechanical shaft seals, accumulated quantities of soft or abrasive debris in the seal flow passages may result in clogging or excessive wear, both of which may lead to increased seal leakage. Catastrophic failure of a shaft seal in the post-LOCA circulation pumps in either PWR or BWR systems as a result of debris ingestion is considered unlikely. In the event of complete failure of shaft seals, pump leakage would be restricted by the throttle or safety bushing incorporated in these seals.

There is a much broader spectrum of both design features and rated performance values for centrifugal pumps used in BWR safety systems than for those used in PWR systems. Although there is a wider variation in BWR pumping capacities, the pumps in BWR systems are also low to medium specific speed designs. They have performance characteristics very similar to those used in PWRs. Pumps in BWRs should be subject to the same technical considerations regarding hydraulic performance as those for PWR pumps (i.e., the criteria used in calculation of NPSH and in considering the quantities of air will apply directly to the BWR pumps).

The main bearings for BWR safety pumps are similar in construction and protection details to those of their PWR equivalents. That is, the main bearings are rolling element or ball bearings, either grease or oil lubricated. These bearings are generally protected from damage as a result of pump leakage by mechanical shaft seals equipped with safety bushings and, in some cases, downstream deflectors. This is true for multistage pumps as well as conventional single-stage pumps. As is the case for comparable PWR pumps, even a complete mechanical seal failure produces only a limited amount of leakage. The outboard ball bearings for these pumps are protected by disaster bushings and deflector disks, and, therefore, total failure of these bearings is not likely.

The BWR pumps are distinguished from PWR safety system pumps principally by the fact that multistage pumps are frequency used in BWR safety systems. When multistage pumps are used, one should be concerned about the effects of particulates and debris on the interstage bushings.

In multistage pumps, interstage bushings are generally cooled and lubricated by the pumped fluid. For plants where it has been determined that significant amounts of abrasive particulates or fiberous debris may be transmitted from the pump inlet screen into the pumps themselves, the interstage bushing systems should be evaluated to determine whether external pressurized cooling or flushing is needed to prevent damage as a result of wear or clogging. Plant operational experience (based on periodic start-up and verification of safety system(s) operation) has shown no problems with interstage bushing assemblies even though the suppression pool water quality is less than that used for reactor recirculation .

2.2 Effects of Debris on Recirculation Capability

The safety concerns related to the effects of LOCA-generated insulation debris on RHR recirculation requirements can be viewed as dependent on the following:

(1) the types and quantities of insulation employed (dependent on plant design and installation)

(2) the potential for a high pressure system break to severely damage or destroy large quantities of insulation (dependent on plant layout and insulation distribution, and on break-targeted insulations)

(3) the potential for LOCA-generated insulation debris to be transported to the PWR sump screen or BWR suction strainer (dependent on plant layout and recirculation velocity)

(4) the extent to which such transported debris would result in blockage of the sump screen or suction strainer (dependent on screen design and size)

(5) the blocked screen head loss impact on RHR recirculation pump available NPSH (dependent on the material and blockage characteristics of the debris transported to the screen)

The variability of plant layout, sump design, insulations employed, and recirculation requirements make debris assessments very plant specific. The results of debris considerations studied can be summarized as follows:

(1) Types of insulation vary from plant to plant and are subject to change with time (i.e., replacement insulation may be different from the original installation).

(2) Generally speaking, insulations can be categorized as

(a) reflective metallic insulation (both stainless steel and aluminum are utilized)
(b) encapsulated, by metallic or other types of coverings, but with various core materials; typical core materials are calcium silicate, fiberglass, mineral wool Cerablanket™, and Unibestos™
(c) nonencapsulated insulations, which are typically fabricated as "blankets" or "pillows" and in which the core materials noted in (b) are used, with varying methods of attachment
(d) molded insulations with closed-cell structure (i.e., foam-glass)
(e) antisweat insulations (typically fiberglass, urethane and polyurethane foams, and closed-cell rubber)

Although encapsulation can afford protection from high pressure jet loads and missile impacts, encapsulated structures must be reviewed to assess the real degree of protection that is afforded. The characterization "totally encapsulated" can be misleading because of the variability of encapsulations and attachment mechanisms provided. Thus assessment should be made to determine whether the insulation is totally encapsulated or semi-encapsulated.

Insulation surveys conducted in 1982 (see Section 3.3) indicated a decreasing trend in the use of insulations such as fiberglass, mineral wool, and calcium silicate, etc., with licensees of newer plants appearing to elect to install reflective metallic insulation. However, feedback received during the "for comment" period (June-July 1983) reversed this finding. More recently, some licensees of operating plants have elected to replace old insulation with fiberglass, and applicants for plants in the operating license (OL) review stage also have selected fiberglass. The more extensive use of fiberglass should be reviewed on a plant-specific basis to assess the screen blockage impact.

LOCA jets are capable of high levels of insulation destruction, as evidenced by the HDR blowdown experiments (see Appendix C). In these HDR experiments, all glass fiber insulation, within 2 to 4 meters of the break nozzle of diameters up to 450 mm was destroyed and distributed throughout the containment as very fine particles. In addition, Sandia National Laboratory (SNL) has analyzed two-dimensional-break jet expansion phenomena and target pressure loads. SNL calculations correlate well with HDR data and show that significant jet loads occur within 3 to 5 L/D's* of the pipe break location. More recent HDR experiments (see Appendix E) illustrate the level of damage that than be incurred by reflective metallic insulation. These experiments revealed severe damage near the break location and much less damage at 7 L/D's from the break. Debris generation is discussed in Section 3.3.3.

Insulation debris transport tests at Alden Research Laboratory (ARL) show that severely damaged or fragmented insulation can be transported at low velocities (0.2 to 0.5 ft/sec). Both fiberglass shreds and thin (0.0025 to 0.004-inch) metallic foils (if undeformed) can be transported at these low velocities. Therefore, the level of damage near the postulated break location(s) becomes a dominant consideration in assessing the type and volume of debris generated as well as in estimating transport probability. Larger or intact pieces require much higher transport velocities (> 1.0 ft/sec). Thus determination of recirculation flow velocities within containment is an important factor in assessing debris transport (See Appendix D). In PWR containments, recirculation flow velocities on the order of 0.2 to 0.6 ft/sec can be calculated; hence, the transport of large pieces of debris is less likely. However, because the types of insulation used, levels of damage, available recirculation paths and sump locations versus break are controlling considerations, such assessments become highly plant dependent.

---

* Here L is the centerline axial distance from the break to the target and D is the pipe break diameter.

Assessment of the probabilities for PWR sump failure (NUREG/CR-3394) has also revealed that:

(1) Principal attention should be given to insulation on the primary coolant system piping and lower half of the steam generators, because insulation on these components is the major source of potential debris, based on postulated break locations and possible break jet targets.
(2) Piping less than 10 inches in diameter is of secondary importance because smaller diameter breaks generate lower quantities of debris. The jet envelope and target area are reduced for these sizes.

Although these findings should not be applied unilaterally, these trends are applicable to PWRs for initial debris assessments and thus provide a means to scope the magnitude of the debris generation potential.

Low density insulations with a closed cell structure will float and are not likely to impede flow through the sump screens, except where the screens are not totally submerged. Low density hygroscopic insulation with submerged densities greater than water require a plant-specific assessment of screen blockage effects. Nonencapsulated insulation (particularly mineral fiber, fiberglass, or mineral wool blanket) requires a plant-specific evaluation to determine the potential for sump screen blockage. If reflective metallic insulation is damaged to the extent of releasing interior foils, transport and potential screen blockage must be assessed on a plant-specific basis. In summary, all insulations should receive a plant-specific evaluation.

Conservative methods have been developed for estimating quantities of debris, break sources, transport mechanisms, and blockage effects based on the findings summarized above. These methods are detailed in Section 3.3 and summarized in Section 5.3.

2.3 Sump Hydraulic Performance Findings

Data obtained from full-scale sump tests provide a sound base for assessing sump hydraulic performance. Both side-suction and bottom-suction designs were tested over a wide range of design parameters, and the effects of elevated water temperatures were also assessed. Scaling experiments (1:4, 1:2, 1:1) were also conducted to provide a means for assessing the validity of previous scaled-model tests. The effectiveness of certain vortex suppression devices was also evaluated. For completeness, plant-specific and LOCA-introduced effects (ice condenser drain flow, break flow impingement, large swirl and sump circulation effects, and sump screen blockage) were evaluated experimentally at full scale. In addition, a limited number of BWR suction tests were performed. The results of this test program can be summarized as follows:

(1) The broad data base from the sump studies resulted in the development of envelope curves for reliably quantifying the expected upper bound for the hydraulic performance of any given sump whose essential features fall approximately within the flow and geometric ranges tested.

(2) Vortices are unstable, randomly formed, and, for cases where air ingestion occurs, cannot be used to quantify air ingestion levels, suction inlet losses, or intake pipe fluid swirl. The full-scale tests show that at water submergences deeper than 9 feet and inlet water velocities of less than 4 ft/sec, significant vortex activity disappears. Correspondingly, air ingestion is negligible or non-existant.

(3) Based on void fraction measurements, air ingestion was found to be less than 2% in most cases. A few test conditions resulted in higher air ingestion, 2% to 8%, with or without perturbations of the approach flow. Maximum air ingestion of 8% to 15% were recorded for only short time periods with deliberately induced adverse approach flow conditions of severely blocked screens. These tests revealed the importance of measuring void fraction and demonstrated the ineffectiveness of visual observations of vortices as a means of quantitatively evaluating air entrainment.

(4) Swirl angles in suction pipes were generally found to have decreased to about 4° at a distance 14 pipe diameters from inlets. Swirl angles of up to 7° at a distance 14 pipe diameters from inlets were observed in some sump tests at low submergence with induced flow perturbations.

(5) Hydraulic grade line measurements for all experiments revealed that the sump intake loss coefficient was insensitive to overall sump design variation. Loss coefficients are basically a function of local intake geometry, and the measured values are consistent with those obtained from standard hydraulic handbooks.

(6) Testing over the temperature range of 70° to 165°F revealed that water temperature (or previously hypothesized Reynolds number effects) had no measurable effect on surface vortexing, air ingestion, pipe swirl, or loss coefficient.

(7) Vortex suppressor testing for PWR applications revealed that cage-type and submerged grid-type designs generally (a) reduce surface vortexing from a full air-core vortex to surface swirl only; (b) reduced air ingestion to essentially zero; (c) reduced pipe swirl to less than 5°; and (d) had no significant effect on the loss coefficient. These vortex suppression structures were fabricated from floor grating materials typically used for walkways.

(8) There were no major differences between the hydraulic performance of vertical outlet sumps and that of horizontal outlet sumps of similar design geometry and similar flow conditions.

(9) Comparison of the results of different scale models showed that scale modeling down to 1:4 scale using Froude number similitude adequately predicted the sump hydraulic performance variables (void fraction, vortex type, swirl, and loss coefficient) of full-scale tests. Tests on 1:4-, 1:2-, and 1:1-scale versions of the same sump under comparable operating conditions showed no significant scale effects in the modeling of air withdrawal because of surface vortices or in free-surface vortex behavior. Additionally, model tests accurately predicted swirl and inlet losses if specified Reynolds number criteria were maintained.

(10) A parametric assessment of nonuniform approach flow into the sump as a result of specific structural features did not reveal any significant adverse effects (see also Section 3.4).

(11) Drain flow impingement on the sump water surface resulted in extensive turbulence that tended to reduce vortexing and did not lead to increased air ingestion.

(12) Break flow impingement tests produced considerable air entrainment at the water surface, but void fractions of the pipe flow were generally small, less than 1%. In one case, a considerably higher void fraction was recorded, 6%, because of a change in approach flow to the sump caused by the break flow.

(13) PWR sump screen blockage tests sometimes revealed slight increases in air ingestion and some degradation of the hydraulic performance of the sump, depending on the sump configuration and test conditions. However, no significant changes were noted. In each case where air-core vortices were generated, the use of a vortex suppressor eliminated the air-core vortex and reduced the air ingestion to zero or negligible levels. Thus, the effectiveness of vortex suppressors (such as submerged floor grating designs) has been demonstrated.

(14) BWR suction intake tests (see Section 3.4.6) revealed that air ingestion was essentially zero for Froude numbers less than 0.6. The suction strainers typically utilized in BWR installations appear to act as vortex suppressors, thereby inhibiting air ingestion (even though air core vortices were observed at lower Froude numbers).

Thus the full-scale sump hydraulic test program conducted at ARL has resulted in an extensive data base that has broad applicability and can be used in lieu of model tests or in-plant tests (if the sump design being evaluated falls within the design and flow envelope investigated). Sump hydraulic design guidelines and criteria for assessing air ingestion potential are in Section 5.

3 TECHNICAL FINDINGS

3.1 Introduction

Before a plan for the resolution of Unresolved Safety Issue A-43 was developed, the following key safety questions were identified:

(1) What are the performance capabilities of pumps used in containment recirculation systems, and how tolerant are such pumps to air entrainment, cavitation, and the potential ingestion of debris and particulates that may pass through screens?

(2) Were a LOCA to occur, would the amount and type of debris generated from containment insulation (and its subsequent transport within containment) cause significant sump screen blockage and, if so, would such blockage be of sufficient magnitude to reduce the NPSH available below the NPSH required?

(3) Can geometric and hydraulic sump system designs be established for which acceptable sump performance can be ensured?

It was recognized that resolution of USI A-43 depended upon the responses to these questions. The effort to resolve these questions was undertaken in three parallel tasks, each designed to respond to one of the key safety questions.

The first question was addressed through an evaluation of the general physical and performance characteristics of RHR and CSS pumps used in existing plants. Conditions likely to cause degraded performance or damage to pumps performance were evaluated. The investigation of pump cavitation, air ingestion, particulate ingestion, and swirl is reported in NUREG/CR-2792 and Creare Technical Memorandum 962. It is summarized in Section 3.2 below.

To address the second question, 19 power reactor plants were surveyed concerning the quantity, types, and location of insulation used within containment (see NUREG/CR-2403 and its Supplement 1). Then, calculational methods were developed for estimating (1) the quantities and sources of debris that could be generated during a LOCA, (2) the transport of such debris, (3) the quantities and properties of insulation debris that could potentially be transported to sump screens, and (4) head losses as a result of debris buildup on sump screens (NUREG/CR-2791). Many of the methods for the assessment of debris blockage in NUREG/CR-2791 are superseded by those described in this report. Experiments were conducted to estimate the onset of jet erosion damage to fibrous insulations (NUREG/CR-3170) and to determine the transport and screen blockage head losses associated with fibrous insulations (NUREG/CR-2982, Rev. 1). The transport and blockage characteristics of reflective metallic insulations are reported in NUREG/CR-3616.

The third key safety question was addressed in an investigation of the behavior of ECCS sumps under diverse flow conditions that might occur during a LOCA. The test program was designed to cover a broad range of geometric and flow variables representative of emergency sump designs. The results are reported in NUREG/CR-2758, NUREG/CR-2759, NUREG/CR-2760, NUREG/CR-2761, and NUREG/CR-2772.

3.2 Performance of Emergency Core Cooling System Pumps

This section summarizes the general physical and performance characteristics of RHR and CSS pumps used in PWRs and RHR, CS and CI pumps used in BWRs. The summary characteristics are based on information from 12 PWRs and 7 BWRs that were sampled in the study. Effects likely to cause degraded performance or damage are identified, and the results of an analysis of these effects on pump performance are presented.

3.2.1 Characteristics of Pumps Used for Emergency Core Cooling Systems

The pumps used in PWR and BWR systems have different characteristics.

3.2.1.1 RHR and CSS Pumps Used in PWRs

A study of pumps used in 12 PWR plants has shown that although individual pump details are plant specific, the pumps used in RHR and CSS services are similar in type, mechanical construction, and performance.

Similarities in the types of pumps are shown in Table 3.1; the table lists the manufacturer, model number, and rated conditions for each of the pumps used in the plants surveyed. The column labeled "Specific Speed" provides a parameter conventionally used by pump manufacturers to specify hydraulic characteristics and, hence, the overall design configuration of a pump. As the table shows, all pumps are relatively high-speed, centrifugal pumps and are in the specific speed range of 800 to 1600 rpm, with specific speed defined as $N_s = (\text{speed})\ (\text{volumetric flow})^{1/2}/(\text{head})^{3/4}$.

The pumps used for RHR and CSS service have the following similarities in mechanical construction:

(1) Impellers and casings are usually austenitic stainless steel, highly resistant to damage by cavitation.

(2) Impellers are shrouded with wear rings to minimize leakage.

(3) Shaft seals are the mechanical type.

(4) Bearings are grease- or oil-lubricated ball type.

Table 3.1 RHR and CSS pump data

Plant	Manufacturer*/Model RHR	CSS	Rated Conditions (RPM) Speed	(FT) Head	(GPM) Flow	Specific Speed
Arkansas Unit #2	I-R 6x23 WD		1800	350	3100	1238
		I-R 8x20 WD	1800	525	2200	851
Calvert Cliffs 1&2	I-R 8x21 AL		1780	360	3000	1205
		B&W 6x8x11 HSMJ	3580	375	1350	1544
Crystal River #3	W 8HN-184		1780	350	3000	1205
		W6HND-134	3550	450	1500	1407
Ginna	Pac 6" SVC		1770	280	1560	1016
Haddom Neck	Pac 8" LX		1770	300	2200	1152
		Pac 8" LX	1770	300	2200	1152
Kewaunee	B-J 6x10x18 VDSM		1770	260	2000	1222
		I-B 4x11 AN	3550	475	1300	1257
McGuire 1&2	I-R 8x20 WD		1780	375	3000	1144
		I-R 8x20 WD	1780	380	3400	1205
Midland #2	B&W 10x12x21 ASMK		1780	370	3000	1156
		B&W 6x8x135 MK	3550	387	1300	1467
Millstone Unit 2	I-R (No Model #)		1770	350	3000	1198
		G3736-4x6-13DV	3560	477	1400	1370
Oconee #3	I-R 8x21 AL		1780	360	3000	1180
		I-R 4x11 A	3550	460	1490	1380
Prairie Island	B-J 6x10x18 VDSM		1770	285	2000	1141
		I-R 4x11 AN	3550	500	1300	1210
Prairie Island 1&2	B-J 6x10x18 VDSM	I-R 4x11 AN	1780	280	2000	1156
			3550	510	1300	1210
Salem #1	I-R 8x20W		1780	350	3000	1205
		G 3415 8x10-22	1780	450	2600	929

*Pac -- Pacific
I-R -- Ingersoll-Rand
W -- Worthington
G -- Gould
B&W -- Babcock & Wilcox
B-J -- Byron Jackson

Specific Speed is defined as N_s = Speed $(Flow)^{1/2}/(Head)^{3/4}$

In this definition: Speed is in rpm, flow in gpm and head in ft.

A pump assembly typical of pumps used for RHR and CSS service is shown in cross-section in Figure 3.1.

Similarities in the performance of pumps used in RHR and CSS service are shown in Figures 3.2 and 3.3. Performance and cavitation data from each of the pumps listed in Table 3.1 have been plotted for comparison. Performance data are given in terms of normalized head versus normalized flow rate where the best-efficiency-point head and flow are used for the reference values. Cavitation data are given in terms of NPSH required.

3.2.1.2 RHR, CS and CI Pumps Used in BWRs

There is a wider variation in rating conditions for pumps used in BWR safety systems than for their counterparts in PWRs. Table 3.2 lists rating points, pump types and specific speeds for a sample of seven BWR plants. Flow rates and rated heads for the BWR pumps are in many cases significantly larger than those conditions for PWR pumps discussed in Section 3.2.1.1. In spite of these plant-specific differences, the pumps are all low to medium specific speed designs with performance characteristics similar to those used in PWRs.

Many of the pumps used in BWR ECC systems are multistage designs. Both the single stage and multistage design pumps used in BWR systems have many construction features similar to those for PWR pumps:

(1) Impellers are usually austenitic stainless steel with high resistance to damage from cavitation.
(2) Impellers are shrouded with wear rings to minimize leakage.
(3) External shaft seals are mechanical.
(4) Main bearings may be grease- or oil-lubricated ball types or oil-lubricated sleeve bearings. In the multistage designs, internal sleeve bushings may be used between stages to provide additional support to the shaft.

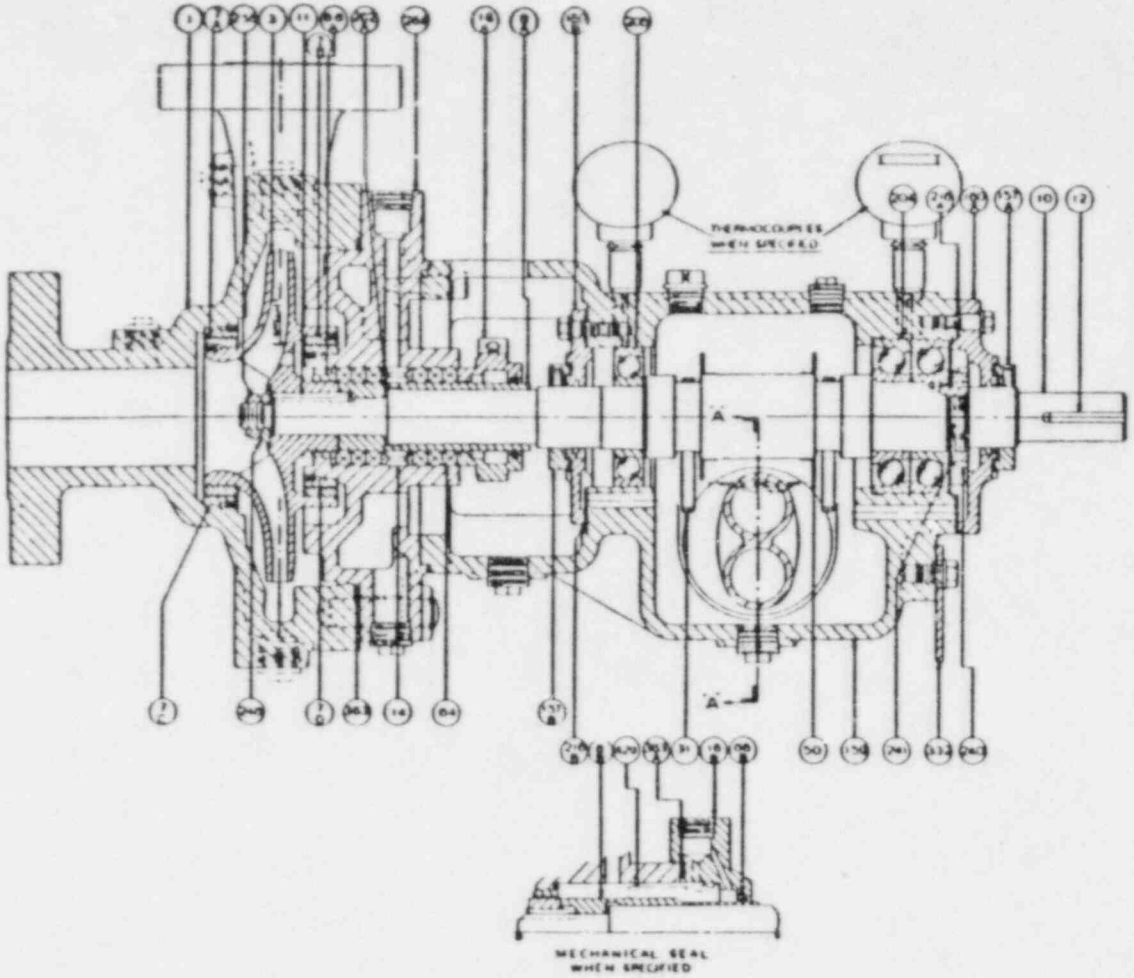

Figure 3.1 Assembly schematic of centrifugal pump typical of those used for RHR or CSS service

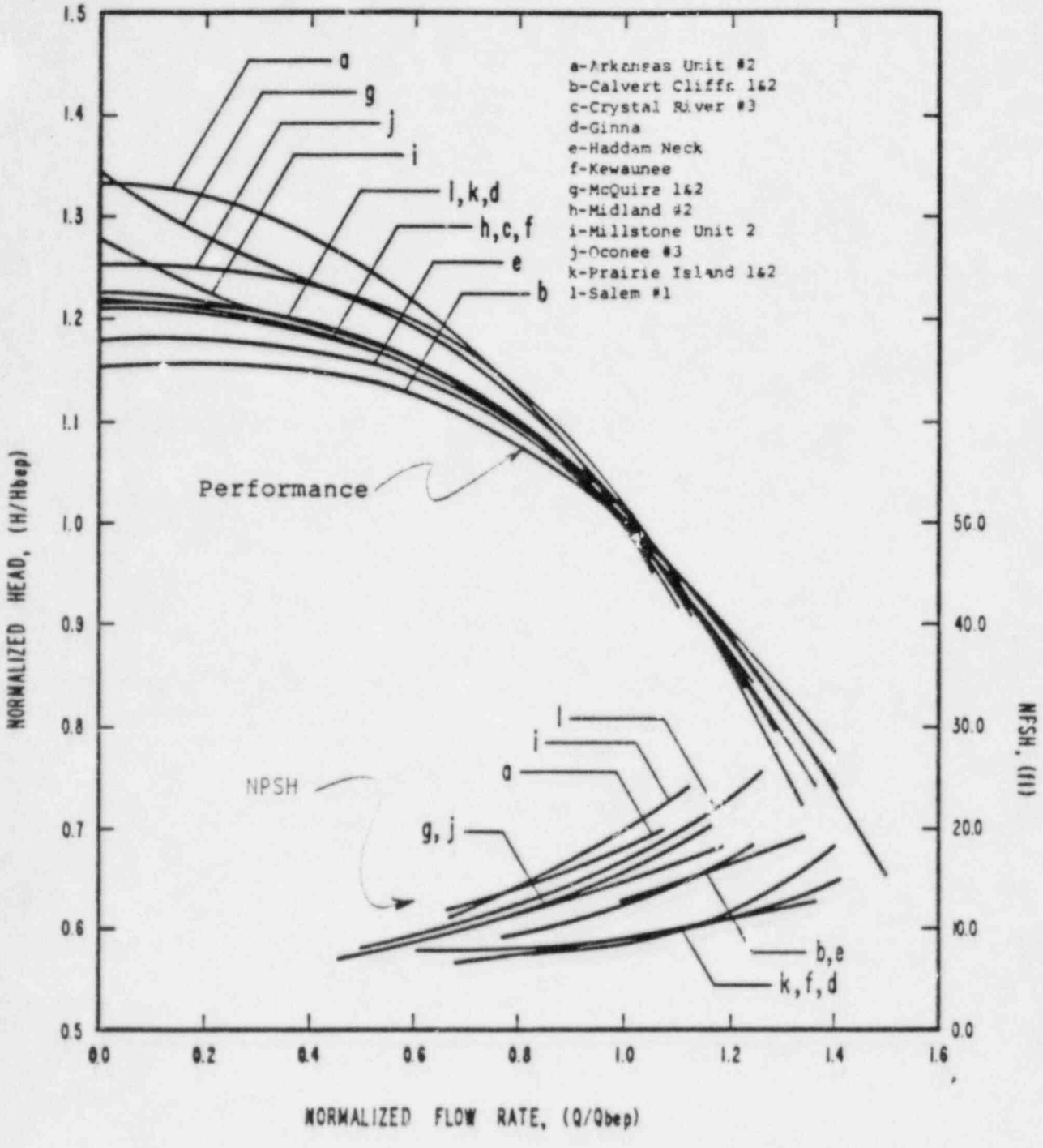

Figure 3.2 Performance and NPSH curves for RHR pumps, head vs. flow rate data normalized by individual best-efficiency-point values

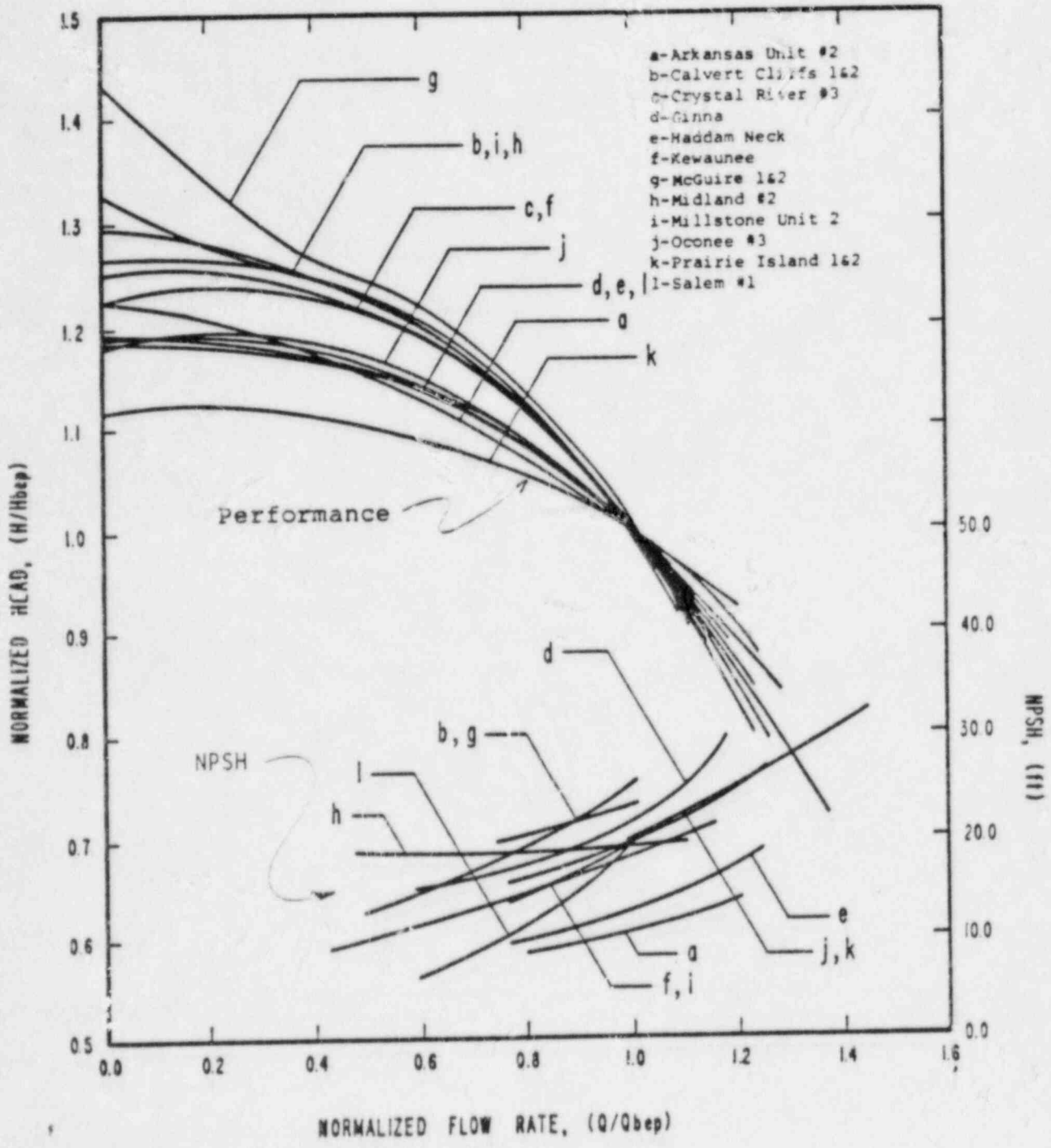

Figure 3.3 Performance and NPSH curves for CSS pumps, head vs. flow rate data normalized by individual best-efficiency-point values

TABLE 3.2

RHR, CS AND CI PUMP DATA FOR BWRs

PLANT	ECCS MODE	PUMP TYPE*	RATED CONDITIONS SPEED (rpm)	HEAD (ft)	FLOW (gpm)	SPECIFIC SPEED
Cooper	CS	VSS				
	LPCI	VSS	1760	420	7800	1675
	HPCI	STD				
Dresden (2)	CS	VSS	3560	585	4700	2052
	LPCI	VSS	3560	570	2700	1585
	HPCI	STD				
Edwin Hatch (1&2)	CS	VMS	1780	670	4700	982
	RHR	VMS	1780	420	7700	1684
	HPCI	STD				
LaSalle (1&2)	LPCS	VMS	1780	725	6350	1015
	HPCS	VMS	1780	1569	6942	595
	RHR	VMS	1780	280	7450	2244
Limerick (1&2)	CS	VMS	1780	668	3175	763
	RHR	VMS	1180	525	10000	1076
Susquehana (1&2)	CS	VMS	1780	668	3175	763
	RHR	VMS	1180	600	10000	973
	HPCI	STD	Varies	525/ 2940	5070	770
Zimmer (1)	LPCS	VMS	1780	690	4750	911
	HPCS	VMS	1780	1347	5142	574
	RHR	VMS	1780	270	5050	1900

* STD - Steam Turbine Drive
VSS - Vertical Single Stage
VMS - Vertical Multistage

The technical considerations relative to hydraulic performance (i.e., cavitation, air ingestion) are the same for single stafe or multistage designs. However, because of the differences in construction details between the two types of pumps, the effects of particulates may be significantly different for each design. Figure 3.4 illustrates the main features of a multistage design typical of those found in BWR emergency cooling systems. These pumps use interstage shaft bushings which are lubricated by the pumped water and are therefore subject to wear or clogging from debris.

3.2.2 Effects of Cavitation, Air or Particulate Ingestion, and Swirl on Pump Performance

Several items have been identified as potential causes of long- or short-term degradation of emergency cooling pumps in PWRs and BWRs. They are

(1) cavitation, which may cause head degradation and damage to impellers
(2) air ingestion, which may cause head degradation
(3) particulate ingestion, which may cause damage to internal parts
(4) swirl at the pump inlet, which may cause head degradation

All of these effects also have the potential for inducing hydraulically or mechanically unbalanced loads. They are discussed below.

3.2.2.1 Cavitation

Net positive suction head (NPSH) is defined as the total pressure at the pump inlet above vapor pressure at the liquid temperature, expressed in terms of liquid head (pressure/specific weight); it is equivalent to the amount of subcooling at the pump inlet. If the NPSH available at the pump is less than the NPSH required, some degree of cavitation is ensured and some degradation of performance and perhaps material erosion are likely.

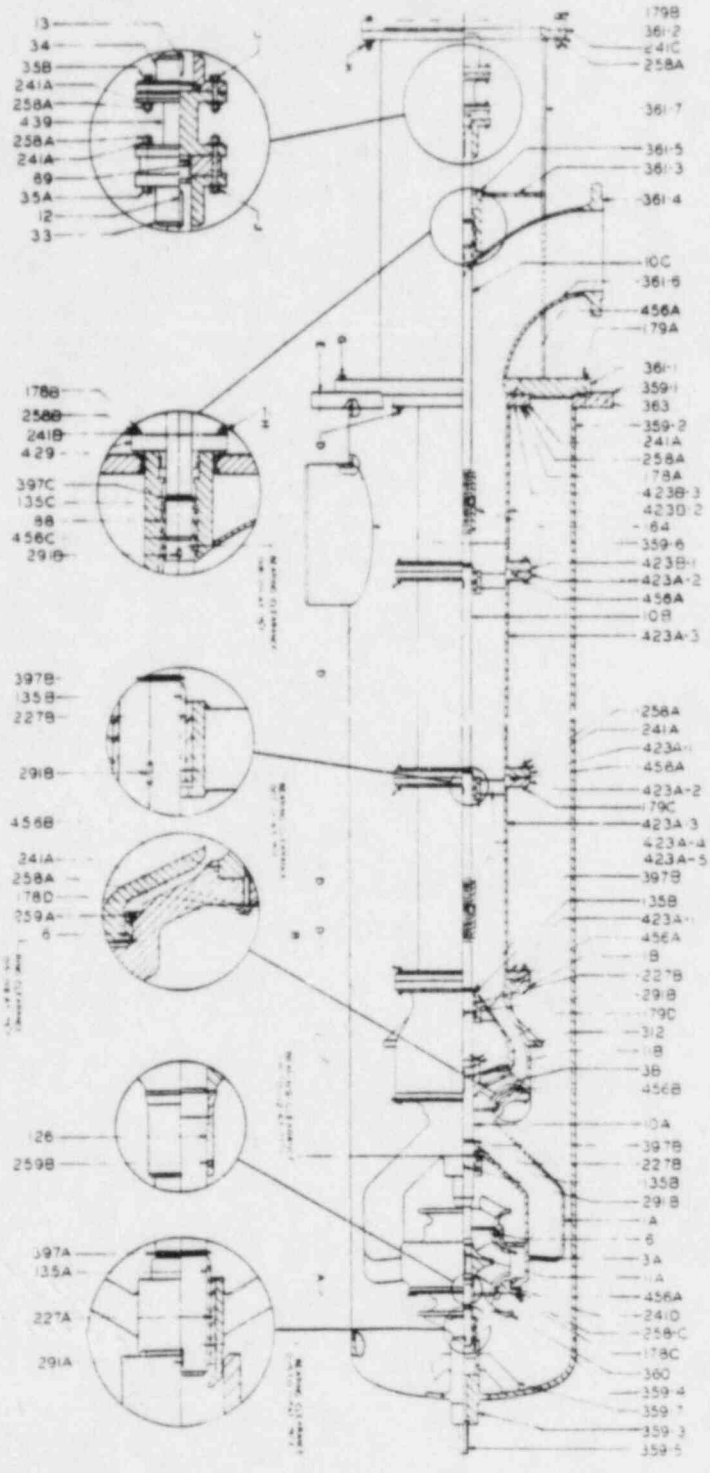

Figure 3.4 Assembly schematic of multistage pump used in BWR emergency cooling systems

There is no standard for identifying the NPSH required for a given pump. Unless there is a stipulation in the specifications, manufacturers have used some percentage (1% to 3%) in head degradation as the criterion for establishing the NPSH required at some flow condition. These are empirically established values for which very rapid degradation occurs (see Figure 3.4) and when cavitation occurs severe erosion is likely to happen. Figure 3.5 illustrates the changes in pump performance at several flow rates as a function of NPSH; these curves are typical of those provided by pump manufacturers to define the NPSH required for their pumps. As NPSH is reduced for each flow rate shown (Q1-Q4), a point is reached below the 3% limit at which substantial degradation begins. Fluid system designers may choose to apply some margin to the NPSH requirements for a pump when designing emergency core cooling systems, but currently no standard margin between NPSH required and NPSH available has been established by NRC regulations.

Some conservatism may be introduced in the calculation of NPSH following guidelines established in RG 1.1 where no credit is allowed for increased containment pressure. However, RG 1.1 does not address subatmospheric conditions in containment with respect to NPSH.

The cavitation behavior of pumps changes at elevated liquid temperatures. Figure 3.6, which is extracted from the Hydraulic Institute Standards (Hydraulic Institute, 1975) shows that as liquid temperatures increase less NPSH is required by the pump. As a result, increases in liquid temperature have two effects on NPSH: (1) the vapor pressure increases, which reduces NPSH available, and (2) the NPSH required is reduced by an amount, as given in Figure 3.6.

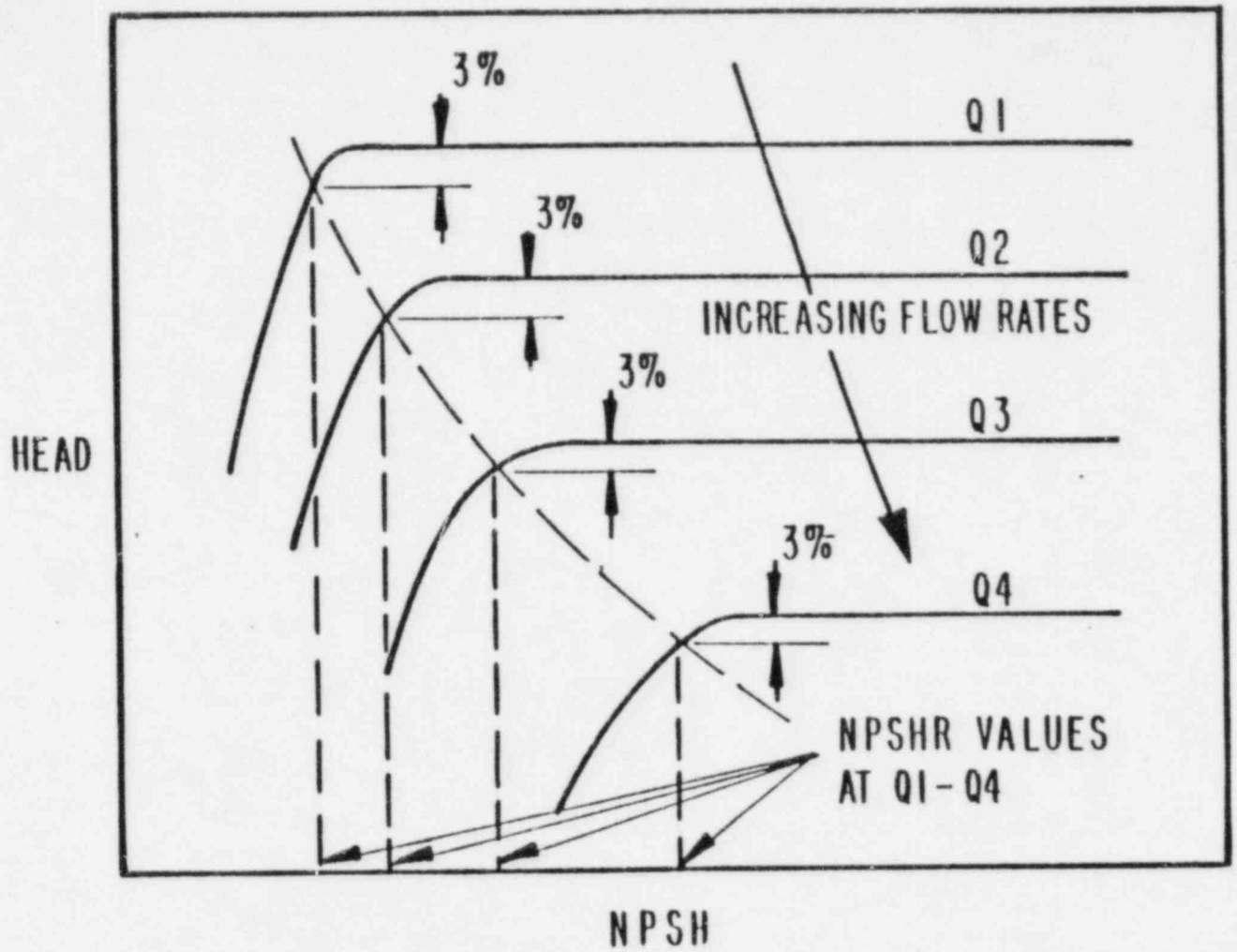

Figure 3.5 Typical head degradation curves due to cavitation at four flow rates (Q1, Q2, Q3, and Q4)

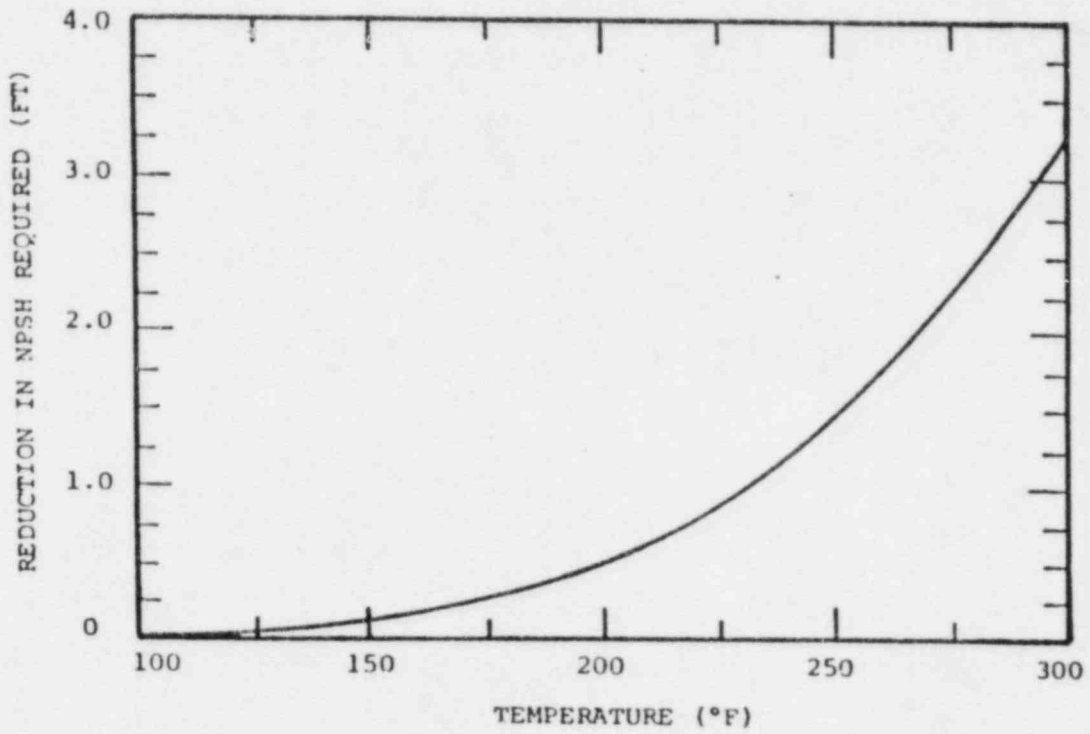

Figure 3.6 Reduction in pump NPSH requirements as a function of liquid temperature (Murakami and Minemura, 1977)

The austenitic stainless steels specified for impellers and casings in these pumps are highly resistant to erosion damage caused by cavitation. Erosion rates for extended operation are not significant as long as the NPSH available exceeds the NPSH requirement of the pump.

3.2.2.2 Air Ingestion

The key findings derived for emergency cooling pumps with respect to air ingestion are based primarily on data from carefully conducted tests in air/water mixtures on pumps of a scale and specific speed range comparable to emergency cooling pumps.* Test data from independent programs on different pumps have been plotted in Figure 3.7 to illustrate the degradation in head at different levels of air ingestion (percent by volume). Performance degradation is indicated by the ratio of the two-phase (air/water) pressure rise to the single-phase (water) pressure rise.

---

*All relevant test data were gathered through reviews of technical papers and interviews with pump manufacturers. Manufacturers' test data on air/water performance of pumps are sparse, and apply primarily to the development of commercial pumps for the paper industry. Although these pumps are similar to those used for emergency cooling service, test methods and results are generally poorly documented. Therefore, manufacturers' data have not been used to establish the air/water performance characteristics of pumps in this report. (Manufacturers' data and testimonials do, however, corroborate published data.) Only sources of information meeting the following criteria were used:

- Pumps must be low specific speed (N_s = 800 to 2000 rpm).
- Pumps must be of reasonable design (with efficiencies $\geq$ 60% and impellers diameter > 6-inch).
- It should also be noted that the quantities of water recirculated in BWRs are significantly larger than those in PWRs.
- Reasonable care must have been used in experimental techniques and in the documentation of results.

Test results meeting these criteria were then reduced to common, normalizing parameters and plotted for comparison.

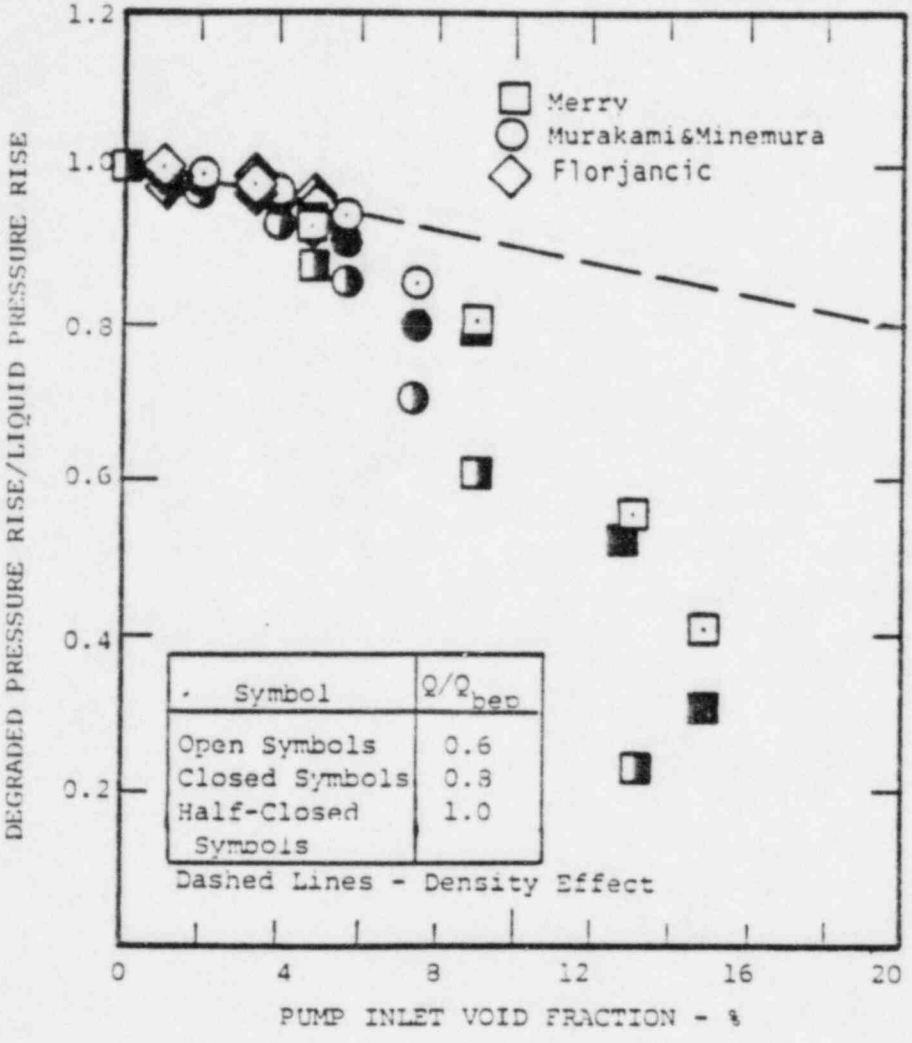

Figure 3.7 Head degradation under air ingesting conditions as a function of inlet void fraction (% of total flow rate by volume)

Figure 3.7 shows that for low levels of air ingestion, the degradation in pump head follows the curve (dashed line) predicted by the change in average fluid density due to the air content. Above 2% void fraction, the data depart from this theoretical line, and the rate of degradation increases. The data in the figure are shown for tests on single stage pumps. Similar tests show that multistage pumps degrade less in performance for comparable quantities of air.

Above void fractions of about 15%, pump performance is almost totally degraded. The degradation process between 2% and 15% void fraction is dependent on operating conditions, pump design, and other unidentified variables. These findings closely approximate the guidelines empirically established by pump manufacturers: at air ingestion levels of less than 3%, degradation is generally not a concern; for air ingestion levels of approximately 5%, performance is pump and site dependent; for air ingestion greater than 15%, the performance of most centrifugal pumps is fully degraded.

For emergency cooling pump operation at very low flow rates (< about 25% of best efficiency point), even small quantities of air may accumulate, resulting in air binding and complete degradation of pump performance.

3.2.2.3 Combined Effects of Cavitation and Air Ingestion

Few data on the combined effects of cavitation and air ingestion are available. Figure 3.8, which uses test results from Merry, (1976), shows that as the air ingestion rate increases, the NPSH requirement for a pump also increases. The curves for this particular pump show that air ingestion levels of about 2% result in a 60% increase in the NPSH required (allowed head degradation based upon 3% degradation from the liquid head performance).

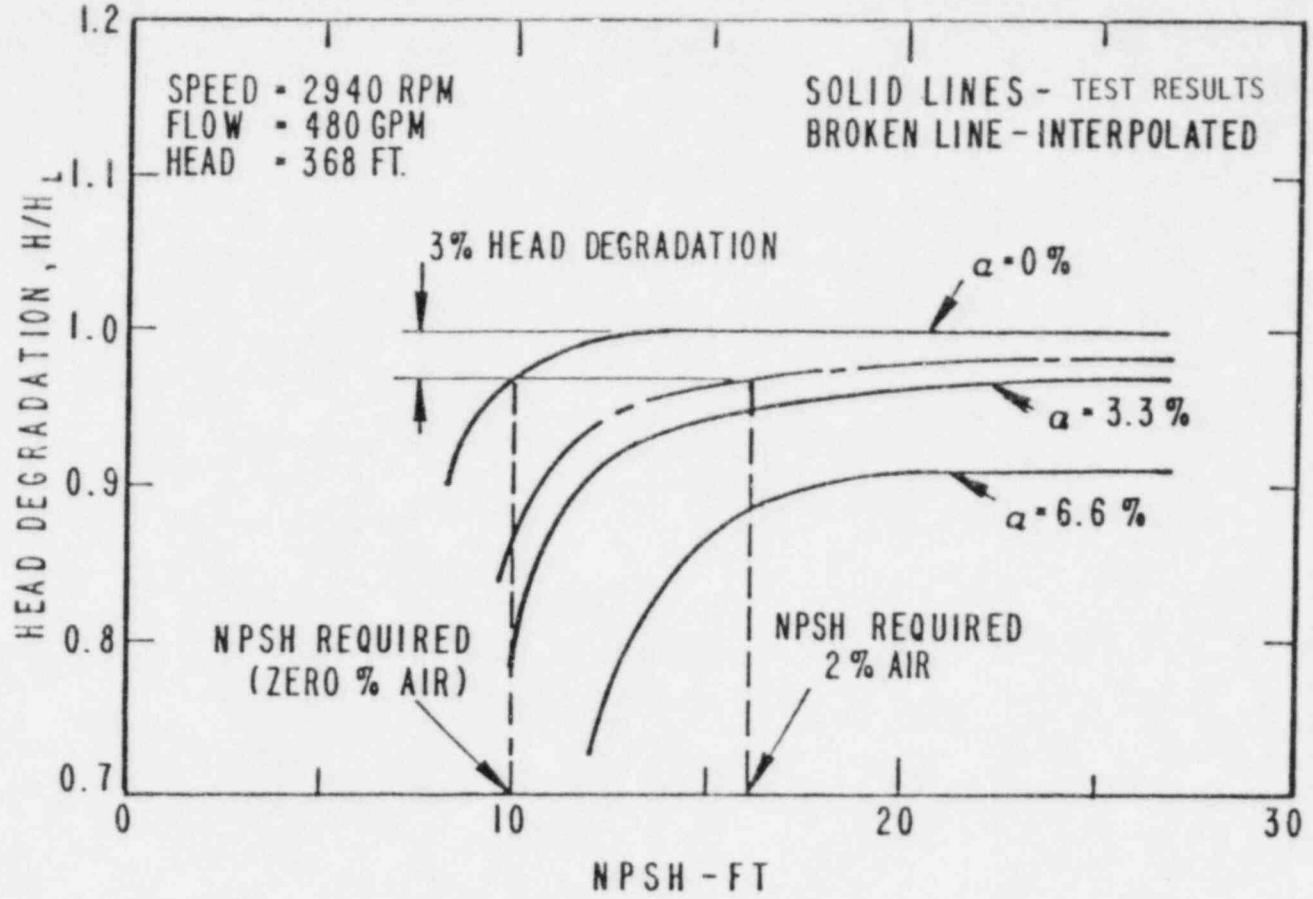

Figure 3.8 Effect of air ingestion on NPSH requirements for a centrifugal pump

3.2.2.4 Particulate Ingestion

The assessment of pump performance under particulate-ingesting conditions is based on estimates of the type and concentrations of debris likely to be transported through the screens to the pump inlet. In the absense of comprehensive test data to quantify types and concentrations of debris that will reach the pumps, it has been estimated that concentrations of fine, abrasive-precipitated hydroxides are of the order of 0.1% by mass and concentrations of fibrous debris are of the order of 1% by volume.* The effects of particulates in these quantities have been assessed on the basis of known behavior of this type pump under similar operating circumstances.

Ingestion of particulates through pumps is not likely to cause performance degradation for the quantities and types of debris estimated above. Because of the upstream screens, particulates likely to reach the pumps should be small enough to pass directly through the minimum cross-section passages of the pumps. Because of generally low pipe velocities on the pump suction side, particulates reaching the pumps should be of near-neutral buoyancy and, therefore, behave like the pump fluid.

Manufacturers' tests and experience with these types of pumps have shown that abrasive slurry mixtures up to concentrations of 1% by mass should cause no serious degradation in performance. Tests on single stage pumps similar in construction to those used in RHR service have shown that quantities up to 4% of fiber paper stock by mass could be handled without appreciable degradation.

---

*The concentration for abrasive AlO(H) was obtained from Niyogi and Lunt, 1981, in which it was estimated that 3000 pounds of precipitate would develop in 30 days and recirculate with 3.7 million pounds of water. The 1% by volume concentration of fibrous debris is based on the quantity of fibrous insulation reaching the sump screens typical of a PWR (see Table 3.4), mixing with 200,000 gallons from the refueling water storage tank and being recirculated through the pumps.

A major concern regarding the effects of particulates on pump performance and operability has been the effects of fibrous or other debris (such as paint chips) on pump seal and bearing systems. Porting within cyclone separators and the flush ports for mechanical shaft seals or water-lubricated bearings may become clogged with debris. In such an event, seal or bearing failure is likely. In the PWR plants that were reviewed, pumps used oil-lubricated or permanently lubricated bearings and mechanical shaft seals. For these configurations, the seals may be subject to failure because of clogging, but the bearings are not. The construction of mechanical face seals used in these pumps is such that complete pump degradation or failure is not likely, even in the event of seal failure. In many of the applications in BWRs, multistage pumps incorporate interstage bushings which are lubricated by the pumped fluid. In these applications, it is possible that excessive wear or clogging due to the presence of particulates or debris may cause bearing failure.

3.2.2.5 Swirl

The effects on pump performance resulting from swirl due to sump vortices are negligible if the pumps are located at significant distances from sumps. Test results discussed in Section 3.4 indicate that swirl angles in the suction pipe were typically 4° in PWR sump configurations (measured at 14 pipe diameters from the sump outlet) and 0 to 7° in BWR configurations. RHR and CSS pumps are generally preceded by valves, elbows, and piping with characteristic lengths on the order of 40 or more pipe diameters. This system of piping components is more likely to determine the flow distributions (swirl) at the pump inlet than the swirl caused by sump hydraulics. However, for swirl angle > 10° it should be noted that swirl induced by the sump causes a higher friction loss than is the case with nonswirling flow. For pumps with inlet bells directly in the sumps, vortices and accompanying swirl in the inlet bell can cause severe problems, because of asymmetric hydraulic loads in the impeller. Hence, this type of installation should be avoided.

3.2.3 Calculation of Pump Inlet Conditions

The steps given below delineate the calculational procedure for assessing the inlet conditions to the pump, based on the findings noted above. The procedure follows routine calculation methods used for estimating NPSH available, except that the procedures incorporate steps to allow for air ingestion effects. Figure 3.9 shows a schematic of the pump suction system with appropriate nomenclature. The procedure is as follows:

(1) Determine the hydrostatic water pressure (gage), P_{sg}, at the sump suction inlet centerline, accounting for temperature dependency and minimum sump water level. An important factor to include in determining the maximum sump water level is pressure head loss across the sump screen (see Section 3.3).

(2) Based on the sump hydraulic assessment, determine the potential level of air ingestion at the sump suction pipe, α_s, as discussed in Section 5.2.

(3) Calculate the pressure losses in the suction pipe between the sump and the pump inlet flange. Pressure losses are calculated for each suction piping element (inlet loss, elbow loss, valves, pipe friction) using the average velocity through each element, V_i, and a loss coefficient, K_i, for each element. The total pressure losses are then

$$P_\ell = (\gamma/144) \sum_{i=1}^{N} K_i \, V_i^2/2g$$

where γ is the specific weight of water (lb/ft^3), 144 is the conversion from psf to psi and N is the number of elements.

The loss coefficients are defined as

$$K_i = \frac{h_{\ell i}}{V_i^2/2g}$$

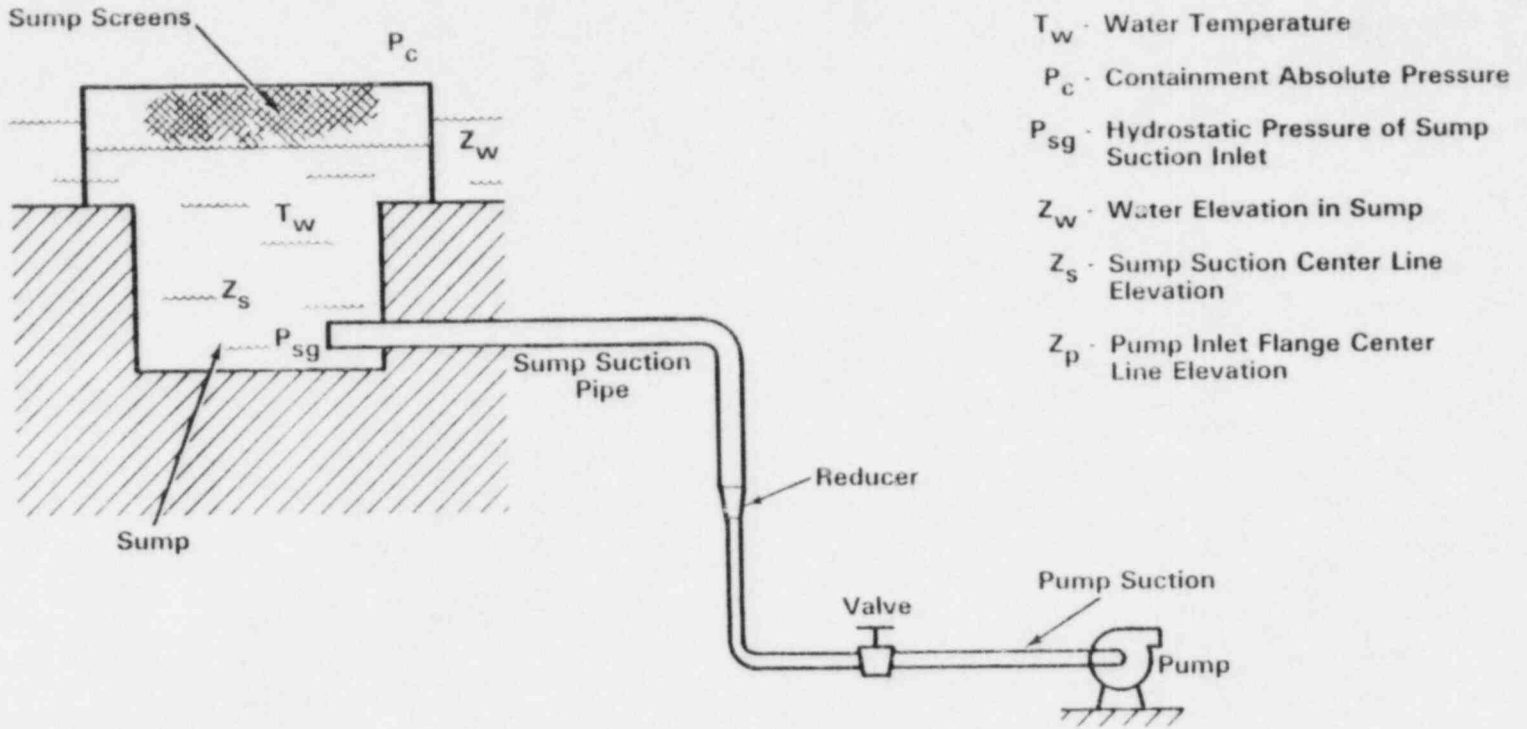

Figure 3.9 Schematic of suction systems for centrifugal pump

where

$h_{\ell i}$ is the head loss in ft of water in element i

g is the acceleration due to gravity

V_i is the average velocity in element i in fps

Loss coefficients can be found in standard hydraulic data references such as Hydraulic Institute Standards (1975).

(4) Calculate a value for P_p that will be used to correct the volumetric flow rate of air at the sump suction pipe for density changes (If air ingestion is zero, Steps 4, 5, and 6 can be ignored):

$$P_p = P_{sa} - P_\ell + P_h - P_d$$

where

P_{sa} = the total absolute pressure at the sump suction pipe centerline, which is the sum of the hydrostatic pressure, P_{sg}, and the containment absolute pressure, P_c (determined in accordance with RG 1.1 and 1.82 for NPSH determination)

P_ℓ = the pressure loss determined in Step 3,

P_h = the hydrostatic pressure due to the elevation difference between the sump suction pipe centerline, Z_s, and the pump inlet flange centerline, Z_p

$$P_h = (\gamma/144)\ (Z_s - Z_p)$$

P_d = the dynamic pressure at the pump inlet flange using the average velocity at the pump suction flange, V_p

$$P_d = \frac{\gamma\ (V_p)^2}{144 \quad 2g}$$

(5) Calculate the corrected air volume flow rate at the pump inlet flange, α_p, based on perfect gas, isothermal process

$$\alpha_p = (P_{sa}/P_p)\alpha_s$$

(6) If α_p is greater than 2%, inlet conditions are not acceptable.

(7) Calculate NPSH at the pump inlet flange, taking into account the requirements of RG 1.1 and 1.82, as follows:

$$NPSH = (P_c + P_{sg} - P_\ell + P_h - P_{vp})\ (144/\gamma)$$

where

P_{vp} = the vapor pressure of the water at evaluation temperature and the other terms are as defined in Steps 1, 3, and 4 above.

(8) If air ingestion is not zero, the NPSH required from the pump manufacturer's curves must be modified to account for air ingestion as follows:

$$\beta = 0.50\ (\alpha_p) + 1.0$$

where

α_p = the air ingestion level percent by volume at the pump inlet flange.

Then

NPSH required (air/water) = βx (NPSH required for water)

The expression for β is empirical. It has been selected because it provides a reasonable amount of conservatism in predicting NPSH requirements in the presence of less than 2% air ingestion at the pump inlet. However, the data on which this conclusion is based are

limited mainly to the tests of Merry, (1976), and the test data scatter mentioned in the published report are not quantified. Therefore, it is important that good judgment be used in the application of the correct factor β to plant calculations. In particular, the conservatisms in assumptions for calculating the pump inlet conditions should be weighed carefully if the calculated NPSH available for air/water operation is marginal with respect to the required NPSH.

(9) If NPSH available from Step 7 is greater than NPSH required from Step 8, pump inlet conditions should be satisfactory.

3.3 Debris Assessment

The safety concerns related to the generation of thermal insulation debris as the result of a LOCA and the potential for sump screen blockage were addressed generically as follows:

(1) Nineteen reactor power plants were surveyed in 1982 to identify insulation types used, quantities and distribution of insulation, methods of attachment, components and piping insulated, variability of plant layouts, and sump designs and locations. Additional information was contributed during a public comment period in 1983.

(2) Experiments were conducted to establish the pressure conditions leading to the onset of damage to typical nonencapsulated mineral wool and fiberglass insulations, and attendant debris generation. The buoyancy and transport characteristics of both fibrous and reflective metallic insulations were investigated, along with screen blockage and head loss.

3.3.1. Overview

Assessing LOCA-generated insulation debris requires consideration of the following elements:

(1) The type and quantities of insulation employed. These are important because the potential for transport and blockage depends upon the insulation material employed. Identification of insulations employed and their distribution on piping and major components is important, as is the identification of methods of attachment.

(2) Long-term cooling. For both PWRs and BWRs, the maintenance of long-term recirculation cooling is the underlying safety concern and breaks (or LOCAs) requiring long-term cooling must be assessed. For PWRs, breaks in the primary coolant system are of principal concern, and evaluations of potential break locations (and size) should be the basis for estimating quantities of debris generated. For BWRs, potential breaks in the feedwater and recirculation loop piping and steamline breaks constitute the LOCAs that necessitate long-term cooling. SRP Section 3.6.2, "Determination of Rupture Locations and Dynamic Effects Associated with the Postulated Rupture of Piping," should be used to identify potential break locations.

(3) Possible break-target combinations. On the basis of the break locations identified in Step 2, possible break-target combinations must be assessed. Sections 3.3.3 and 3.3.4 provide guidance for defining the break jet envelope. Analyses should consider the effects in close proximity of the break (within $\leq$ 7 L/D's of the break) where insulation destruction will be highest. Beyond 7 L/D's, insulation could be dislodged in the as-fabricated state, depending on the methods of attachment.

(4) Level of insulation damage and volume of LOCA-generated insulation debris. The level of damage can be severe, partly damaged or dislogement of as-fabricated insulation segments. Insights regarding potential levels of destruction can be derived from the HDR (Heissdampfreaktor or superheated steam reactor) experiments (see Appendix C). In those experiments, destruction of insulation (particularly fiberglass insulation material) within 2 to 4 meters of the break was very severe.

Analytical studies (see Section 3.3.4) of expanding two-phase jets also show very high stagnation pressures near the break location (within 3 to 5 L/D's). The insulations and coverings within this region will be subjected to stagnation pressures on the order of 10 to 50 bars.

Small-scale experimental studies on some typical fibercloth-jacketed insulation pillows (see Section 3.3.3) revealed that the onset of destruction (the start of tearing of the fibercloth jacket) occurred at stagnation pressures of 20 to 35 psi.

Thus the estimation of debris generation is complex and material dependent. Sections 3.3.3 and 3.3.4 provide means for making such estimates.

(5) Transport Characteristics. The transport of LOCA-generated insulation debris will be controlled initially by the blowdown phase (when the jet forces will distribute debris). Long-term transport will occur during the recirculation phase when containment-flow forces (or velocities) control the transport of debris. This long-term transport depends on the type of insulation, level of damage and flow velocity. Both fibrous insulation and RMI debris fragments transport at low velocities (0.2 to 0.5 ft/sec). RMI debris generally accumulate at the lower portion of debris screen while fibrous insulation debris builds up uniformly on the screen. Thus, highly damaged insulation debris will exhibit transport characteristics significantly different (i.e., transport can occur at low velocities) from the as-fabricated insulation segments.

The plant layout, particularly for PWRs, is an important consideration in the initial transport (or blowdown) phase. If the sump and break locations are such that the break jet can target the sump region directly, direct transport to the vicinity of the sump screen can be postulated immediately. Moreover, if the break jet can target the sump screen, screen survivability relative to jet loads should be assessed.

(6) Screen blockage (or suction strainer blockage). This blockage is dependent on the material characteristics of the debris transported to the screen and on the local velocities, which can pull such debris to the screen, as well as on the findings obtained for the transport of fibrous and metallic materials and as-fabricated sections of typical insulation materials.

There are two parts to this element:

(a) Will the debris be transported? Transport is dependent on recirculation flow velocities within containment.

(b) Will blockage occur? Blockage is dependent on the approach velocities near the screen or suction strainer, and the approach velocity will establish the blockage patterns that will occur.

Shredded fibrous debris is transported at near-neutral buoyancy conditions and is deposited (in a general sense) uniformly across a screen structure. Metallic foils (such as those used internally in reflective metallic insulations) exhibit transport characteristics and screen blockage patterns that are a function of foil thickness (or rigidity) and screen- approach velocities. Development of a blockage model for foils is more difficult than it is for fibrous debris.

(7) Head loss as a result of the estimated screen blockage. The results of Step (6) dictate the estimating methods applicable. Results of experiments have shown that blockage losses for fibrous insulation

materials can be described as a power function such as

$$\Delta H = a\, U^{b} t^{c}$$

where

a, b, and c are coefficients that should be derived from experimental data
t(thickness) = volume of debris/effective screen area
U = approach velocity

Head losses that result from impervious materials (such as metallic sheets) are dependent on the potential blockage patterns resulting from the plant-specific reviews. For example, a PWR sump with a horizontal debris screen will incur a different type of blockage than will a sump with high vertical debris screens. Sections 3.3.5 and 5.3 provide additional information relative to these considerations.

(8) Accurate predictions of recirculation flow velocities within the containment during the long-term cooling mode. These are as important as the experimentally derived debris transport velocities discussed above. If predicted recirculation velocities exceed transport velocities, debris will move toward the sump. An analytic method that permits estimation of velocities within containment is reported in NUREG/CR-2791. However, because of simplifications inherent in that modelling technique, a more refined analysis may be warranted if the predicted fluid velocities are within a factor of two of the transport velocity determined experimentally for each of the insulation types. That is to say, although the recirculation flow velocities discussed in Appendix D would predict one-half of the critical transport velocity (thereby indicating zero transport), transport might actually occur because of flow field variabilities within containment that are not accounted for.

3.3.2 Types of Insulations Employed

Insulations utilized in nuclear power plants can be categorized in two major groups, as discussed in the following paragraphs.

(1) Reflective Metallic Insulation

This is an all-metallic insulation design based on the concept of utilizing a series of highly reflective foils to retard heat transfer. reflective metallic insulation (RMI) is generally constructed from stainless steel, although aluminum interior foils have been used in conjunction with stainless steel inner and outer liners. Figure 3.10 provides details for typical, as-fabricated RMI segments and details of the internal foil construction. Generally RMI is manufactured in half-shell segments or other geometric shapes that are prefabricated to fit piping or other major components (reactor vessels, steam generators, and the like) and that use snap-on latching for attachment.

There are currently at least four different manufacturers of RMI: Diamond Power Speciality Company, TRANSCO, Johns-Manville, and ROMET. All vendor designs vary. Some designs have open ends; others have sides sealed with foils. Interior foils range in thickness from 0.0025 inch to 0.010 inch. Inner and outer liners are generally thicker (on the order of 0.030 inch to 0.040 inch) and may be flat, corrugated, or dimpled.

(2) Conventional or Mass Type Insulation

Mass type insulation is an industry-derived term that encompasses a wide range of insulation materials and differentiates them from RMI.

In mass type insulation, the materials used as the insulation filler are from one of two broad categories, fibrous and others.

Fibrous insulations include.

Calcium Silicate Molded Block

Calcium silicate molded block insulation is a molded, high-temperature pipe and block insulation composed of hydrous calcium silicate. It is light weight, has low thermal conductivity and high structural strength, and is insoluble in water. Its density (dry) is 13 to 14 lb. per cubic foot. Its compressive strength (based on 1-1/2 inch thickness) is 60 to 250 psi. The molded blocks are provided in thicknesses of up to 4 inches and lengths of up to 3 ft.

Expanded Perlite Molded Block

Expanded perlite molded block insulation is composed of expanded perlite with reinforced mineral fiber and inorganic binders. It is an insulating material with properties similar to those of calcium silicate insulation. The average maximum density is 14 lb. per cubic foot. Its flexural strength should be not less than 35 psi, and its compressive strength dry is 60 psi and wet is 25 psi.

Fiberglass Molded Block

Fiberglass molded block insulation is composed of glass that has been foamed or cellulated under molten conditions, annealed, and set to form a rigid incombustible material with hermetically sealed cells. The density is between 7.0 and 9.5 lb. per cubic foot. Its flexural strength is 60 psi, and compressive strength is 75 psi.

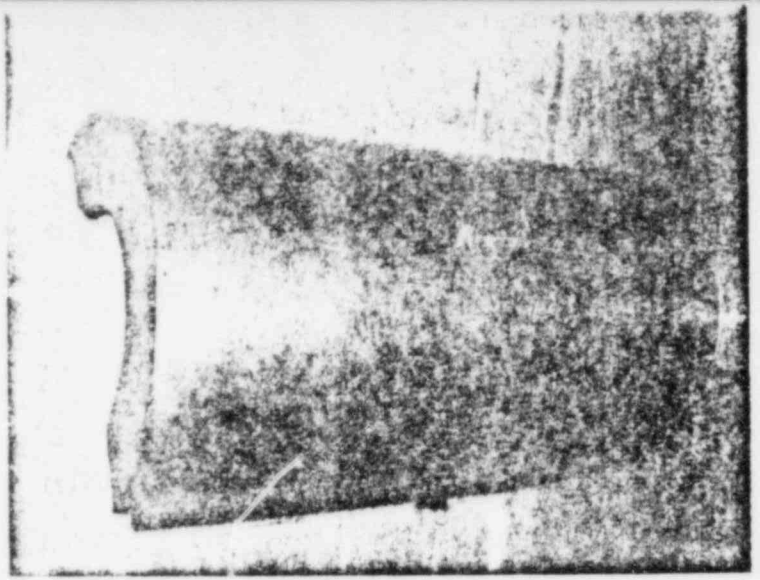

HALF SHELL (OUT-SIDE)

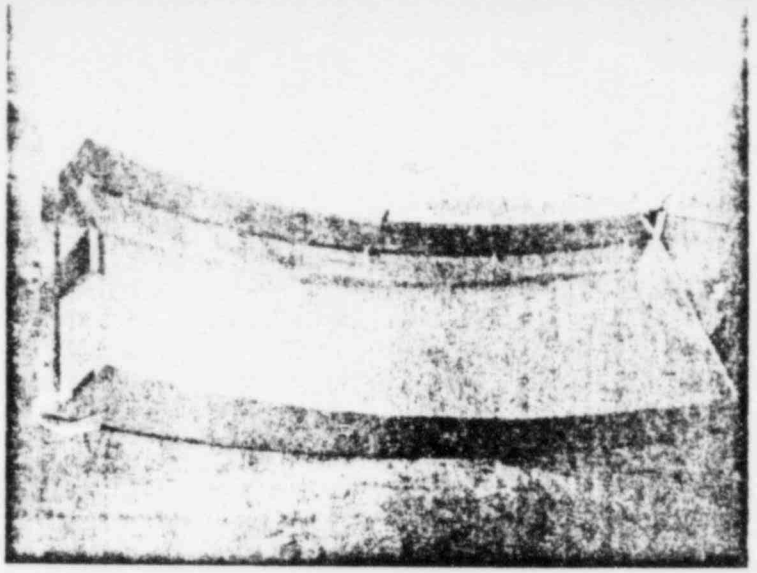

TYPICAL OUTER SHELL

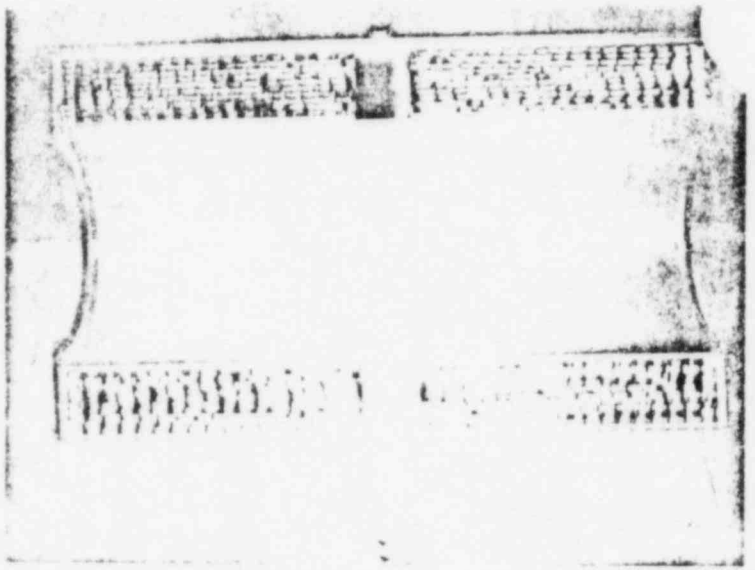

HALF SHELL (IN-SIDE)

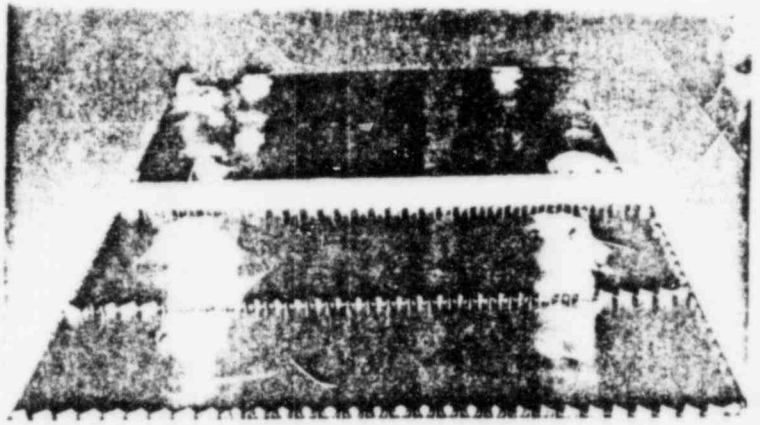

INNER FOILS (.0025 inches thick)

Figure 3.10 As-fabricated, reflective metallic insulation components

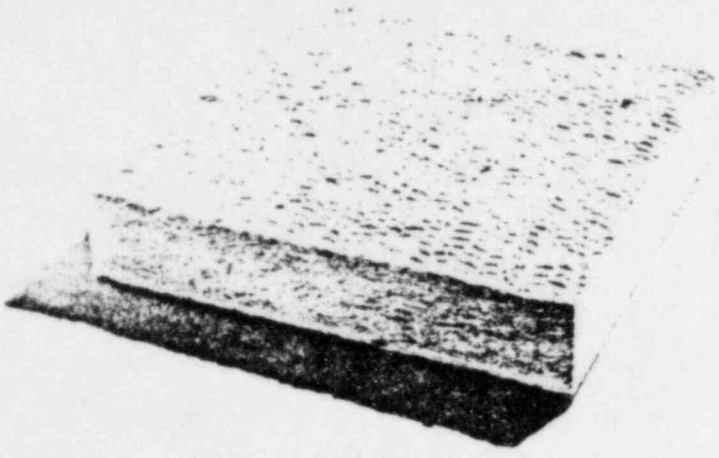

MINERALWOOL

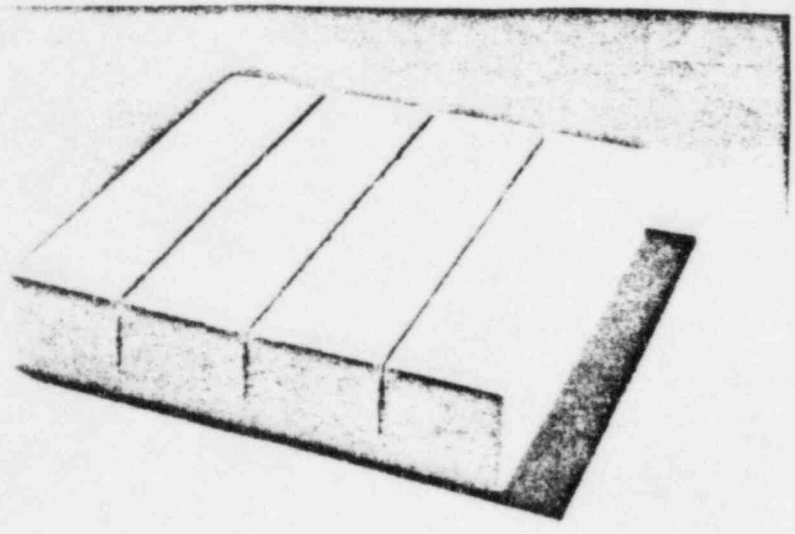

CALCIUM SILICATE

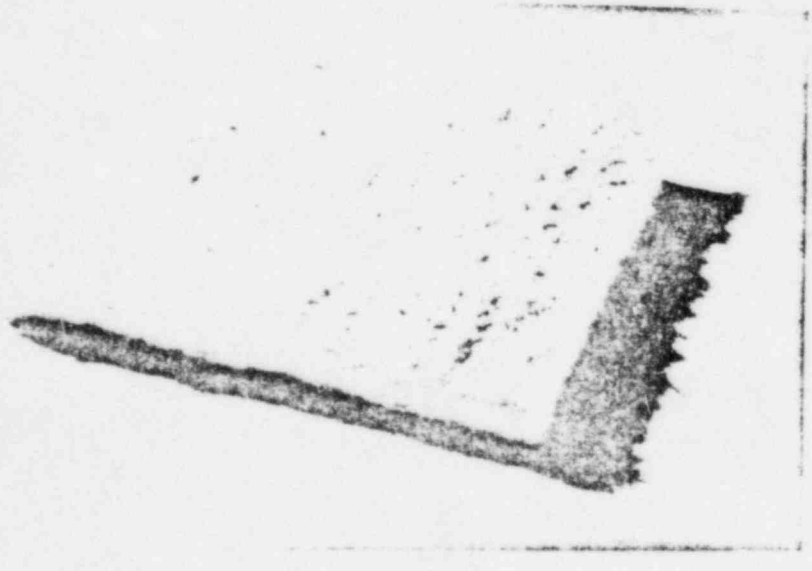

NEEDLED FIBERGLASS
(E - TYPE)

Figure 3.11 Mass-type insulations

Nukon Fiberglass Blankets

The leading manufacturer of this type insulation is Owens-Corning which makes thermal insulation system called NUKON for use in the containment areas of light water nuclear power plants. NUKON™ is a blanket insulation consisting of fiberglass insulating wool reinforced with fiberglass scrim and sewn with fiberglass thread. The blanket may have secondary holding straps attached to it and wrapped completely around it. This material has a low density (i.e., 2 to 4 lbs. per cubic foot). Figure 3.13 shows this type of insulation as fiberglass core material.

Mineral Wool Fiber Block

Mineral wool fiber block insulation is made of a mineral substance, such as rock, slag, or glass processed from a molten state into fibrous form. The density, depending on kind, ranges from 10 to 20 lb. per cubic foot. The strength varies considerably with the classes of insulation. The moisture is less than 1.0 percent by volume.

Other insulations include.

Cerablanket

Cerablanket™, manufactured by Johns-Manville, is a ceramic fibrous insulation material with a density of 6 lb. per cubic foot. The Cerablanket is enclosed in 0.006 inch metal foil and then encapsulated in a reflective insulation structure.

Unibestos

Unibestos™ insulation is composed of lime and diatomaceous silica taken from natural deposits. These basic ingredients are bonded with asbestos fiber possessing the tensile strength of piano wire. This composition is then encased in stainless steel sheet.

Figure 3.11 illustrates a variety of materials of this type of insulation. (NUREG/CR-2403 provides a more extensive description of insulations employed, particularly those used in older plants.) Any of the above described mass type insulations can sometimes be enclosed in an outer shell or jacket or cloth covers. The following categories are currently being used by the industry:

Totally Encapsulated or Semi-Encapsulated Insulation

Internal insulation in this category can be mass type materials that act as the principal heat barrier. The outer shell is generally made of sheet metal and in some cases the ends are closed. The encapsulation is being utilized to contain the mass insulation and to ease installation and removal.

Caution is recommended in assessing encapsulated insulation because of the generalized use of this category and wide variability of designs procured and installed in plants. Figure 3.12 illustrates some encapsulated insulations. Survivability under break jet loads requires assessment of the specific insulation employed and the structural capability of the encapsulation provided.

The construction of semi-encapsulated insulation modules is exactly the same as that of totally encapsulated ones, except that semi-encapsulated modules are assembled in the field and clamped, not welded, together.

Jacketed Insulations

In this category the principal heat barrier (internal insulation) is the same as it is for mass type insulation. The jacket (which is usually a separate outer metal cover such as a stainless steel sheet, asbestos cloth, fiberglass cloth or aluminum) is simply an outer cover to protect the core material. Thus jacketed insulations are an intermediate arrangement between encapsulated and nonencapsulated insulation. Generally banding or latching mechanisms are employed for jacketed insulations such as shown on Figure 3.13.

Urethane and polyurethane foam antisweat is another jacketed type insulation. It is a rigid cellular foam plastic that combines light weight and strength with exceptional thermal insulating efficiency. The foam is a vast cross-linked netwook of closed cells; each cell is a tiny bubble full of gas that accounts for 90 percent of its volume. Its density ranges from 1.8 to 4.0 lb. per cubic foot. The insulation is sealed with a vapor barrier of aluminum foil or a metal jacket.

Regardless of the type of insulation employed, the assessment of debris effects must focus on types and quantities of materials present and their survivability during a LOCA, as discussed in Sections 3.3.3 and 3.3.4.

Plant insulation surveys were performed in 1981 and 1982, and the results are summarized in Table 3.3. (The details associated with these surveys are in NUREG/CR-2403 and its Supplement 1.) These surveys showed that there was a wide variability in types of insulations employed, but that the newer plants were electing to utilize RMI. Moreover, based on the two BWRs surveyed, the trend appeared to be total use of RMI or totally encapsulated insulation.

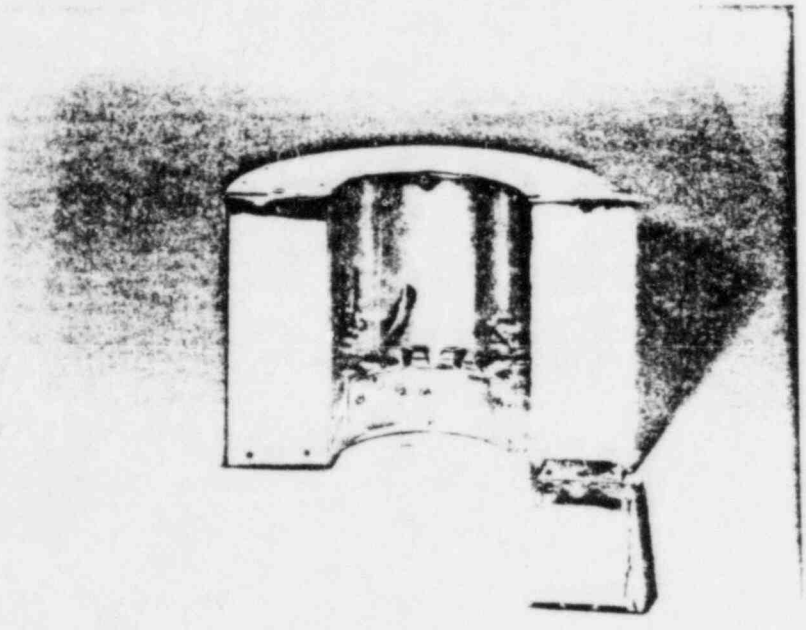

ENCAPSULATED FIBERGLASS

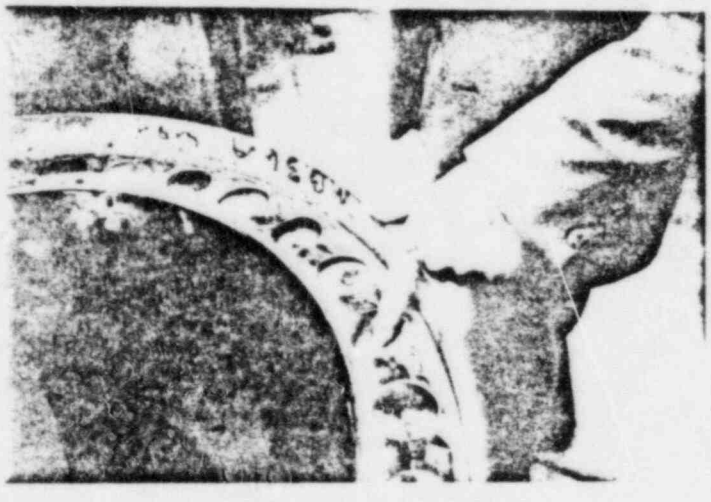

ENCAPSULATED REFLECTIVE METALLIC

Figure 3.12 Encapsulated insulation assemblies

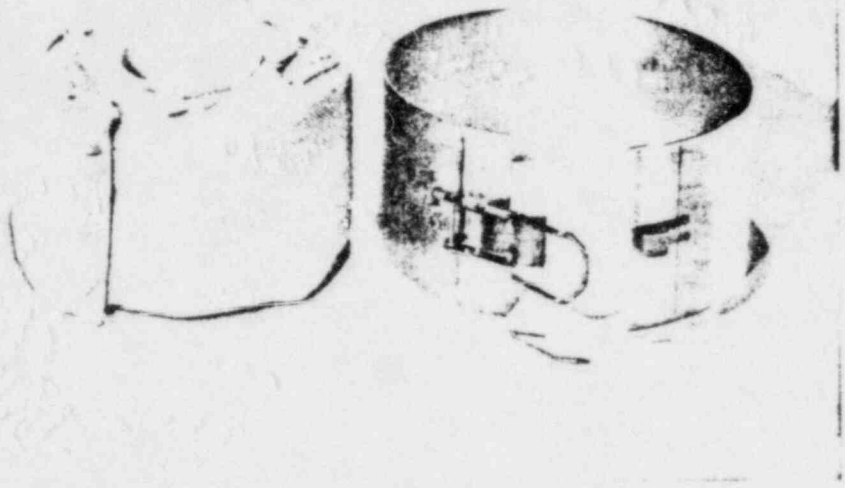

FIBERGLASS CORE MATERIAL JACKET AND LATCH

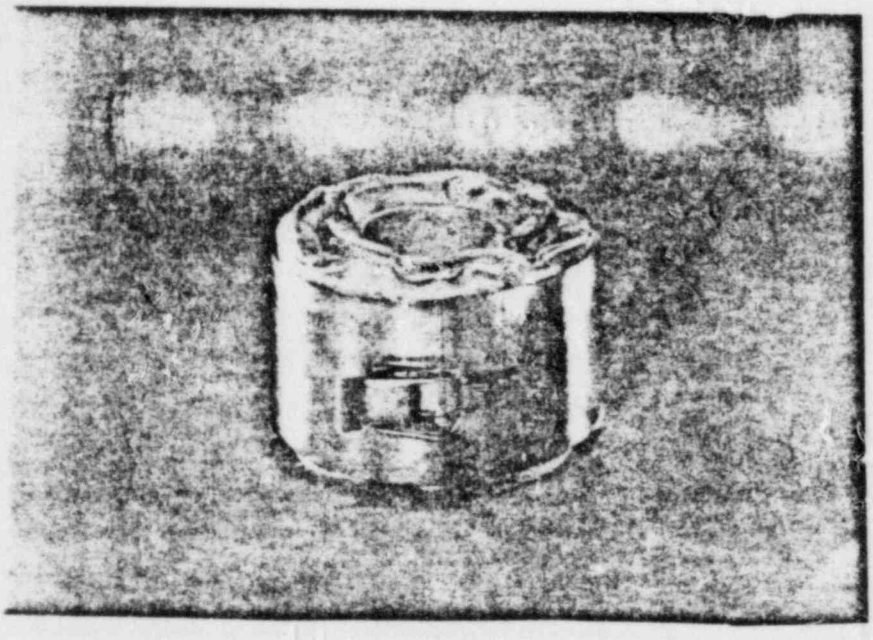

JACKETED ASSEMBLY

Figure 3.13 Jacketed insulation assemblies

Table 3.3 Types and percentages of insulation used within the primary coolant system shield wall in plants surveyed

Plant	Types of Insulation and Percentage*					
	Reflective Metallic	Totally Encapsulated	Mineral Fiber/Wool Blanket	Calcium Silicate Block	Unibestos Block	Fiberglass
Oconee Unit 3	98	--	--	--	--	2
Crystal River Unit 3	94	5	1	--	--	--
Midland Unit 2	78	--	--	--	--	22
Haddam Neck	3	--	--	--	95¶	1
Robert E. Ginna	--	--	5	80	10	--
H. B. Robinson	--	--	--	15	85	--
Prairie Island Units 1 & 2	98	--	--	--	--	2
Kewaunee	61	--	--	--	39	--
Salem Unit 1	39	8	53**	--	--	--
McGuire Units 1 & 2	100	--	--	--	--	--
Sequoyah Unit 2	100	--	--	--	--	--
Maine Yankee	13	--	48	25	13	1
Millstone Unit 2	25	35	5	30	--	--
St. Lucie Unit 1	10	--	--	90	--	--
Calvert Cliffs Units 1 & 2	41	59	--	--	--	--
Arkansas Unit 2	46	53	--	--	--	1
Waterford Unit 3	15	85	--	--	--	--
Cooper	30	70	--	--	--	--
WPPSS Unit 2	100	--	--	--	--	--

*Tolerance is ± 20 percent

**Both totally and semi-encapsulated Cerablanket is used, however, inside containment only totally encapsulated is employed.

¶Unibestos is currently being replaced by Calcium Silicate. However, both types of insulation have the same sump blockage characteristics.

Table 3.4 Insulation types used on nuclear plant components*

	Vessel	Coolant Piping	Coolant Pumps	S. G. (less bottom head)	S. G. Bottom	Pressurizers
Rs						
dam Neck	Rm	C	C	C	C	C
-2 & IP-3	Rm	C	C	C	C	C
ine Yankee	Rm	C	C	C	C	C
lstone-3	Rm	C	C	C	C	C
nkee	C	C	C	C	C	C
isades	Rm	C	C	C	C	C
f Creek	Rm	C	C	C	C	C
Calhoun	Rm	C	C	C	C	C
laway	Rm	C	C	C	C	C
inson-2	Rm	C	C	C	C	C
key Pt-3	Rm	C	C	Rm	Rm	C
key Pt-4	Rm	C	C	C	C	C
Lucie-2	Rm	C	C	C	C	C
erford-3	Rm	E	E	E	E	E
th Texas 1&2	Rm	C	C	C	C	C
Onofre-1	Rm	C	C	C	C	C
na	Rm	C	Rm	Rm	C	C
ble Hill	Rm	Rm	Rm	C	Rm	Rm & C
-2	Rm	Rm	Rm	C	Rm	Rm
Rs						
erick 1&2	Rm	C	C	N/A	N/A	N/A
zpatrick	Rm	C	C	N/A	N/A	N/A
ry 1&2	Rm	C	C	N/A	N/A	N/A
ticello	Rm	C	C	N/A	N/A	N/A
ch-1	Rm	C	C	N/A	N/A	N/A

sulation Legend:

- Reflective Metallic Insulation
- Conventional Insulations (e.g., fibrous & mass materials)
- Encapsulated Insulation

*Based on material obtained during a public comment period; may be obtained by writing to Generic Issues Branch, NRC, Washington, DC 20555.

However, comments received during the public "for comment" period associated with USI A-43 (June-July 1983) presented a changing picture (see Table 3.4). Some older operating plants (e.g., Monticello) have been reinsulated with fibrous insulation. Newer BWRs (e.g., Limerick) are being insulated with fiberglass, and the increasing use of fiberglass is evident. Replacement of selective insulation also occurs during, or following, inservice inspections. These recent observations re-emphasize the large varibility of insulations employed, the plant-specific aspects associated with insulations used (plants handle insulation on a site-specific basis and changes need not be reported), and the time dependency factor. As new insulation products are developed new materials are being introduced into nuclear plants.

3.3.3 Insulation Debris Generation

Jet impingement forces are the dominant insulation debris generator. Other contributors, such as pipe whip and impact, have been studied and shown to be of secondary importance (NUREG/CR-2791).

The criteria for defining break or rupture locations should be consistent with the requirements of SRP Section 3.6.2, which provides guidance for selecting the number, orientation, and location of postulated ruptures within a containment.

The safety concerns associated with debris relate to ensuring long-term recirculation capability. Therefore, for PWRs, the postulated breaks of concern are those in the primary coolant system and in components (or other systems) that are connected to the primary coolant system. For BWRs, the postulated breaks of concern are in the feedwater and recirculation systems and in the steam lines.

The destructive nature of high pressure break jets has been experimentally demonstrated in blowdown experiments conducted in the HDR facility (see Appendix C). Figures 3.14 and 3.15 show damage to reinforced concrete structures in the HDR. Figures 3.16, 3.17, and 3.18 show the damage to insulation and insulated components in the HDR.

These blowdown tests (blowdown was from 110 bars and 280°C to 315°C, under steam and subcooled water conditions) revealed that all glass fiber insulation was destroyed within 2 meters of the break nozzle and distributed throughout the HDR containment as very fine particles. In addition iron wrappers were thrown away from vessels within 4 to 6 meters of the break nozzle, with glass fiber untouched. With enforced shieldings (steel bandages) around the vessels, the damage was reduced. Mineral wool insulation that was encapsulated in iron plate, withstood the rough blowdown conditions well. Break sizes 200-mm, 350-mm, and 430-mm diameter have been investigated.

3.3.4 Two-Phase Jet Loads Under LOCA Conditions

Determination of the extent of potential damage requires estimation of pressure and flow field forces resulting from the expanding jet. On the other hand, the flow field for a two-phase jet is extremely complicated and multidimensional. The jet impingement model discussed in this section is based on a study of HDR experimental data by Sandia National Laboratory. This model is under peer review by the ANS-58.2 Committee on Pipe Rupture and has not yet been incorporated in SRP 3.6.2 as an endorsed approach. Sandia National Laboratory has analytically studied two-phase jet impingement on targets over a range of pressures and temperatures representative of postulated LOCAs for BWRs and PWRs. Those results are reported in NUREG/CR-2913.

In the expanding jet flow field, there are three natural divisions of the field (see Figure 3.19). There is a nozzle (or break) region where the flow chokes. In this region, there is a core at choked flow thermodynamic properties that projects downstream of the nozzle at distances that depend on the degree of subcooling. Downstream of this region there is the free jet region. Here the jet expands almost as a free, isentropic expansion; the flow is supersonic throughout this entire region. The free jet region terminates at a stationary shock wave near the target. This shock wave arises because the target propagates pressure waves

Figure 3.14 Structural damage to railings and walls in the HDR facility following a blowdown experiment

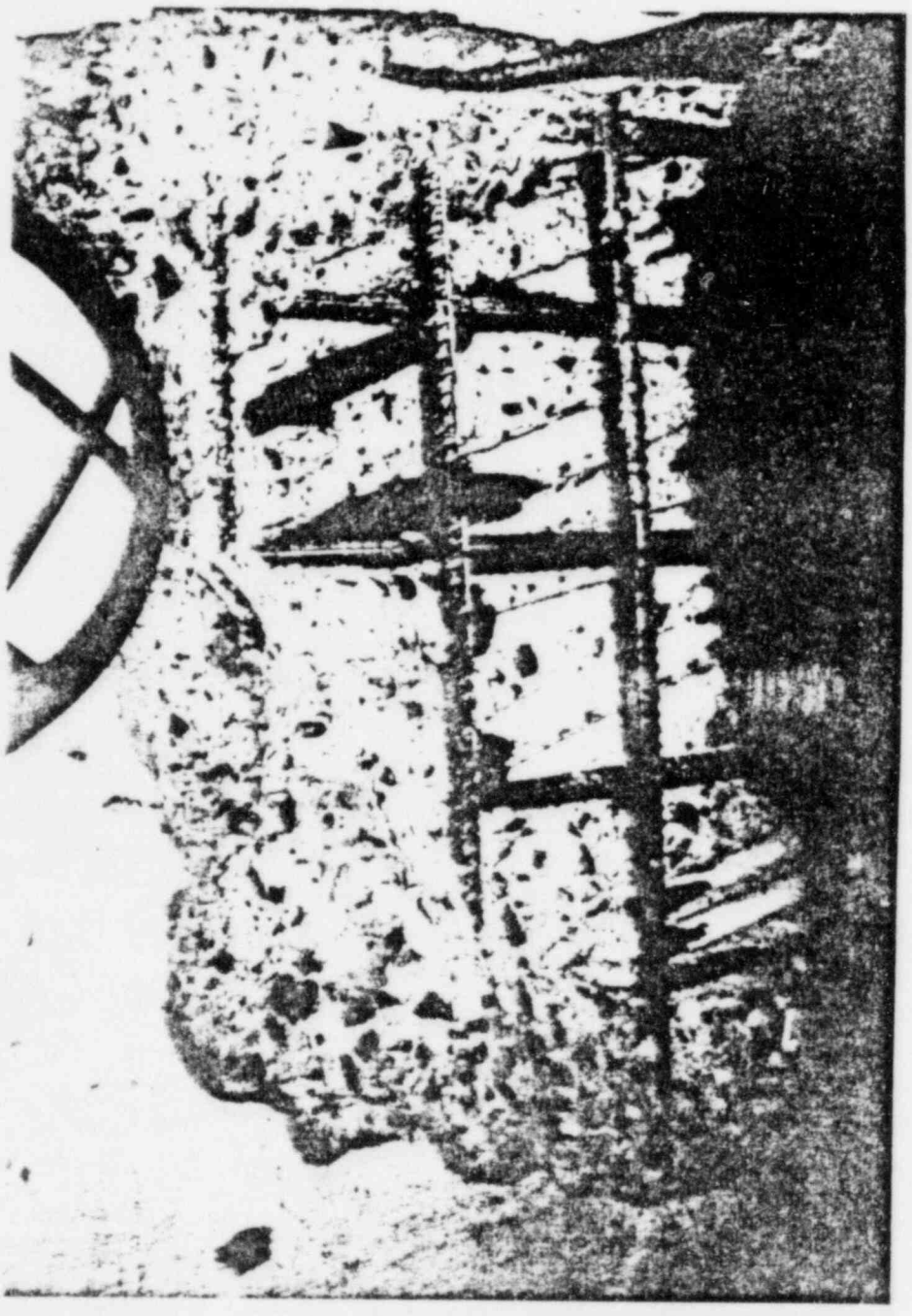

Figure 3.15 Erosion of reinforced concrete in the HDR facility due to direct break jet impingement

Figure 3.16 Blowdown damage to fiberglass insulation covering the HDR pressure vessel

Figure 3.17 Distribution of fiberglass insulation after an initial HDR blowdown test

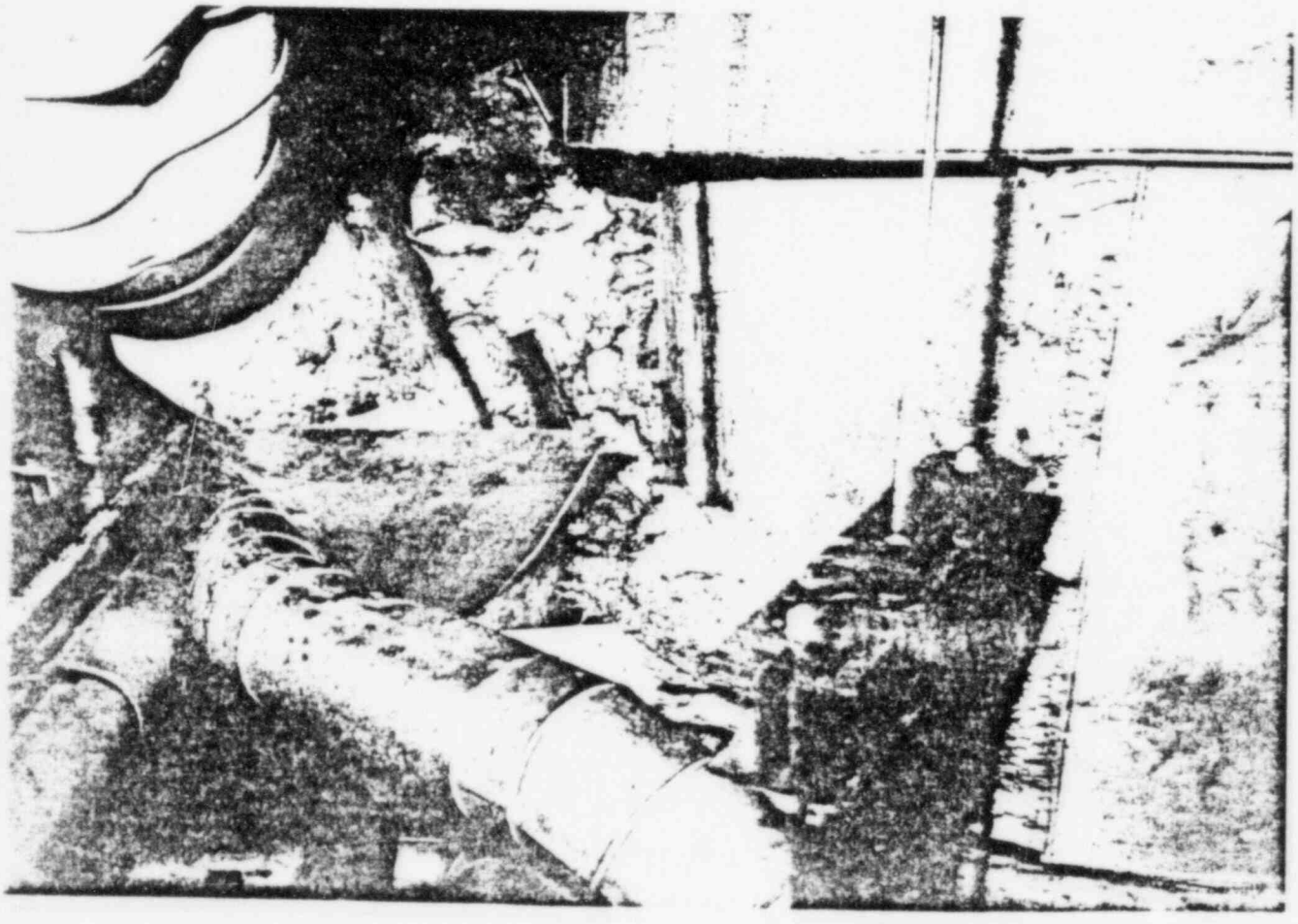

Figure 3.18 Blowdown damage to jacketed (sheet metal cover) reinforced (with wire mesh) fiberglass in the HDR blowdown compartment

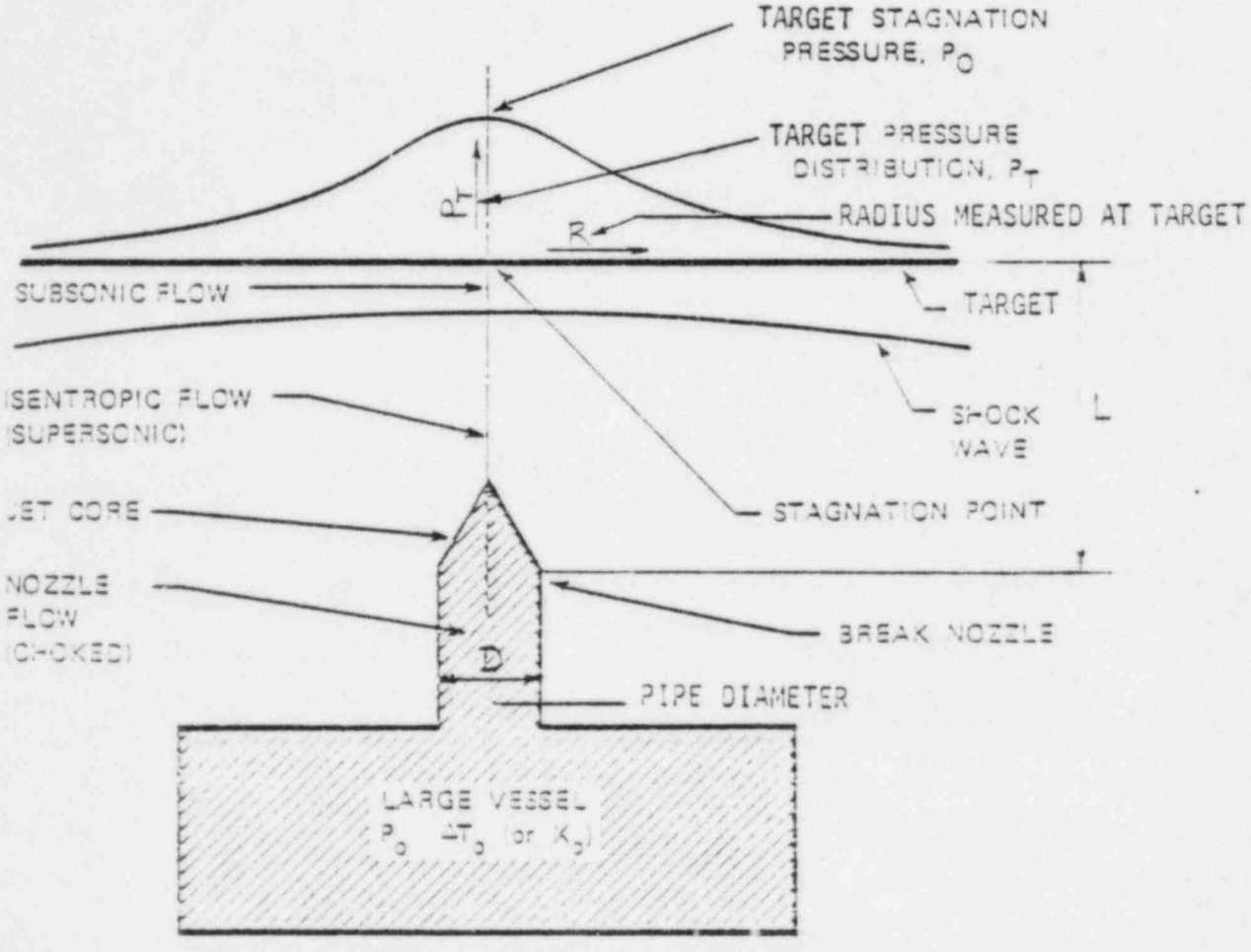

P_o = Stagnation pressure at break

ΔT_o = Subcooling of stagnation temperature at break

X_o = Stagnation quality at break

Figure 3.13 Schematic of jet impinging on target

upstream and, thus, produces a pressure gradient that will direct the fluid around the target. Downstream of the shock is the target region where the local flow field imposes a pressure loading on the target. Depending upon the upstream flow conditions and the L/D's of the target, there may be a substantial total pressure loss across the shock wave. This loss arises because of the irreversible physics that characterize the shock. The pressure loss across the shock and radial velocity components can lead to negative pressure loads across the target, which can lift away materials (such as insulation segments) from targeted components. The HDR tests revealed evidence of such loadings.

NUREG/CR-2913 addresses the centerline behavior of two-phase jets and the radial loading for axisymmetric impinging two-phase jets. The method developed for calculating centerline behavior indicates that the jet stagnation pressure at a given target distance from the break (in terms of L/D) is a function of the stagnation pressure and steam quality or the degree of subcooling in the vessel. This functional dependence (on pressure and subcooling) largely disappears at about 5 L/D's from the break. At approximately 7 L/D's downstream of the jet origin along the centerline of the jet, stagnation pressure falls to roughly 20 psig regardless of the break thermodynamic conditions.

Two-dimensional pressure distributions were calculated and are reported in NUREG/CR-2913. These results indicate that the region targeted by an impinging two-phase jet is highly dependent on the thermodynamic conditions at the break. The constant pressure contours (as a function of target L/D)

form complex shapes in space. Figures 3.20 through 3.23, which are reproduced from NUREG/CR-2913, illustrate axial and radial pressure distributions of an expanding jet representative of PWR and BWR blowdown conditions. Figure 3.24 is a comparison of Sandia calculations (taken from NUREG-2913) with HDR experiment V21.1.

The significant findings to be derived from the calculations contained in NUREG/CR-2913 are

(1) Target pressure loadings increase asymptotically at L/D's less than 3.0 to break exit pressures. At L/D's less than 3, survivability of insulation materials is highly unlikely.

(2) At L/Ds from 5 to 7, the centerline stagnation pressure becomes essentially constant at approximately 2 ± 1 bars.

(3) The multidimension pressure field loads the target over a large region (see Figures 3.22 and 3.23); this region may be approximated by a 90° jet cone expansion model. A hemispherical expansion model could be another approximation for this expanding pressure field. These two-dimensional calculations do not support the use of the Moody jet model (a narrow jet cone) for target close to the break locations.

The two-phase jet modelling results and the levels of insulation damage evidenced by the HDR experiments lead to the development of a three-region jet-debris-generation model which is shown in Figure 3.25. Region I ($\leq$'3 L/D from the break) is where extremely high levels of destruction would occur due to the very high break jet pressures (see also Figures 3.20 and 3.21) and total destruction can be assumed to occur. Region II ($3 < L/D < 7$) is a zone where high levels of damage (or destruction) are possible; but with the recognition that the types of insulation employed (e.g., reflective

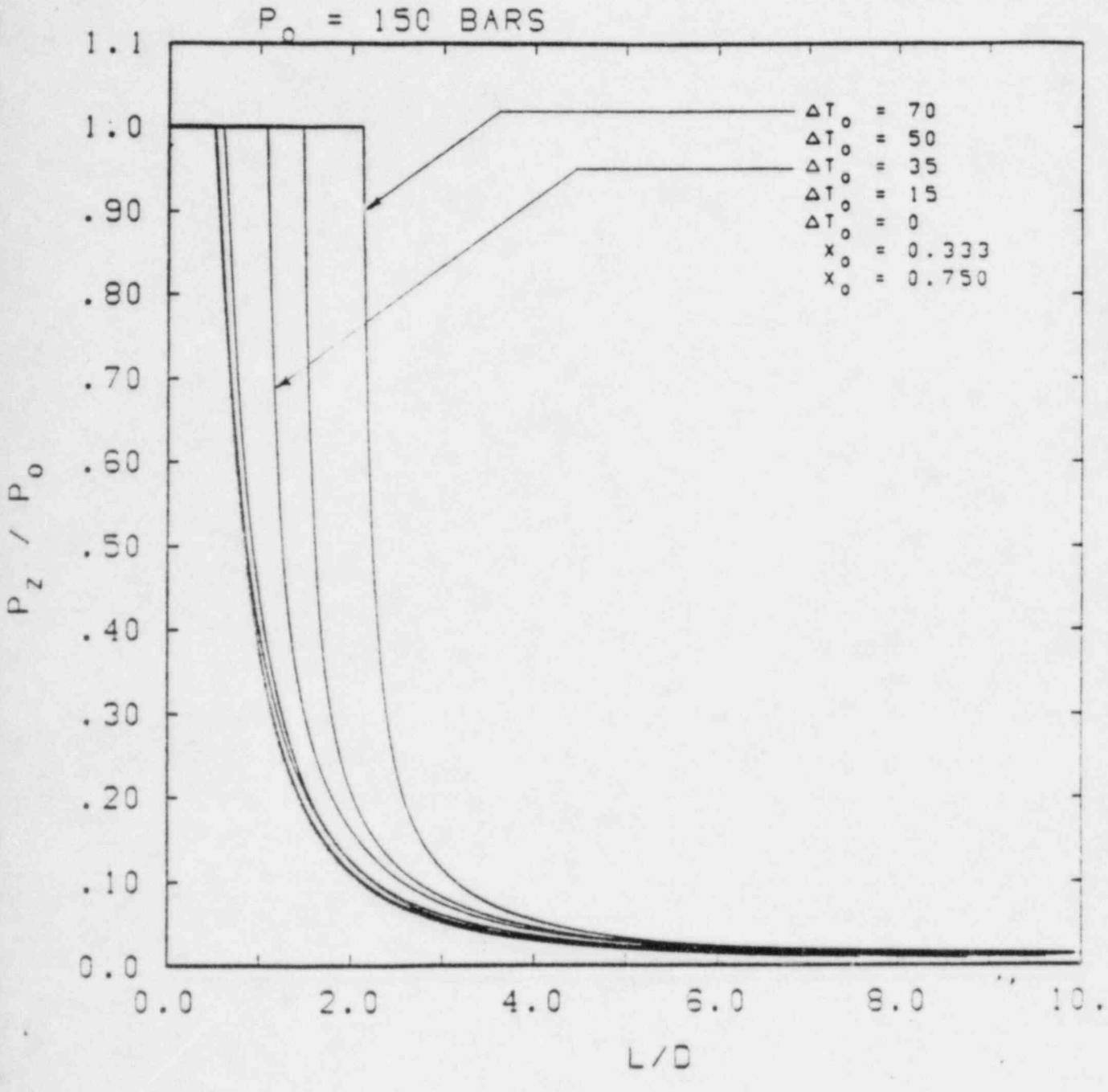

Figure 3.20 Centerline target pressure as a function of axial target position (L/D) for break stagnation conditions of 150 bars and various subcoolings and qualities. L is the target position, D is the pipe diameter P_z is the centerline pressure, and P_o is the stagnation pressure at the break.

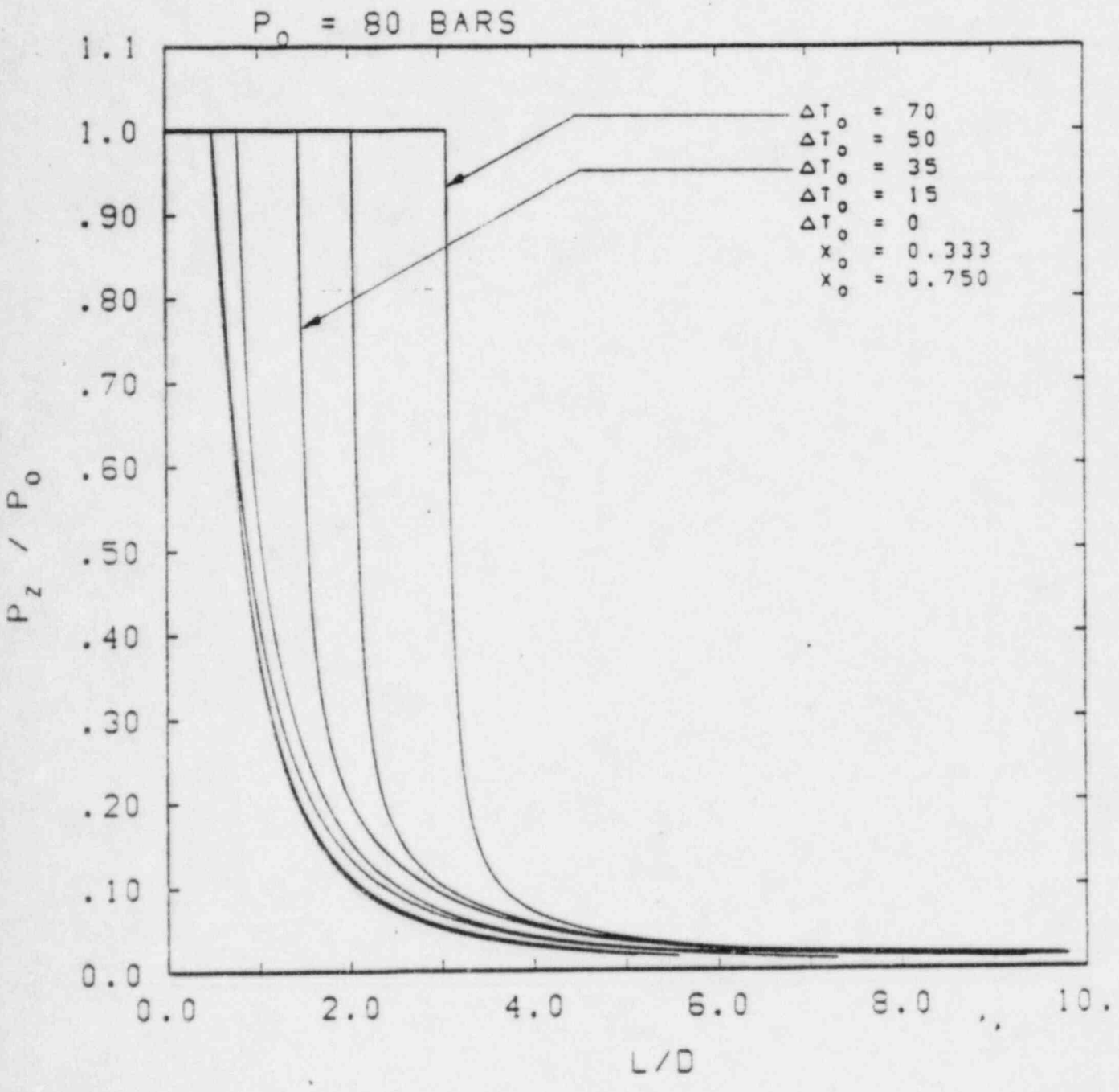

Figure 3.21 Centerline target pressure as a function of axial position (L/D) for break stagnation conditions of 80 bars and various subcoolings and qualities. L is the target position, D is the pipe diameter, P_z is the centerline pressure, and P_o is the stagnation pressure at the break.

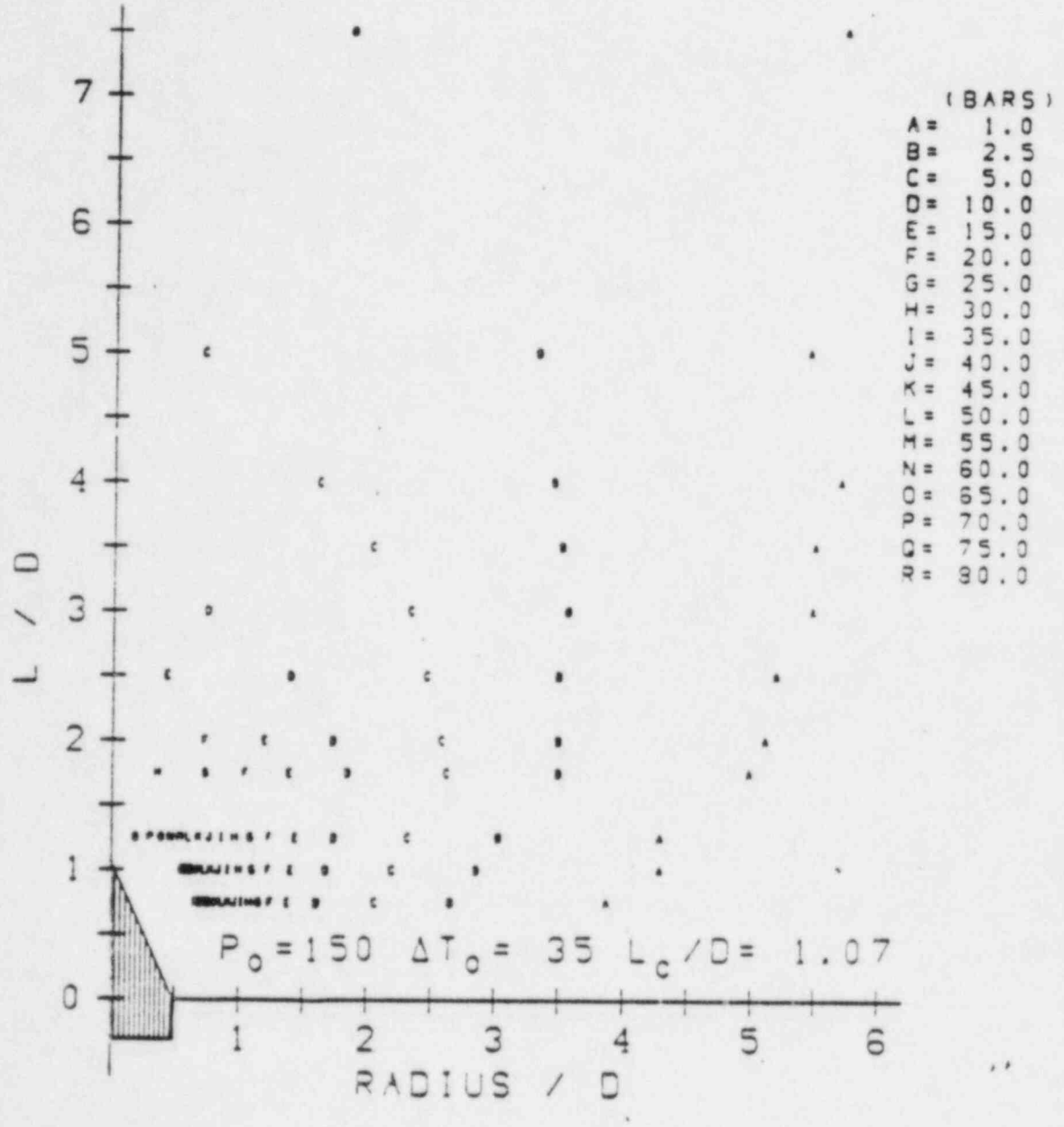

Figure 3.22 Composite target pressure contours as a function of target length/jet diameter (L/D) and target radius/jet diameter (RADIUS/D) for stagnation conditions of P_o = 150 bars and 35 degrees of subcooling. Smooth lines connecting like alphabetic letters form an approximate pressure contour corresponding, in bars, to the pressure versus alphabetic letter key. This contour is approximate and is only informational.

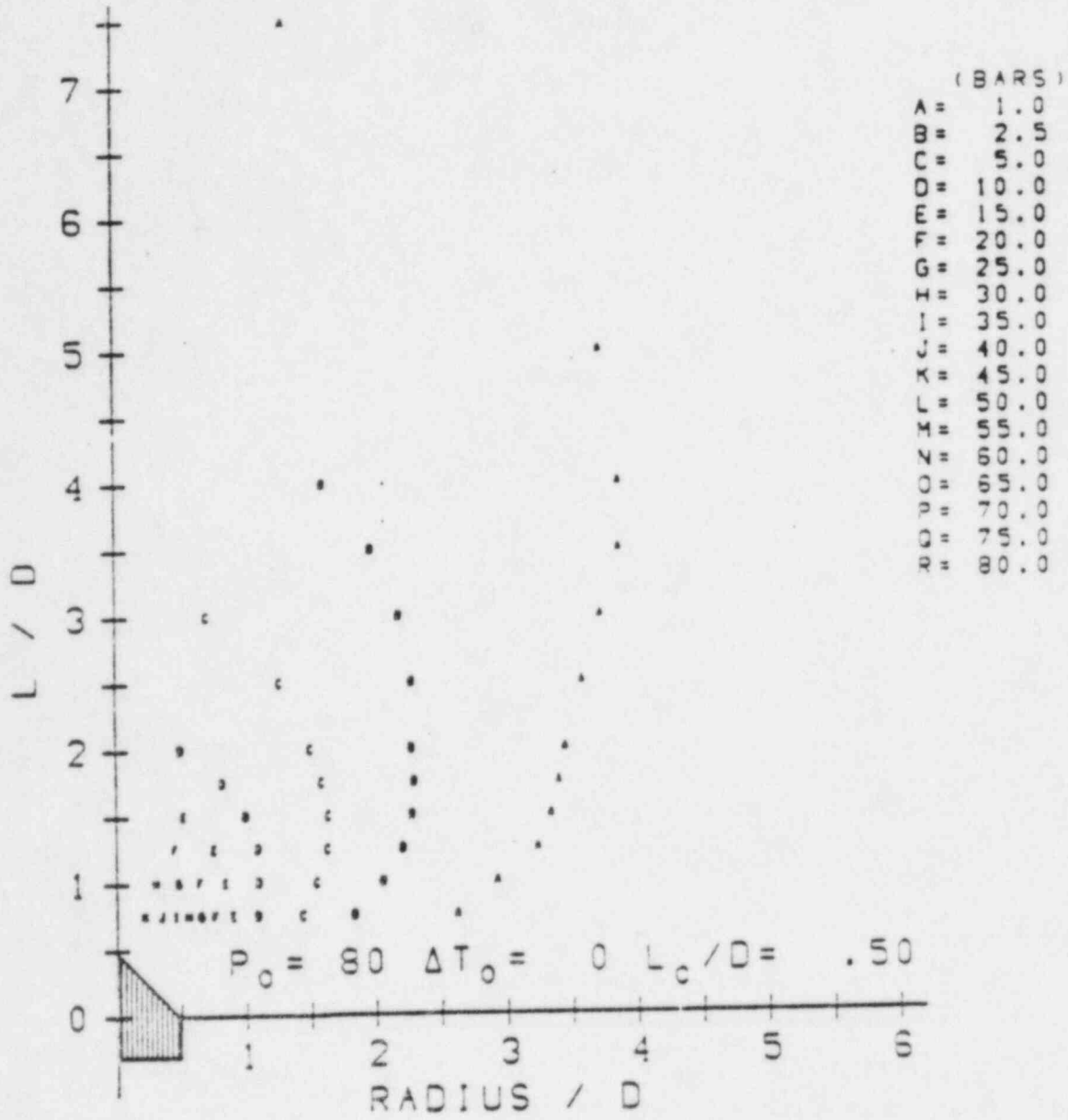

Figure 3.23 Composite target pressure contours as a function of target length/jet diameter (L/D) and target radius/jet diameter (RADIUS/D) for stagnation conditions of P_o = 80 bars and saturated liquid. Smooth lines connecting like alphabetic letters form an approximate pressure contour corresponding, in bars, to the pressure versus alphabetic letter key. This contour is approximate and is only informational.

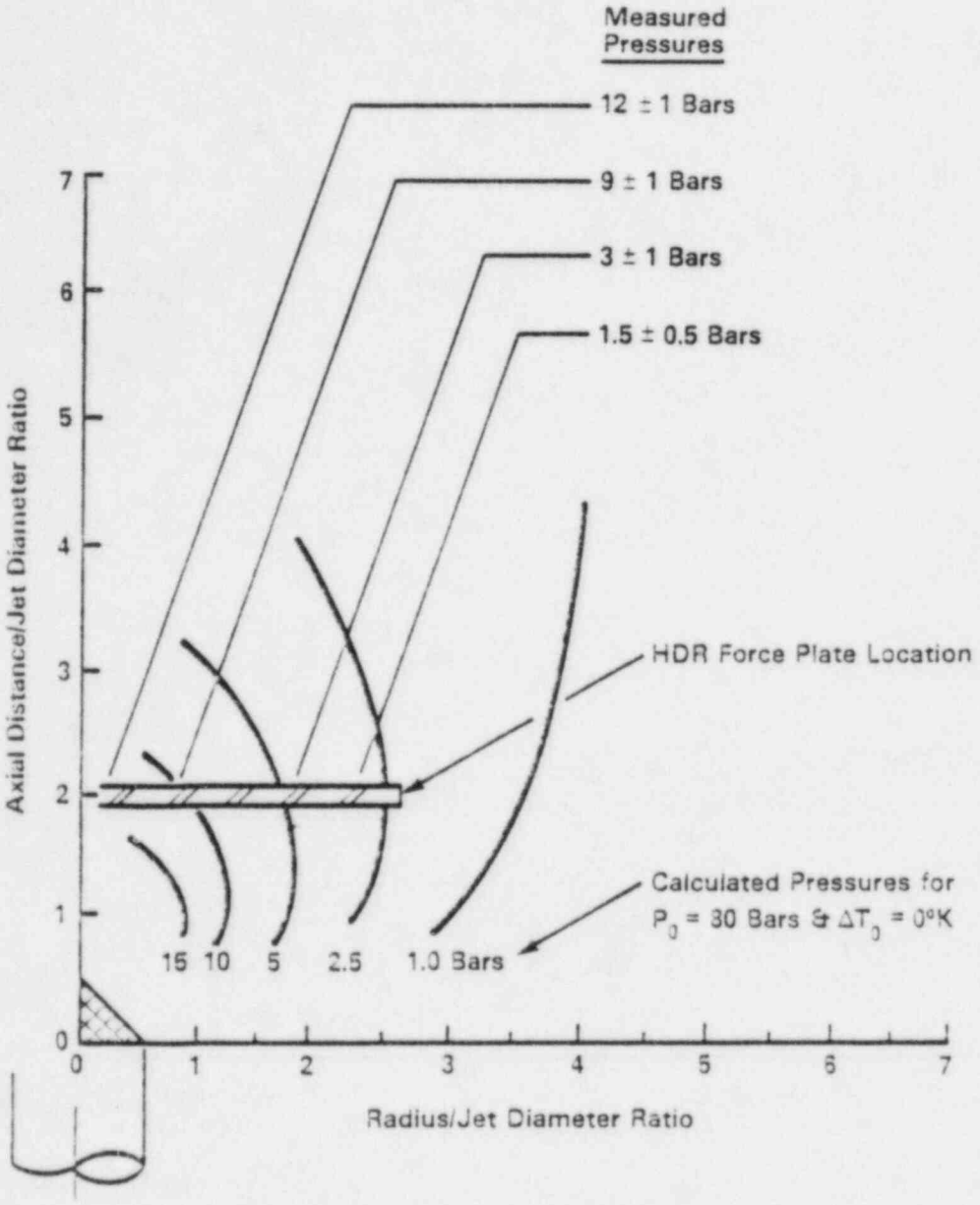

Figure 3.24 Comparison of calculated target pressures with HDR experiment V21.1

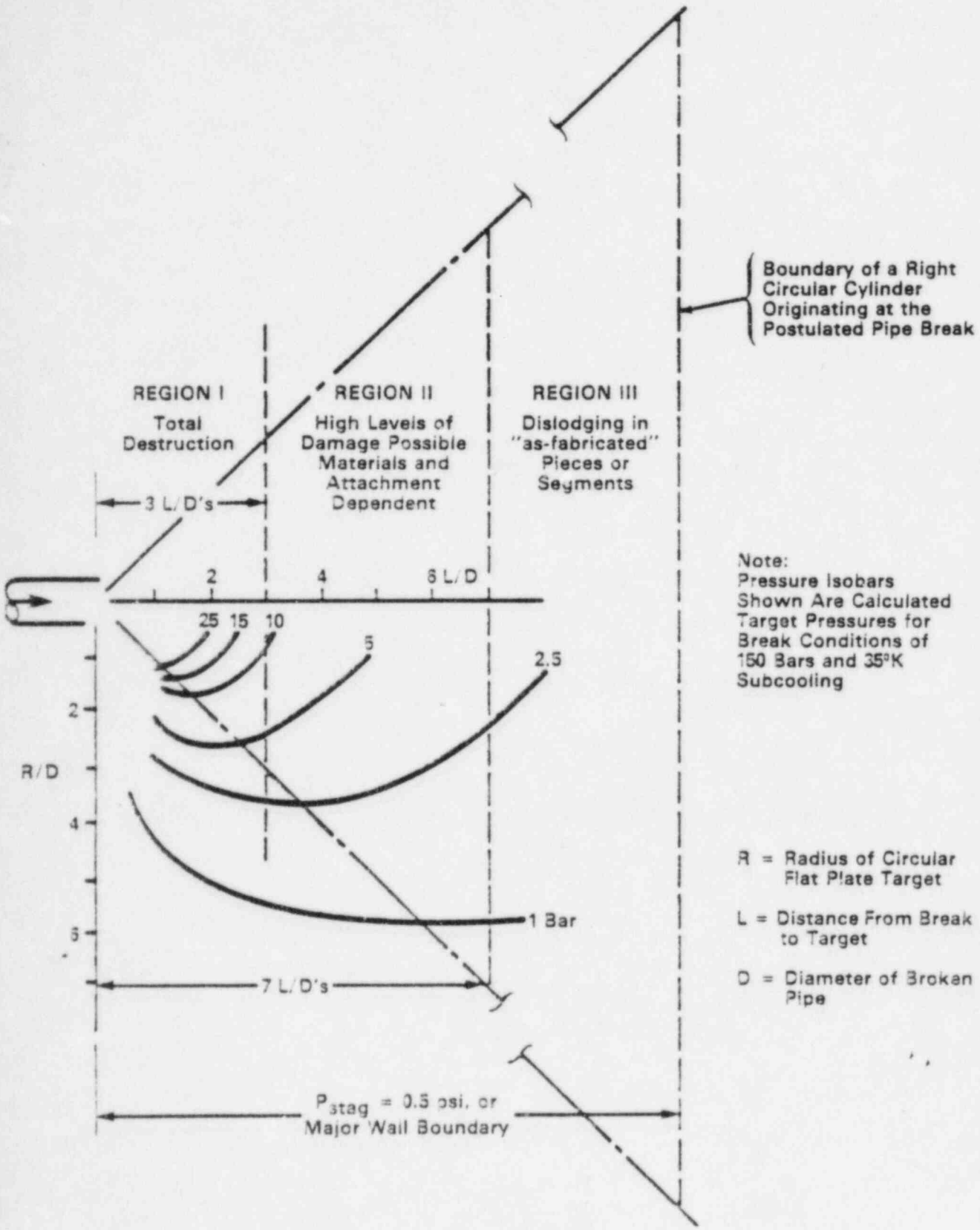

Figure 3.25 Multiple region insulation debris generation model

metallic, fibrous, foamglass, etc), methods of attachment, whether the materials are encapsulated,etc. are factors which should be considered in estimating the types and volumes of debris generated in Region II. Region III ($L/D \geq 7$) is a zone where destruction (or damage) will likely be dislodgement of insulation in the as-fabricated mode, or as modules. Beyond 7 L/D, break jet pressures have decayed to 1 to 2 bars. It should also be noted that superimposed pressure field on Figure 3.25, is representative of a PWR primary coolant system break. BWR jet expansion fields decay more rapidly (see pressures in Figure 3.21 versus Figure 3.20).

Despite the calculational simplification afforded by a three-region model, determination of the types and quantities of insulation debris will always be material (or type) dependent. Figure 3.26 has been constructed to illustrate the possible variation of debris types as a function of distance from the break jet and the relative quantities of different types of possible debris. A quantified debris distribution model would require extensive experiments designed to develop such data; these do not exist. On the other hand, results from HDR experiments (see Appendices C,E, and F) do provide insights regarding debris generation and were used to construct Figure 3.26.

First of all, the assumption of severe damage or total fragmentation within 3 L/D's is supported by experiments and is applicable to both reflective metallic insulation (RMI) assemblies and fibrous insulation assemblies. However, the hypothesis of "exploded" RMI assemblies releasing free, or undamaged interior foils (which can transport at very low velocities), is not supported by the experimental evidence reported in Appendix E.

Pursuing those potential levels of damage expected in Region II (see Figure 3.25) it appears that the RMI debris could consist of damaged inner foils and damaged assembly or components that were the result of further LOCA damage. Experimental data available for fibrous insulations indicate that shredding and damage can extend into Region II, with such damage decreasing with distance from the jet. However, if the "inner core" of fibrous insulation

is exposed to the break jet (such as would occur if the cover blanket was breached), blowdown transport of this material would be expected to extend for distances much greater than 7 L/D's. Jacketing of fibrous insulations does appear to provide some protection provided such jackets are not blown away by the initial blowdown jet forces, as demonstrated by HDR blowdown tests (Appendix F) where unjacketed fibrous insulations or insulations covered by a metal mesh are nearly totally destroyed within 3L/D's with some damaged and partially destroyed segments within 7 L/D's. But the same blankets enclosed in stainless steel jacket withstand the blast better (see Appendix F). Figure 3.26 illustrates examples of debris generation for RMI, fibrous jacketed and fibrous non-jacketed insulation materials.

Thus, debris generation in Region II can be very complex, and generic conclusions should not be drawn nor extrapolated to cover different materials or conditions. The specific materials and products used as insulation should be carefully reviewed in light of the data base available as results of tests (see Appendices C, E, and F). The assessment for the volume of debris generation, transport and screen blockage should be made on a plant-specific basis. If such a determination shows that estimated blockage head losses do not exceed the NPSH margin, a conservative safety assessment has been made.

The size of the third volume (Region III) was established using the Moody jet analysis as modified and discussed in NUREG/CR-2791. It begins at L/D = 7 and extends to an axial position in the jet where the jet thrust (as calculated by the Moody jet expansion model) would be equal to 0.5 psig when calculated for a flat axisymmetric target. The Moody-type jet expansion model was selected for establishing the outer boundary of Region III because it always results in a larger L/D value for the boundary than the two-phase jet analysis in NUREG/CR-2913, thus ensuring that the effects of debris modeling uncertainties are mitigated by a conservative outer boundary selection.

Break location(s) and insulation(s) targeted by the break jet are the key factors in estimating debris generation. This is illustrated in Figure 3.27 for a typical PWR where the influence of an expanding jet is shown. A break

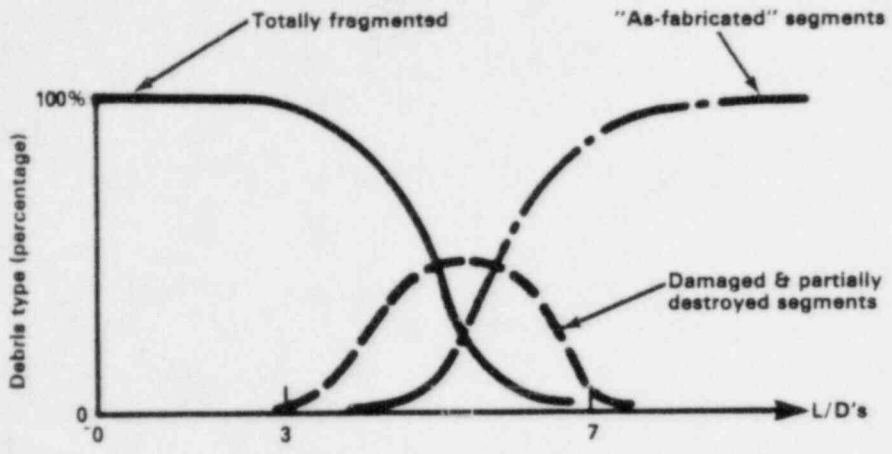

Example for non-jacketed fibrous insulation materials.

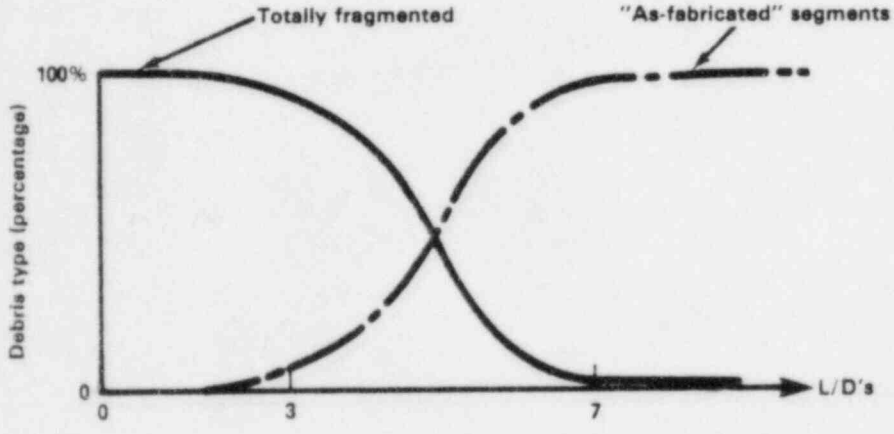

Example for jacketed fibrous insulation materials.

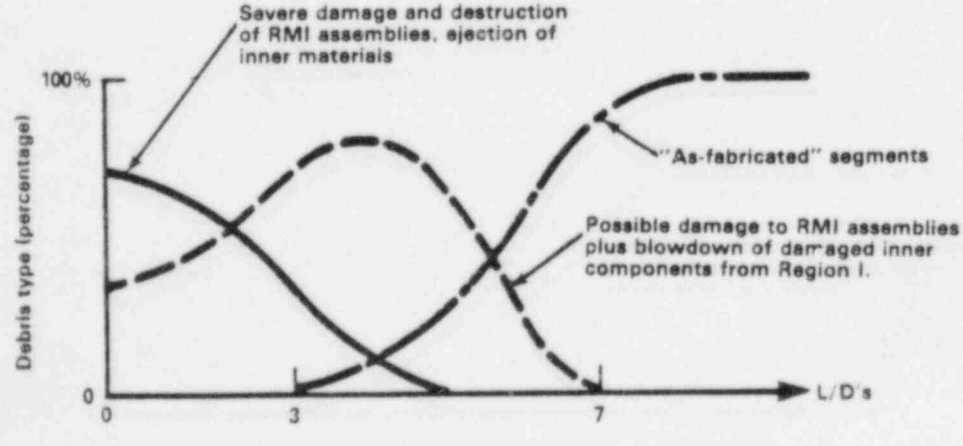

Example for reflective metallic insulation materials.

Figure 3.26 Possible variation of debris types and relative quantities in regions of the three-region jet model (see Figure 3.25)

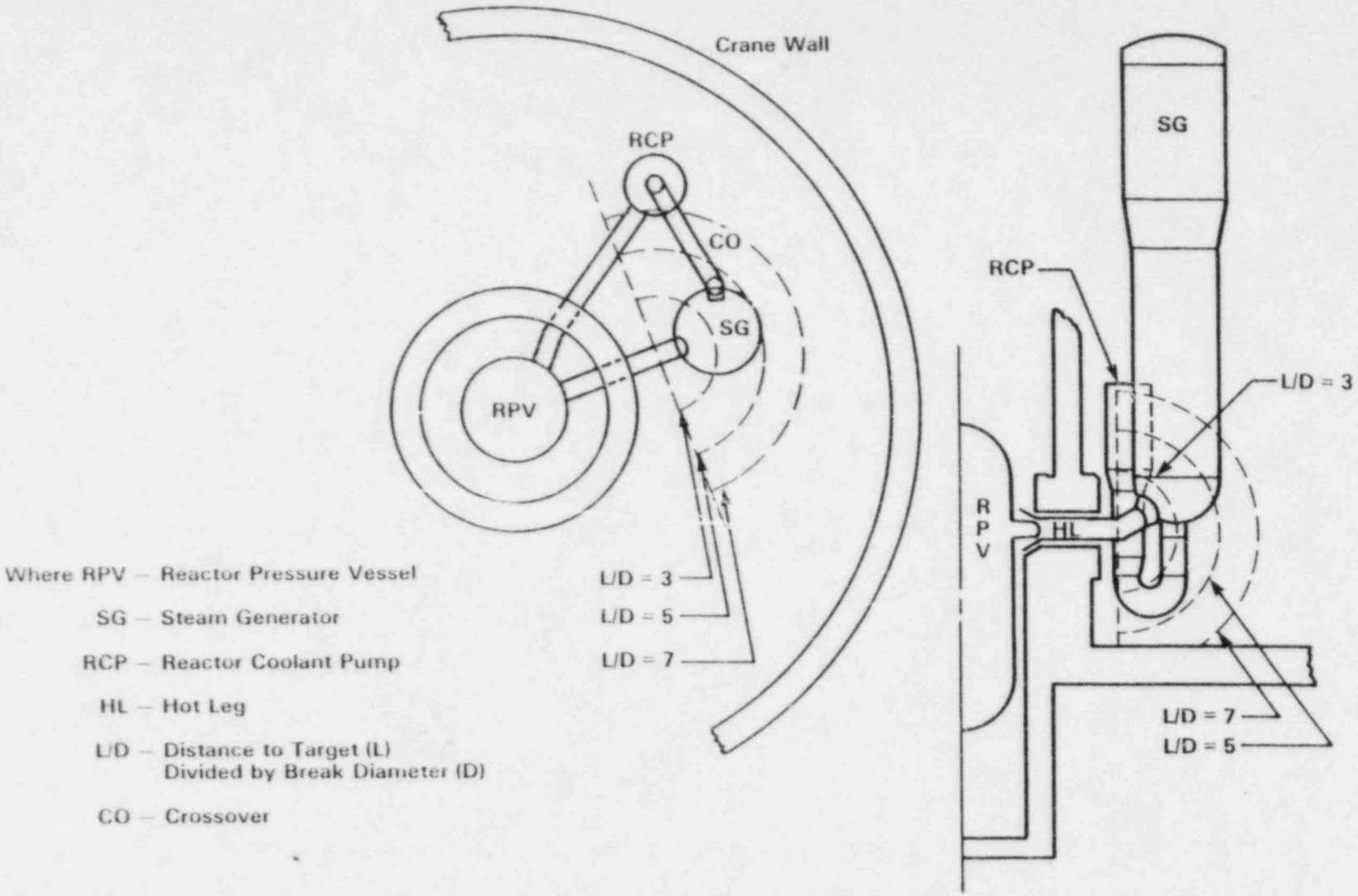

Figure 3.27 Zones of influence for debris generation

Table 3.5 Maximum LOCA-generated insulation debris summarized by break size

Pipe diameter (inches)	Total fibrous debris (ft^3)	Total all types (ft^3)
2	1	1
6	2	22
8	2	3
10	4	31
14	227	227
16	270	270
32	144	295
34	315	726
36	118	408

Notes:

(1) These values correspond to break locations in the primary system within the crane wall and represent the largest quantity of debris generated by a single break of a given pipe diameter.

(2) The insulation types and distribution within containment are those used in Salem-1. All insulation within 7 L/D of a break location is assumed to be destroyed and released as fragmented debris.

(3) For reference see NUREG/CR-3394.

in the primary coolant system piping will target large quantities of insulations located in the lower portions of the steam generators. Although break locations are identified in SRP Section 3.6.2, the reviewer (or analyst) should determine which breaks are most significant and estimate the extent (or volume) of insulation debris generation. Such a detailed break evaluation was carried out for a reference PWR (Salem Unit 1) and is reported in NUREG/CR-3394. Although this study was primarily directed at estimating the probability of sump blockage, the analyses revealed that breaks in large diameter piping ($\geq$ 10-inch diameter) were the dominant contributors to debris generation (see Table 3.5). This finding can be used by the analyst in scoping the extent of LOCA debris generation.

Table 3.6, which illustrates typical volumes of insulation employed (for two typical PWRs) on the primary coolant system and related components, provides an insight regarding volumes of insulations employed and their distribution on the PWR primary coolant system and components.

Although a generic conclusion cannot be drawn from these studies, because of plant variabilities, the results do indicate that PWR debris assessments should concentrate on the primary coolant system insulation within the crane wall region and for pipe breaks of pipe diameter $\geq$ 10 inches. Because such a detailed break study has not been done for BWRs, the reviewer should consider debris generation as occurring for breaks postulated in the BWR feedwater and recirculation piping and for postulated breaks in BWR main steamlines.

Table 3.6 Typical volumes of primary system insulation employed[1]

Component	Salem		Maine Yankee	
	Volume (ft^3)	Type of Insulation	Volume (ft^3)	Type of Insulation
Steam Generator	1284	reflective metallic/ fibrous	1144	calcium silicate/ fibrous
Hot Leg	160	reflective metallic	149	fibrous
Cold Leg	144	reflective metallic	156	fibrous
Cross-Over	60	reflective metallic	279	fibrous
Pressurizer	160	reflective metallic	302	calcium silicate/ fibrous
Press. Surge Line	129	reflective metallic	57	calcium silicate/ fibrous
RCP	570	reflective metallic	149	calcium silicate/ fibrous
Bypass	N/A	N/A	88	fibrous
TOTAL[2]	2507		2324	
SUBTOTAL[3] (excluding reflective metallic and calcium silicate)	1284(=4402 ft^2)		1527(=5234 ft^2)	

(1) This table is based on information provided by the operators in 1981. Plant changes since 1981 have made the data less accurate for these two specific reactors. However, as representative data for reactors in general, the table is still valid.

(2) This volume includes all of the insulation that could be hit by a water jet from a LOCA pipe break (in pipes $\geq$10" diameters). If the volume was restricted to only insulation within L/D = 7 of a break, it might be significantly smaller.

(3) In order to be conservative, Salem's steam generator is assumed to be covered entirely with fibrous insulation. 50% of the insulation of Maine Yankee's steam generator, pressurizer, and reactor coolant pump is assumed to be fibrous.

Table 3.7 Transport and blockage characteristics of reflective metallic insulation materials (see also NUREG/CR-3616)

Sample Description	Velocity to initiate motion (ft/sec)	Velocity to transport to screen (ft/sec)	Comments
Undamaged half jacket normal to flow			
concave side up	1.0	1.0	Either flipped on screen (see Figure 3.28) or got stuck partially flipped
concave side down	above 2.2		Never moved.
Outside Cover (0.037" thick diameter = 19"			
concave side up	0.7	0.8	Same blockage mode as undamaged half jackets.
concave side down	above 1.8		
Inside Cover (0.015" thick diameter = 13")			
concave side up	0.7	0.8	With both initial positions, covers flipped against the screen on arrival and got flattened against it by the flow force.
concave side down	1.1	1.6	
End Covers	above 2		Never moved.
Single sheet Inner Foil (0.0025" thick 36" x 25") uncrumpled with and without separating crimp	0.35	0.5	Moves in folding and tumbling mode. Flips vertically against screen as soon as it reaches it. (Figure 3.29) May be folded on screen, i.e., not cover full sheet area. Never covered screen higher than maximum sheet dimension, even for flow velocity of 2 ft/sec, and water depth of 60 inches.

Table 3.7 continued

Sample Description	Velocity to initiate motion (ft/sec)	Velocity to transport to screen (ft/sec)	Comments
Single sheet Inner Foil (0.0025" thick 36" x 25")	0.20	0.25	Moves in folding and tumbling mode. Flips against screen as soon as it reaches it. Gets flattened on screen by current.
Four sheets inner foil (0.0025" thick 36" x 25") two crumpled two uncrumpled	0.25	0.4 to 1.8	When numerous foil sheets are used they tend to jam up in piles that may need high velocity to unjam. Significant overlapping on screen.
Single cut-up sheet inner foil (0.0025" thick 24" x 21")			
uncrumpled	0.20	0.25	Folding and tumbling transport mode. Flip veritically on screen upon arrival, sometimes folded.
crumpled	0.20	0.25	Flip veritically on screen upon arrival, sometimes folded. (See Fig. 3.30)
Several cut-up sheets inner foil (0.0025" thick 8" x 8")			
uncrumpled	0.5	1.2	Pieces not folded by flow as larger ones. Sliding transport mode. One piece reached screen at 0.5 ft/sec - all flipped vertically on arrival to screen. (See Fig. 3.31)
crumpled	0.5	1.2	One piece reached screen at 0.9 ft/sec - all flipped vertically on arrival to screen.

Table 3.7 continued

Sample Description	Velocity to initiate motion (ft/sec)	Velocity to transport to screen (ft/sec)	Comments
Several cut-up sheets inner foil (0.0025" thick 3" x 3") uncrumpled	0.8	2.0	Pieces not folded by flow as larger ones. Sliding transport mode.
Several cut-up sheets inner foil (0.0025" thick 3" x 3") (continued) crumpled	0.6	1.0	Pieces flip vertically on screen unless a corner gets trapped under screen bottom, in which case the piece stays flat on bottom.

3.3.5 Transport and Screen Blockage Potential for Reflective Metallic Insulation Materials

A limited amount of testing has been conducted with reflective metallic insulation components to gain an insight into the transport and possible screen blockage configurations. The results are reported in NUREG/CR-3616. The thrust of these tests was to determine velocity levels that would transport various compononts, particularly thin foils that are used internally. As might be expected, intact units were not transported until flow velocities exceeded 1 ft/sec. On the other hand, very thin, stainless steel foil (0.0025 inch thick) materials were transported at low velocities (0.2 to 0.5 ft/sec) if such foils were in an uncrumpled and intact state. Table 3.7 summarizes experimental findings. In these tests, as the foil material became more rigid (increased thickness), the foil type debris was transported by sliding along the floor, rather than in a tumbling mode, and higher velocities were required to flip the material into a vertical orientation against the debris screen.

Of more significance are the screen blockage patterns observed during these transport tests. Intact shells (or halves) can flip against a debris screen if velocities exceed 1 ft/sec (see Figure 3.28). On the other hand, free thin foil sheets tend to crumple resulting in the blockage configurations shown in Figures 3.29 and 3.30. Multiple foil sheets can form a blockage pattern such as shown in Figure 3.31. Generally blockages occurred at the lower portion of the debris screen. Although enough sheet material to totally block the screen was introduced into the transport flume, total blockage did not occur (see Figure 3.29). The very thin foil material (when in large sheets) is transported with a tumbling, lifting-type motion; however, lack of structural rigidity results in transport deformations, as shown in Figure 3.29. Another significant finding was that none of the foil samples tested became water borne. This is particularly important in BWR considerations because the RHR suction intakes are generally 6 to 8 feet above the suppression pool floor.

Thus transport of metallic insulation debris at fairly low velocities cannot be discounted and therefore plant-specific assessments should be made for those plants employing this type of insulation. The transport and blockage findings discussed above can be used to estimate levels of potential blockage. Of equal importance is the severity of LOCA induced damage (see Section 3.3.4) and types of RMI debris generated (see Appendix E). The HDR tests discussed in Appendix E do not support a debris generation model consisting of free, undamaged interior foil materials being available for transport.

3.3.6 Buoyancy, Transport, and Screen Blockage Characteristics of Mass Type Insulations

The buoyancy and transport characteristics of fibrous insulation materials are important because long-term screen blockage is a function of whether, and how, such debris material would be transported. Information regarding transport of shredded mineral wool insulation is provided in the Finnish tests conducted in the late 1970s (see Imatran Voima Oy, "Model tests of the Loviisa Emergency Core Cooling System and Model Tests of Containment Sumps of the Emergency Core Cooling System"). These tests showed that shredded mineral wool would be transported at low velocities and build up uniformly on a debris screen, and thus could result in high head losses.

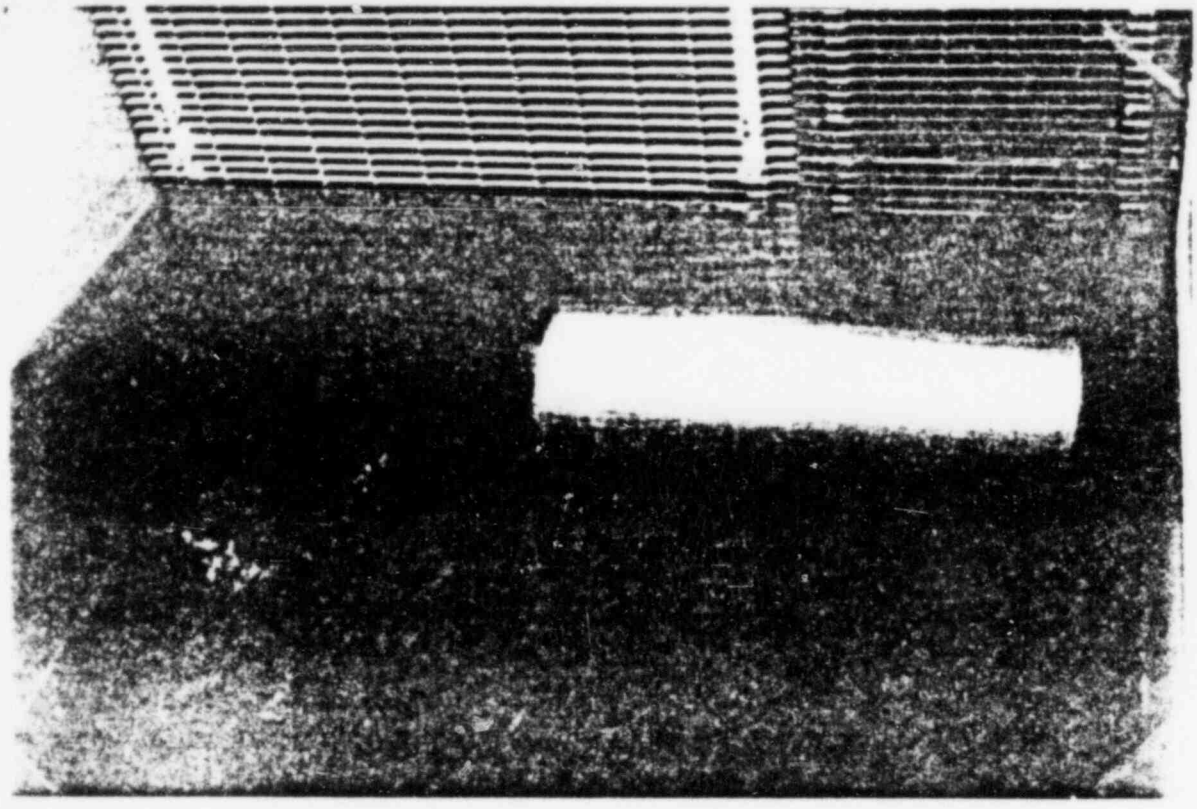

Figure 3.28 A half segment flipped onto screen

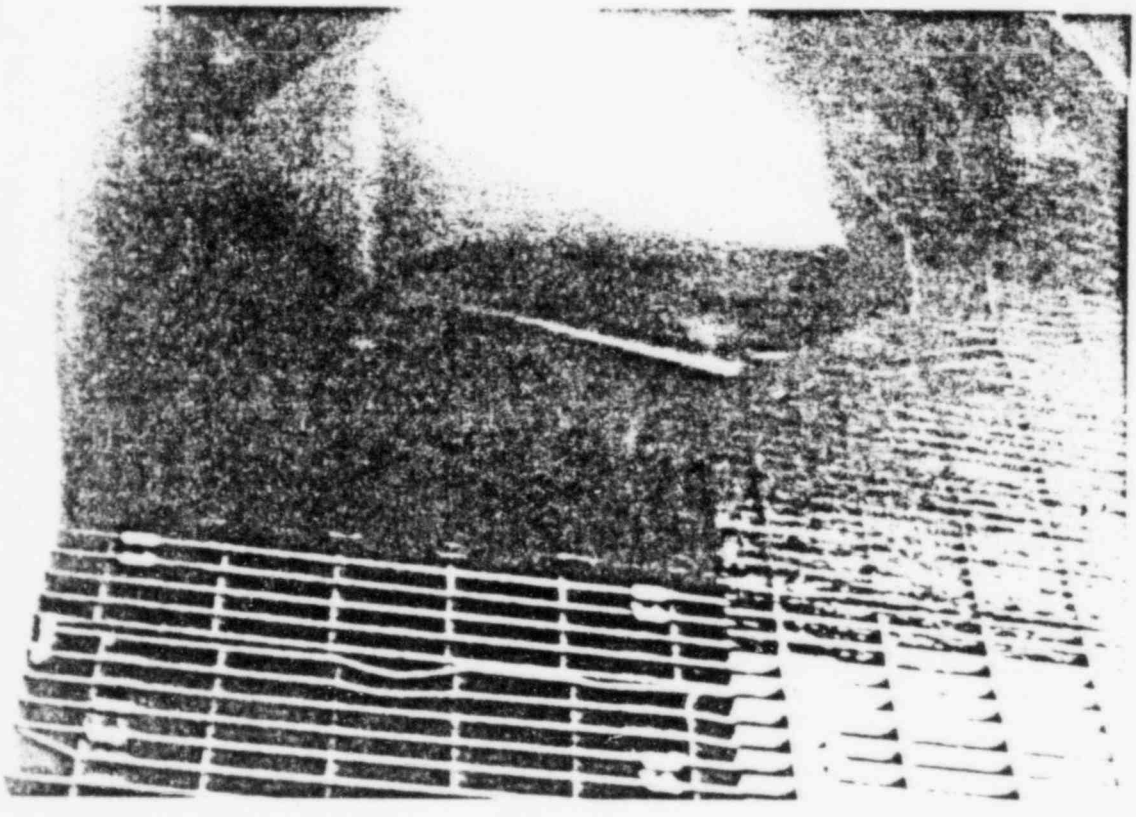

Figure 3.29 Uncrumpled foil sheet flipped vertically on screen (flow velocity = 0.5 ft/sec)

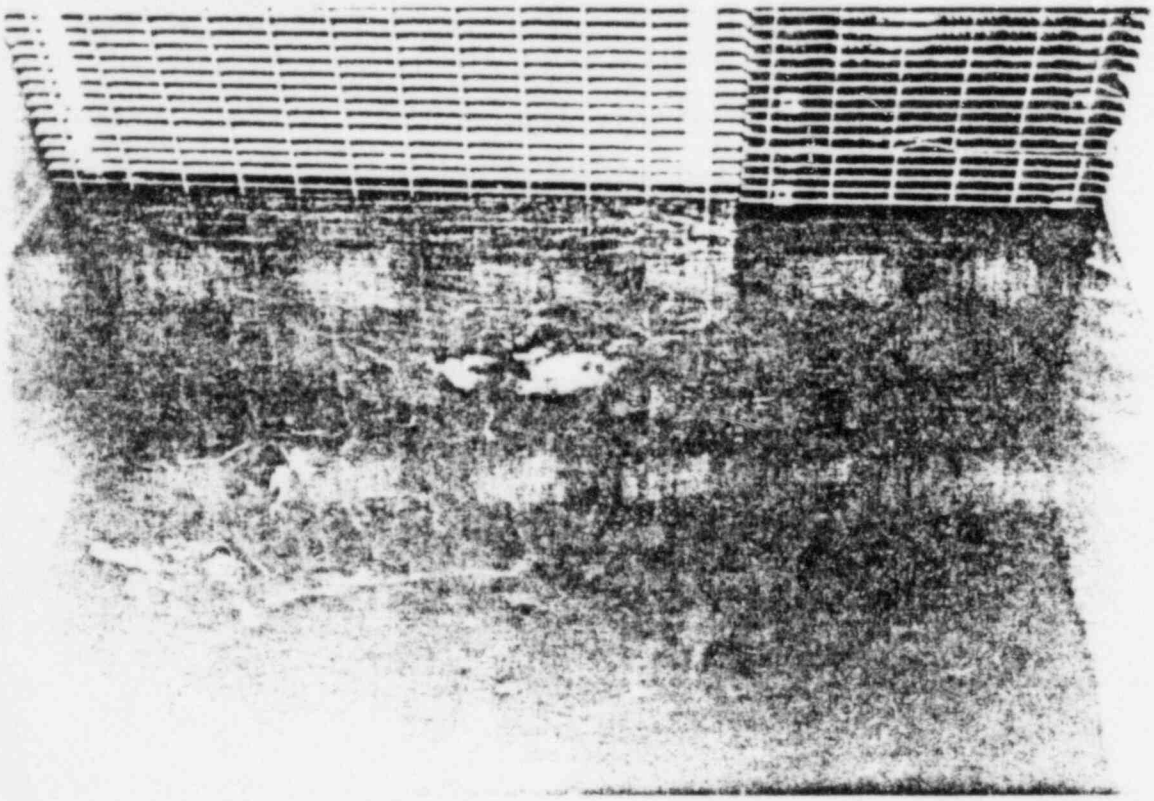

Figure D.30 Crumpled foil sheet against screen (flow velocity = 0.3 ft/sec

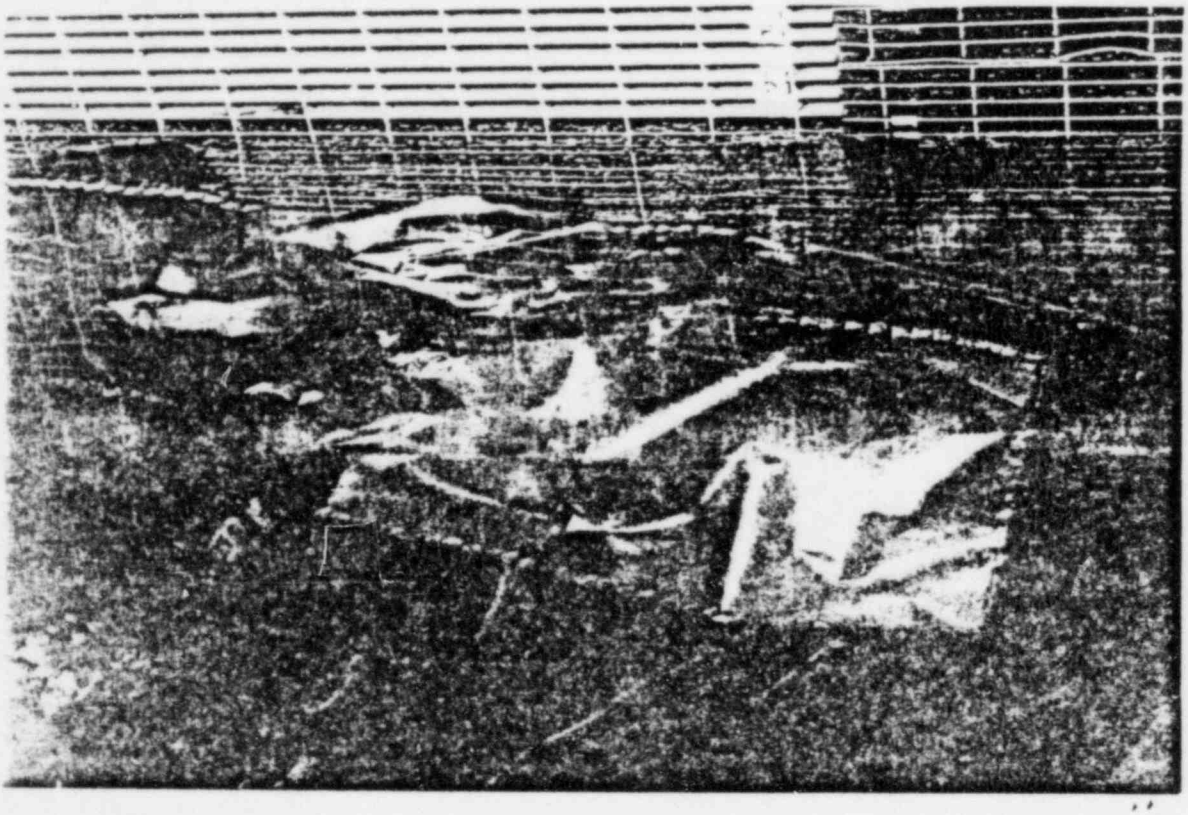

Figure 3.01 Several foil sheets on screen (flow velocity = 0.7 ft/sec)

Similar tests were conducted under NRC sponsorship at the Alden Research Laboratory and are reported in NUREG/CR-2982, Revision 1. The results of those tests are summarized below.

Buoyancy, transport, and head loss experiments were conducted with three types of as-fabricated insulation panels and with fragmented fibrous insulations. The three types of as-fabricated insulation panels were

Type 1: 4-inch mineral wool or refractory mineral fiber core mineral (6 lb density), covered with Uniroyal 6555 asbestos cloth coated with 1/2-mil Mylar.

Type 2: 4-inch Burlglass 1200, or 4 layers of 1-inch-thick Filomat D (fiberglass) core material, an inner covering of knitted stainless steel mesh, and an outer covering of Alpha Maritex silicone aluminum cloth, product 2619.

Type 3: Same insulation core materials as Type 2, but with an inner and outer covering of 18-ounce Alpha Maritex cloth, product 7371.

The fiberglass core material in Types 2 and 3 is a high density fiberglass ($\sim$10 lb/ft^3). Various types of fiberglass insulation are employed in nuclear plants, and, as evidenced by the data reported (Durgin and Noreika, September 1983) for the Owens Corning Fiberglass product NUKON™, they can exhibit different characteristics. Therefore, evaluations should be based on the actual material(s) utilized in a given plant.

The buoyancy tests revealed

(1) In general, the time needed for both mineral wool and fiberglass insulation to sink was less at higher water temperatures.

(2) Mineral wool (Type 1) does not readily absorb water and can remain afloat for several days.

(3) Fiberglass insulation (Types 2 and 3) readily absorbs water, particularly hot water, and sinks rapidly (from 20 seconds to 30 seconds in 120°F water).

(4) Undamaged fiberglass pillows of Type 3 (and possibly also of Type 2) can trap air inside their covers and remain afloat for several days.

(5) Based on the observed sinking rates, it may be concluded that mineral wool pillows and some undamaged fiberglass pillows (those that trap air inside their cover) will remain afloat after activation of the containment recirculation system (approximately 20 minutes after the beginning of LOCA). Those floating pillows will move at any water velocity and can be transported to the sump before activation of the recirculation system.

The transportation tests revealed

(1) Water velocities needed to initiate the motion of insulation are on the order of 0.2 ft/sec for individual shreds, 0.5 to 0.7 ft/sec for individual small pieces (up to 4 inches on the side), and 0.9 to 1.5 ft/sec for individual large pieces (up to 2 feet on the side).

(2) For whole sunken pillows to flip vertically onto the screen, flow velocities of 1.1 ft/sec for Type 1 (mineral wool) and 1.6 to 2.4 ft/sec for Types 2 and 3 (fiberglass) are required.

(3) Whole floating pillows require a water velocity in excess of 2.3 ft/sec to flip vertically against the screen.

(4) Insulation pillows broken up in finite size sunken fragments tend to congregate near the bottom of the screen if there is no turbulence generator, and, depending on the water depth, unblocked space can remain near the top of the screen. With turbulence generators (vertical posts 2 feet upstream of the screen), some insulation fragments are lifted from the bottom and collect higher on the screen.

(5) Once insulation shreds are in motion, they tend to become suspended in the water column and collect over the entire screen area.

The head loss tests revealed

(1) The measured head loss across a vertical screen in a flume as a result of blockage by insulation released upstream varies from 7 to 10 times the approach velocity head, $U^2/2g$, for whole sunken pillows; from 13 to 36 times the approach velocity head as that for opened or broken up pillows; and more than 240 times the approach velocity head for shredded pillows. These results are for an equivalent volume for 50% screen blockage with the undamaged pillows.

Opened pillows with separated, fragmented, or shredded insulation layers had enough area to block the entire screen. However, the screen was entirely (but not uniformly) covered only in the test with the shredded insulation. In the other tests, open space remained on the screen.

For these conditions, the maximum measured head loss of 240 times the approach velocity head (for shredded pillows) would result in screen head losses of 0.15 foot to 0.60 foot for approach velocities of 0.2 ft/sec to 0.4 ft/sec.

(2) Measured head losses through beds of accumulated fragments or shreds of mineral wool or fiberglass insulation varied nonlinearly with approach velocity and bed thickness.

For mineral wool fragments, the larger head losses were observed for the tests of larger fragments (3 x 2 to 4 x 1/8 inch). For an original insulation thickness of 1 inch, the maximum head loss was 0.4 foot at 0.2 ft/sec and 1.4 feet at 0.4 ft/sec.

For fiberglass insulation fragments and shreds, the larger head losses were observed for the shreds. For an original (as-fabricated) insulation thickness of 1 inch, the maximum head loss was 1.2 feet at 0.2 ft/sec and 6 feet at 0.4 ft/sec.

(3) The head loss through as-fabricated insulation material is higher, by a factor of up to 10, than that for accumulated fragments. For example, with water at 105° to 120°F and with an approach velocity of 0.2 ft/sec, the head loss through 2 inches of undisturbed mineral wool is about 3.5 feet, and the head loss through 1 inch of undisturbed fiberglass is about 20 feet. These head losses are for insulation samples sealed to the walls to prevent leakage. The head loss would be less if leakage occurred around the sample.

(4) In addition to the variables of insulation thickness and approach flow velocity, the actual head loss that may be expected across a sump screen depends critically on how the screen is blocked. If some unblocked screen area remains, or if water can flow between pieces of insulation,

the head loss would be small; if the entire screen area is uniformly covered with mats of undisturbed insulation or accumulated fibers, the head loss can be many feet.

(5) Best-fit expressions for the head loss through shredded fibrous insulation, were derived as follows:

for mineral wool (Type 1): $\Delta H = 123U^{1.51}t^{1.36}$

for fiberglass (Types 2 and 3): $\Delta H = 1653U^{1.84}t^{1.54}$

where

U is the screen approach velocity (ft/sec)
t is the original (as fabricated) insulation debris thickness (ft)
ΔH is the head loss (ft H_2O)

Table 3.8 summarizes these transport and head loss characteristics.

The strong dependence on material characteristics cannot be overemphasized. Owens Corning Fiberglass conducted similar tests with fiberglass utilized in NUKON™ (a low density fiberglass, 2 lb/ft^3). The transport characteristics were similar to those reported in NUREG/CR-2982, Revision 1, in that the transport of fragments occurred in the 0.2 to 0.3 ft/sec range. However, the screen blockage head loss correlation for fragments (experimentally derived) was

$$\Delta H = 68.3U^{1.79}t^{1.07}$$

This equation is significantly different from the two previous equations, and these results are reported in ARL Report No. 110-83/M489F (Brocard, D. N., September 1983). Thus, the reviewer should base evaluations on the particular type of insulation material(s) employed in a given plant application.

Table 3.8 Summary of transport and screen blockage characteristics of high density fiberglass

Condition	Pillow Type	V_i (ft/sec)	V_s (ft/sec)	V_v (ft/sec)	ΔH (ft)	$\frac{\Delta H}{\frac{V^2}{2g}}$ *	Comments
Floating whole pillows	1	N/A	N/A	> 2.3			Never flipped
	2	N/A	N/A	N/A			Sunk while against screen; flipped vertical
	3	N/A	N/A	N/A			Sunk while against screen; flipped vertical
Sunken whole pillows	1	1.1	1.1	1.1	0.13		Only one pillow tested
		0.9	1.1	1.1	0.07		Only one pillow tested folded in half on screen
	2	1.2	1.8	2.0	0.44	7.1	
		1.4	1.6	2.4			
	3	1.5	1.7	2.0	0.60	9.4	
		1.1	1.6	1.6	0.33	8.3	Pillows on screens overlap by 2 inches
Sunken pillows with covers removed but included and separated insulation layers	1	1.1	1.1	1.1	0.67	36.0	
		0.9	1.5		0.96	27.5	Not all pieces vertical
	2 or 3	1.1	1.6				
		0.9	1.2	1.2	0.71	32.0	
Sunken pillows with covers and insulation layers in 5 pieces (see Figure 2.6)	1	1.0	1.9		1.4	25.0	Not all pieces vertical
		1.1	2.0		1.6	26.0	
	2 or 3	1.0	1.4	1.6	0.54	14.0	Significant overlap of pieces on screen

*For details in the size and amount of the insulation materials utilized in these tests see NUREG/CR-2982, Revision 1.

Table 3.8 continued

Condition	Pillow Type	V_i (ft/sec)	V_s (ft/sec)	V_v (ft/sec)	ΔH (ft)	$\frac{\Delta H}{\frac{V^2}{2g}}$	Comments
Sunken pillows in 4" x 4" x 1" fragments. Covers not included.	1	0.4	1.4	1.6	1.35	34.0	Fragments collect on bottom 1 ft of screen
		0.6	1.3	1.4	2.45	80.0	With turbulence generators. Fragments collect on bottom 3 ft of screen
	2 or 3	1.0	> 1.6				Not all pieces reached the screen. Collected near screen bottom, Figure 4.6
		1.0	> 1.6		0.72	18.1	With turbulence generators. Only about half the pieces on screen. Some pieces at mid-height.
Sunken pillows in shreds. Covers not included.	2 or 3	0.4	> 1.3	N/A	3.7 for 1.0 fps	240	Not all pieces on screen. Screen entirely but not uniformly covered.
Sunken single fragments							Tests conducted in 1 ft wide flume with 7 inch water depth
4"x4"x1"	1	0.6					
	2 or 3	0.7					
4"x1"x1"	1	0.3					
	2 or 3	0.5					
Shreds	1	0.3					
	2 or 3	0.2					

NOTATIONS: V_i = velocity needed to initiate motion of at least one piece of insulation (not including covers when separated from pillows)

V_s = velocity needed to bring all material on screen

V_v = velocity needed to flip all pieces vertically on screen

ΔH = head loss at V_v (or V_s if V_v not given)

In summary, the following consideration should be made for determination of fibrous insulation blockage effects:

(1) Recirculation velocities and break jet loads must be evaluated to determine that they are high enough to transport debris to PWR sump screens or BWR suction strainers? (See Appendix D.) If not, blockage is not likely to occur.

(2) If the material can be shredded by the break jet, transport can occur at low velocities and a determination of screen head losses must be made, provided recirculation velocities are high enough to result in transport of the fragmented insulation debris.

3.3.7 Effects of Combined Blockage (Reflective Metallic and Mass Type Insulations)

Assessment of the effects of combined blockage, wherein both reflective metallic and mass type (fibrous) insulations are employed, is more difficult. As described above, both types of insulations can be transported at low velocities and block debris screens. Because metallic-type debris does not become water borne, blockages that can be ascribed to metal foils would occur at the lower (or bottom) portions of vertical screens. Fibrous insulation fragments can be transported at near-neutral buoyancy and do migrate to open flow passages. Therefore, a combined-effects model should be applied. Unfortunately, not enough experimental data are available to allow for development of a combined generic blockage model. Plant-specific evaluations should also consider the potential for this type of combined debris blockage.

3.4 Sump Hydraulic Performance

To investigate ECCS sump behavior under flow conditions that might occur during a LOCA, a test program was undertaken that covered a broad range of geometric and flow variables representative of PWR containment emergency sump designs. To avoid scaling uncertainties, a full-scale experimental facility

at the Alden Research Laboratory was used. Scaling effects resulting from the use of reduced-scale hydraulic models were subsequently evaluated. The three broad areas of interest for ECCS sump design investigated were

(1) fundamental behavior of the sump with reasonably uniform approach flow conditions

(2) changes in the fundamental behavior of the sump as a result of potential accident conditions (screen blockage, break and drain flow, obstructions, nonuniform approach flow, etc.) that could cause degraded performance in the recirculation system

(3) design and operational items of special concern in ECCS sumps

Information from initial testing was used to plan or redirect later tests; hence, the tests were not necessarily conducted in the order listed below.

The tests performed may be divided into six series as follows:

(1) Factorial Tests

A fractional factorial matrix of tests was used to study primary sump flow and geometric variables. The factorial matrix provided a wide range of parameter variations and a method for effectively testing a large number of variables and determining their interdependencies.

(2) Secondary Geometric Variable Sensitivity Tests

The effects on sump performance of secondary geometric variables and design parameters of special concern in ECCS sumps were tested by holding all sump variables constant except one, for which several values were tested.

(3) Severe Flow Perturbations Tests

The behavior of selected sump geometries subjected to approach flow perturbations was investigated. Major flow disturbances considered were screen blockage (up to 75%), nonuniform approach velocity distribution, break-flow and drain-flow impingement, pump startup transients, and obstructions, as illustrated in Figures 3.32 and 3.33.

(4) Vortex Suppression Tests

The effectiveness of several types of vortex suppressors and inlet configurations was evaluated.

(5) Scale Tests

Scaling effects in geometrically scaled models using Froude number similitude and pipe velocity similitude were tested.

(6) BWR Suction Pipe Inlet Tests

The hydraulic performance of BWR suction pipe geometries typical of Mark I, II, and III RHR suction inlet designs was evaluated.

Data generated during the sump performance studies were analyzed using two approaches as follows:

(1) Functional Correlations of Dependent Variables

Correlations using response-surface regression analysis of nondimensional empirical data fitting were developed. Because of the extremely small values of the dependent variables and the complex time-varying nature of the three-dimensional flows in the sump, the use of functional correlations showed no

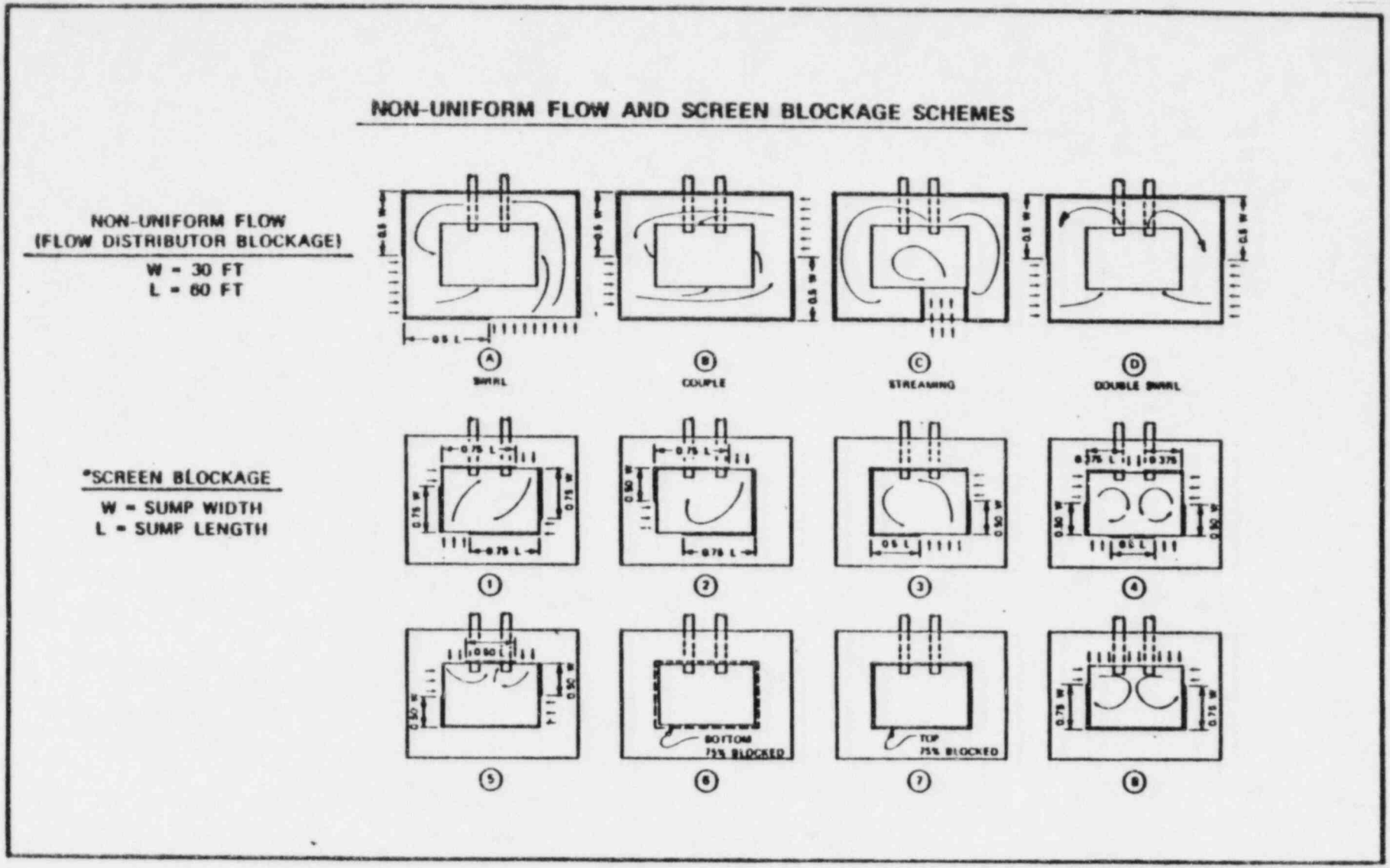

Figure 3.32 Approach flow perturbations and screen blockage schemes

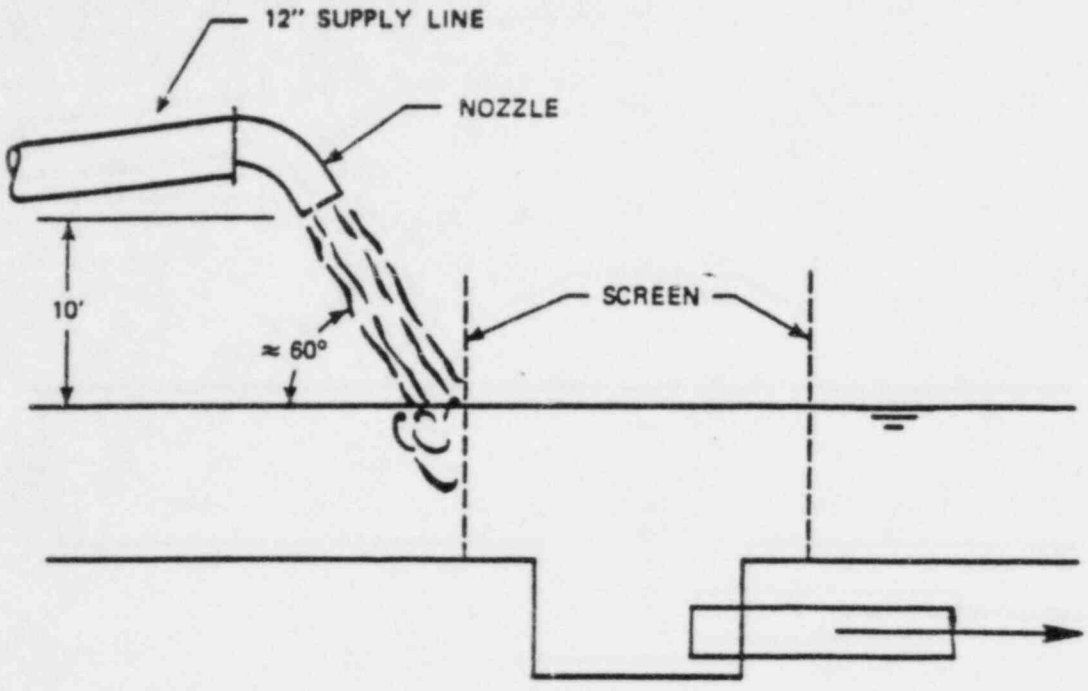

a. Break Flow Jet Impingement

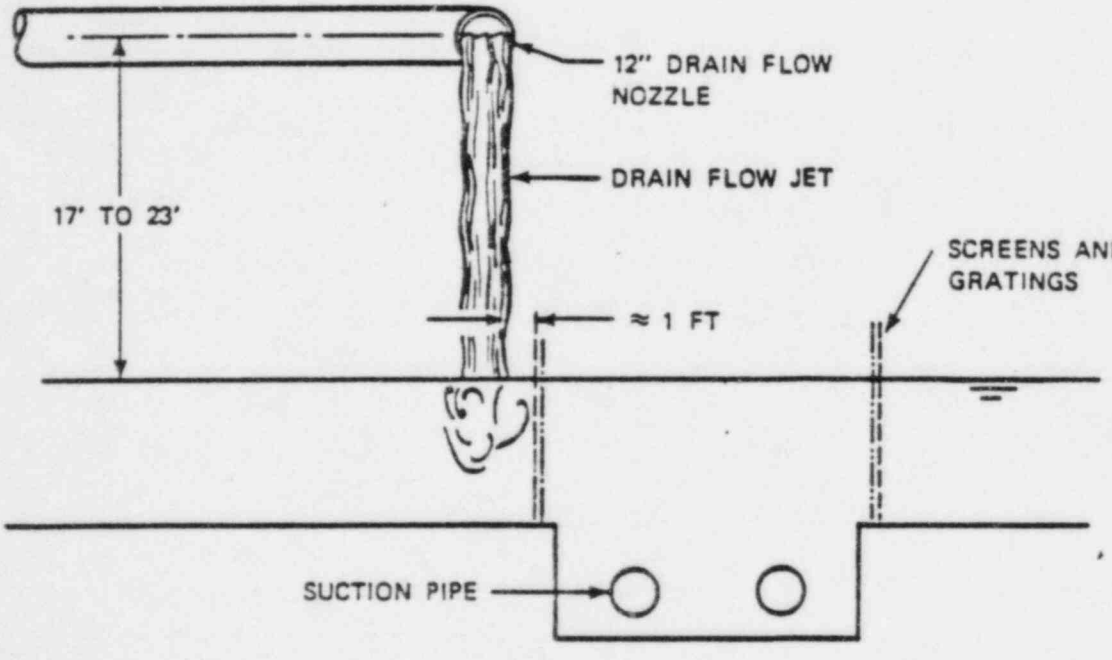

b. Drain Flow Jet Impingement

Figure 3.33 Break and drain flow impingement

consistent, or generally applicable, correlation between the dependent and independent variables. Thus, the hydraulic performance of a particular sump under given flow and submergence conditions could not be reliably predicted using this approach.

(2) Bounding Envelope Analysis

The broad data base that resulted from the sump studies made possible the use of envelope analysis for reliably predicting the expected upper bound for the hydraulic performance (void fraction, vortex type, swirl angle, and inlet loss coefficient) of any given sump whose flow and geometric features fall approximately within the ranges tested. The data boundary curves generated indicate the maximum response of the data for each of the hydraulic performance parameters as a function of the sump flow variables, particularly when plotted as a function of Froude number. Thus, the ability to describe the performance of PWR ECCS sumps, with or without flow perturbations, using bounding envelope curves was the most significant result of the ARL test program. The application of an envelope analysis to test data resulting from all the sump performance tests is discussed in Section 3.4.1. Findings of the sump performance tests are described in greater detail in subsequent sections.

3.4.1 Envelope Analysis

The sump performance test program generated a data base covering a broad range of ECCS geometric variables, flow conditions (including potential accident conditions), and design operations (horizontal or vertical inlets, single or dual pipes, etc.). An envelope analysis applied to this broad range of data resulted in boundary curves for vortex activity, swirl, and sump head loss as a function of key sump flow variables (Froude number, velocity, etc.).

Figures 3.34, 3.35, and 3.36 show typical envelope analysis curves for air ingestion, surface vortex activity, and swirl in PWR sumps with dual horizontal pump suction intakes. Figures 3.37, 3.38, and 3.39 show typical envelope analysis curves for air ingestion, surface vortex activity, and swirl in PWR sumps with dual vertical intakes.

3.4.2 General PWR Sump Performance (All Tests)

The following items were studied while testing for the sump performance.

(1) Free Surface Vortices

Vortex size and type (see Figure 3.40) resulting from a given geometric and flow condition are difficult to predict and are not reliable indicators of sump performance. Performance parameters (void fraction, pressure loss coefficient, and swirl angle) are not well correlated with observed vortex formations.

(2) Air Ingestion

Measured levels of air ingestion, even with air core vortices, were generally less than 2%. Maximum values of air ingestion with deliberately induced swirl and blockage conditions were less than 7% for horizontal inlets and 12% for vertical inlets. These high levels always occurred for high flow and low submergence (Froude number (Fr) generally greater than 1.0). For submergences of 8 feet or more, none of the configurations tested indicated air-drawing vortices ingesting more than 1% over the entire flow range, even with severe flow perturbations.

(3) Swirl (measured at a distance 14 diameters from suction inlet)

Flow swirl within the intake pipes, with or without flow perturbations, was very low. In almost all cases, the swirl angle was less than 4 degrees, an

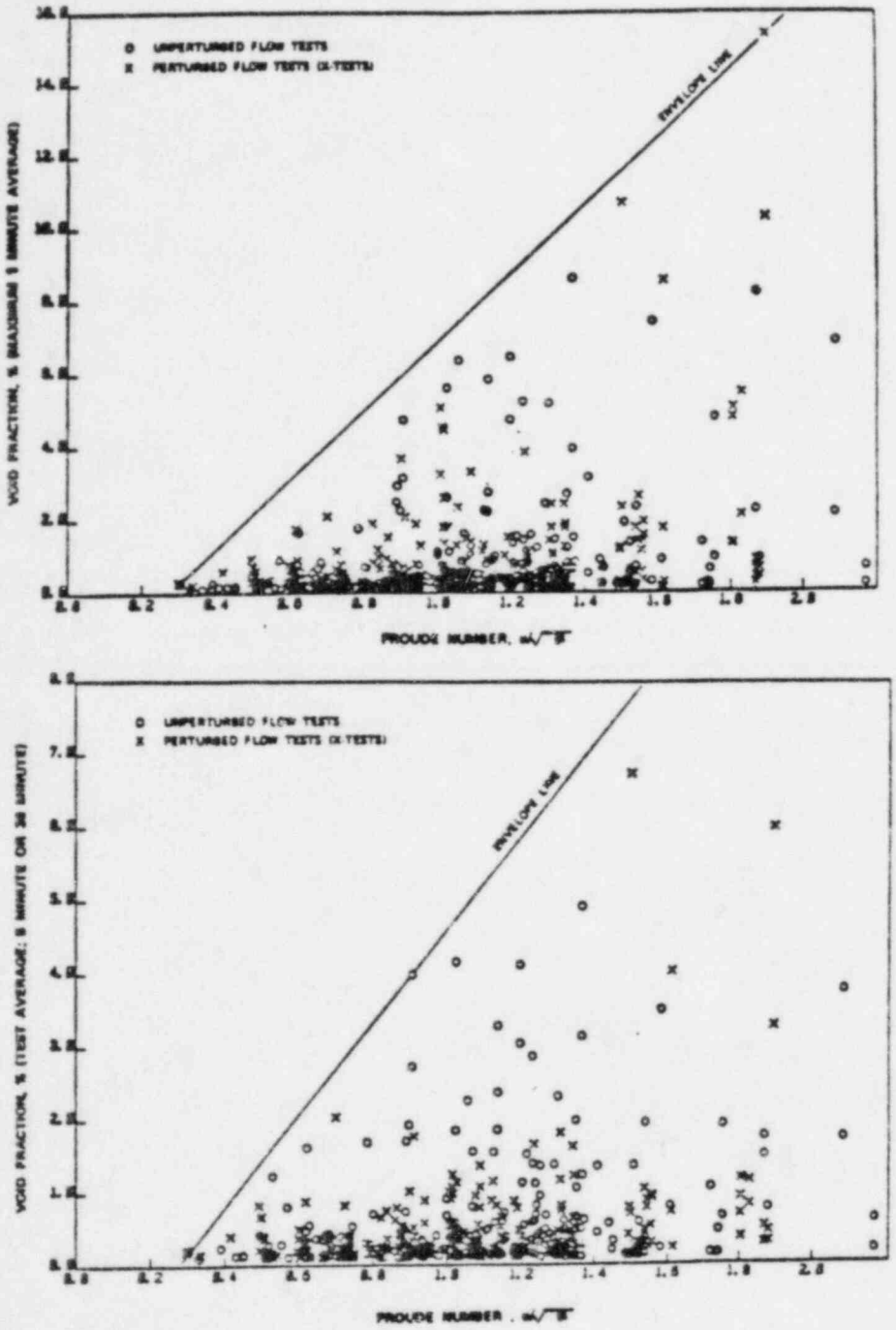

Figure 3.34 Void fraction (% by volume) as a function of Froude number; horizontal intake configuration; only data points indicating nonzero void fraction are plotted

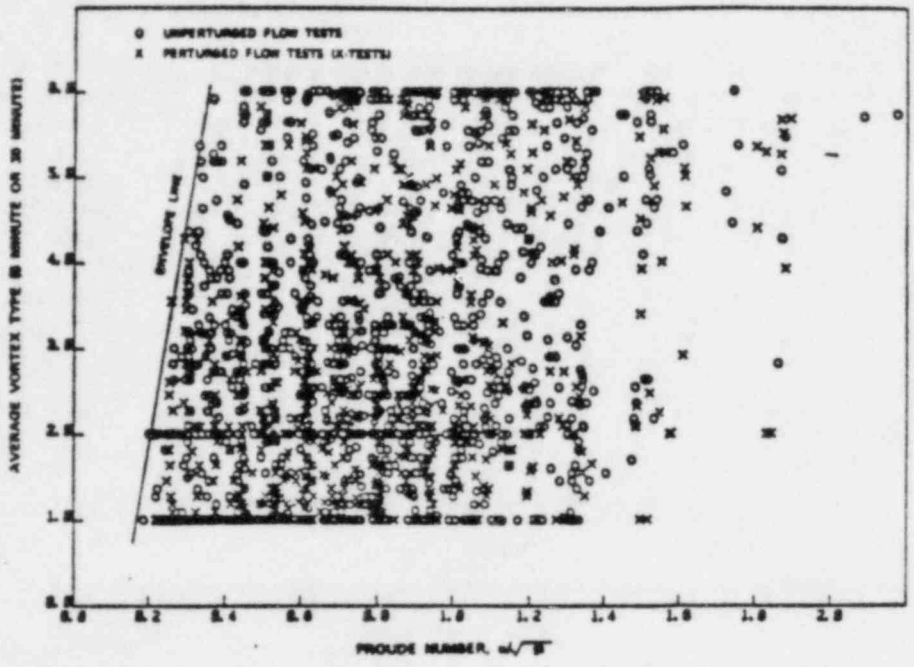

Figure 3.35 Surface vortex type as a function of Froude number; horizontal intake configuration (Type 1: surface swirl only, Type 6: full air core to intake)

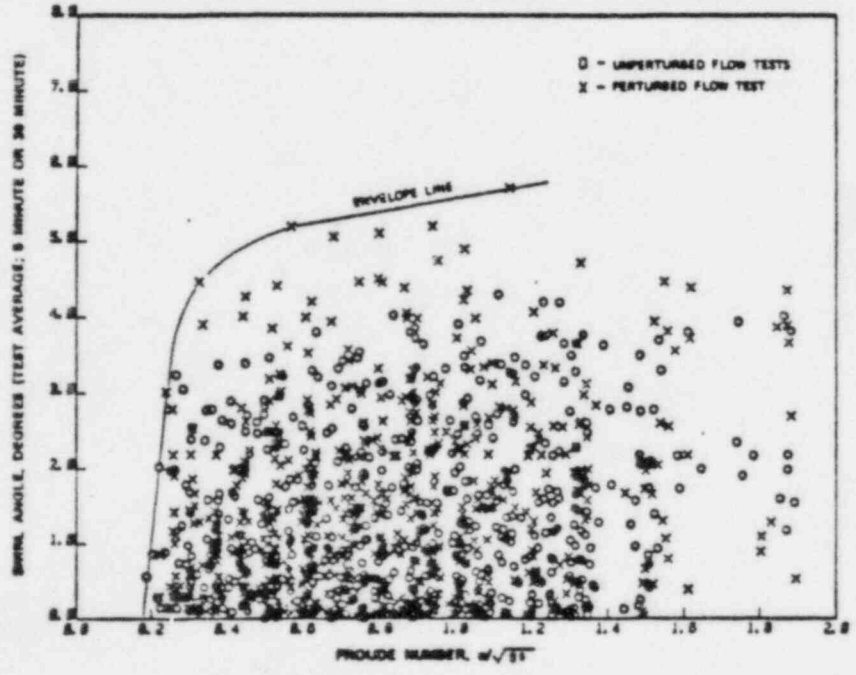

Figure 3.36 Swirl as a function of Froude number; horizontal intake configuration

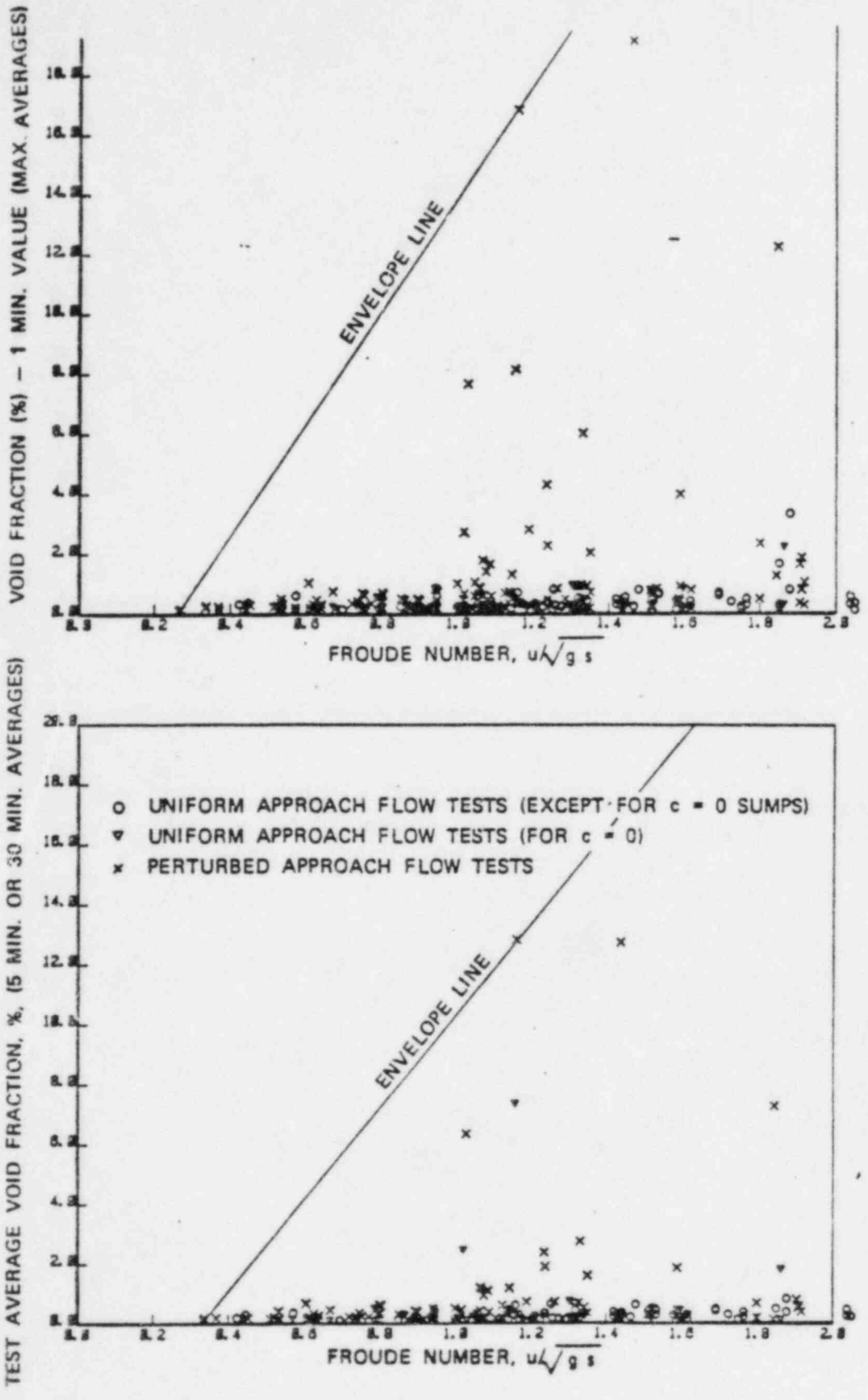

Figure 3.37 Void fraction data for various Froude numbers; vertical intake configuration; only data for nonzero void fraction plotted

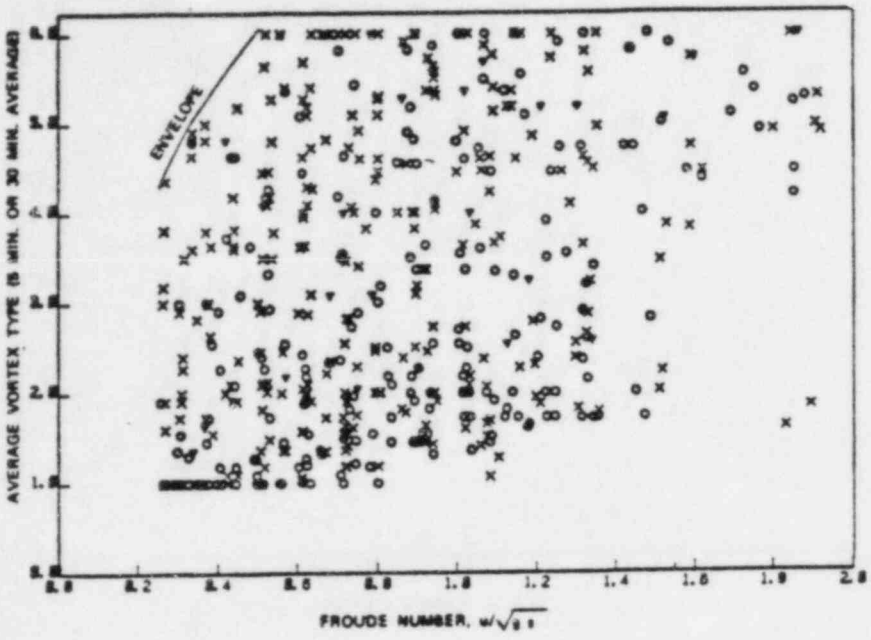

Figure 3.38 Surface vortex type as a function of Froude number; vertical intake configuration (Type 1: surface swirl only; Type 6: full air core to intake)

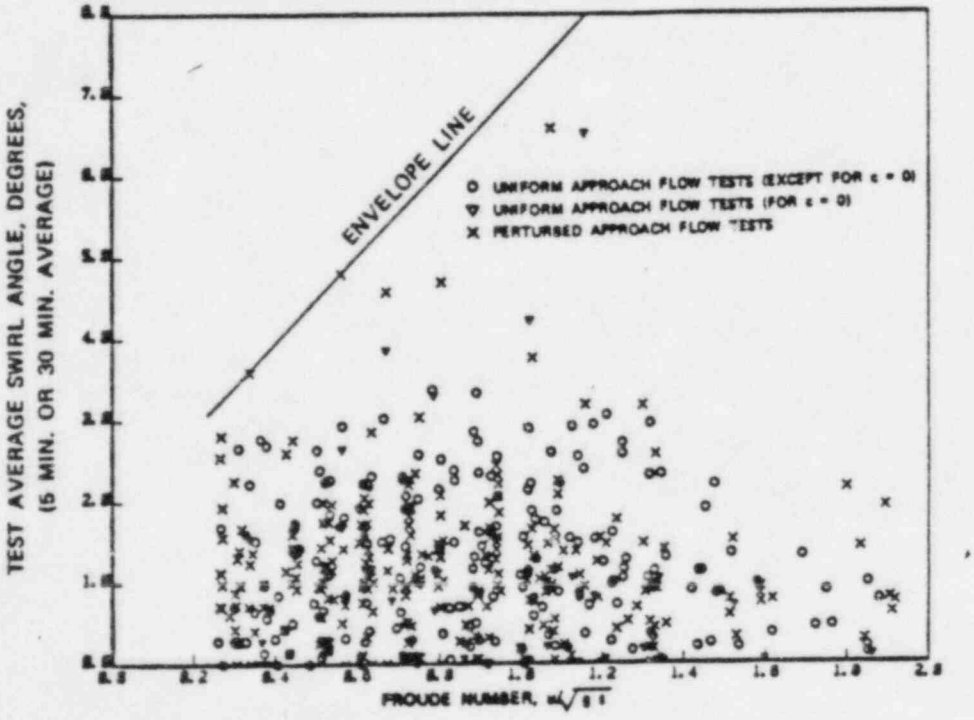

Figure 3.39 Swirl as a function of Froude number; vertical intake configuration

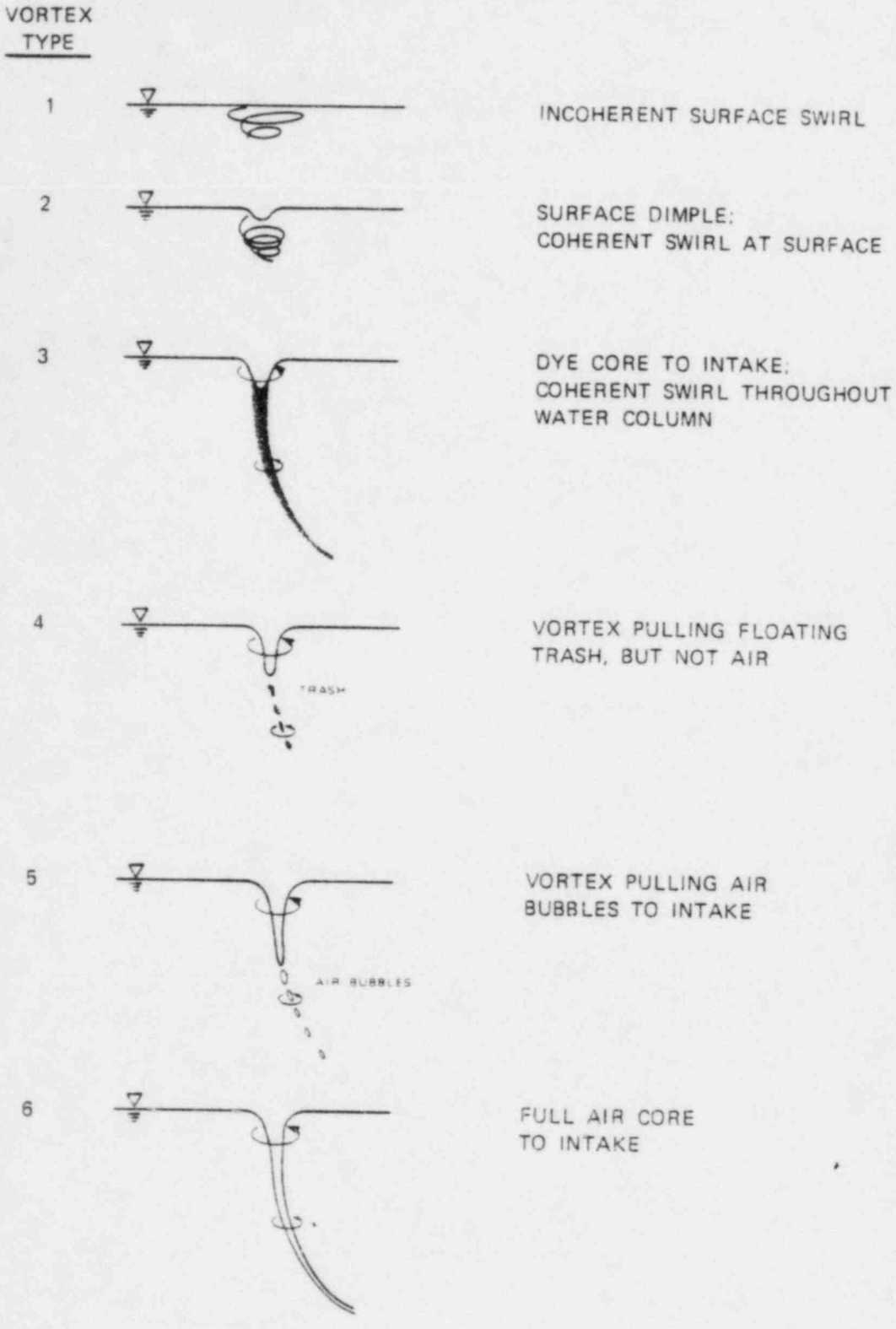

Figure 3.40 Vortex type classification

acceptable value for RHR and CSS pumps. The maximum value for severely perturbed flows was about 8 degrees and occurred during the screen blockage test series.

(4) Sump Head Losses

The suction pipe intake pressure loss coefficient for most of the tests, with and without flow perturbations, was in the range of 0.8 ± 0.2 and agreed with recommended values in standard hydraulic handbooks.

3.4.3 PWR Sump Performance During Simulated Accident Conditions (Perturbed Flow)

The following items were considered for sump performance under perturbed flow conditions.

(1) Screen Blockage

Screen blockages up to 75% of the sump screen resulted in air ingestion levels similar to those noted under 3.4.2(2) above.

(2) Nonuniform Approach Flow Distributions

Nonuniform approach flows, particularly streaming flow, generally increased surface vortexing and the associated void fraction.

(3) Drain and Break Flow

Drain and break flow effects were generally found not to cause any additional air ingestion. They reduced vortexing severities by surface wave action.

(4) Obstructions

Obstructions 2 feet or less in cross-section had no influence on vortexing, air withdrawals, swirl, or inlet losses.

(5) Transients

Under transient startup conditions, momentary vortices were strong, but no air-core vortices giving withdrawals exceeding 5% void fraction (1- minute average) were observed.

3.4.4 Geometric and Design Effects (Unperturbed Flow Tests)

In general, no consistent trends applicable for the entire range of tests were observed in the data between the hydraulic response of the sump (air withdrawal, swirl, etc.) and secondary geometric parameters. However, for some ranges of flow and submergence, the following observations are applicable:

(1) Greater depth from containment floor to the pipe centerline reduces surface vortexing and swirl.

(2) Lower approach flow depths with higher approach velocities may cause increased turbulence levels serving to dissipate surface vortexing.

(3) Suction pipe inlets located with less distance to the adjacent sump wall and greater pipe spacing reduces vortexing and swirl.

(4) There is no advantage in extending the suction pipe beyond 1 pipe diameter from the wall.

3.4.5 Design or Operational Items of Special Concern in PWR ECCS Sumps

(1) Pump Intake Orientation

Comparison of vertical intake data to corresponding horizontal intake data showed minor differences in hydraulic performance for sumps of the same geometry and flow conditions. Average vortex types agreed within ± 1 (types range from 1, incoherent surface swirl, to 6, full air core to pump intake);

air withdrawals were somewhat higher for vertical intake sumps but usually within 1% (30-minute averages) to 4% (1- and 5-minute averages); swirl angles differed only within ± 1 degree. Both vertical and horizontal intake sumps performed better under perturbed flow when the pipe inlets were closer to an adjacent wall rather than at the center of the sump.

(2) Single Intake Sumps

Two sump configurations (4 x 4 feet and 7 x 5 feet in plan, both 4.5 feet deep with 12-inch-diameter intakes) were tested under unperturbed (uniform) and perturbed approach flows with screen blockages up to 75% of the screen area. For both the configurations, unperturbed flow tests indicated air withdrawals were always less than 1% by volume for the entire range of tested flows and submergences (Fr = 0.3 to 1.6.). Even with perturbed flows, zero or near zero air withdrawals were measured in both sumps for Froude numbers less than 0.8, suggesting insignificant vortexing problems. For Froude numbers above 0.8, a few tests indicated significantly high air withdrawal (up to 17.4% air by volume; 1 minute average) especially for the smaller sized sump. Measured swirl values in the pipes were insignificant for both the tested sumps, in the range of 2 to 3 degrees, even with flow perturbations. The inlet loss coefficients for both sump configurations were in the expected ranges for such protruding inlets, 0.8 ± 0.2.

(3) Dual-Intake Sumps with Solid Partition Walls

Four dual-intake sump configurations (one 20 x 10-foot sump with 24-inch diameter intakes and three 8 x 10-foot sumps with 24-inch, 12-inch, and 6-inch intakes, respectively) were tested with solid partition walls in the sumps between the pipe inlets and with only one intake operational. None of the tests indicated any significant increases in vortexing, air withdrawal, swirl, or inlet losses compared to dual pipe operation without partition walls. Thus, a partition wall in a sump should not cause any additional problems when only one pipe is operating.

(4) Bellmouths at Pipe Entrance

Limited tests on a sump configuration were conducted with and without a bellmouth attachment to the 12-inch intakes. Adding bellmouths at the pipe entrances did not result in any significant changes in the vortex types, air withdrawals, and pipe swirl compared to those that otherwise existed under the same hydraulic conditions. An expected reduction of up to about 40% in inlet losses was noticed with the addition of a bellmouth.

(5) Cover Plate

A solid top cover plate over the sump was effective in suppressing vortices as long as the cover plate was submerged and proper venting of air from underneath was provided. No air drawing vortices were observed for the submerged cover plate tests, and no significant changes in swirl or loss coefficients occurred.

(6) Vortex Suppressors

Cage-shaped vortex suppressors made of floor grating in the form of cubes 3 and 4 feet on a side and single or multiple layers of horizontal floor gratings over the entire sump area were found to be effective in suppressing vortices and reducing air ingestion to zero. These suppressors were tested in sump configurations using 12-inch-diameter intake pipes, and with the water levels ranging from 0.5 foot to 6.5 feet above the top of the suppressors. Adverse screen blockages were imposed on these sump configurations, which produced considerable air ingestion and strong vortexing without the suppressors; thus, the effectiveness of the suppressors was tested when hydraulic conditions were least desirable. The suppressors also reduced pipe swirl and did not cause any significant increase in inlet losses. Both the cage-shaped grating suppressors and the horizontal floor grates were made of standard 1.5-inch floor grates.

Tests on a cage-shaped suppressor less than 3 feet on a side indicated the existence of air-core vortices for certain ranges of flow and submergences, even though air withdrawals were found to be reduced to insignificant levels.

Therefore, either properly sized cage shaped suppressors made of floor grating, or floor grating over the entire sump area, may be used to reduce air-ingestion to zero in cases where the sump design and/or approach flow creates otherwise undesirable vortexing and air-ingestion.

(7) Scale Model Tests

To evaluate the use of reduced scale hydraulic models to determine the performance of containment emergency sumps and to investigate, in particular, possible scale effects in modeling the hydraulic phenomenon of concern, a test program involving two reduced-scale models (1:2 and 1:4) of a full-size sump (1:1) was undertaken (NUREG/CR-2760).

The test results show that the hydraulic models predicted the hydraulic performance of the full-sized sump; namely, vortexing, air-ingestion from free surface vortices, pipe flow swirl, and the inlet loss coefficient. No scale effects on vortexing or air-withdrawals were apparent within the tested range for both models. However, an accurate prediction of pipe flow swirl and inlet loss coefficient was found to require that the approach flow Reynolds number and the pipe Reynolds number be above certain limits.

Based on these results, it is concluded that properly designed and operated reduced scale hydraulic models of geometric scales 1:4 or larger could be used to properly evaluate the hydraulic performance of a sump design. Evaluations of sump hydraulic model studies conducted in the past can be derived from this series of tests.

(8) Pump Overspeed Tests

Two 8 x 10 x 4.5 ft sumps (one with horizontal suction intakes and one with vertical suction intakes) were tested at higher flow rates to simulate pump overspeed or run out (to Froude number = 1.6) conditions. No strong air-core vortices were observed with air-withdrawals greater than 1 percent (1 minute or 30 minute averages).

Maximum recorded pipe swirl angle was 0.9° (at 14.5 pipe diameters from entrance); inlet loss coefficients averaged 0.8 (NUREG/CR-2761).

(9) High Temperature Tests

A series of tests were performed on horizontal suction intake, and the conclusion was that changing water temperatures over the range from 40°F to 165°F had no significant effect on sump hydraulic performance parameters (see NUREG/CR-2758, Section 4.6.).

3.4.6 BWR Suction Pipe Intakes

Because BWR plants do not have a sump or a floor depression with surrounding screens and gratings, typical residual heat removal system suction pipe inlet configurations applicable to Mark I, Mark II, and Mark III containment designs were investigated in full-scale flow experiments. Figure 3.41 shows the two inlet pipe and strainer configurations of the three designs under consideration.

Key parameters of interest were air-ingestion levels, vortex formation, suction pipe swirl, and the RHR inlet pressure loss coefficient. The tests were conducted with both perturbed and unperturbed approach flows to the inlets, as indicated in Figure 3.42. Flows ranged from 2000 to 12000 gpm per pipe, while submergences varied from 2 to 5 feet. The resulting Froude numbers ranged from about 0.2 to 1.1.

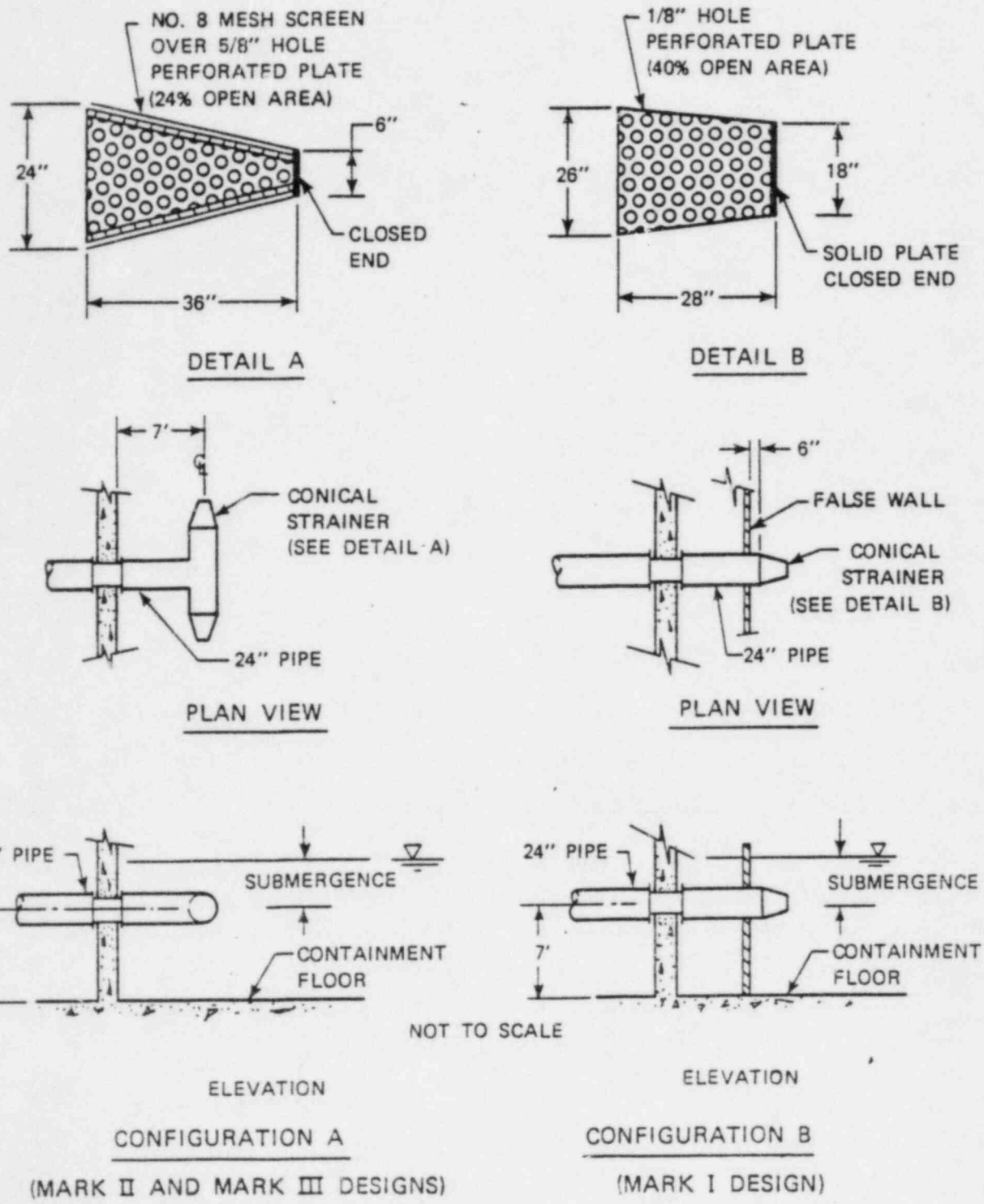

Figure 3.41 BWR pipe inlet configurations as built in full-size facility

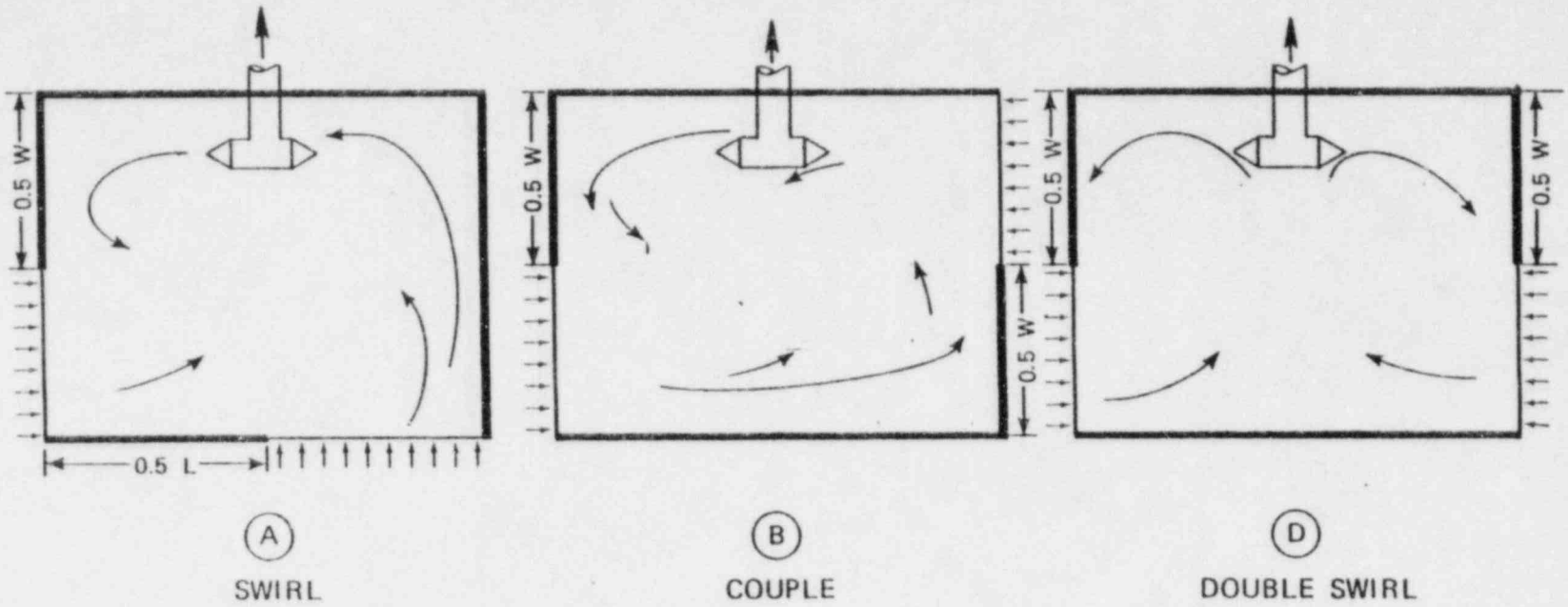

NON-UNIFORM FLOW
(FLOW DISTRIBUTOR BLOCKAGE)

W=30 FEET
L=60 FEET

Figure 3.42 Perturbed flow schemes; schemes A, B, and D used for BWR inlet tests

Figures 3.43 and 3.44 show the test-average (30-minute) and 1-minute void fractions for the two inlet configurations (A and B) and the various flow schemes examined. Essentially zero air withdrawal was measured for both configurations at Froude numbers less than or equal to 0.6 under all tested approach flows. For the double inlet or tee inlet design (Configuration A), maximum air withdrawal was less than 0.5% at all Froude numbers examined. For the single inlet design (Configuration B), air core vortices drawing up to 4% air by volume were observed to form at a Froude number above 0.6 under perturbed approach flows.

No air-core vortices were observed for either inlet configuration over the entire range of tested flows at submergences equal to or above 3.5 feet (Froude numbers less than 0.6). Swirl angle in the Configuration B inlet pipe ranged from 0 to 3 degrees, while the Configuration A pipe swirl angle fell between 2 and 7 degrees for the Froude numbers tested.

The measured inlet loss coefficients expressed in terms of suction pipe velocity head averaged to about 1.7 and 1.0 for Configurations A and B respectively. The loss coefficients reflect entrance, strainer, and tee losses (if applicable).

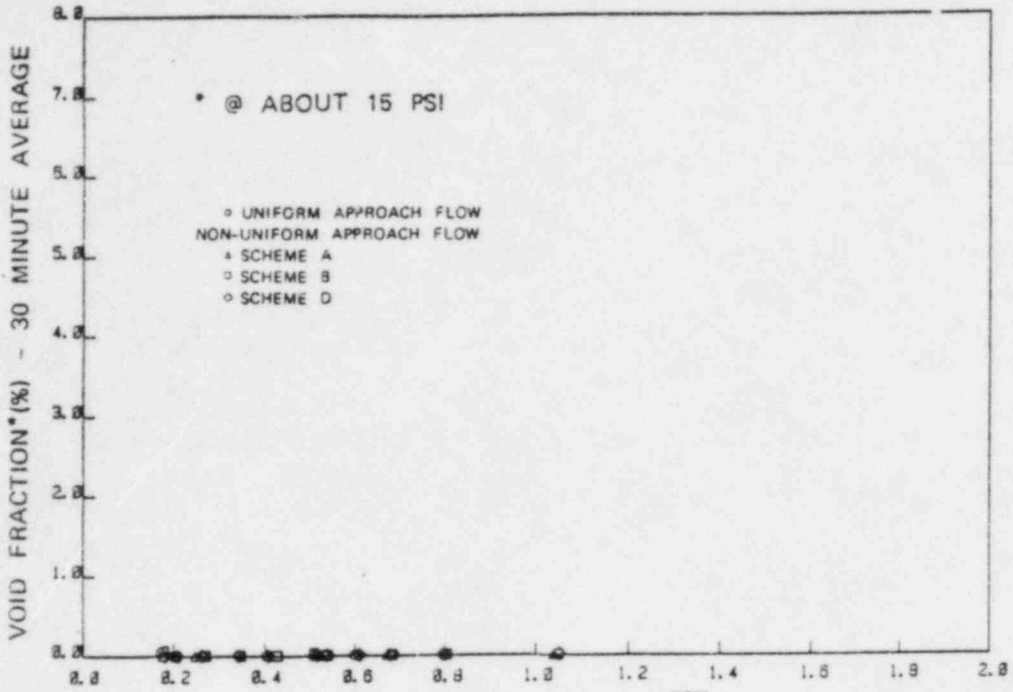

a. CONFIGURATION A

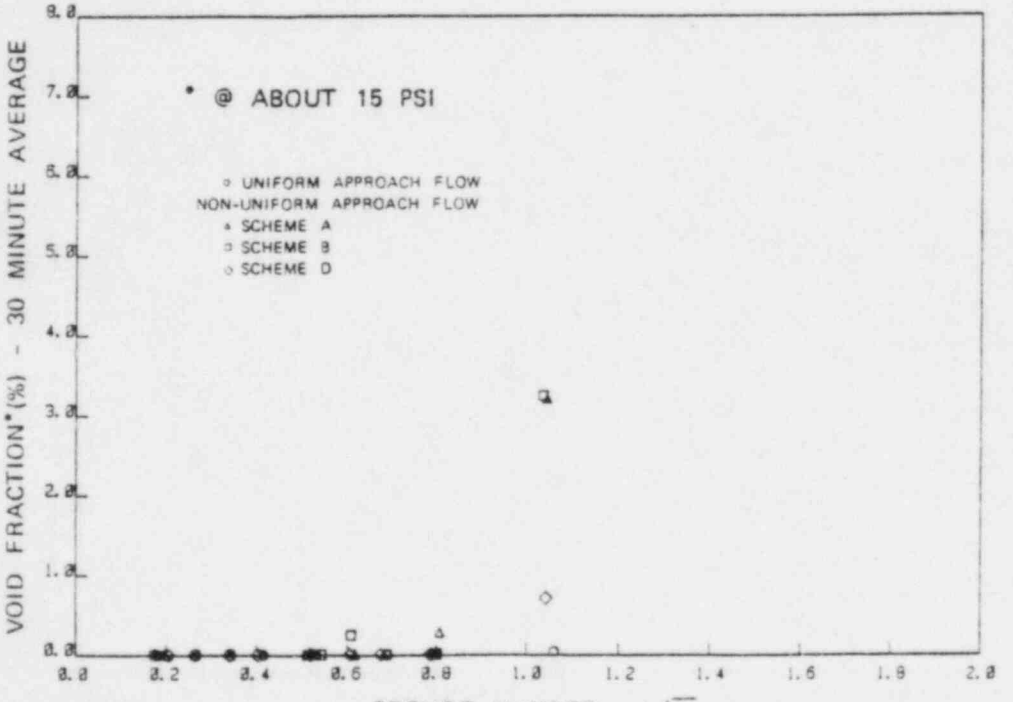

b. CONFIGURATION B

Figure 3.43 Test-average void fractions for tested BWR suction intakes

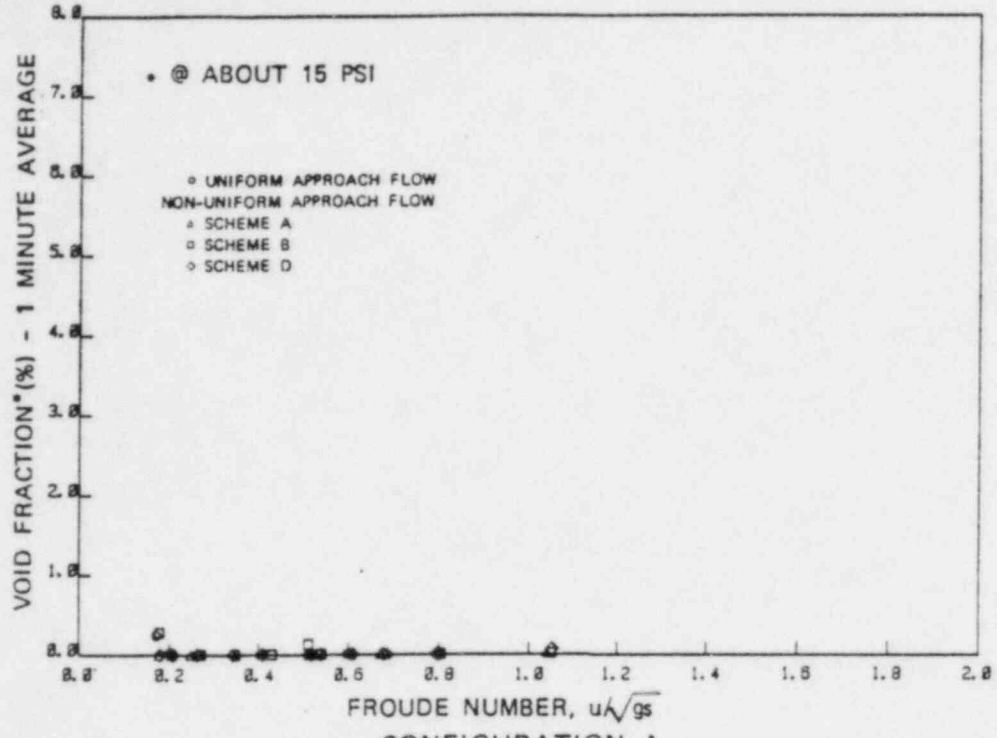

a. CONFIGURATION A

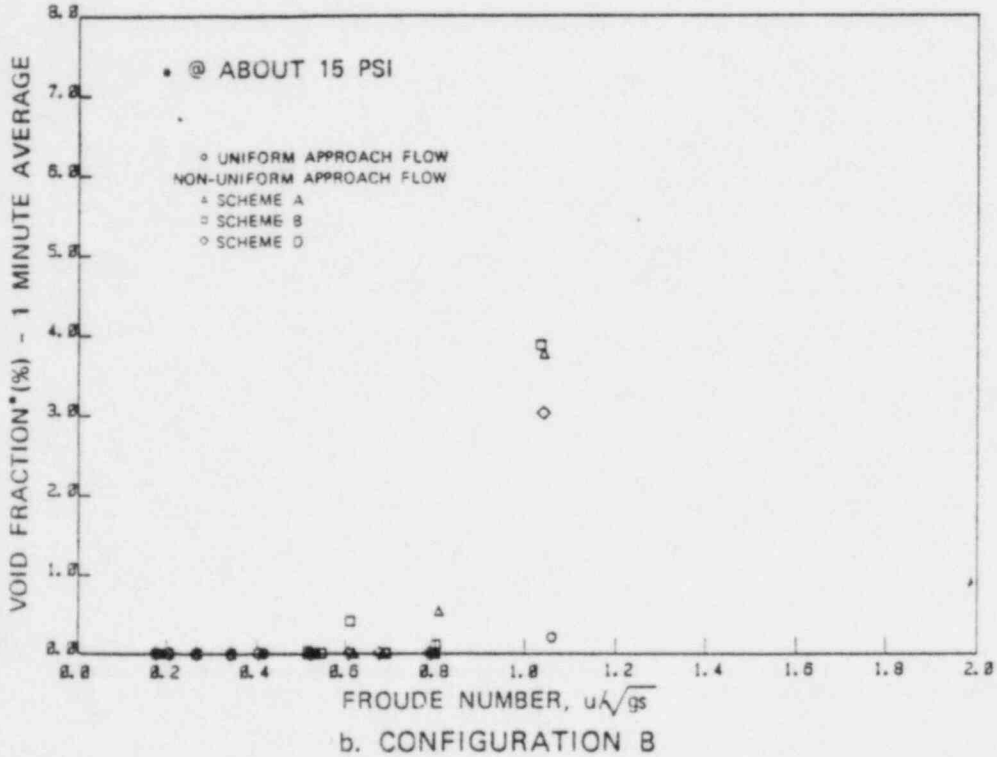

b. CONFIGURATION B

Figure 3.44 1-minute average void fraction for tested BWR suction intakes

4 INDEPENDENT PROGRAM TECHNICAL REVIEWS

Independent program technical reviews were conducted before and during key phases of the work reported in Section 3 to solicit comments and technical views about the program's direction and goals from experts not connected with the implementation and execution of Task Action Plan (TAP) A-43. The reviewers were selected from among the foremost authorities in each of the areas reviewed. Two reviews were conducted: sump hydraulic performance and insulation debris calculational methods effects.

4.1 Sump Hydraulic Performance Review

The sump hydraulic performance review consisted of two panel meetings,* held on March 17 and June 4, 1981. The primary purpose of the first meeting was to introduce in detail the program plan and initial test results. The second meeting was primarily for reviewer followup response and comment. Additionally, at both meetings the reviewers were provided with preliminary program redirections, and were asked to comment on results to date and give an analysis of the proposed future program plan. Overall, the reviewers approved of the program, the experimental test plan, its conduct, and data analysis. They concluded that the program was appropriate for resolving the sump hydraulic performance issues.

---

*Meetings were held on March 17, 1981, at Germantown, Maryland, and June 4, 1981, at Alden Research Laboratory of Worcester Polytechnic Institute, Holden, Massachusetts. Those attending and their affiliations were P. Tullis/Utah State University; D. Simons/Simons, Li and Associates; R. Gardiner/Western Canada Hydraulic Laboratories; D. Canup/Duke Power Company; W. Butler/NRC; S. Vigander/Tennessee Valley Authority (TVA); J. Kennedy/University of Iowa; and R. Letendre/Combustion Engineering, Inc. (R. Letendre did not attend the meeting of June 4, 1981.) Those attending were asked to provide formal written responses and comments at the close of the second meeting. Copies of the responses are available through the Office of Light Water Safety Research, Department of Energy, Washington, DC.

Divergent opinions emerged during the review concerning the potential for pump performance degradation when the fluid temperature was near saturation. Some concerns were expressed regarding the possibility of degraded pump performance as a result of cavitation or the release of dissolved air into the water in the suction lines leading to the pumps. Other opinions suggested that pump performance should be satisfactory at coolant temperatures near saturation, because the (1) solubility of air in water is low near saturation and, (2) if cavitation were not occurring in the pump, any voids would collapse as a result of the static pressure increase with depth in the sump. These collapsing bubbles would then form a turbulent environment and inhibit surface vortex activity. Although the pump issues raised by the reviewers are indirectly pertinent to the sump hydraulics program, they are a part of USI A-43 and have been addressed (see Section 3.2).

In direct response to reviewer comments, elevated temperature tests were performed immediately following the first 25 configurations, which was earlier in the program than originally planned. The experimental research program did not examine the effects on operation at temperatures near saturation conditions due to the operational limits of the experimental facility (about 165°F). However, up to that limit, no significant, or adverse, temperature effects on sump system performance were detected.

An area of general peer review group agreement was that sump system performance with respect to air entrainment could be improved in most sump configurations by the addition of a vortex suppression device(s). One reviewer, however, commented that such a device(s) might be removed during

some phase of reactor operations and not be replaced. Such a possibility, in his judgment, was sufficient justification for an experimental research program that would allow the development of adequate sump design guidelines that were based upon justifiable physical criteria (in the absence of vortex suppressors). The results of the studies provided in Section 3.4 confirm the effectiveness of vortex suppressors to reduce air ingestion to zero and provide hydraulic results for developing acceptable sump design guidelines.

The adequacy of recirculation sump pumps for performing reliably when ingesting air/water mixtures was a matter of some concern to the review group. These concerns have been resolved by the development of sump design guidelines that take into account pump performance specifications under such conditions.

4.2 Insulation Debris Effects Review

The purpose of the insulation debris effects review was to determine the adequacy of methods (described in Section 3.2 and in detail in NUREG/CR-2791) to conservatively estimate quantities of insulation debris that might be produced in containment, its transport, and its potential for sump screen blockage.

The review was conducted in two phases. In the initial phase, a draft report describing the methods was provided to peer panel and other reviewers* to solicit their comments. Reviewers provided highly useful criticisms and comments with recommendations for improvements in the physical basis and rigor of the development of the debris generation and transport models.

---

*The peer panel reviewers and their affiliations were R. Gardiner/Western Canada Hydraulic Laboratories; D. Simons/Simons, Li & Associates, Inc.; D. Canup/Duke Power Company; R. Mango/Combustion Engineering, Inc.; P. Tullis/Utah State Unviersity; J. Kennedy/University of Iowa; W. Butler/NRC; and S. Vigander/TVA. Other reviewers included G. Weigand/Sandia and R. Bosnak, G. Mazetis, and T. Speis/NRC. Their written review comments are available through the NRC Division of Safety Technology, NRC, Washington, DC 20555.

The draft document was then modified in response to the comments of the reviewers. The modified document was transmitted to the reviewers, who were then requested to prepare comments for a formal peer panel review, which was the second phase of the review process.

Formal peer panel review took place at NRC Headquarters on March 31, 1982. Panelists Kennedy and Canup were unable to attend the meeting; however, a number of other persons, in addition to peer panel members, participated in the review.* Questions that were raised during the meeting and their disposition are given below.

It was observed that, under some circumstances, the amount of debris generated with the potential to migrate to the sump could be greater than that estimated in the draft report. This concern was resolved by determining that the report would require the selection of those pipe break locations and jet targets that would generate the maximum quantities of potentially transportable debris without regard to initial blowdown and transport direction.

Questions were raised about (1) the applicability of the jet model used in the debris generation portion of the report, (2) the assumption of uniform distribution of debris across the face of the jet and, (3) the use of a 0.5 psi stagnation pressure cutoff for debris generation. Resolution of (1) was arrived at by agreement that a modified Moody jet model (Moody, 1973) would be allowed to model the jet. It was agreed that the stripping of all insulation from plant and piping within the crane wall and within the jet represented a conservative treatment of insulation debris generation.

---

*Other attendees were: S. Hanauer, K. Kniel, C. Liang, P. Norian, F. Orr, A. Serkiz, J. Shapaker/NRC; G. Hecker/Alden Research Laboratory; E. Gahan, J. Wysocki/Burns and Roe; W. Swift/Creare, Inc.; and P. Strom and G. Weigand/Sandia.

Discussions of (2) concluded that a definite probability existed that debris distribution across the face of the jet would not be uniform. It was agreed that a distribution of debris across the jet face would be provided that would represent the geometric distribution of insulation targeted by the jet in the containment. In addition, because of uncertainties in jet transport to walls, it was agreed that the quantities of debris estimated to exit through crane wall openings would be doubled.

The use of a 0.5 psi stagnation pressure cut-off (item (3)) for insulation damage was questioned by a number of reviewers. Technical views were put forward by a Sandia staff member on the expected performance of jets under LOCA conditions. He stated that centerline stagnation pressures above 15 psig could be expected for at least five diameters downstream of high-energy, high pressure breaks. An Atomic Energy Commission report (Glasstone, 1981) was cited by Burns and Roe as the origin of the cut-off estimate for debris generation. Alden Research Laboratory personnel reported on preliminary experiments at ARL that have shown that little insulation damage occurred to fibrous insulation assemblies up to 6.5-psi water jet pressures. It was agreed* that the 0.5 psi stagnation pressure represented a conservative treatment for the onset of insulation debris generation. It was further agreed that the assumption that all insulation within the jet cone would be transformed to insulation debris was conservative. This assumption was chosen to represent the volume within which insulation debris would be generated under the treatment provided in NUREG/CR-2791. The results of work performed subsequently on these issues are provided in Sections 3.3 and 5.3 of this report.

---

*This decision has been superseded by information discussed in Section 3.3.

Discussions were held on the physical accuracy of the model in representing pipe whip, pipe impact, and the direction of motion of dislodged insulation and its trajectory. It was first pointed out that the quantity of insulation generated by this mechanism would amount to 10% or less of that generated by jet forces. It was further pointed out that the use of the treatment in the report would conservatively estimate the quantities of insulation debris produced by a minor contributor to debris production and, as such, was satisfactory.

Questions were raised on the treatment of long term transport following blowdown. These questions related to

(1) recirculation flow velocities within containment
(2) hydraulic lift provided to sunken debris
(3) drawdown of floating debris onto less than fully submerged sump screens (ice-jam effect)
(4) transport mechanisms of sunken debris, such as tumbling and sliding

In the resolution of (1), agreement was reached to account for obstructions in flow paths and subsequent flow expansion (Appendix D and NUREG/CR-2791).

Agreement was reached on (2) that for horizontal orientation, lift would be approximated by drag for horizontal debris, would be zero for vertically oriented debris, and would be disregarded for tumbling debris.

Item (3) was recognized as a potentially important mechanism for screen blockage. It will be treated by established methods available as described in the literature, (Uzuner, July 1977; NUREG/CR-2791).

Tumbling and other transport mechanisms, as noted under (4), could significantly affect the movement of debris towards screens. Panelists agreed to treatments that they considered to be conservative in dealing with debris transported by these mechanisms. Recent experiments at ARL have shown a wide variability of transport characteristics depending on the debris geometry (section 3.3; NUREG/CRs-2982 and -3616).

Arguments were raised that a period of debris transport (intermediate- to short-term transport and long-term transport, as defined here) might exist. It was postulated that transport during such an interim period might seriously affect potential sump blockage. Because the report assumes that all floating debris reaches the sump, such an interim migration period would not affect the consequences of such transport. With respect to debris of density equal to or greater than unity and its transport, discussions brought out views that the likelihood of a significant effect during such an interim period would be minor, flow patterns would show no preferential transport toward the sump, and entrainment would be higher in the recirculation mode than in the interim period.

An issue that was not resolved concerned the behavior of fibrous insulation in its migration toward a sump and the potential for blockage by such material. Because this problem appears to exist at only a few plants, it is considered plant-specific. Nevertheless, it was an open issue at the time of the meetings. Following the meetings, experimental studies were conducted at ARL to estimate stagnation pressures required for the onset of debris generation for nonencapsulated mineral wool and fiberglass insulations (NUREG/CR-3170), the transport characteristics of such debris, and the pressure losses

at sump screens caused by the accumulation of fibrous debris on screens (NUREG/CR-2982). These findings are reflected in the findings provided in Sections 3.3 and 5.3 of this report.

All panelists, except S. Vigander of TVA, concluded that the use of the methods discussed would result in conservative estimates of sump screen blockage. Vigander commented that while he was of the opinion that the treatment would yield conservative, perhaps ultra-conservative, results, he could not with certainty arrive at that conclusion. He suggested that uncertainty analyses be conducted to establish the levels of conservatism (if any) that are provided in the development. Other panelists agreed that quantitative or qualitative error analyses would be desirable, although the needs for such analyses were deemed not to be immediate or pressing.

5 SUMMARY OF SUMP PERFORMANCE TECHNICAL FINDINGS

5.1 General Overview

Emergency core cooling systems require a clean and reliable water source for maintaining long-term recirculation following a LOCA. PWRs rely on the containment emergency sump to provide such a water supply to residual heat removal pumps and containment spray pumps. BWRs rely on pump suction intakes located in the suppression pool, or wet well, to provide a water source to residual heat removal pumps and core spray pumps. Thus, recirculation pump performance under post-LOCA conditions must be evaluated for both BWRs and PWRs.

Typical technical considerations are shown in Figure 5.1. Each major area of concern--pump performance, sump hydraulics, and debris generation potential--can be assessed separately, but the combined effects of all three areas should then be assessed to determine the overall effect on both the available and required NPSH requirements of the pumps. The sections below summarize technical findings and provide concise data sets.

5.2 Sump Hydraulic Performance

Full scale tests show that adequate PWR sump (or BWR RHR suction intake) hydraulic performance is principally a function of depth of water (the submergence level of the suction pipe) and the rate of pumping (suction inlet water velocity). These variables can be combined to form a dimensionless quantity defined as the Froude number

$$\text{Froude number} = U/\sqrt{gs}$$

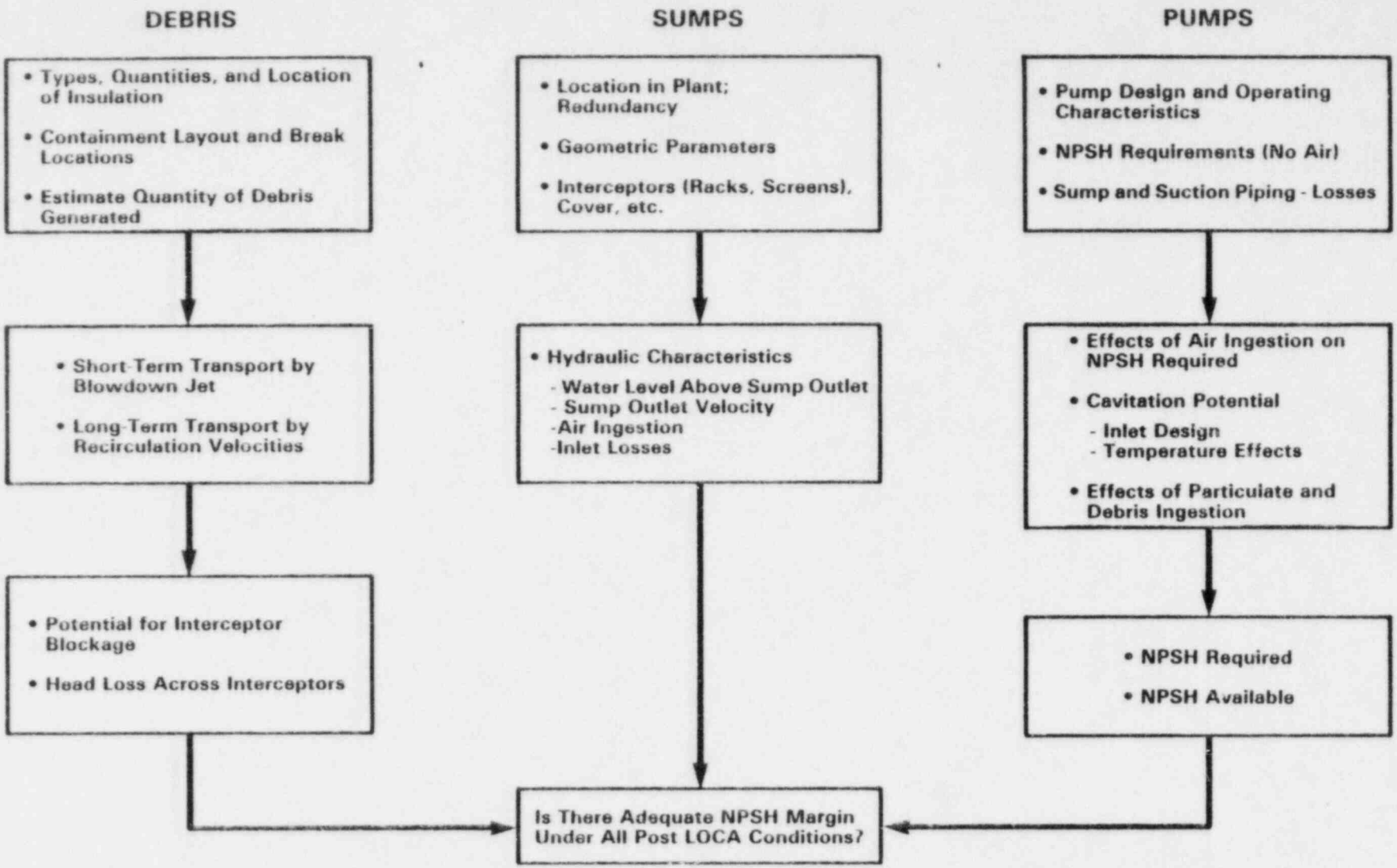

Figure 5.1 Technical considerations relevant to ECCS sump performance

where

U = suction pipe mean velocity
s = submergence (water depth from surface to suction pipe centerline)
g = acceleration due to gravity

The extent of air ingestion is the principal parameter to be determined. Small amounts of air (less than 2% by volume) do not significantly degrade pumping capacity (Merry, 1976; Murakami and Minemura, 1977; and Florjancic, 1970). Generally speaking, full-scale tests revealed low levels of air ingestion (< 2%) over a wide range of Froude numbers despite the presence of air-core vortices. Other hydraulic effects, such as intake swirl, were found to be small, and inlet loss coefficients were in agreement with handbook values for similar intake geometries.

Section 3.4 summarizes the results of full-scale PWR sump hydraulic tests and BWR suction inlet tests. Figures 3.34 and 3.37 show typical void fraction data as a function of Froude number for PWR sumps; Figures 3.43 and 3.44 show void fraction data for BWR suction inlets. More detailed results are provided in NUREG/CR-2758; NUREG/CR-2759; NUREG/CR-2760; NUREG/CR-2761; and NUREG/CR-2772. Generally, sump (or suction intake) design acceptability should be based upon $\leq$ 2% air ingestion criteria.

PWR sump hydraulic performance can, therefore, be assessed as follows:

(1) Table 5.1 summarizes the conditions for PWR type sump designs where negligible (or zero) air ingestion would exist. Adequate submergence and low intake velocities are the key parameters derived from ARL tests.

Table 5.1 Hydraulic design findings* for zero air ingestion

Item	Horizontal Outlets	Vertical Outlets
Minimum submergence, s (ft) (m)	9 2.7	9 2.7
Maximum Froude Number, Fr	0.25	0.25
Maximum Pipe Velocity, U (ft/s) (m/s)	4 1.2	4 1.2

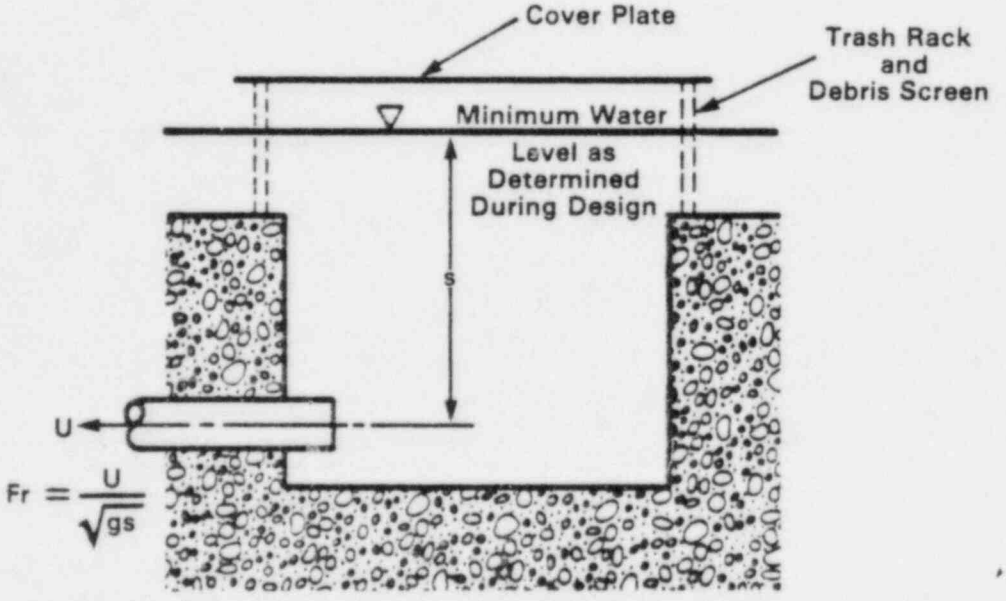

*The hydraulic findings were established using experimental results from NUREG/CRs-2758, -2759, and -2760, and the variable ranges over which such data were taken for sump geometries which were of rectilinear design.

(2) If the adequacy of the sump geometric design and hydraulic performance is to be based on air ingestion levels of $\leq$ 2%, such assessments can be made using Tables 5.2, 5.3, 5.4, and 5.5. Under such conditions, sump design features should be comparable with those sump geometries tested at ARL and as noted in these tables.

(3) Vortex suppressors provide a very effective means to achieve zero air ingestion. Vortex suppression devices such as those shown in Table 5.6 have been shown to reduce air ingestion measured levels to zero on PWR sump designs.

(4) Table 5.7 provides additional information pertinent to screens and grates that could affect PWR sump hydraulic performance and represents the types tested at ARL.

(5) Elevated water temperature has been shown to have negligible effect on sump hydraulic performance in full-scale tests conducted at temperatures up to 165°F.

BWR pump suction intake designs (employing suction strainers) that result in a Froude number of $\leq$ 0.6 were found to have insignificant air ingestion. NUREG/CR-2772 reports experimental findings for Mark I, Mark II, and III intake designs.

5.3 Debris Assessments

Debris assessments should consider the initiating mechanisms (pipe break locations, orientations, and break jet energy content), the amount of debris that might be generated, short- and long-term transport, the potential for PWR sump screen or BWR suction strainer blockage, and head losses that could degrade available NPSH. In addition, an evaluation of the effects of small

Table 5.2 Hydraulic design findings* for air ingestion $\leq$ 2%
Air ingestion α is empirically calculated as
$\alpha = \alpha_o + \alpha_1 \times Fr$

where α_o and α_1 are coefficients derived from test results as given in the table below

Item	Horizontal Outlets		Vertical Outlets	
	Dual	Single	Dual	Single**
Coefficient α_o	-2.47	-4.75	-4.75	-9.14
Coefficient α_1	9.38	18.04	18.69	35.95
Minimum Submergence, s (ft) (m)	7.5 2.3	8.0 2.4	7.5 2.3	10 3.1
Maximum Froude Number, Fr	0.5	0.4	0.4	0.3
Maximum Pipe Velocity, U (ft/s) (m/s)	7.0 2.1	6.5 2.0	6.0 1.8	5.5 1.7
Maximum Screen Face Velocity (blocked and minimum submergence) (ft/s) (m/s)	3.0 0.9	3.0 0.9	3.0 0.9	3.0 0.9
Maximum Approach Flow Velocity (ft/s) (m/s)	0.36 0.11	0.36 0.11	0.36 0.11	0.36 0.11
Maximum Sump Outlet Coefficient C_L	1.2	1.2	1.2	1.2

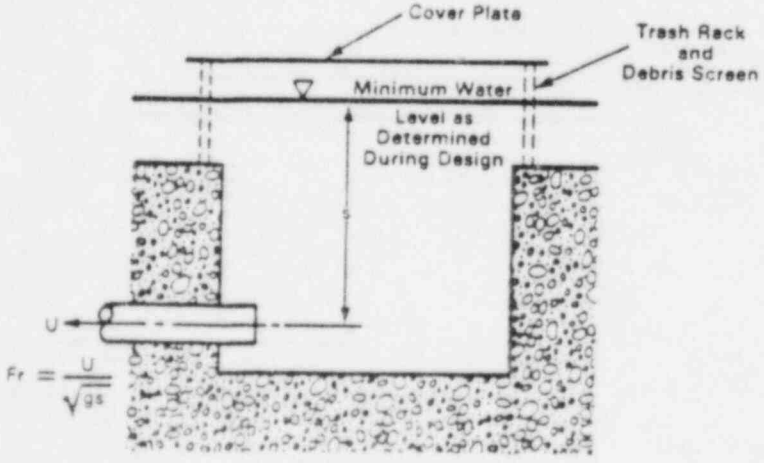

*See note on Table 5.1
**These numbers are not from test data, but are extrapolated.

Table 5.3 Geometric design envelope guidelines for horizontal suction outlets **

Sump Outlet	Size			Sump Outlet Position*						Screen	
	Aspect Ratio	Min. Perimeter (ft)	(m)	e_y/d	$(B - e_y)/d$	c/d	b/d	f/d	e_x/d	Min. Area (ft^2)	(m^2)
Dual	1 to 5	36	11	≥ 1	≥ 3	≥ 1.5	≥ 1	≥ 4	≥ 1.5	75	7
Single	1 to 5	16	4.9					-		35	3.3

*Preferred location.
**Dimensions are always measured to pipe centerline.

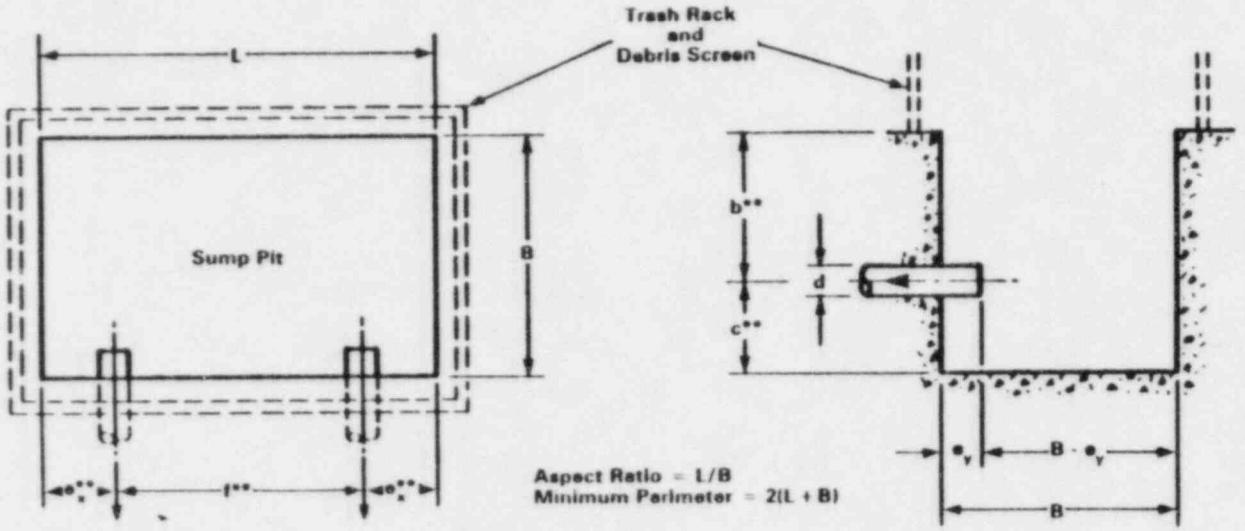

Table 5.4 Geometric design envelope guidelines for vertical suction outlets**

Sump Outlet	Size			Sump Outlet Position*						Screen	
	Aspect Ratio	Min. Perimeter (ft)	(m)	e_y/d	$(B - e_y)/d$	c/d	b/d	f/d	e_x/d	Min. Area (ft^2)	(m^2)
Dual	1 to 5	36	11	≥ 1	≥ 1	≥ 0	≥ 1	≥ 4	≥ 1.5	75	7
Single	1 to 5	16	4.9			≤ 1.5		-		35	3.3

*Preferred location.
**Dimensions are always measured to pipe centerline.

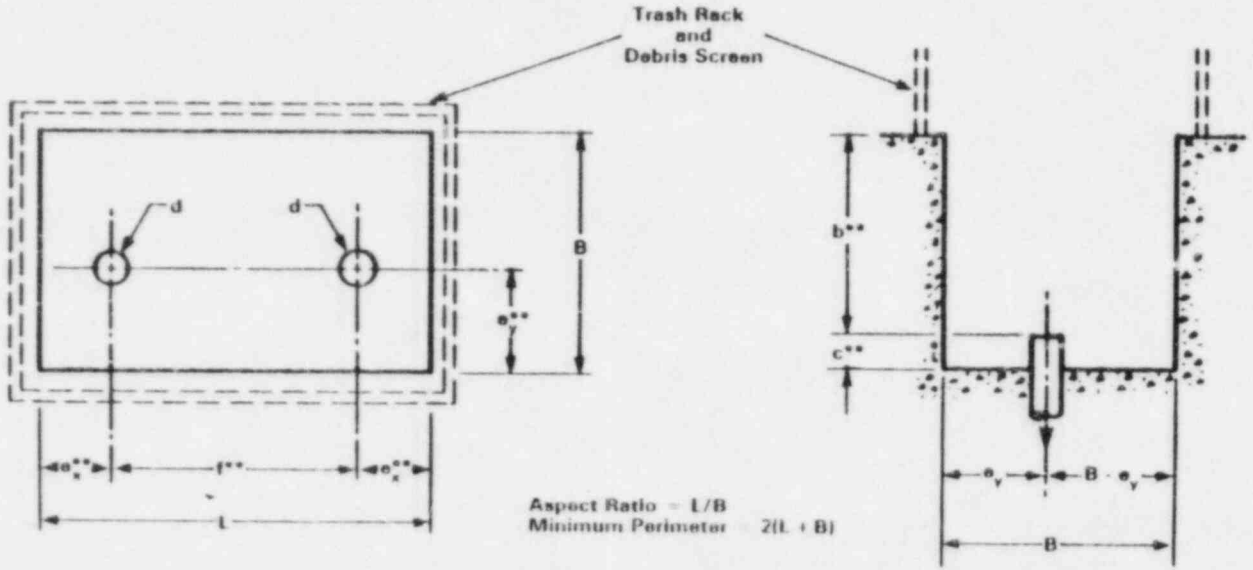

Table 5.5 Additional considerations related to sump size and placement

1. The clearance between the trash rack and any wall or obstruction of length ℓ equal to or greater than the length of the adjacent screen/grate (B_s or L_s) should be at least 4 ft (1.2 m).

2. A solid wall or large obstruction may form the boundary of the sump on one side only, i.e., the sump must have three sides open to the approach flow.

3. These additional considerations are provided to ensure that the experimental data boundaries (upon which Tables 5.1, 5.2, 5.3, and 5.4 are based) resulting from the experimental studies at Alden Research Laboratory are noted.

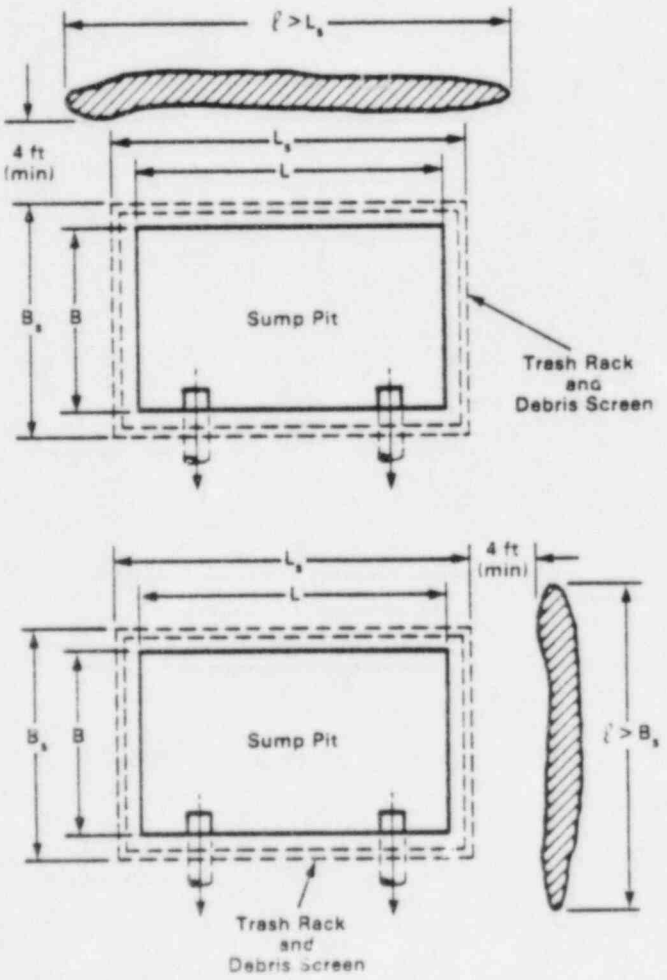

Table 5.6 Findings for selected vortex suppression devices*

1. Cubic arrangement of standard 1-1/2-inc (38-mm) deep or deeper floor grating (or its equivalent) with a characteristic length, ℓ_v, that is $\geq$ 3 pipe diameters and with the top of the cube submerged at least 6 inches (15.2 cm) below the minimum water level. Noncubic designs with $\ell_v \geq$ 3 pipe diameters for the horizontal upper grate and satisfying the depth and distances to the minimum water level given for cubic designs are acceptable.

2. Standard 1-1/2-inch (38-mm) or deeper floor grating (or its equivalent) located horizontally over the entire sump and containment floor inside the screens and located between 3 inches (7.6 cm) and 12 inches (30 cm) below the minimum water level.

*Tests on these types of vortex suppressors at alden Research Laboratory have demonstrated their capability to reduce air ingestion to zero even under the most adverse conditions simulated.

Design #1:

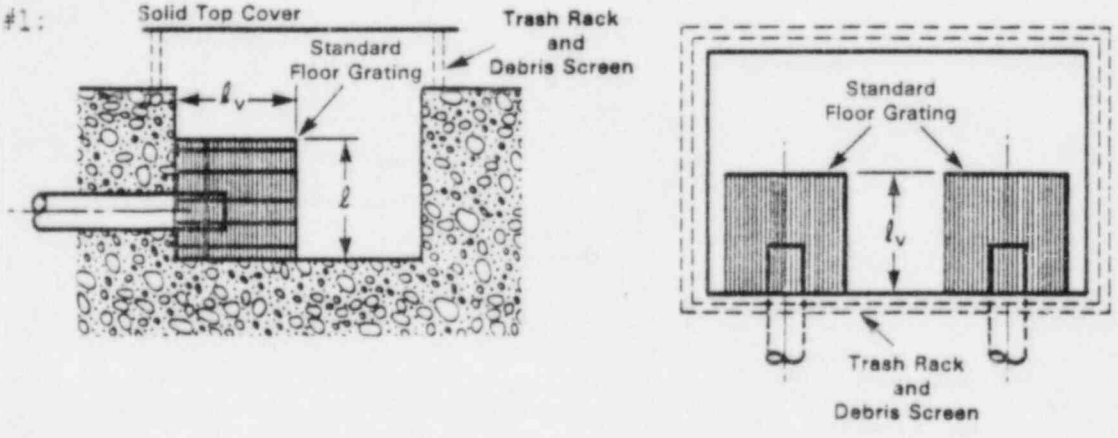

Design #2:

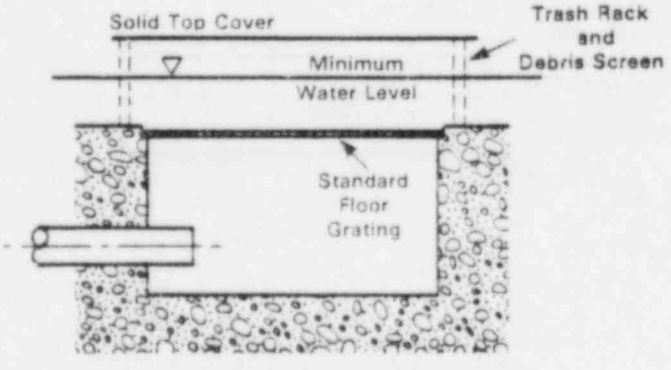

Table 5.7 Screen, trash rack, and cover plate design findings*

1. Minimum plane face screen area should be obtained from Tables 5.3 and 5.4.

2. Minimum height of open screen (debris interceptors) should be 2 feet (0.61 m).

3. Distance from sump side to screens, g_s, may be any reasonable value.

4. Screen mesh should be 1/4 inch (6.4 mm) or finer.

5. Trash racks should be vertically oriented 1- to 1-1/2-inch (25- to 38-mm) standard floor grate or equivalent.

6. The distance between the screens and trash racks should be 6 inches (15.2 cm) or less.

7. A solid cover plate should be mounted above the sump and should fully cover the trash rack. The cover plate should be designed to ensure the release of air trapped below the plate (a cover plate located below the minimum water level is preferable).

---

*These design findings are based on full-scale tests conducted at the Alden Research Laboratory.

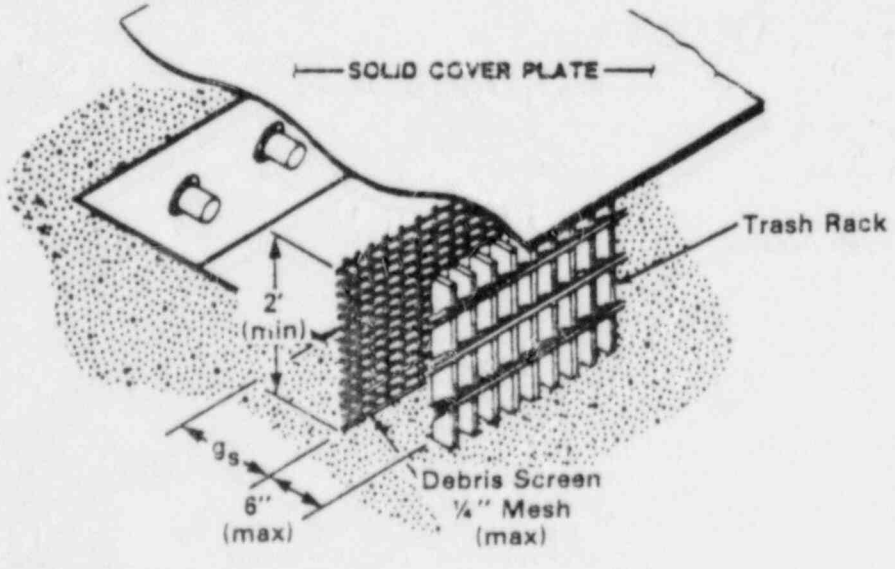

debris (or particulates) that can pass through screens or strainers should be made. Particulate effects on bearing and seal systems should be evaluated. Table 5.8 outlines key considerations requiring evaluation.

Evaluation of potential debris effects requires the following information:

(1) Identification of major break locations (per SRP 3.6.2) and jet energy levels.

(2) Types and quantities of insulations employed, and methods of fabrication and installation (i.e., mechanical attachments). Material characteristics of the insulations utilized are important for determination of transport and head loss characteristics. The primary and secondary system piping, reactor pressure vessel, and major components (PWR steam generators, reactor coolant pumps, pressurizer, tanks, etc.) that can become targets of expanding jet(s) identified under Item (1) are of importance in assessing debris generation. For BWRs, the feedwater and recirculation piping and the steamlines are of importance in assessing potential debris generation.

(3) Containment plan and elevation drawings showing high-energy line piping runs, system components, and the piping that are sources of insulation debris should be reviewed. Structures and system equipment that become obstructions to debris transport, and sump location(s) are important. Drawings showing PWR sump design and debris screen details are needed; for BWRs, downcomer inlet design (from drywell to wetwell), RHR suction inlet and debris strainer design details are needed.

(4) Expected containment water levels and recirculation velocities during the post-LOCA recirculation period are needed to assess debris transport and NPSH effects (see Appendix D).

Table 5.8 Debris assessment considerations*

	CONSIDERATION	EVALUATE
(1)	Debris generator (pipe breaks and location as identified in SRP Section 3.6.2)	° Major Pipe Breaks and Location ° Pipe Whip and Pipe Impact ° Break Jet Expansion Envelope (the (major debris generators)
(2)	Expanding jets	° Jet Expansion Envelope ° Piping and Plant Components Targeted (i.e., steam generators) ° Jet Forces on Insulation ° Insulation That Can Be Destroyed or Dislodged by Blowdown Jets. ° Sump and Suction Structures (i.e., screens), Survivability Under Jet Loading
(3)	Short-term debris transport (by blowdown jet forces)	° Jet/Equipment Interaction ° Jet/Crane Wall Interaction ° Sump Location Relative to Expanding Break Jet
(4)	Long-term debris transport (transport to the sump during the recirculation phase)	° Containment Layout and Sump (or Suction) Locations ° Debris Physical Characteristics ° Recirculation Velocity ° Debris Transport Velocity
(5)	Screen (or suction intake) blockage effects (impairment of flow and/or NPSH margin)	° Screen (or suction strainer) Area ° Water Level Under Post-LOCA Conditions ° Recirculation Flow Requirements ° Head Loss Across Blocked Screen or Suction Intakes
	Key elements for assessment of debris effects	° Estimated Amount and Type of Debris That Can Reach Sump ° Predicted Screen (or Suction) Blockage ° ΔP Across Blocked Screens or Suction Intakes ° NPSH Required vs. NPSH Available

*Per debris estimation methods described in Section 3.3

Generic findings regarding debris that might be generated, transported, and lodged against sump screens (and the plant-specific dependence of these phenomena) are discussed in Section 3.3. The following paragraphs summarize the findings.

Break locations, type and size of breaks, and break jet targets are major factors to consider in the estimation of potential quantities of debris generated. The break jet is a high-energy, two-phase expansion that is capable of shredding insulation and insulation coverings into small pieces or fibers by producing high-impingement pressures and large jet loads.

If the PWR sump location can be directly targeted by an expanding break jet, a close examination should be made of possible jet load damage to such insulations at that location and their possible prompt transport to the sump; jet loads on sump screens, etc., also should be evaluated.

Low-density insulations, such as calcium silicate and Unibestos, that have closed cell structures can float. Thus, they are unlikely to impede flow through screens if water levels are above screen height. Partially submerged screens should, however, be evaluated for pulldown of floating debris Uzuner, July 1977). Low-density hygroscopic insulations that, upon being wetted, have submerged densities greater than water require plant-specific determinations of screen (or strainers) blockage effects.

Fibrous insulations (such as mineral wool and fiberglass materials) that are transported at low velocities have been shown to present the possibility for total screen blockages (NUREG/CR-2982). Even if these materials are deposited onto screens in layers of relatively small thickness (on the order of an inch or less), high pressure drops can result. The potential for

screen blockage can be calculated using the methods provided in Sections 3.3.5, 3.3.6, and 3.3.7.

The methods for debris assessment noted above should also be reviewed in light of the appendices E and F. Appendix E provides information received from Diamond Power Company about HDR test results on MIRROR insulation performance during LOCA conditions. Appendix F provides information received from Owens-Corning about HDR blowdown tests with NUKON insulation blankets. The NRC staff response to above mentioned information is included in Appendix A.

5.4 Pump Performance Under Adverse Conditions

The pump industry historically has determined NPSH requirements for pumps on the basis of a percentage of degradation in performance. The percentage is arbitrary, but generally is 1% or 3%. A 2% limit on allowed air ingestion was selected in this review because data show that air ingestion levels exceeding 2% have the potential to produce significant head degradation. Either the 2% limit in air ingestion or the NPSH requirement to limit cavitation may be used independently when the two effects act independently. However, air ingestion levels less than 2% will affect NPSH requirements. In determining these combined effects, the effects of air ingestion on NPSH required must be taken into account.

A calculational method for assessing pump inlet conditions is shown in Figure 5.2. For a given sump design, the following procedure can be followed:

(1) Determine the static water pressure at the sump suction pipe after debris blockage effects have been evaluated (see Section 5.3.). For PWRs, the water level in the sump should not be so low that a limiting critical water depth occurs at the sump edge in a way that flow is restricted into the sump.

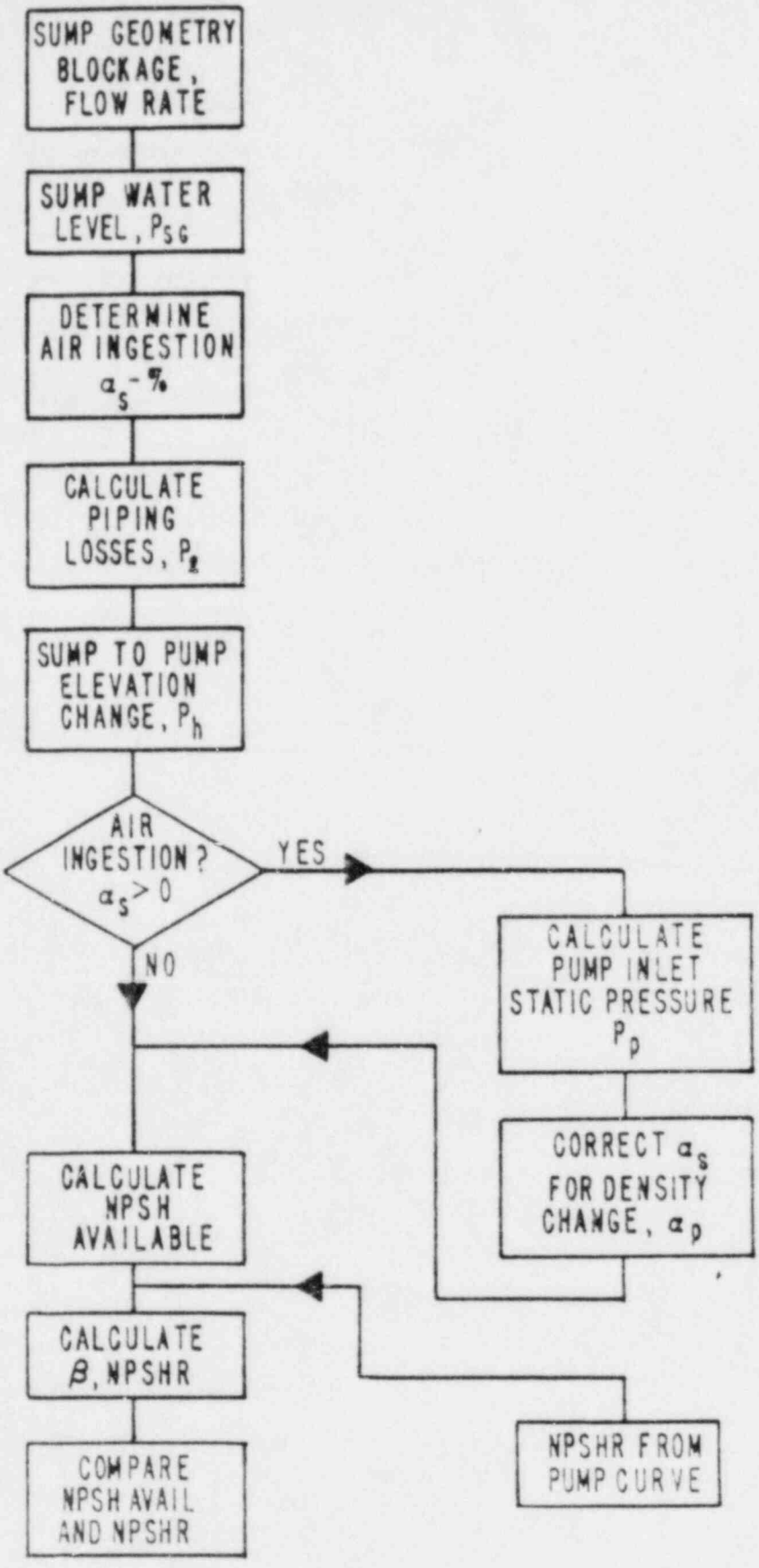

Figure 5.2 Flow chart for calculation of pump inlet conditions

(2) Assess the potential level of air ingestion (see Table 5.2) using the criteria in Section 5.2.

(3) Determine pressure losses between suction pipe inlet and pump inlet flange for the required RHR and CSS flows. If the pump inlet is located less than 14 pipe diameters from the suction pipe inlet, the effect of sump-induced swirl should be evaluated (see Section 3.4).

(4) Calculate the static pressure at the pump inlet flange. Static pressure is equal to containment atmospheric pressure plus the hydrostatic pressure due to pump elevation relative to sump or suppression pool surface level, less pressure losses and the dynamic pressure due to velocity. Note that no credit is allowed for containment overpressure, per SRP Section 6.2.2.

(5) Calculate the air density at the pump inlet, then calculate the air-volume flow rate at the pump inlet, incorporating the density difference from suction pipe to the pump.

(6) If the calculated air ingestion is found to be less than, or equal to 2%, proceed to Step 7. If the calculated air ingestion is greater than 2%, reassess the sump design and operation per Section 5.1.

(7) Calculate the NPSH available.

(8) If air ingestion is indicated, correct the NPSH requirement from the manufacturer's pump curves by the following relationship:

$$NPSH_{required}(air/water) = NPSH_{required}(water) \times \beta$$

where

$$\beta = 1 + 0.5\ \alpha_p$$

and α_p is the air ingestion rate (in percent by volume) at the pump inlet flange.

(9) If the NPSH available from Step 7 is greater than the NPSH requirement from Step 8, inlet considerations will be satisfied.

If the above review procedure leads to the conclusion that an inadequate NPSH margin exists, further plant-specific discussions must be undertaken with the applicant/licensee for resolution of differences, uncertainties in calculations, plant layout details, etc. The lack of credit for containment overpressure should be recognized as a conservatism that should be assessed on a plant-specific basis.

In addition, an evaluation of small particulate (or debris) ingestion should be made to assess pump bearing and seal design effects. Small particulates (which can pass through PWR screens or BWR suction strainers) should be assessed for adverse impacts on pump operation and pump bearings.

5.5 Combined Effects

The findings summarized in Sections 5.2, 5.3, and 5.4 can be combined as shown in Figure 5.3 for determination of adequate sump performance. This sequence is straight forward; it begins with assessing air ingestion potential, followed by assessing debris blockage effects on NPSH margins, and concluding with pump performance under post-LOCA conditions.

To facilitate first round, or scoping evaluations, the following guidance is provided:

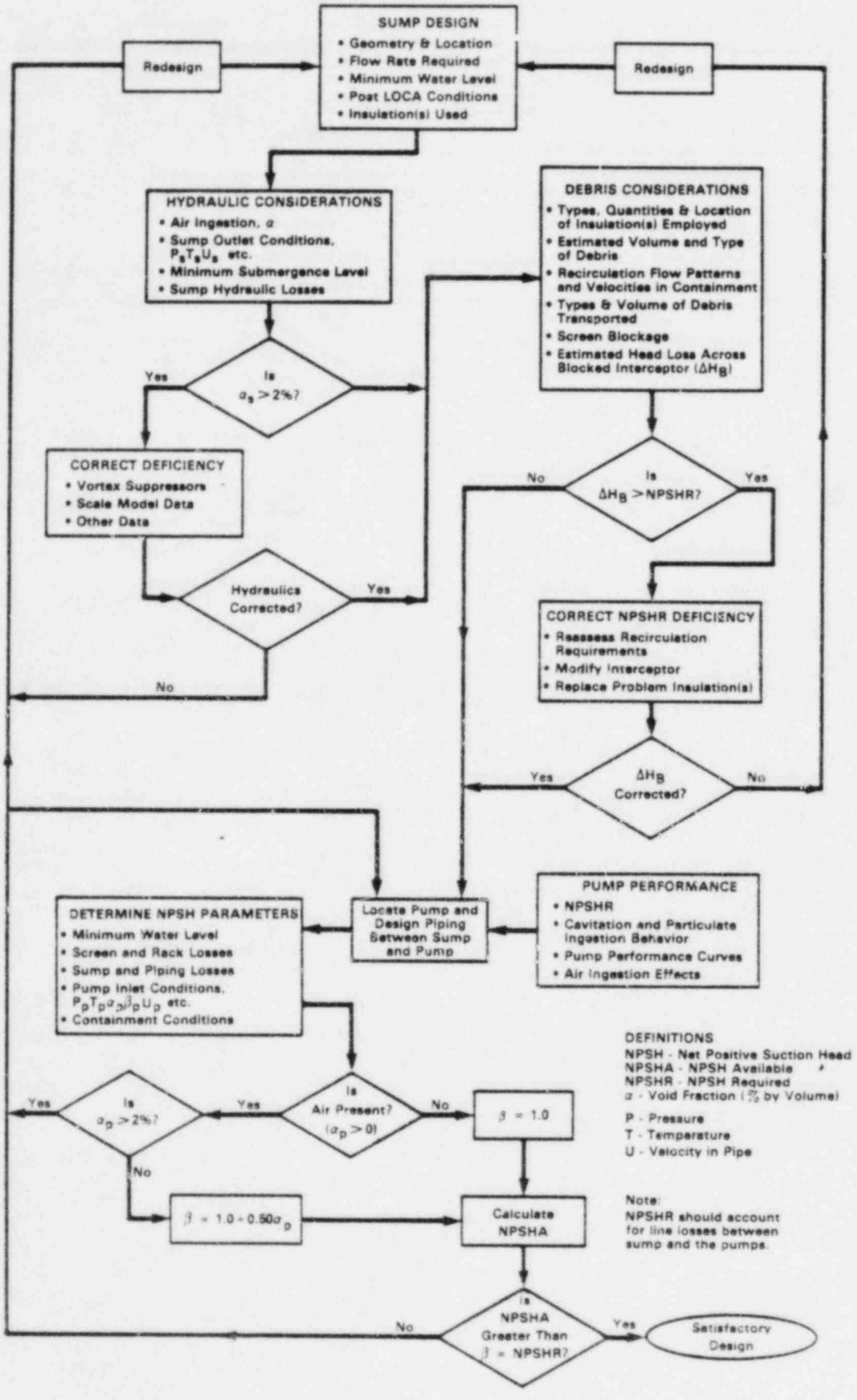

Figure 5.3 Combined technical considerations for sump performance

(1) Air Ingestion Potential

(a) If submergence > 10 feet, intake velocity < 4 ft/sec, and Froude number < 0.25, $\alpha = 0$ (see Table 5.1).

(b) If α (see Table 5.2) > 2%, vortex suppressors should be considered to reduce α to 0 (see Table 5.6).

(2) Debris Blockage Potential

(a) If recirculation flow velocities are low ($\leq$ 0.15 ft/sec), transport of any debris is highly unlikely (see Table 5.9 for a scoping assessment).

(b) When considerable quantities of fibrous (i.e., fiberglass) insulation are employed, the significance of potential blockage can be quickly scoped by assuming material within the 7 L/D cone envelope (see Figure 3.25) is totally destroyed and that debris volume is transported to the debris screen. Because fibrous debris blockage head losses (see Section 3.3.5) are a power function such as

$$\Delta H_B = a\, U^b t^c \qquad \text{Equation (1)}$$

which can be rewritten as

$$\Delta H_B = a\, (Q/A)^b (V/A)^c \qquad \text{Equation (2)}$$

where

Δ_B = head loss across blocked screen
Q = recirculation flow rate
A = effective (wetted) screen area
V = volume of fibrous debris transported to debris screen and distributed uniformly thereon

Criteria for "Zero" Potential for Screen Blockage			
	Criteria 1	Criteria 2	Criteria 3
V_{fb}	0	0	> 0
V_{rm}	0	> 0	any value
V_{cc}	any value	any value	any value
V_{hg}	0	0	0
U_f	any value	$\leq$ 0.2 ft/sec	$\leq$ 0.15 ft/sec
H_w	$\geq H_s$	$\geq H_s$	$\geq H_s$

V_{fb} = volume of fibrous insulation employed
V_{rm} = volume of reflective metallic insulation employed
V_{cc} = volume of closed cell insulation with a specific gravity less than 1.0 (for $H_w \geq H_s$) this insulation will float on water surface above the sump.
V_{hg} = volume of hygroscopic insulation employed
H_w = water level at sump screen
H_s = sump screen height
U_f = flow velocity at the screen based upon the smaller of (1) the screen area that is shielded from prompt transport of insulation and below the minimum water level or (2) the smallest immediate, total approach-flow-area to the screens/grates below the minimum water level.

Table 5.9 First round assessment of screen blockage potential

Therefore, a quick assessment of the head loss across blocked screen area can be made and compared with the NPSHR. Figures 5.4 and 5.5 provide plots of transported debris volumes versus blockage head loss for high density and low density fiberglass debris and are based on experimentally derived head loss data for specific materials (see Section 3.3.6). Material density dependence is illustrated by these figures, and necessitates obtaining similar correlation for other materials used.

Thus, if a prior assumption is made that total transport occurs and the blocked screen calculated head loss is within NPSH margins, the most conservative calculation has been made.

If unacceptable screen blockage losses are calculated, more extensive evaluations, such as outlined in Figure 5.6, will be necessary.

(c) Reflective metallic insulation debris and associated blockage effects should be evaluated on a plant-specific basis utilizing the debris considerations and findings discussed in Sections 3.3.4 and 3.3.5.

(d) Combinations of insulations are more difficult to assess (see Section 3.3.7) and require estimating combined blockage effects.

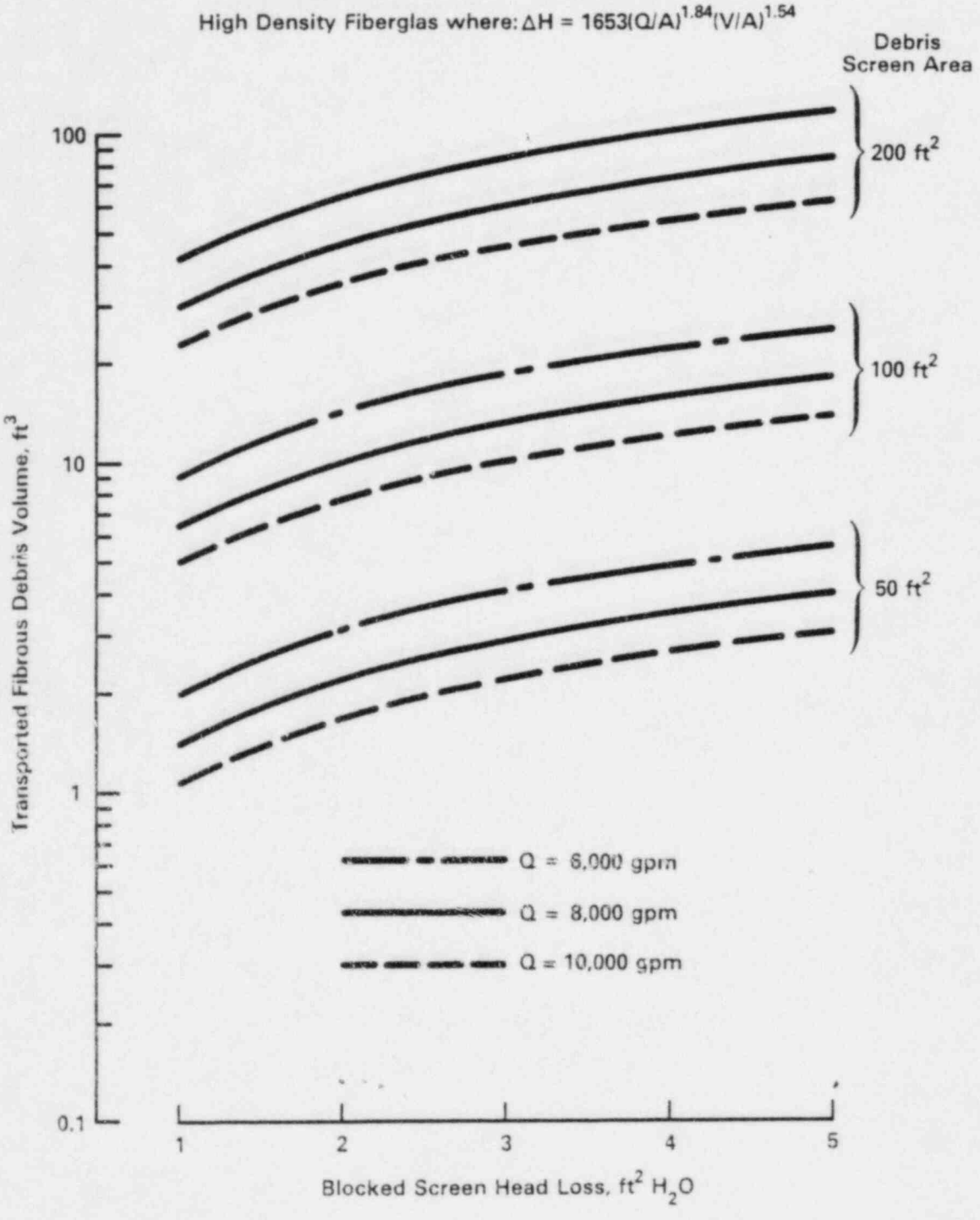

Figure 5.4 Debris volume versus debris screen area, recirculation flow rate and blocked screen head loss, for high density fiberglass

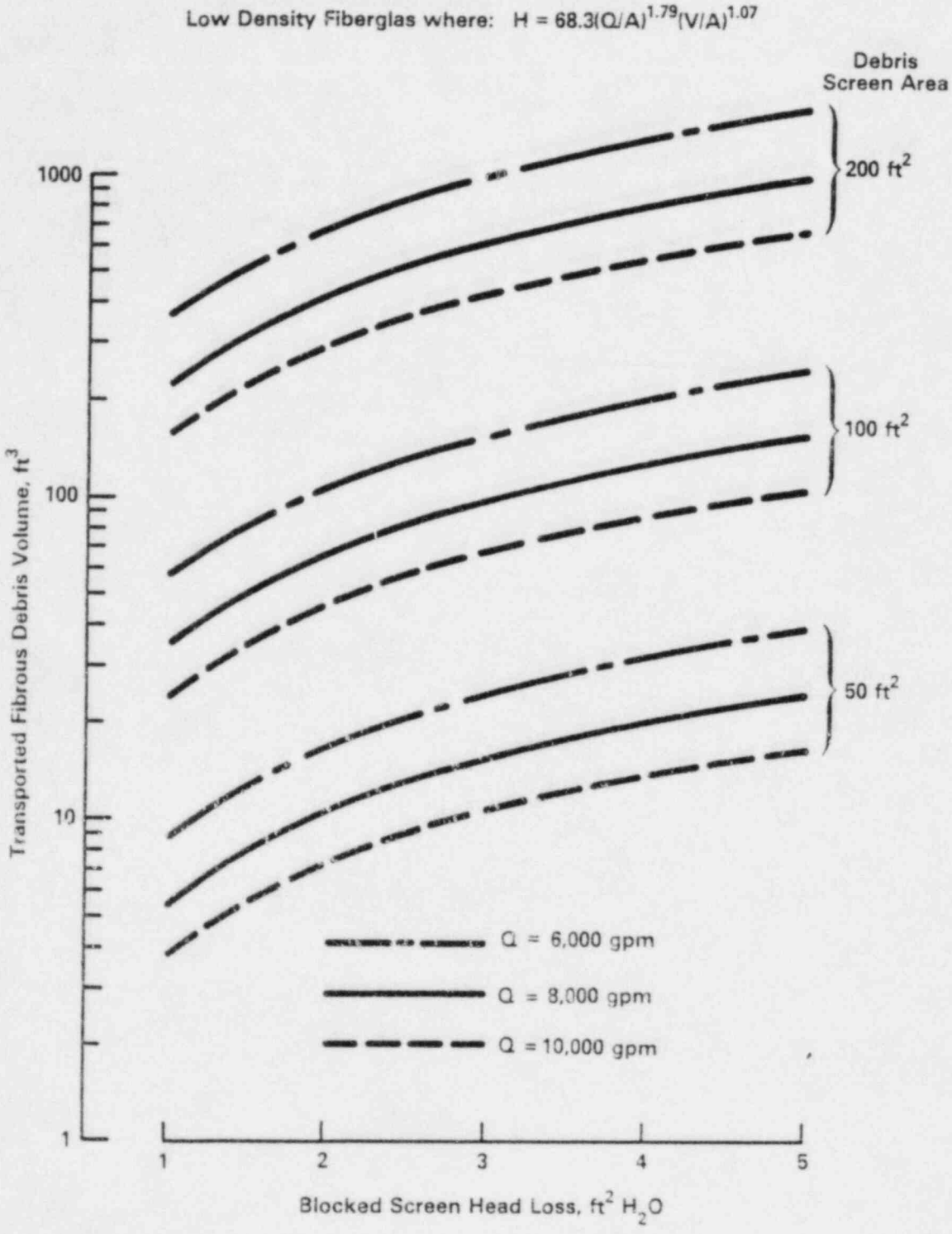

Figure 5.5 Debris volume versus debris screen area, recirculation flow rate and blocked screen head loss, for low density fiberglass

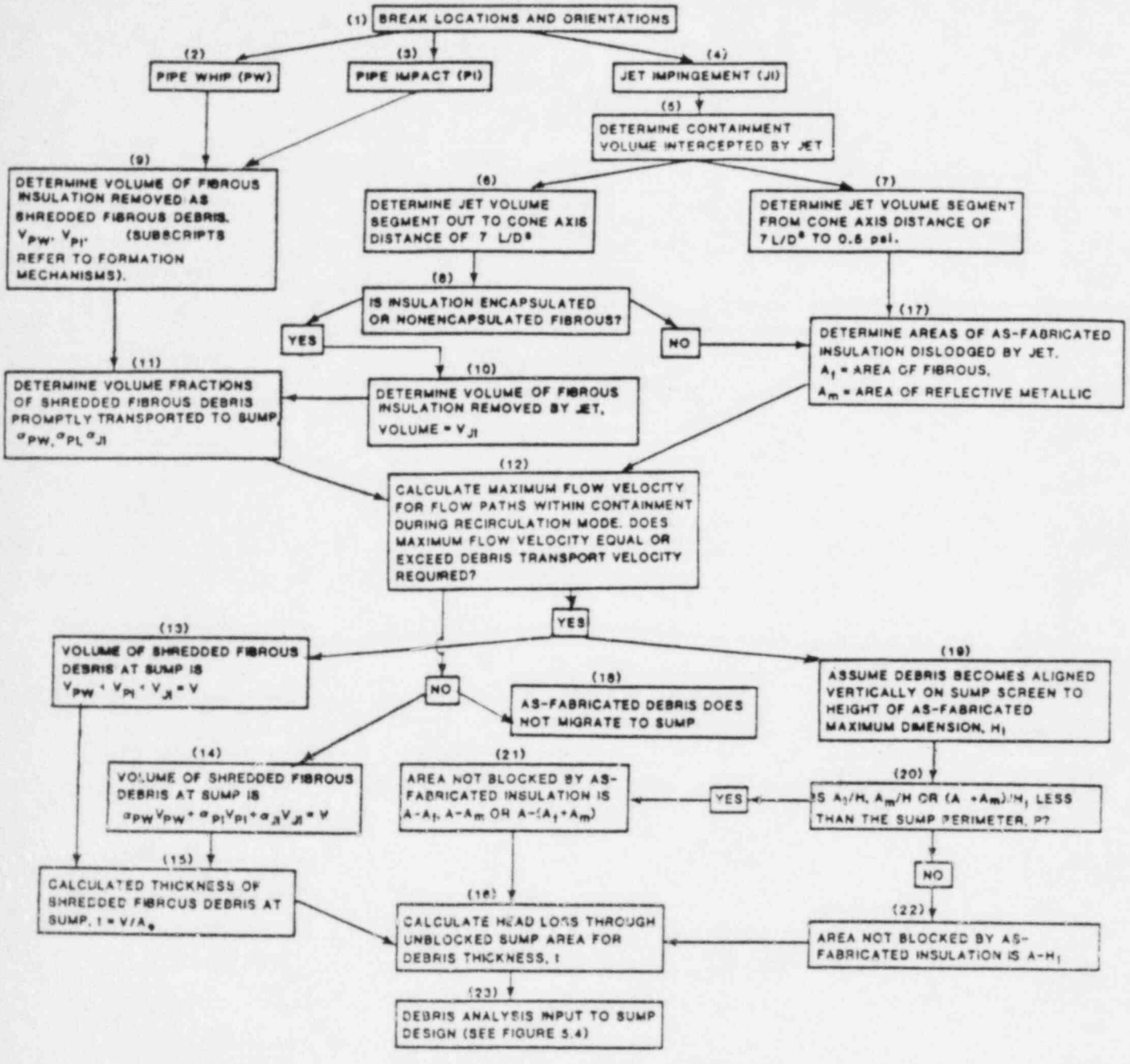

V_{PW} - VOLUME OF SHREDDED FIBROUS INSULATION REMOVED BY PIPE WHIP. (FT^3)
V_{PI} - VOLUME OF SHREDDED FIBROUS INSULATION REMOVED BY PIPE IMPACT. (FT^3)
V_{JI} - VOLUME OF SHREDDED FIBROUS INSULATION REMOVED BY JET IMPINGEMENT. (FT^3)
α_{PW} - FRACTION OF VOLUME OF SHREDDED INSULATION CAUSED BY PIPE WHIP PROMPTLY TRANSPORTED TO SUMP.
α_{PI} - FRACTION OF VOLUME OF SHREDDED INSULATION CAUSED BY PIPE IMPACT PROMPTLY TRANSPORTED TO SUMP.
α_{JI} - FRACTION OF VOLUME OF SHREDDED INSULATION CAUSED BY JET IMPINGEMENT PROMPTLY TRANSPORTED TO SUMP.
L/D - RATIO OF JET LENGTH TO PIPE DIAMETER.
V - TOTAL VOLUME OF SHREDDED DEBRIS TRANSPORTED TO SUMP SCREEN. (FT^3)
A_f - AREA OF AS-FABRICATED FIBROUS INSULATION DISLODGED BY JET. (FT^3)
A_m - AREA OF AS-FABRICATED REFLECTIVE METALLIC INSULATION DISLODGED BY JET. (FT^2)
A - AREA OF SUMP SCREEN. (FT^2)
A_e - EFFECTIVE UNBLOCKED SUMP SCREEN AREA (AREA AVAILABLE FOR FLOW) (FT^2)
H_1 - MAXIMUM LINEAR DIMENSION OF AS-FABRICATED INSULATION (FT)
P - PERIMETER OF EFFECTIVE SUMP SCREEN (FT)
t - CALCULATED THICKNESS OF SHREDDED DEBRIS MAT ON SUMP SCREEN. (IN)

Figure 5.6 Flow chart for the determination of insulation debris effects

6 REFERENCES

U.S. Nuclear Regulatory Commission Documents

Information supplied during a public comment period, 1983 (available in the NRC Public Document Room, 1717 H Street, NW, Washington, DC 20555).

Information supplied by insulation companies during a public comment period, 1983 (available in the NRC Public Document Room, 1717 H Street, NW, Washington, DC 20555).

NUREG/CR-2403, "Survey of Insulation Used in Nuclear Power Plants and the Potential for Debris Generation," R. Reyer, et al., Burns and Roe, Inc., October 1981.

NUREG/CR-2403, Supplement 1, "Survey of Insulation Used in Nuclear Power Plants and the Potential for Debris Generation," R. Kolbe, and E. Gahan, Burns and Roe, Inc., May 1982.

NUREG/CR-2758, "A Parametric Study of Containment Emergency Sump Performance," G. G. Weigand, et al., July 1982 (also Sandia National Laboratory, SAND-82-0624 and Alden Research Laboratory ARL-46-82).

NUREG/CR-2759, "Results of Vertical Outlet Sump Tests," Alden Research Laboratory/Sandia National Laboratory, joint report, September 1982 (also Alden Research Laboratory, ARL-47-92 and Sandia National Laboratory, SAND-82-1286).

NUREG/CR-2760, "Assessment of Scale Effects on Vortexing, Swirl, and Inlet Losses in Large Scale Sump Models," M. Padmanabhan, and G. E. Hecker, Alden Research Laboratory, June 1982.

NUREG/CR-2761, "Results of Vortex Suppressor Tests, Single Outlet Sump Tests, and Miscellaneous Sensitivity Tests," M. Padmanabhan, Alden Research Laboratory, September 1982.

NUREG/CR-2772, "Hydraulic Performance of Pump Suction Inlet for Emergency Core Cooling Systems in Boiling Water Reactors," M. Padmanabhan, Alden Research Laboratory, June 1982.

NUREG/CR-2791, "Methodology for Evaluation of Insulation Debris Effects," J. J. Wysocki, et al., Burns and Roe, Inc., September 1982.

NUREG/CR-2792, "An Assessment of Residual Heat Removal and Containment Spray System Pump Performance Under Air and Debris Ingesting Conditions," P. Kamath, T. Tantillo, and W. Swift, Creare, Inc., September 1982.

NUREG/CR-2913, "Two Phase Jet Loads," G. G. Weigand, S. L. Thompson, D. Tomasko, Sandia National Laboratory, January 1983 (also Sandia National Laboratory, SAND-82-1935).

NUREG/CR-2982, Rev. 1, "Buoyancy, Transport, and Head Loss of Fibrous Reactor Insulation," D. N. Brocard, Alden Research Laboratory, July 1983 (also Sandia National Laboratory, SAND-82-7205).

NUREG/CR-3170, "The Susceptibility of Fibrous Insulation Pillows to Debris Formation Under Exposure to Energetic Jet Flows," W. W. Durgin, and J. Noreika, Alden Research Laboratory, January 1983 (also Sandia National Laboratory, SAND-83-7008).

NUREG/CR-3394, "Probabilistic Assessment of Recirculation Sump Blockage Due to Loss of Coolant Accident," J. J. Wysocki, Burns and Roe Inc., July 1983 (also Sandia National Laboratory, SAND-83-7116).

NUREG/CR-3616, "Transport and Screen Blockage Characteristics of Reflective Metallic Insulation Materials," D. N. Brocard, December 1983 (also Alden Research Laboratory, ARL-124-83 and Sandia National Laboratory, SAND-83-7471).

Other Documents

Brocard, D. N., "Transport and Head Loss Tests of Owens Corning Nukon™ Fiberglass Insulation," Alden Research Laboratory, ARL-110-83/M489F, Holden, MA, September 1983.

Durgin, W. W., and J. F. Noreika, "The Susceptibility of Nukon™ Insulation Pillows to Debris Formation Under Exposure to Energetic Jet Flows," Alden Research Laboratory, ARL-111-83/M489F, Holden, MA, September 1983.

Durgin, W. W., M. Padmanabhan, and C. R. Janik, "The Experimental Facility for Containment Sump Reliability Studies," NRC Generic Task A-43, Alden Research Laboratory, ALO-132, Holden, MA, 1980.

Florjancic, D., "Influence of Gas and Air Admission on the Behavior of Single- and Multi-Stage Pumps," Sulzer Research Number 1970, Sulzer Brothers, Ltd., of Winterthur, Switzerland, 1970.

Glasstone, S., "Effects of Nuclear Weapons," Superintendent of Documents, U.S. Government Printing Office, Washington, D.C., 1981.

Hydraulic Institute, Hydraulic Institute Standards for Centrifugal, Rotary and Reciprocating Pumps, 13th edition, Cleveland, OH, 1975.

Imatran Voima Oy, "Model Tests of the Loviisa Emergency Cooling System," Report No. 275, August 1976, Civil Engineering Department, Construction Laboratory, Finland.

Imatran Voima Oy, "Model Tests of Containment Sumps of the Emergency Core Cooling System," Report No. 291, April 1980, Civil Engineering Department, Construction Laboratory, Finland.

Merry, H., "Effects of Two-Phase Liquid/Gas Flow on the Performance of Centrifugal Pumps," Institution of Mechanical Engineers Conference on Pumps and Compressors, Paper No. C130/76, 1976, 1, Birdcage Walk, London, S.W. 1H 9JJ U.K.

Moody, F. J., "Fluid Reaction and Impingement Loads, Specialty Conference on Structural Design of Nuclear Plant Facilities," Vol 1, Chicago, IL, December 1973, "American Society of Civil Engineers, 345 East 47th Street, New York, N.Y. 10017.

Murakami, M. and K. Minemura, "Flow of Air Bubbles in Centrifugal Impellers and its Effect on Pump Performance," presented at sixth Australian Hydraulics and Fluid Mechanics National Conference, Publication No. 77/12, December 1977, Institution of Engineers, Adelaide, Australia.

Niyogi, K. K. and R. Lunt, "Corrosion of Aluminum and Zinc in Containment Following a LOCA and Potential for Precipitation of Corrosion Products in the Sump," United Engineers and Constructors, Inc., Philadelphia, PA, September 1981.

Uzuner, M. S., "Stability Analysis of Floating and Submerged Ice Floes," Proc. ASCE, 103, HY7, Journal Hyd. Div., pp. 713-722, July 1977.

APPENDIX A

SUMMARY OF PUBLIC COMMENTS RECEIVED AND ACTIONS TAKEN

(REF. USI A-43)

APPENDIX A

SUMMARY OF PUBLIC COMMENTS RECEIVED AND ACTIONS TAKEN

1 INTRODUCTION

The technical findings related to Unresolved Safety Issue (USI) A-43 were published for comment in May 1983. Notice of the publication was placed in the Federal Register on May 9, 1983. The official comment period lasted for 60 days and ended on July 11, 1983. However, comments were received into September 1983, with followup comments received into November 1983. A listing of those who responded during the period and afterwards is shown in Table 1. Copies of the comment letters are on file in the NRC Public Document Room, 1717 H Street, NW, Washington, DC.

A public meeting was held on June 1 and 2, 1983, at Bethesda, Maryland, to offer additional opportunity for public comments; however, attendance was very small. Followup discussions were held with respondees to clarify issues raised at this meeting and in the written comments.

An overview of the comments received is provided in Section 2 below. Section 3 contains summaries of significant comments and the actions planned to resolve them.

2 OVERVIEW OF COMMENTS RECEIVED

The major written comments received addressed seven specific subject areas. The comment categories and commentors are listed in Table 2 below. The commentors are identified in Table 2 as follows: Alden Research Laboratory (ARL); Atomic Industrial Forum (AIF); BWR Owners Group (BWR); Commonwealth Edison (CEd); Consumers Power Co. (CPC); Creare Research and Development (CRD); Diamond Power Co. (DPC); General Electric (GE); Gibbs and Hill, Inc. (GH); Northeast Utilities (NE); and Owens-Corning Fiberglass, Inc. (OCF).

Table 1 Persons who commented on the technical findings related to USI A-43*

Alden Research Laboratory (ARL), M. Padmanabhan, letter to A. Serkiz (NRC), "Comments on NUREG-0897 and 0869," June 13, 1983.

ARL, M. Padmanabhan, letter to A. Serkiz (NRC), "Revision to Table A-3 in NUREG-0869," June 22, 1983.

Atomic Industrial Forum, R. Szalay, letter to the Secretary of the Commission, "NRC's Proposed Resolution of Unresolved Safety Issue A-43, Containment Emergency Sump Performance, Contained in NUREG-0869," July 22, 1983.

Atomic Industrial Forum, J. Cook, letter to R. Purple (NRC) and enclosure "Examples of Staff Review Going Beyond Approved Regulatory Criteria," June 4, 1984.

BWR Owners Group, T. J. Dente, letter to T. P. Speis (NRC), "BWR Owners' Group Comments on Proposed Revision to Regulatory Guide 1.82, Rev. 1," October 18, 1983.

BWR Owners Group, D. R. Helwig, letter to V. Stello (NRC), BWR Owners' Group comments on Regulatory Guide 1.82, Revision 1, July 16, 1984.

Commonwealth Edison, D. L. Farrar, letter to the Secretary of the Commission, "NUREG-0897, Containment Emergency Sump Performance; Standard Review Plan Section 6.2.2, Rev. 4, Containment Emergency Heat Removal Systems; and NUREG-0869, USI A-43 Resolution Positions (48FR2089; May 9, 1983)," July 13, 1983.

Consumers Power, D. M. Budzik, letter to the Secretary of the Commission, "Comments Concerning Regulatory Guide 1.82, Proposed Revision 1 (File 0485.1, 0911.1.5, Serial: 23206)," July 15, 1983.

Creare, W. L. Swift, letter to P. Strom (SNL), "Comments on Figure 3-6 of NUREG-0897 and Table A-9 of NUREG-0869," June 13, 1983.

Diamond Power Company, R. E. Ziegler and B. D. Ziels, letter to K. Kniel (NRC), "Containment Emergency Sump Performance, USI A-43," July 11, 1983.

Diamond Power Specialty Company, B. D. Ziels, letter to A. Serkiz (NRC), "HDR Test Result Summary, MIRROR Insulation Performance During LOCA Conditions," December 6, 1984.

General Electric (GE), J. F. Quirk, letter to K. Kniel (NRC), "Comments on Emergency Sump Documents," July 11, 1983.

*Including comments on NUREG-0869, NUREG-0897, proposed Revision 1 to Regulatory Guide 1.82, and proposed Revision 4 to Section 6.2.2 of the Standard Review Plan (SRP, NUREG-0800).

Table 1 (Continued)

GE, J. F. Quirk, letter to T. P. Speis (NRC), "Comments on Proposed Regulatory Guide 1.82, Rev. 1," October 17, 1983.

Gibbs and Hill, Inc., M. A. Vivirito, letter to the Secretary of the Commission, "Comments on Proposed Revision No. 1 to RG 1.82," July 11, 1983.

Northeast Utilities, W. G. Counsil, letter to K. Kniel (NRC), "Haddam Neck, Millstone Nuclear Power Station, Unit Nos. 1, 2, and 3, Comments on NUREG-0897, SRP Section 6.2.2 and NUREG-0869," September 2, 1983.

Owens Corning Fiberglass (OCF), G. H. Hart, letter to A. Serkiz (NRC), "Comments on NUREG-0897 and NUREG-0869," June 23, 1983.

OCF, G. H. Hart, letter to A. Serkiz (NRC), "Updated Comments on NUREG-0897 and NUREG-0869," July 14, 1983.

OCF, G. P. Pinsky, letter to K. Kniel (NRC), "Comments on NUREG-0879 and -0896," July 14, 1983.

OCF, G. H. Hart, transmittal to A. Serkiz (NRC), "HDR Blowdown Tests with NUKON Insulation Blankets," February 18, 1985.

Power Component Systems, Inc., D. A. Leach, letter to A. Serkiz (NRC), "Nuclear Grade Blanket Insulation," November 8, 1984.

Table 2 Categories addressed in major written comments

Comment Category	ARL	AIF	BWR	CED	CPC	CRD	DPC	GE	GH	NE	OCF
(1) Survey of insulation used is not current or complete.							X				X
(2) Cost estimates are low.		X								X	
(3) Estimates of sump blockage probabilities are high.		X		X	X			X			
(4) Value-impact analysis questioned.		X		X				X		X	
(5) BWRs should be exempt; A-43 is a PWR issue.			X					X		X	
(6) Insulation material definitions and descriptions need revision for clarity and completeness.							X			X	
(7) Technical comments on and clarifications of subject matter in NUREG-0897 and NUREG-0869.	X			X	X	X	X		X	X	X

By category, the actions taken in response to these comments are as follows:

Categories 1 and 6: Tables have been added to NUREG-0897, Revision 1 and NUREG-0869, Revision 1 to include the additional plant insulation information provided during the public comment period. The text of the NUREGs has been revised to reflect recommended insulation definitions and the need to evaluate the specific insulation employed.

Categories 2 and 4: The cost estimates provided by different industry groups have varied over a wide range. With the exception of Diamond Power Company, respondees claimed that the cost estimates in value/impact analysis were too low. The revised value/impact analysis reflects an averaged value derived from costs provided.

Category 3: A detailed sump blockage probability analysis has been performed and is reported in NUREG/CR-3394. The results were used in the revised value/impact analysis. These results show a sump blockage probability range for pressurized water reactors (PWRs) of 10^{-6} to 5×10^{-5}/Rx-yr and a strong dependence on plant design.

Category 5: NUREG-0869 and Regulatory Guide 1.82 have been revised to specifically identify areas of concern for boiling water reactors (BWRs) and for PWRs.

Category 7: Technical corrections and clarifications have been made in the appropriate sections of NUREG-0897 and NUREG-0869.

The NRC staff greatly appreciates the review and comments provided by the respondees. The time and effort they have taken to review USI A-43 has resulted in an improved report that will reflect current findings and a balanced position with respect to this safety issue.

3 COMMENTS RECEIVED AND PROPOSED ACTION (OR RESPONSE) ACTIONS

The NRC staff has given complete and careful consideration to all comments received on USI A-43. Summaries of significant comments and the actions taken by the NRC staff in response are provided in Table 3. Comments are presented in alphabetical order, based on the name of the commenting institution.

Table 3 Comments received on USI A-43 and NRC staff response

Comment	NRC Staff Response
Alden Research Laboratory	
ARL noted typographical errors and proposed technical clarification to several tables	These corrections and clarifications have been incorporated into NUREG-0897 and NUREG-0869.
Atomic Industrial Forum	
The cost impact of $550,000/plant used in value/impact analysis is low by at least a factor of 2.	Costs impacts were re-evaluated based on cost estimate information received from AIF and other respondees
Economic considerations related to reduced probability of plant damage should be excluded from the cost-benefit balancing. Decisions should be based primarily on the value/impact ratio.	The essence of a value/impact analysis is that it attempts to identify, organize, relate, and make "visible" all the significant elements of value expected to be derived from a proposed regulatory action as well as all significant elements of impact. The net values are compared with the net impacts. Thus if a proposed safety improvement is accompanied by an adverse side effect, the impairment is subtracted from the improvement to arrive at a net safety value for consideration in the value/impact assessment. Similarly, when the immediate and prospective cost impacts are summed, they should include all elements of economic impact on licensees, such as costs to design, plan, install, test, operate, maintain, etc. Plant downtime or decreased plant availability is included when applicable. The summed impacts, however, should be net impacts, for comparison with net values. Thus, any reductions in operating costs, improvements in plant availability, or reductions in the probability of plant damage are properly a factor in determining net adverse economic impact. Future economic costs and savings are appropriately discounted.

Table 3 (Continued)

Comment	NRC Staff Response
	Qualitative differences among impact elements are respected, and distinctive elements of impact (of which averted plant-damage probability, as a favorable rather than adverse impact, is a prominent example) are separately identified, for appropriate consideration in regulatory decision making. The ratio of avoided public dose to the gross cost of implementation is ordinarily a major decision factor. However, it is not by itself always a good guide to a sound regulatory decision. The issues involved are often too complex for a decision on this criterion alone. Other factors that enter, often in important ways, may include any economic benefits that reduce a net adverse economic impact, the safety importance of the issue, and values and impacts that cannot or cannot readily be quantified; for example, jeopardy to a defense layer in the defense-in-depth concept or expected reductions in plant availability that can be foreseen but not precisely estimated. A sound regulatory decision rests on adequate consideration of all significant factors. An overly simple approach can mislead if it simplifies away complexities that are the essence of the issue at hand.
The assumption that sump failure will occur in 50% cases of the large LOCAs should be justified.	A detailed sump blockage probability analysis has been performed and is reported in NUREG/CR-3394. The results show a wide range of sump blockage failure probabilities (i.e., 3E-6 to 5E-5/reactor-year) and a high dependency on plant design and operational requirements. These results are reflected in a revised value impact analysis utilizing a range of sump failure probabilities.
The use of PWR release categories from WASH-1400 is too conservative. Containment failure probabilities used in WASH-1400	The containment failure probabilities and release categories used in the regulatory analysis for USI A-43 were based on information presented in WASH-1400, and

Table 3 (Continued)

Comment	NRC Staff Response
are inadequate to describe the nuclear industry's present knowledge in this field. Releases due to "vessel steam explosion" are unrealistic and should not be considered.	also on other considerations. The comments presented by an AIF subcommittee regarding the validity of continued use of WASH-1400 assumptions, etc. are being evaluated through other activities such as: reevaluation of source terms, SASA studies, etc. USI A-43 regulatory analyses were based on the following considerations and for the reasons noted: (1) WASH-1400 assumptions were utilized to provide a common baseline calculations for reference plants and were used to estimate increases in releases due to a postulated loss of recirculation flow capacity. Until revised failure mechanisms and new source terms are determined, this approach provides a consistent set of calculations. (2) Although using a small containment failure probability associated with steam explosion would be more appropriate, release category PWR-1 (which includes steam explosion) was not a dominant contributor to release. Release categories PWR-2, -4, and -6 were the dominant pathways contributing to increases releases due to a failed sump for the plants analyzed. (3) Basing release effects on the assumption of simultaneous failure of core cooling and loss of containment sprays is conservative. If containment were not lost (as would be the situation for PWRs that have dry containments with safety-grade fan cooler systems), the LOCA energy could be disspated without containment overpressurization and failure. Thus releases associated with PWR-2 and -4 categories could be discounted and PWR-6 releases only used. Such considerations have been incorporated into this revised regulatory analysis.

Table 3 (Continued)

Comment	NRC Staff Response
	(4) Other factors--such as containment structural design margins that argue against gross containment failures (as postulated in WASH-1400), realignment to alternate water sources, controlled venting for BWRs, etc.--have also been considered this revised regulatory analysis.
The use of the CRAC Code and a "no-evacuation," 50-mile-radius model to develop public doses is unrealistic.	The 50-mile radius reflects a substantial part (though not all) of the total population dose, and is thus a reasonable index of the radiological effect on the public. Standardization of calculations to that radius is helpful in comparing risks associated with different issues and average such risks for use with the 1000 person-rem/$M criteria. Evacuation of people is not considered because calculations suggest that, although it may sometimes be important for people directly affected, the effect of evacuation on the total population dose is likely to be small.
NRC should utilize information developed more recently (i.e., NUREG-0772) to reassess and reduce the source terms, rather than continue to use the PWR-2 and PWR-3 release categories from WASH-1400.	Possible changes in the source terms are being considered by the special task force established by the Commission to review the source-term issue. Changes would be premature before this group completes its evaluation and the new values are accepted by all parties involved.
NRC should utilize the "leak before break" concept in evaluating the safety significance of A-43.	Elastic-plastic fracture mechanics analysis techniques to analyze pipe break potential has been used in USI A-2, with a limited number of PWRs being analyzed. For USI A-2, the submittal of such analyses for specific break locations (on a plant-specific basis) will require obtaining an exemption from the requirements of GDC 4. Submittal of such analyses to address the USI A-43 debris blockage issues would be reviewed by staff on a plant-specific basis, should a licensee or applicant elect to utilize this approach.

Table 3 (Continued)

Comment	NRC Staff Response
BWR Owners Group	
After quick review of the proposed revision to the regulatory guide, the BWR Owners Group and GE maintain that USI A-43 is not a generic issue for BWRs.	The requirement for long-term decay heat removal is applicable to light-water reactors, both BWRs and PWRs.
The revisions to RG 1.82, which now proposes specific criteria for BWRs, should apply only to light-water reactors that have any potential for harmful debris generation (i.e., light water reactors that extensively use fibrous insulation).	All types of insulation should be evaluated for the potential of debris generation, transport, and suction strainer blockage. The wide variation in plant designs and insulation employed does not support a generic statement.
These comments and any future comments by the BWR Owners Group should not substitute for the normal notice and comment procedure that allows potentially affected licensees to respond to proposed regulatory guide changes.	RG 1.82, Revision 1 (along with NUREG-0897, NUREG-0869 and SRP 6.2.2, Revision 4) was issued "for comment" in May 1983. Only 14 responses were received as of September 1983. Some of these comments (in particular GE's July 11, 1983 letter) cited a need to specifically address BWR-related concerns in the RG. This was done and copies were sent to GE and the BWR Owners Group. Given the previous extensive distribution of "for comment" reports and regulatory positions and the rather small number of responses, the staff does not plan to reissue RG 1.82, Revision 1 for comment. The NRC staff will incorporate additional valid technical points received from the BWR Owners Group and GE. The most recent input from the BWR Owners Group (July 16, 1984) does not provide new significant findings; rather this input re-expresses concerns previously voiced and stresses possible misinterpretations of wording in RG 1.82, Revision 1.

Table 3 (Continued)

Comment	NRC Staff Response
Commonwealth Edison	
The Commission has not sufficiently justified the need to impose retrofit requirements on either operating or near-term operating license units.	A-43 resolution does not mandate retrofits; rather, applicants are requested to assess long-term recirculation capability utilizing RG 1.82, Revision 1 and to then determine what corrective actions may be needed. The use of an information bulletin to the majority of the plants does not constitute imposition of a retrofit.
Cost estimates for surveys, design reviews, and retrofitting are questionable.	The A-43 value/impact evaluation has been revised based on detailed sump blockage probability studies (NUREG/CR-3394) and cost estimates received from industry responses.
The proposed RG 1.82 is overly conservative. However, given the need for assurance that the recirculation sump remains a reliable source of cooling water, the commentor agrees that an evaluation of sump designs, potential for debris, air ingestion, and adequate net positive suction head (NPSH) is fully justified.	The NRC staff acknowledges that conservatisms exist in RG 1.82, Revision 1. However, such conservatisms are prompted by the limited amount of available information regarding insulation destruction due to high pressure jets and attendant debris generation, and the wide variability of plant designs and types of insulation used.
The commentor questions the assumption that 50% of LOCAs lead to sump loss, the value/impact ratio given uncertainties in estimated costs, the basis for assuming 23 years remaining plant life, etc.	A detailed sump failure probability analysis was performed and is reported in NUREG/CR-3394. The "averaged" sump failure probability was 2E-5/reactor-year with a range of 3E-6 to 5E-5/reactor-year.
Consumers Power	
Regarding the proposed Revision 1 to RG 1.82, the commentor stated (1) that Appendix A should be clearly delineated as being an information and guidance source, not as presenting design requirements, and (2) that consistency is needed with respect to NPSH terminology.	Appendix A of proposed RG 1.82, Revision 1 was always intended to provide additional information and/or guidance, not design requirements. Appendix A has been clearly labeled as such.

Table 3 (Continued)

Comment	NRC Staff Response
Regarding the value/impact analysis, the commentor questioned the assumption that 50% of the loss-of-coolant accidents (LOCAs) lead to sump blockage and cites a sump failure frequency of 2×10^{-4} per demand from another probabilistic risk analysis.	That 50% of LOCAs lead to sump blockage has been reevaluated (see NUREG/CR-3394), and the results of that detailed study have been used in revising the A-43 release estimates.
The commentor questioned the direct application of core melt frequency reduction for computing avoided accident cost. The commentor disagrees with taking credit for loss of plant cost. Rather, the commentor states that loss-of-plant costs should be deducted from avoided accident costs.	The calculation of avoided accidents costs, loss-of-plant costs, etc., are consistent with current NRC staff evaluation practices. Recalculation of the parameters previously used will be carried out with the revised blockage frequencies.
Creare	
The beta factor used to predict a pump's required NPSH in an air/water mixture is based on data whose scatter was not reported. The NUREG should note this and caution the applicant and reviewer to carefully consider the adequacy of the NPSH margin if it is marginal.	Efforts were made to obtain the original data tapes and calculate the data's scatter; however, this information was not readily available. The suggested cautionary note has been added to NUREG-0897.
The use of an arbitrary minimum allowable NPSH margin, either as a fixed value (i.e., 1 foot) or as a percentage value (i.e., 0.5 x margin with no screen blockage), is not justifiable. It should be recognized that what constitutes a safe NPSH margin is a plant-specific judgment.	NUREG-0897 and RG 1.82, Revision 1 no longer recommend a minimum allowable NPSH margin. Instead, they note that whatever NPSH margin is available (after accounting for hydraulic and screen blockage effects) should be evaluated with respect to each plant's long-term recirculation requirements.
Diamond Power Company	
NUREG-0897 resolves a significant safety problem in a thorough and equitable manner.	The NRC staff concurs.

Comment	NRC Staff Response
The commentor provides recommendations regarding the classification of various insulating materials, particularly on the need to distinguish between totally encapsulated insulation and jacketed insulation.	The proposed classifications have been combined with other similar proposals to revise and clarify the insulation classification and descriptions used in NUREG-0897.
The commentor provides listings of the types of insulations purchased since 1980 and the types of insulations used in recent retrofittings.	The information has been added to NUREG-0897 and NUREG-0869, along with data received from other manufacturers.
The commentor states that the costs in the value/impact analysis are in agreement with its costs and provides the following figures: Cost of MIRROR™ reflective metallic insulation = $\$40/ft^2$ for material alone. Installation cost, excluding material = \$25/hour. Productivity = 1.24 hours/ft^2 of insulation.	This cost information has been reflected in the revised value/impact analysis (NUREG-0869), along with other industry cost figures.

Table 3 (Continued)

Comment	NRC Staff Response
Reflective metallic insulation is not the predominant type of insulation used in newer plants. Recently insulated plants mainly use fiberglass insulation.*	Information supplied by Owens-Corning Fiberglass Co. and the Diamond Power Co. regarding types of insulation used in existing and future reactors has been added to NUREG-0897 and NUREG-0869. These reports have been revised to reflect this new information. The trend appears to be toward a greater use of fibrous insulations.
A report on HDR test results on MIRROR™ insulation performance during LOCA conditions was submitted to provide additional information for the existing data base used in resolution of USI A-43.**	This report has been included as Appendix E in NUREG-0897, Rev. 1. The results of this report do not support a hypothesis which postulates free and undamaged inner foils being available to transport at low velocities and to cause blockage. However, the limited data base precludes developing a detailed debris generation model.

* Letter of July 11, 1983.
** Letter of December 6, 1984.

Table 3 (Continued)

Comment	NRC Staff Response
General Electric Company	
SRP 6.2.2 and RG 1.82, Revision 1 make no distinction between BWRs and PWRs; regulatory criteria should differentiate between various plant designs.*	RG 1.82, Revision 1 and SRP 6.2.2 have been modified to identify PWR- and BWR-related concerns. Regulatory Guide 1.82, Revision 1, has been renamed "Water Sources for Long-Term Recirculation Cooling Following a Loss-of-Coolant Accident."
Reference should be made to technical findings that imply that A-43 concerns do not pose a serious problem for BWRs.*	Based on the responses received, the A-43 technical findings will be revised to reflect (1) that there is a more extensive use of fibrous insulations (i.e., NUKON™) than previously identified and (2) that BWRs are reinsulating with NUKON™. NUREG-0897 will reflect current findings and identify both PWR- and BWR-related concerns.
The value impact analysis utilizes a PWR for the risk assessment and PWR-oriented industry impacts and, as such, is not directly applicable to BWRs.*	GE's point on utilizing a PWR probabilistic risk assessment for drawing conclusions for a BWR is acknowledged. Similar assessments have been made for BWRs and those results have been utilized in preparing this revised regulatory analysis.
General Electric has reviewed the proposed revisions and has concluded that the design requirements proposed in RG 1.82, Revision 1 are excessively prescriptive and not generically applicable to the BWR.**	The requirement for long-term decay heat removal is applicable to both BWRs and PWRs. RG 1.82, Revision 1, Appendix A contains a series of tables (or guidelines) that have been derived from extensive tests and analytical studies. This information is provided for ease of referral and can, or need not, be used--at the user's option. RG 1.82, Revision 1 is general, and not prescriptive. The applicant has the responsibility for design submittal and justification of the safety aspects thereof.

* Letter of July 11, 1983.
** Letter of October 17, 1983.

Table 3 (Continued)

Comment	NRC Staff Response
The proposed RG should be revised so that no further requirements are imposed on designs that have already included precautions that preclude air ingestion into, or blocking of, suction lines used for long-term decay heat removal.*	The technical findings in 1983 (versus earlier findings) are considerably different, particularly with respect to insulation employed currently and the transport characteristics of insulation debris. The air ingestion potential has been experimentally quantified and found to be small. However the 50% blockage criterion in the current RG 1.82 permitted applicants to essentially bypass the debris blockage question. For those plants where design precautions can be clearly demonstrated, further actions (retrofits) are not necessary.
In addition, the proposed RG should be further revised to provide for alternative means of ensuring that long-term heat removal is not lost as a result of suction blocking or air ingestion.*	The licensee and/or applicant always has the option to propose alternate means to deal with a particular design or safety problem.
In the SER for GESSAR, the NRC indicated that USI A-43 posed no problem for the Mark III containment configuration.*	At the time the SER for GESSAR II was written, A-43 concerns relative to BWRs were still under evaluation. The staff's SER cited several elements of the GESSAR II design that tended to reduce the probability for blockage of the RHR suction inlets due to LOCA-generated debris. The staff concluded that plants referencing the GESSAR II design could proceed, pending resolution of USI A-43, without endangering the health and safety of the public while the staff completed its evaluation of GESSAR. The unique aspects of each Mark III plant design should be evaluated during plant-specific reviews of A-43 concerns.

*Letter of October 17, 1983.

Table 3 (Continued)

Comment	NRC Staff Response
The tests performed by Alden Research Laboratory (see NUREG/CR-3616) may even be very conservative for BWRs since it appears the tests utilized sump screens directly on the sump floor.*	The comment is partially correct, because BWR RHR suction inlets are located at some elevated distance above the wetwell or suppression pool floor. However, the insulation debris transport characteristics (see NUREG/CR-2982, Rev. 1) showed that low velocities (i.e., 0.2 - 0.3 ft/sec) can transport fragmented debris and are applicable to both BWRs and PWRs.
The proposed regulatory guide should be revised to include criteria that will allow alternative measures for precluding loss of long-term decay heat removal due to air ingestion or blockage.*	RG 1.82, Revision 1 states: "This regulatory guide has been developed from an extensive experimental and analytical data base. The applicant is free to select alternate calculation methods which are based on substantiating experiments and/or limiting analytical considerations." Thus, the applicant is free to select alternate methods or measures for precluding loss of long-term decay heat removal.
Earlier surveys on the use of insulation in light water reactors have concluded that most BWRs utilize metallic insulation, which minimizes the potential for formation and subsequent transport of debris to the sump screens.*	As stated above, current findings do not support the earlier surveys or conclusions. NUREG-0897 is being revised to incorporate findings from public comments received (particularly with respect to insulations currently used and the change to fibrous insulation from previously used reflective metallic insulations). Recent tests on the transport of thin stainless steel foils show that this material can be transported at low velocities (i.e., 0.2 to 0.3 ft/sec).

*letter of October 17, 1983.

Table 3 (Continued)

Comment	NRC Staff Response
Gibbs and Hill, Inc.	
Section B does not discuss the fact that sump configurations that differ significantly from the criteria of Appendix A may be equally acceptable. Gibbs and Hill recommends adding the following concluding paragraph to Section B: "If the sump design differs significantly from the guidelines presented in Appendix A, similar data from full-scale or reduced-scale tests, or in-plant tests can be used to verify adequate sump hydraulic performance."	Appendix A (page 19) has wording very similar to the commentor's suggested wording.
Tables A-1 and A-3 are inconsistent and Table A-2 has inconsistencies in water level noted.	The inconsistencies have been corrected.
Northeast Utilities	
Tests show that gratings are as effective as solid cover plate in suppressing vortices.	Gratings were very effective in reducing air ingestion to essentially zero.
The procedure in Appendix B is too prescriptive. The NRC should allow licensees to define and develop their own evaluation methods.	Appendix B in NUREG-0897 presents the staff's technical findings for A-43. Appendix B was included to illustrate major considerations. RG 1.82, Revision 1 is the regulatory document.

Table 3 (Continued)

Comment	NRC Staff Response
Credit should be given for top screen area if it is deep enough to reduce the potential for clogging (RG 1.82, Revision 1, Section C, Item 7).	For those plant designs and calculated plant conditions where this point could be unconditionally substantiated, credit would be given.
The licensee should be free to determine methods of inspection and access requirements (RG 1.82, Revision 1, Section C, Item 14).	Regulatory Guide 1.82, Revision 1 has been revised accordingly.
RG 1.82, Revision 1 will be used to evaluate sumps in operating plants. This may require backfitting at substantial costs.	The need for backfitting will be based on plant-specific analyses that will reveal the need for and the extent of backfitting that might be required. The cost of backfit should be weighed against core melt costs.
Appendix A to RG 1.82, Revision 1 requires obtaining performance data if sump design deviates significantly from the guidelines provided. For operating plants, this may result in costly sump testing.	Appendix A states: "If the sump design deviates significantly from the boundaries noted, similar performance data should be obtained for verification of adequate sump hydraulic performance."
NRC estimates for man-rem costs associated with insulation replacement are grossly underestimated.	The value impact analysis has been revised based on cost data received during "for comment" period.
The value impact analysis addresses only PWRs. If the NRC has concluded that this issue only applies to PWRs, the document should reflect this.	The value impact analysis revision clearly addresses BWR and PWR concerns.
The commentor concurs with the comments submitted separately on this document by the AIF.	The AIF comments are addressed separately; see above.

Table 3 (Continued)

Comment	NRC Staff Response
Owens-Corning	
Detailed comments addressed the wide variation of insulations employed, descriptions, suggested terminology, etc.*	Detailed comments received on insulation types; descriptions, etc. have been used to revise NUREG-0897.
Comments recommended including transport and head loss data for NUKON™ fiberglass tests.*	Data from NUKON™ tests have been referenced and major findings summarized in the revised NUREG-0897.
The commentor questioned Table B-1, Criterion 2, that reflective metallic insulation foil debris would not be transported at velocities less than 2.0 ft/sec.*	Transport tests on reflective metallic foils revealed that they can be transported at low velocities (0.2 - 0.5 ft/sec).
The commentor questioned the concept that if there is all reflective metallic insulation there is no problem.*	Inputs received have been used in revising NUREG-0869.
The commentor recommended changes to various tables as discussed at the June 1 and 2, 1983, public meeting.*	Inputs received have been used in revising NUREG-0869.
The commentor suggested word changes that would minimize singling out fibrous type insulations as the screen blockage concern without considering blockages due to reflective metallic insulation materials.*	Inputs received have been used in revising NUREG-0869.
The commentor addressed the recommended revision to reflect current status of insulations employed in nuclear power plants.*	Inputs received have been used in revising NUREG-0869.

*Letter of June 23, 1983.

Table 3 (Continued)

Comment	NRC Staff Response
The potential for screen blockage by reflective metallic debris has not been adequately addressed. In particular, the water velocities required to transport debris and hold it against the sump screen have not been studied.*	A set of experiments to determine transport velocities (similar to those performed on fibrous insulations) has been completed by Alden Research Laboratory. The results are summarized in NUREG-0897 and used in RG 1.82.
The assumption that all fibrous blankets and pillows within 7 L/D of a break are destroyed is overly conservative. Different designs of pillows have varying resistances to destruction by water jets.*	The 7 L/D criterion is based on experimental studies of representative samples of fibrous pillows exposed to high-pressure water jets. These small water jet studies showed that increasing pressure (40-60 psia) results in destruction of pillow covers and release of core material. Furthermore, blowdown experiments in the German HDR facility showed that fiberglass insulations (even when jacketed) were destroyed within 6 to 12 feet of the break, and distributed throughout containment as very fine particles. Unless conclusive experimental evidence is obtained that accurately replicates the variety of conditions that may exist in a LOCA, it is prudent to retain the conservative 7 L/D criterion. The 7 L/D envelope is a significant reduction from the previously proposed 0.5 psia stagnation pressure destruction criterion in NUREG/CR-2791 (September 1982) and (in general) limits the zone of maximum destruction to the primary system piping and lower portions of the steam generators.

*Letter of July 14, 1983.

Table 3 (Continued)

Comment	NRC Staff Response
The commentor stated that estimated costs for insulation installation and replacement are too low. OCF cost estimates were* Cost of NUKON™ = $90/ft^2 for material (as fabricated) Cost of reflective metallic = $100/ft^2 for material (as fabricated) Installation cost = $112/ft^2 for labor and related support	OCF cost data are utilized in revisions to the value/impact analysis.
The commentor provided recommendations for classification of various insulating materials, stressing differences between NUKON™ (an OCF product) and other fiberglass and mineral wool materials. The commentor also noted the differences between NUKON™ and high density fiberglass.*	Descriptive classifications provided for insulation types have been combined with similar classifications obtained from Diamond Power Company for inclusion in NUREG-0897, Revision 1 and NUREG-0869, Revision 1.
The commentor identified 14 nuclear power plants that have been reinsulated with NUKON™, are in the process of installing NUKON™, or may install NUKON™.*	OCF plant information has been utilized, along with information from Diamond Power Company, to develop a current picture of insulation utilization in nuclear power plants. The major finding is that the number of plants using or planning to use fibrous insulation is larger than previously estimated. For example, the Diamond Power list reveals that 25 of 130 operating and projected plants are utilizing fibrous insulation on primary system components.

*Letter of July 14, 1983.

Table 3 (Continued)

Comment	NRC Staff Response
The commentor recommended inspection surveys of plants to identify actual insulations employed and recommended the modification of a draft generic letter to include this requirement.*	The recommendation for physical plant surveys (or inspection to identify types and quantities of insulations employed) is a good one. However, the generic letter for plant specific evaluation based on actual types and quantities of insulation employed will address this concern.
A report on "HDR Blowdown Tests with NUKON Insulation Blankets" was submitted to support the capability of NUKON™ insulation to withstand the impact of a high pressure steam-water blast.**	This report has been included as Appendix F in NUREG-0897, Rev. 1. The tests demonstrated that jacketed and unjacketed NUKON™ blankets within 7 L/D will be nearly totally destroyed. NUKON™ blankets enclosed in standard NUKON™ stainless steel jackets withstood the blast better; not enough of these tests were performed to allow conclusions to be drawn for similar insulations.
Power Component Systems, Inc.	
A report on "Buoyancy, Transport and Head Loss Characteristics of Nuclear Grade Insulation Blankets," was submitted to describe relative efforts in the area of fibrous insulations.***	The formula provided for fibrous debris blocakge head loss is included in Section 5 of NUREG-0897, Rev. 1.

* Letter of July 14, 1983.
** Letter of February 18, 1985
*** Letter of November 8, 1984

APPENDIX B

PLANT SUMP DESIGNS

AND CONTAINMENT LAYOUTS

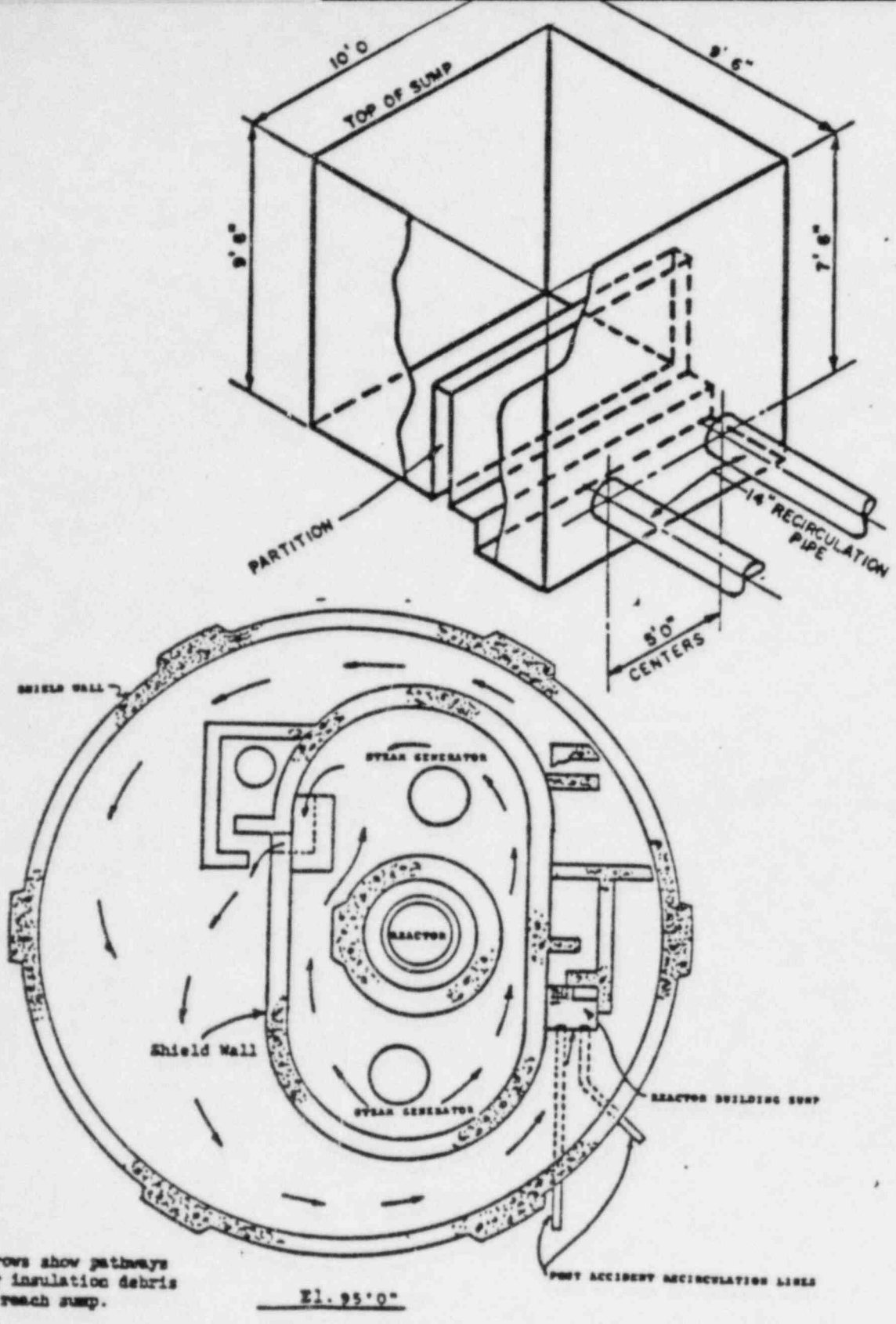

Figure B-1. ECCS Sump and Containment Building Layout, Crystal River Unit 3

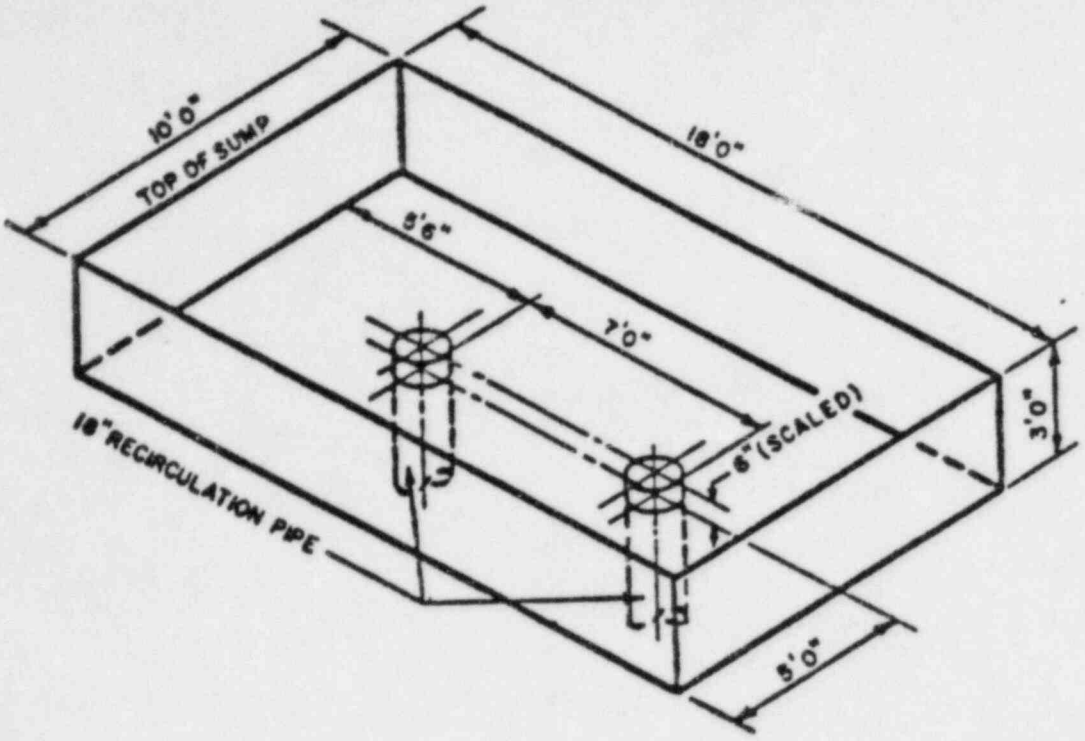

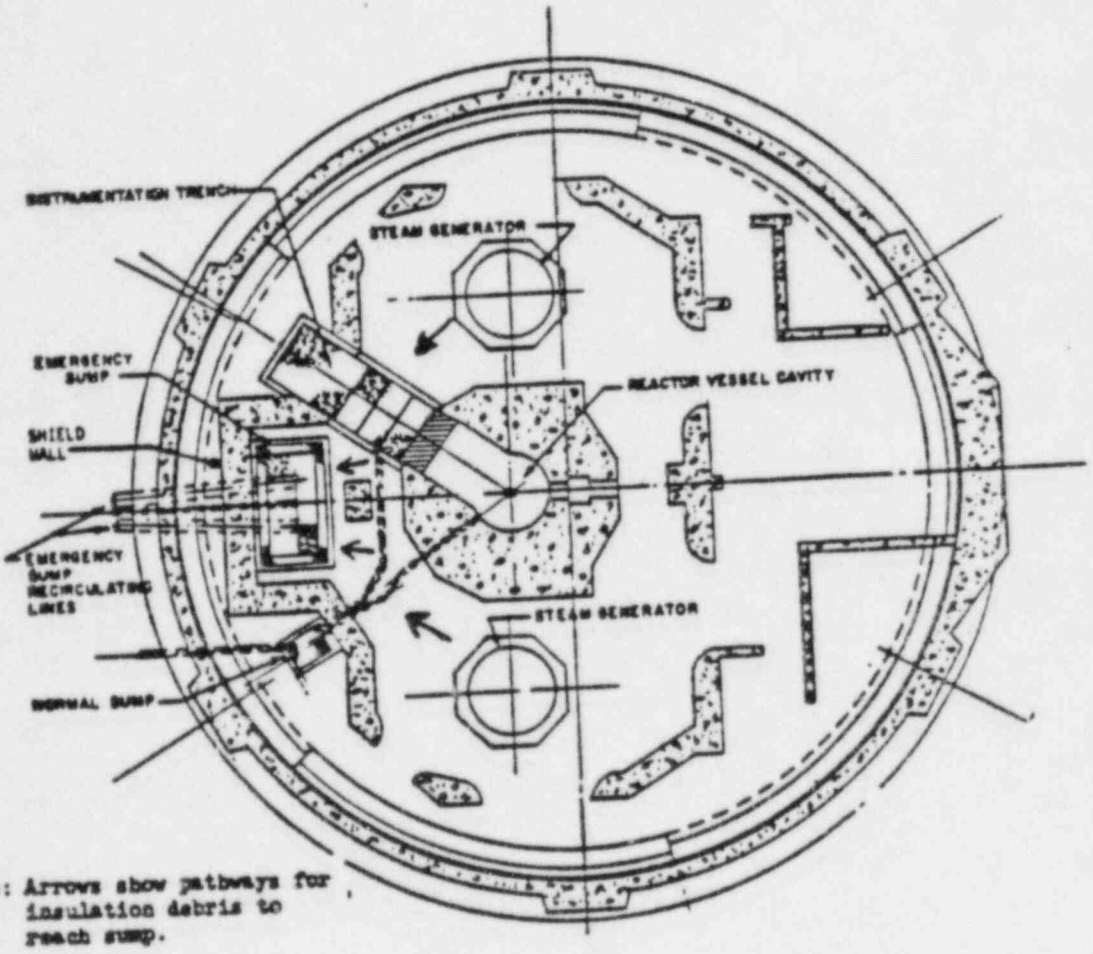

Note: Arrows show pathways for insulation debris to reach sump.

Figure B-2. ECCS Sump and Containment Building Layout, Oconee Unit 3

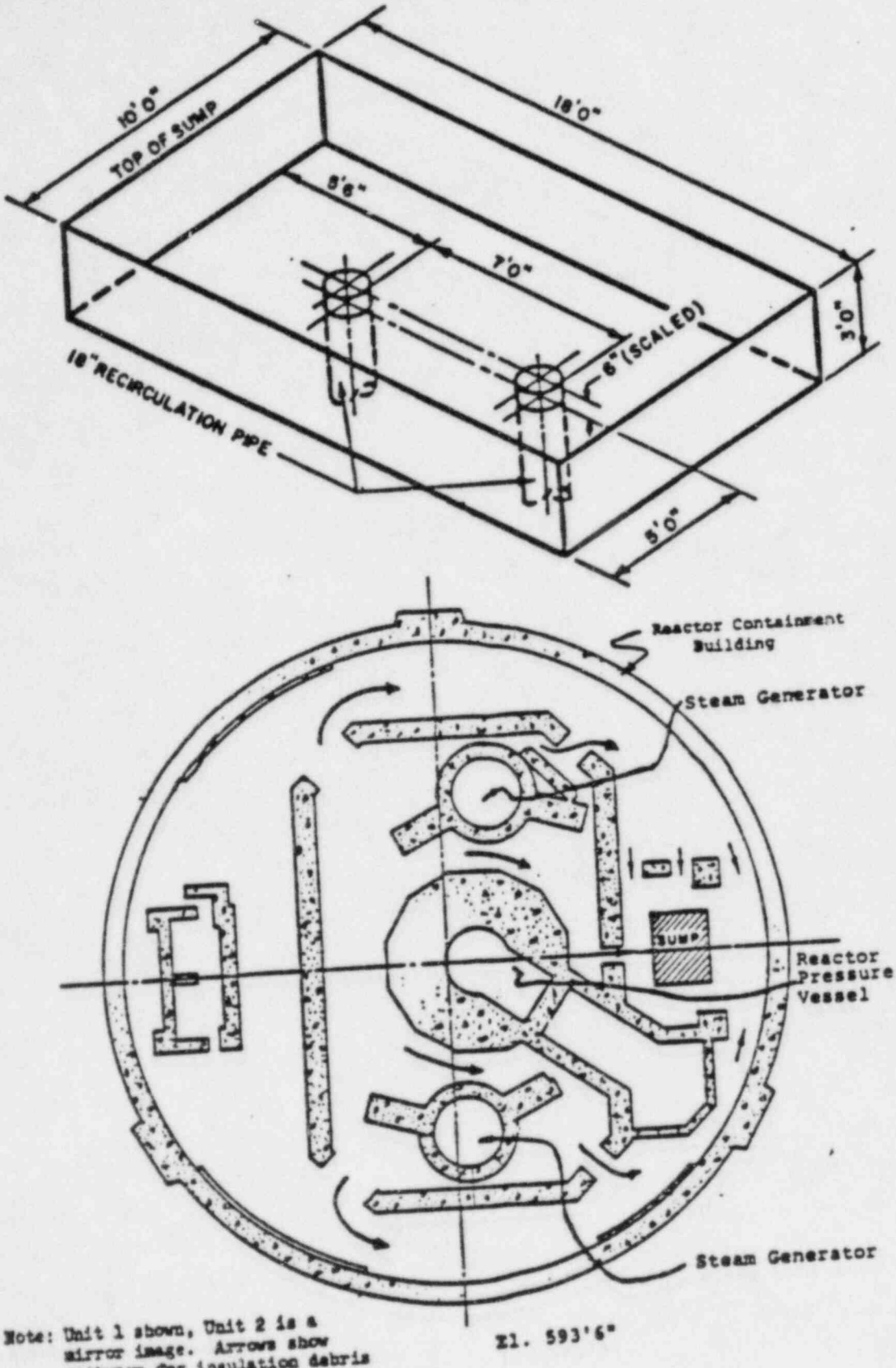

Note: Unit 1 shown, Unit 2 is a mirror image. Arrows show pathways for insulation debris to reach sump

Figure B-3. ECCS Sump and Containment Building Layout, Midland Unit 2

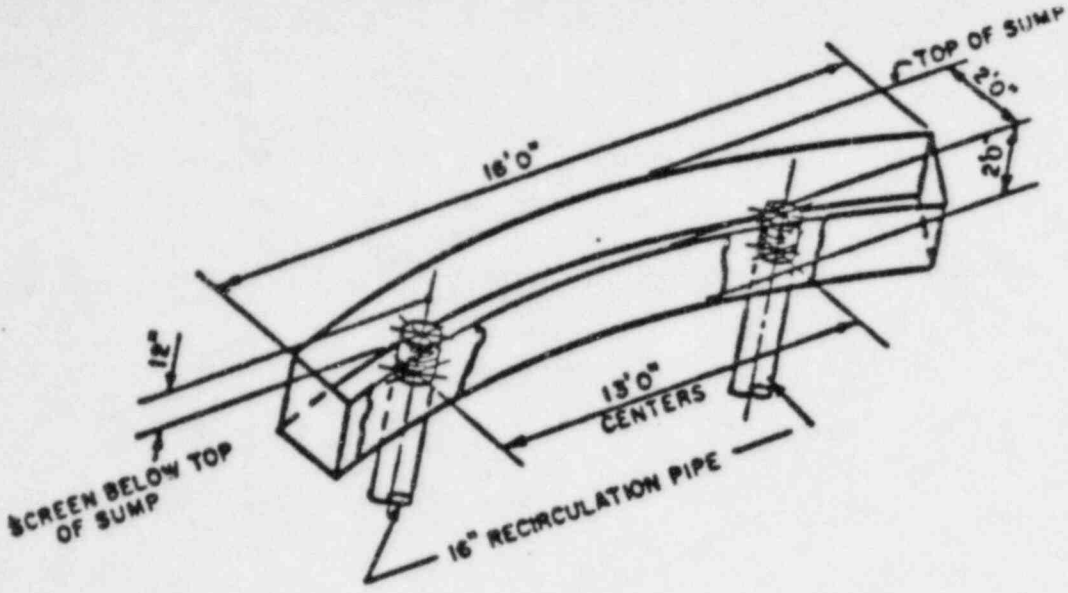

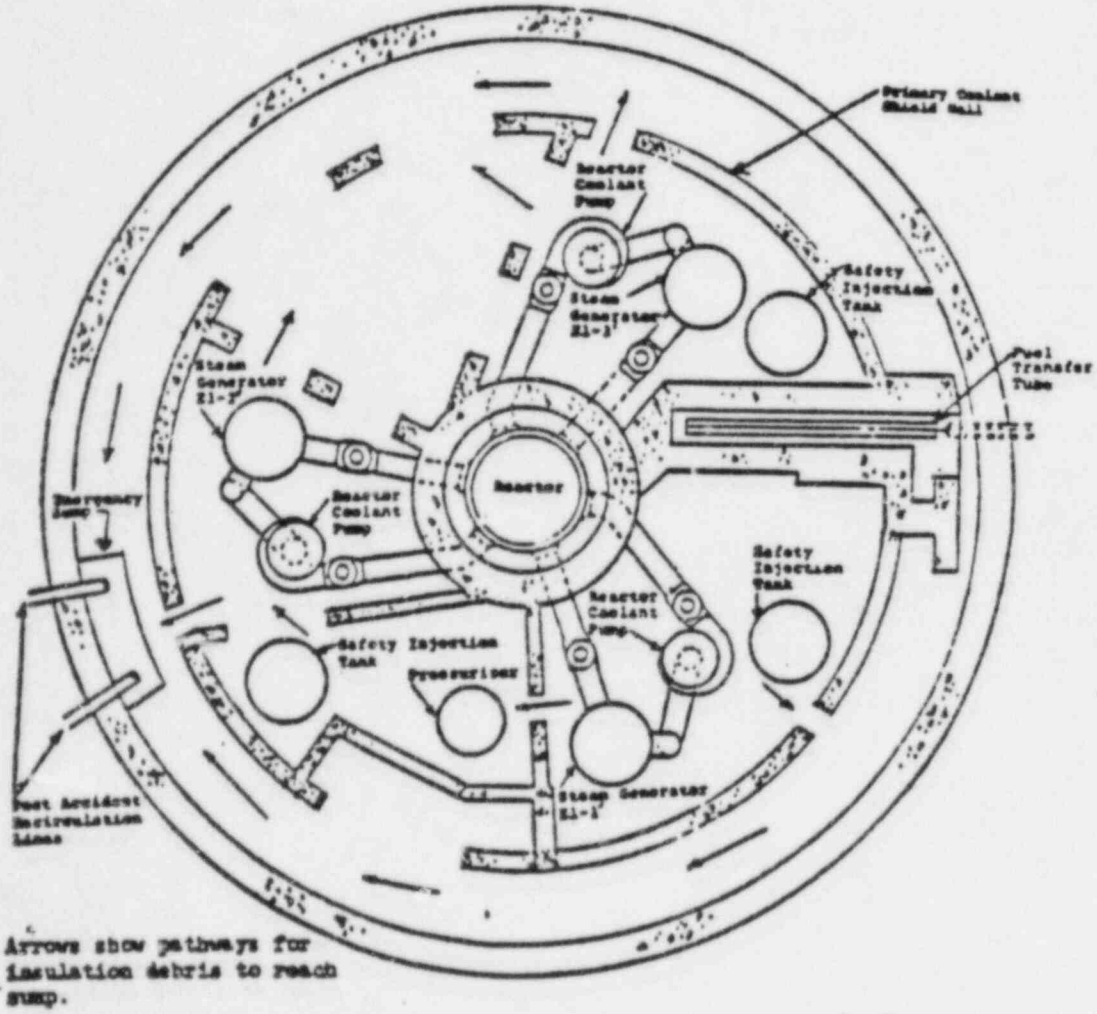

Note: Arrows show pathways for insulation debris to reach sump.

El.-2' 0"

Figure B-4. ECCS Sump and Containment Building Layout, Maine Yankee

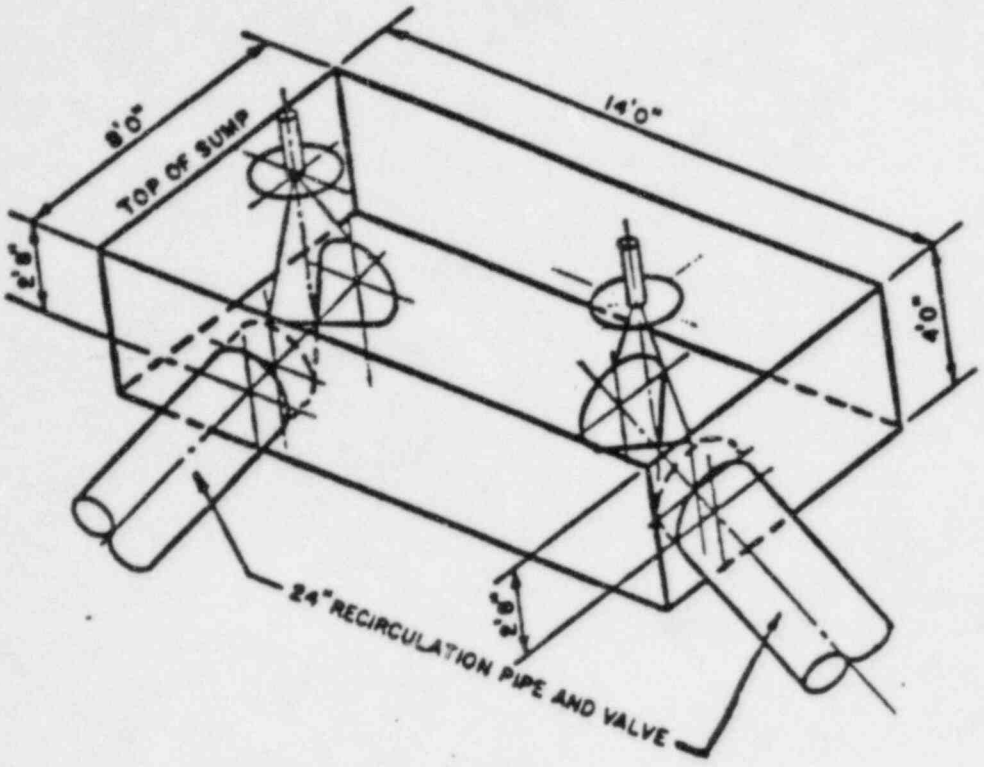

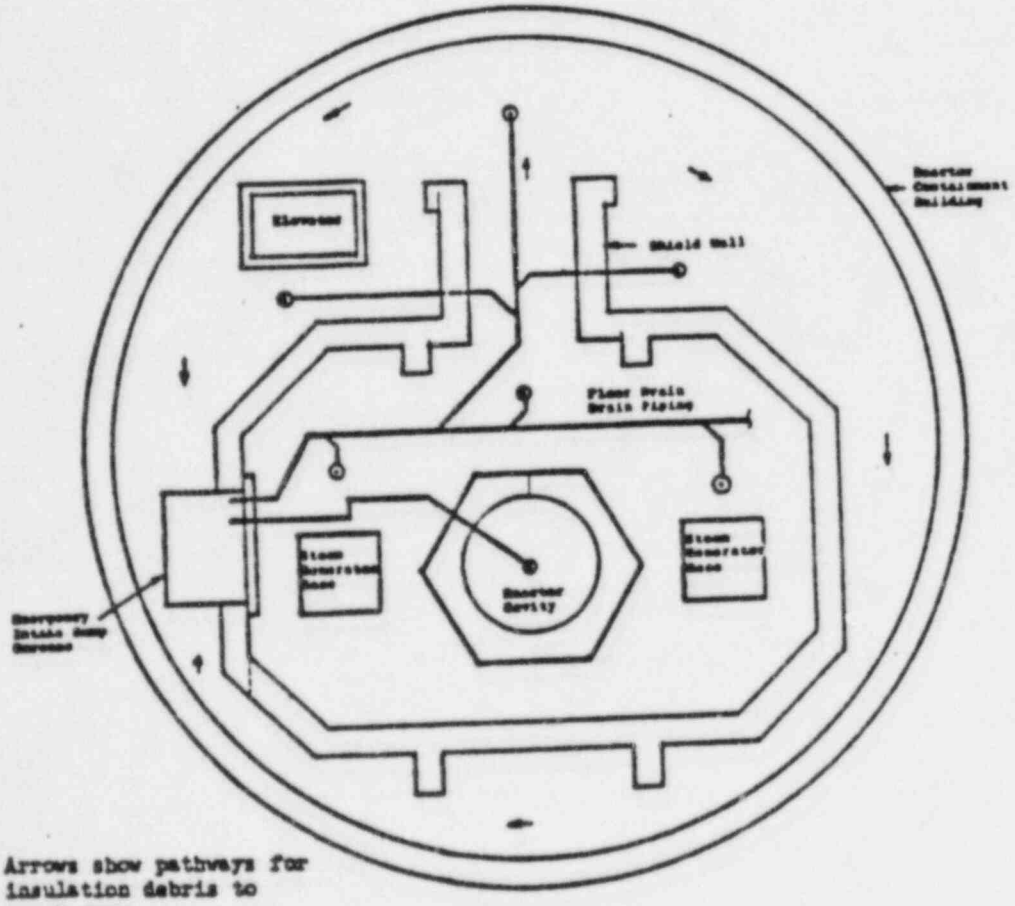

Note: Arrows show pathways for insulation debris to reach sump.

Figure B-5. ECCS Sump and Containment Building Layout, Arkansas Unit 2

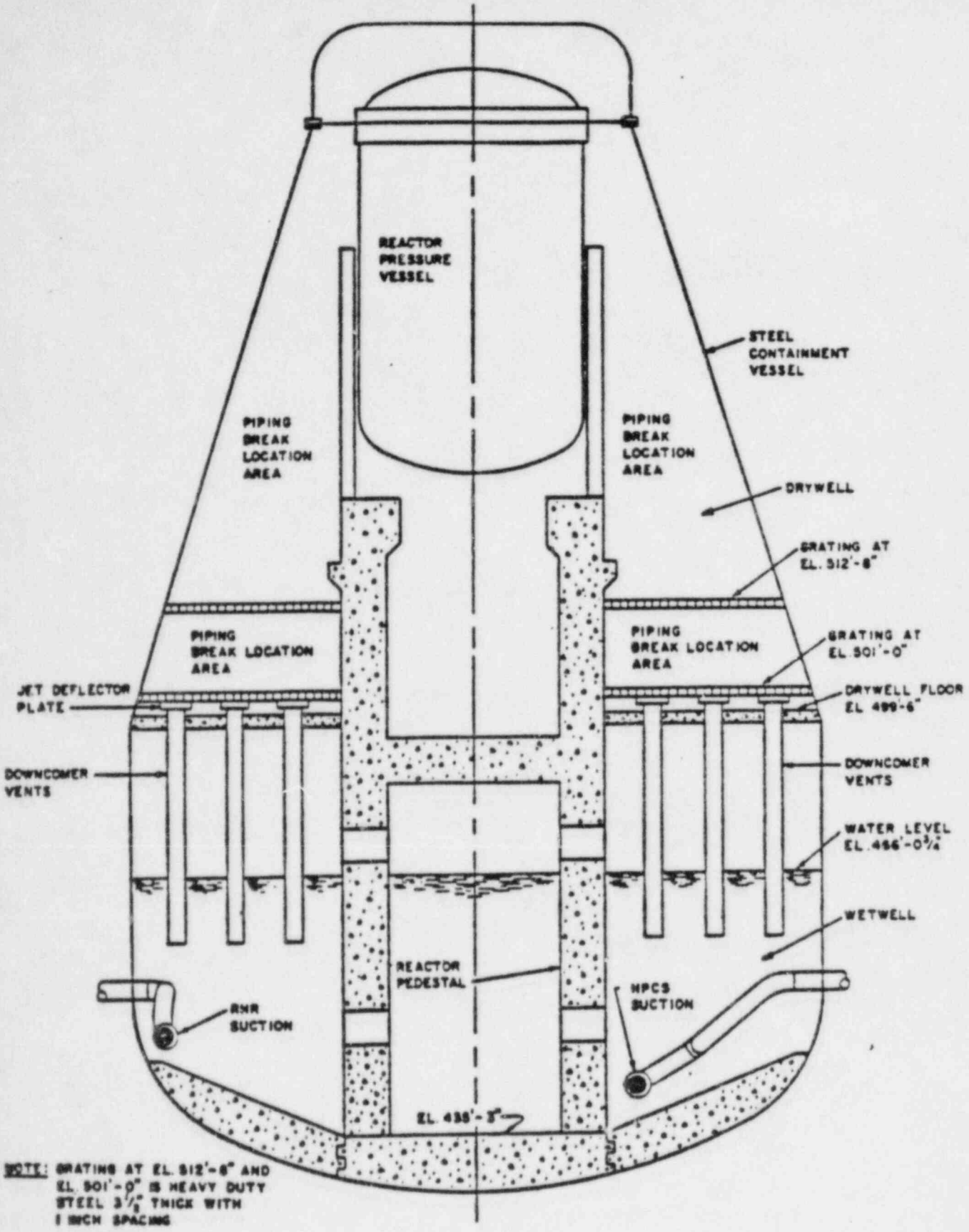

Figure B-6. Primary Containment Vessel, WPPSS Unit 2

APPENDIX C

INSULATION DAMAGE EXPERIENCED IN THE HDR PROGRAM

APPENDIX C

INSULATION DAMAGE EXPERIENCED IN THE HDR PROGRAM

HDR Program and Facility Description*

The Heissdampfreaktor(HDR) safety program (PHDR) represents a major research effort in the Federal Republic of Germany addressing the safety of nuclear power plants. Funded by the Federal Ministry for Research and Technology (Bundesministerium für Forschung and Technologie, or BMFT) and directed by the Kernforschungszentrum Karlsruhe (KfK), HDR experiments at a decommissioned nuclear power plant cover a broad range of topics relevant to nuclear safety. The program was conceived with two basic objectives

(1) to improve understanding of reactor system behavior under upset conditions and define margins of safety

(2) to evaluate and improve design and testing techniques for nuclear systems and components

HDR research is concentrated in the following five areas:

(1) reactor pressure vessel blowdown from typical LWR operating conditions

(2) response of structures and components to such extreme external loads as earthquakes and aircraft impact

(3) structural response and fracture behavior of pressure vessels and piping under both thermal and mechanical loading

---

*Source: Scholl and Holman, 1983.

(4) nondestructive examination of materials

(5) measurement of containment leak rates, both under normal operating conditions and following simulated accidents

The HDR (Heissdampfreaktor or superheated steam reactor) achieved initial criticality in October 1969 as a prototype 100 MWt boiling water reactor (BWR). Although the facility was originally intended to demonstrate the commercial feasibility of direct nuclear superheat, numerous operating problems forced its final shutdown after less than 2000 hours of operation. Rather than restart the HDR as a nuclear facility, the BMFT decided in late 1973 to refit the HDR for light water reactor (LWR) safety research. The reactor internals were removed and the facility decontaminated; new equipment was installed specifically for test purposes. The first blowdown tests at the recommissioned HDR test facility took place in 1977.

The HDR is a real nuclear power plant. That is to say, although it was originally designed nearly 20 years ago, the HDR still offers the following test capabilities relevant to more modern commercial plants:

(1) Actual reactor systems and components can be tested up to 1:1 scale.

(2) HDR systems and components are generically similar in construction and materials to those in use today.

(3) The HDR containment provides a representative basis for investigating pressurization and flow effects in multicompartmented structures following a loss-of-coolant accident.

(4) The HDR can be placed under thermal-hydraulic conditions that subject systems and components to pressure, temperature, and mass flow loads typical of postulated accident scenarios.

The initial thermal-hydraulic state required for HDR blowdown tests (typically 110 bar, 310°C) reflects nominal PWR operating conditions and is produced by a specially designed test loop. The experimental test loop (Versuchskreislauf, or VKL) includes a 4-MW electric boiler for heating circulating water, a cooler with 8 MW of heat rejection capacity, and an appropriate volume and pressure control system. Warm water is fed in at the top of the reactor pressure vessel (RPV) and cold water at the bottom, and water at a mix temperature is withdrawn through a feedwater inlet nozzle. The system is designed to produce either pressure vessel temperature gradients typical of normal PWR operating conditions or uniform (standby) temperatures. Initial tests on the VKL proved it capable of maintaining pressures stable within 1 bar, and temperatures stable within 3°C.

Damage Incurred During Blowdown Tests*

Blowdown tests conducted in the HDR facility showed there were high dynamic loads in the vicinity of the immediate break area. Inspections following these blowdown tests revealed: spalled concrete (attributed to thermal shock), blown open and damaged hatchways (in some compartments doors were torn from their frames), bent metal railings, damaged protective (or painted) coatings, peeled and heavily damaged thermal insulation on the piping and vessels, and scattered insulation debris throughout the containment building. The damage to, and the scattering of, glass wool insulation was particularly severe.

*See Holman, Müeller-Dietsche, and MTller, 1983.

Figure C-1 shows the HDR containment and break compartment. The large number of compartments at various elevations should be noted and utilized when making use of findings for application to U.S. nuclear plants, which are generally much more open, without many intervening compartments. Figures C-2 to C-5 are photographs illustrating damage that recurred. Figure C-7 shows a typical pressure and temperature plot for containment following a blowdown.

Insulation Damage Experienced During Blowdown Tests

NUREG/CP-0033 reports insulation damage as described below.

(1) Insulation (Vessel and Piping)

Standard glass wool insulation with sheet metal covering was torn away within a radius of 3 to 5 meters and distributed throughout containment. A significant improvement was achieved through replacing the glass wool insulation with foam-glass insulation on the pipes.

Insulation on larger vessels in the pressure wave path could be protected by steel bands as long as the pressure loading was from outside to the inside. However, at times the wave pressure loading penetrated beneath the surface and lifted off the protective sheathing.

(2) Insulation (RPV)

The RPV, with its nozzle openings and complex flow patterns, is an exception because the pressure wave propagates to a certain extent from inside to outside. Several types of insulation were tested here with the following results:

- Glass wool with sheet metal sheathing was peeled off and destroyed.
- Foam-glass was destroyed by larger inner overpressure because of its brittleness.

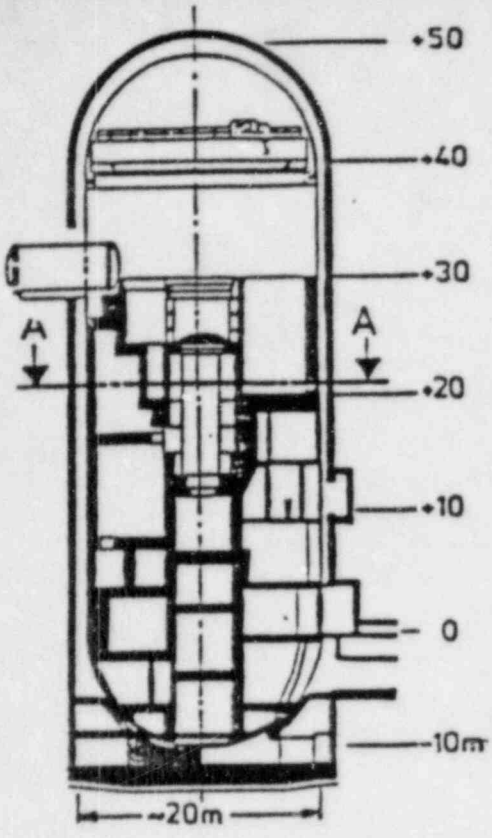

HDR containment.

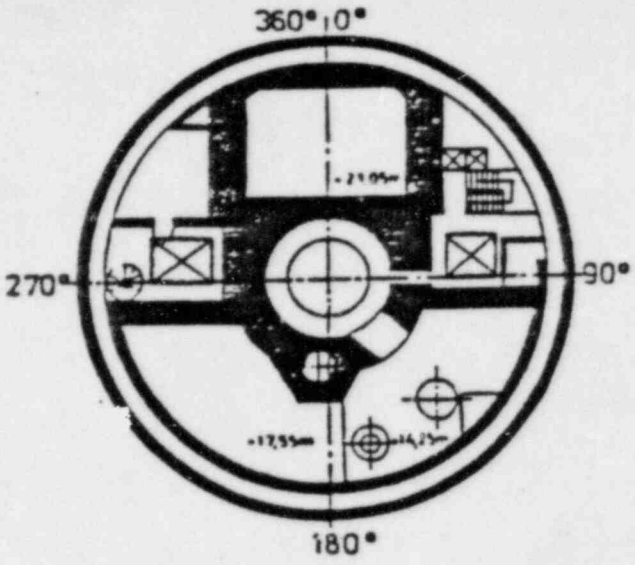

Cross Section A-A

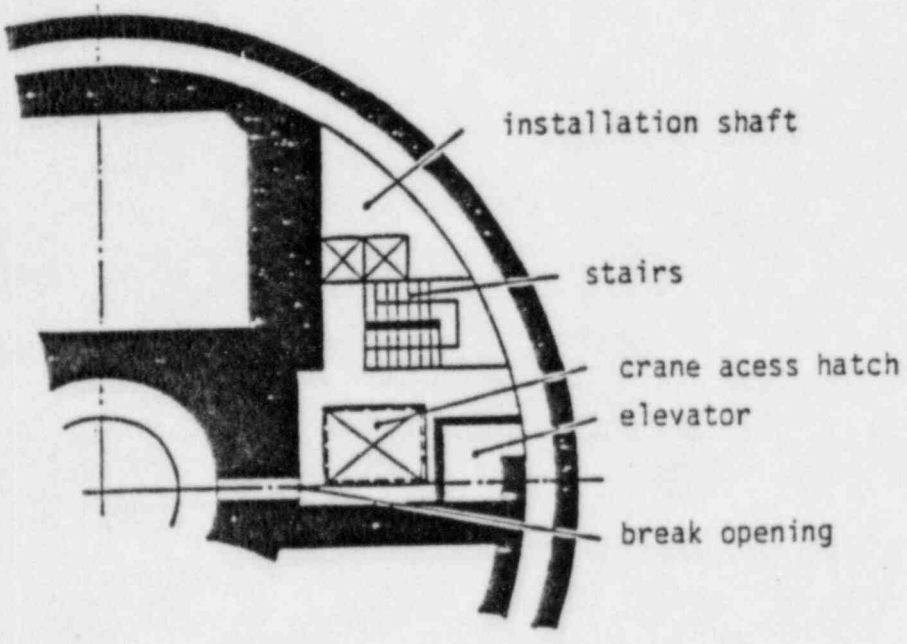

Figure C-1 HDR containment and break compartment

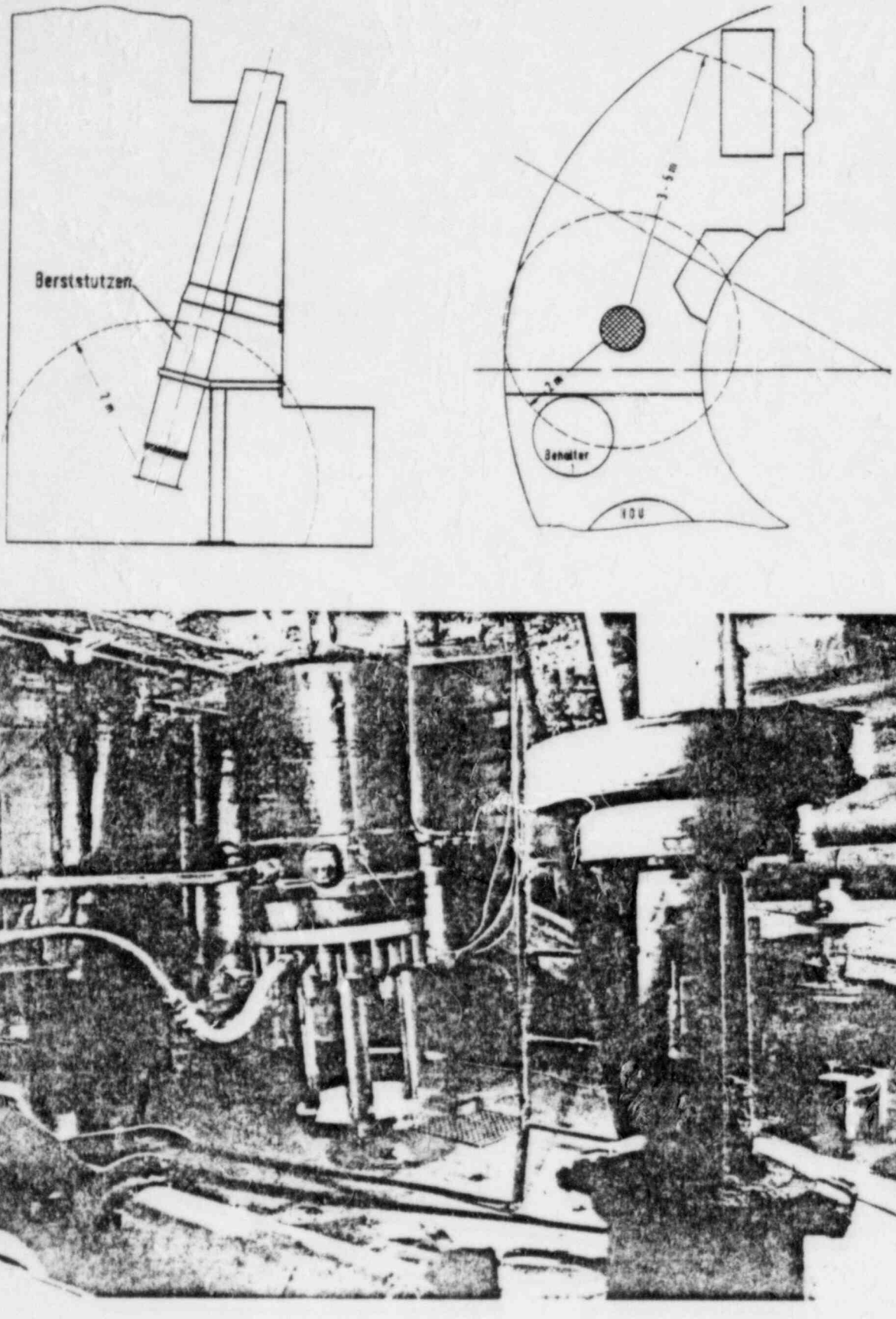

Figure C-1 HDR blowdown compartment and photo of local damage near the break nozzle

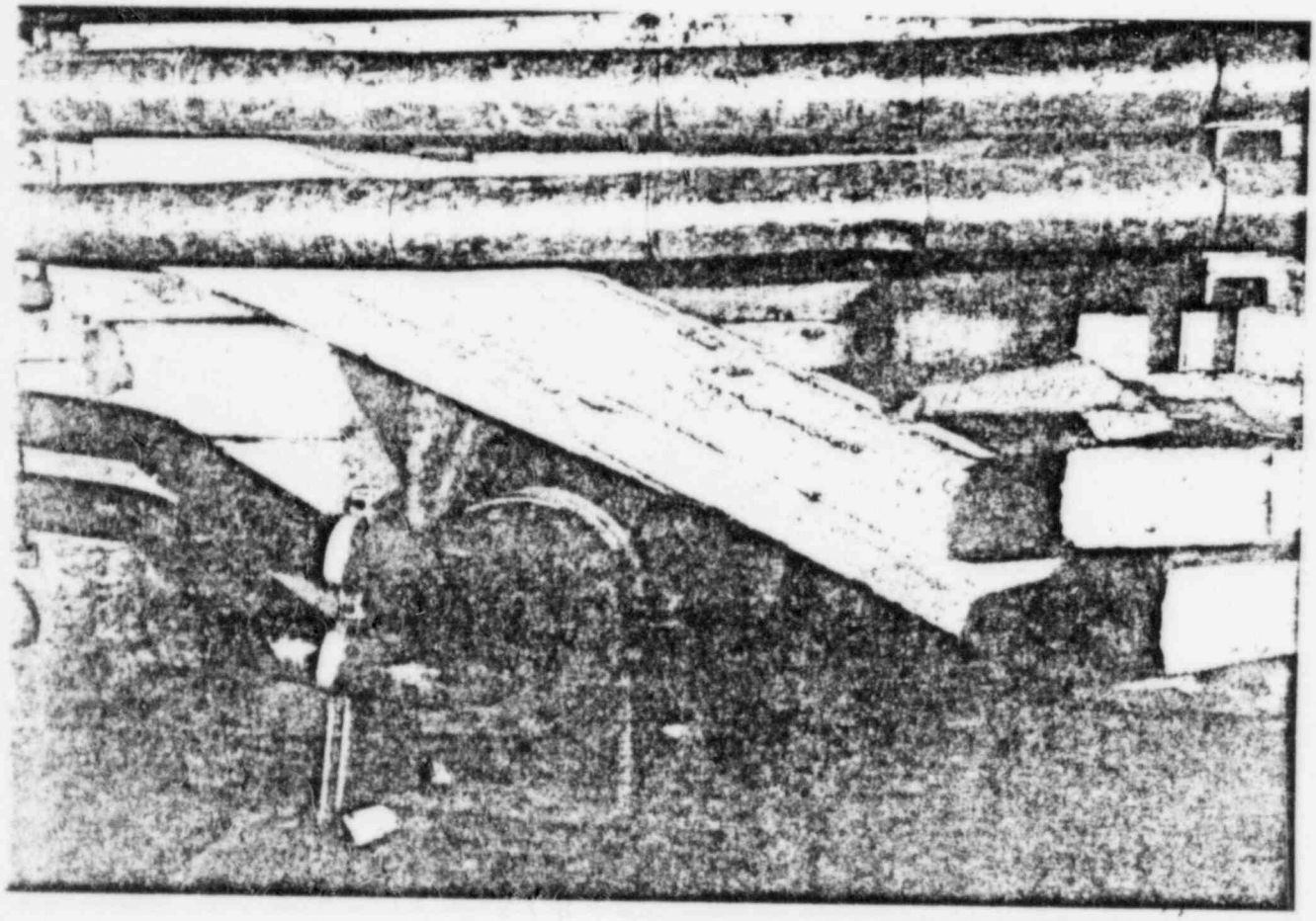

Figure C-3 HDR post-blowdown damage to concrete structures within blowdown compartment

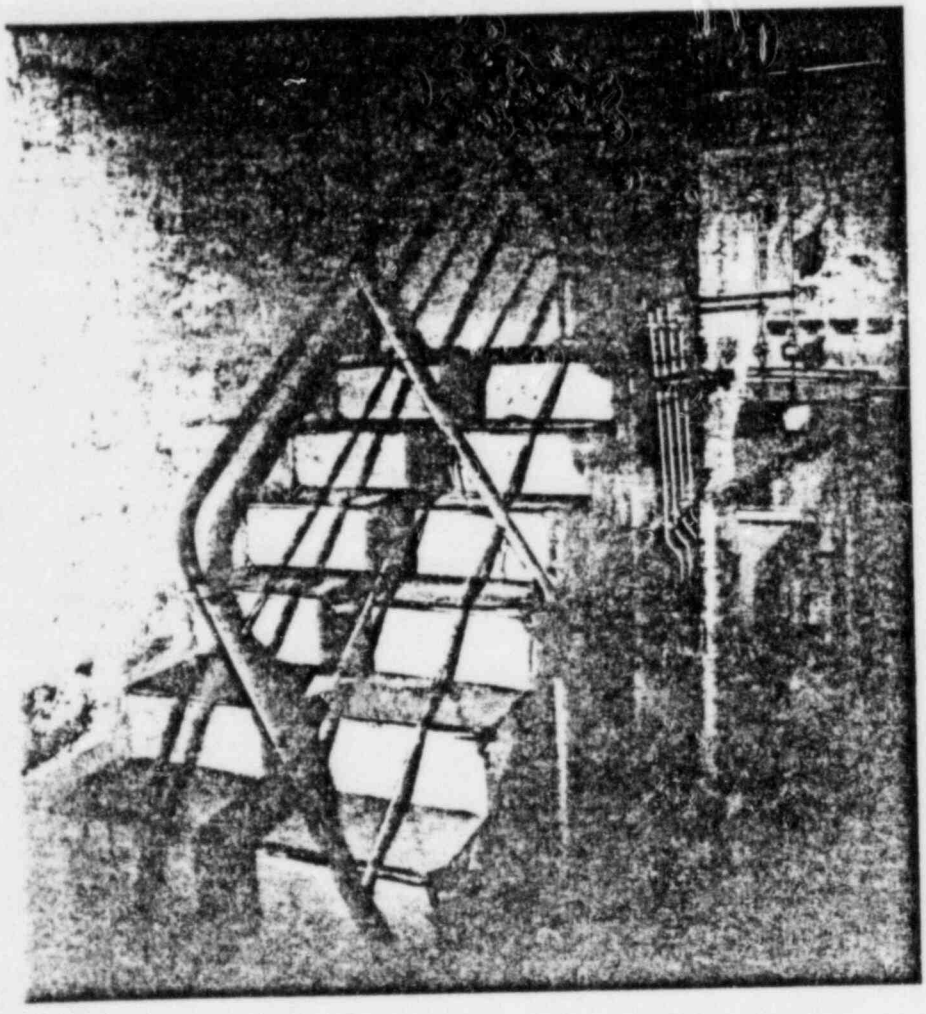

Figure C-4 HDR post-blowdown damage to railing structures in compartment near blowdown chamber

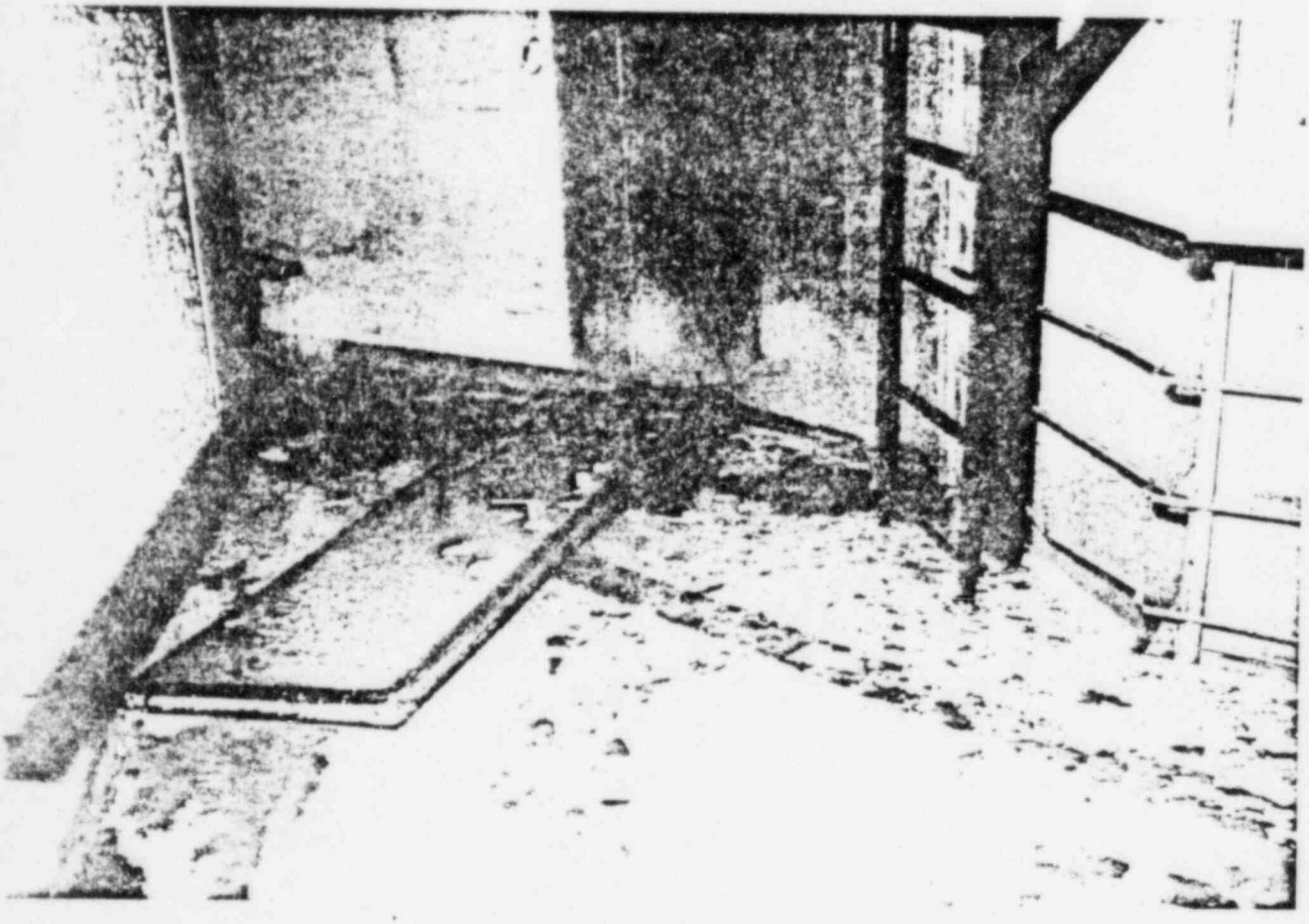

Figure C-5 HDR post-blowdown damage to compartment doors due to pressure wave. Debris shown is spalled concrete from stairwell located near blowdown compartment.

Figure C-6 HDR post-blowdown damage to insulated piping within the blowdown compartment

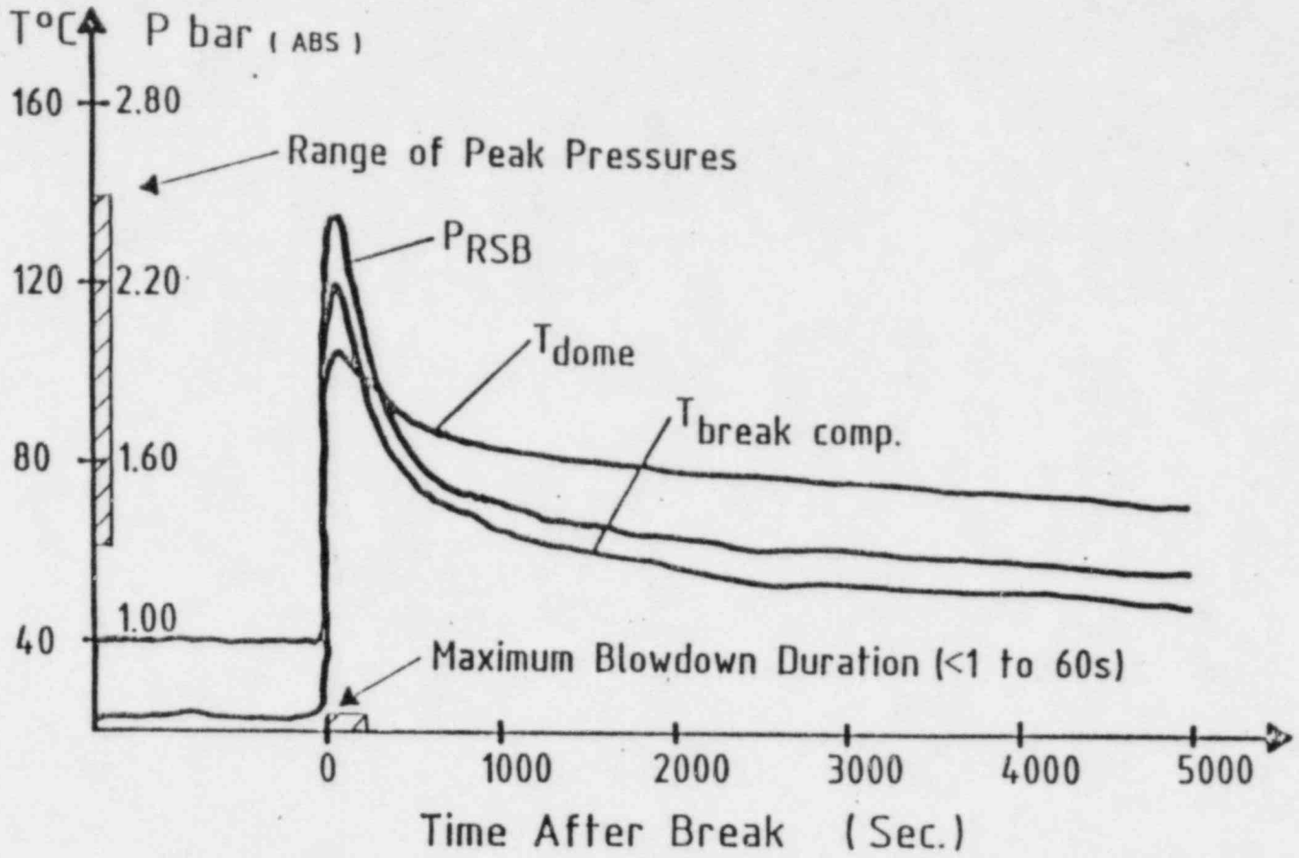

Figure C-7 Typical pressure and temperature in containment after blowdown

Foam-glass insulation sheathed in stainless steel proved more resistant to pressure waves and jet impingement loads because its connecting joints yield to inner overpressure and suppress it.

Insulation mats with glass wool inserts and pure textile or wire-weave-strengthened covers resisted pressure waves and jet forces equally well.

Figures C-8 and C-9 illustrate the insulation damage incurred.

Two letters from the HDR staff that provide further information regarding insulation are included in their entirety in this appendix. Two other documents that are pertinent to this subject are "Investigations of the Transport Behavior of Particles During a Blowdown Test at HDR," GKSS Report 83/E/9, and "Considerations Related to Accident Induced Debris Distribution in a Pressurized Water Reactor Containment," GKSS Report 83/E/8, December 1982. Both documents were written by M. Kreubig and translated by G. Holman of Lawrence Livermore National Laboratory.

References

Holman, G., W. Müeller-Dietsche, and K. Muller, "Behavior of Components Under Blowdown and Simulated Seismic Loading," paper presented at the ASME Pressure Vessel and Piping Conference, Orlando, Florida, July 2, 1982.

Müller, K., G. Holman, and G. Katzenmier, "Behavior of Containment Structures During Blowdown and Static Pressure Tests at the HDR Plant," in Proceedings of the Workshop on Containment Integrity, Vol II of II, U.S. Nuclear Regulatory Commission Report NUREG/CP-0033, October 1982 (see also Sandia National Laboratory, SAND-82-1659).

Scholl, K. H. and G. S. Holman, "Research at Full Scale: the HDR Program" in Nuclear Engineering International, January 1983.

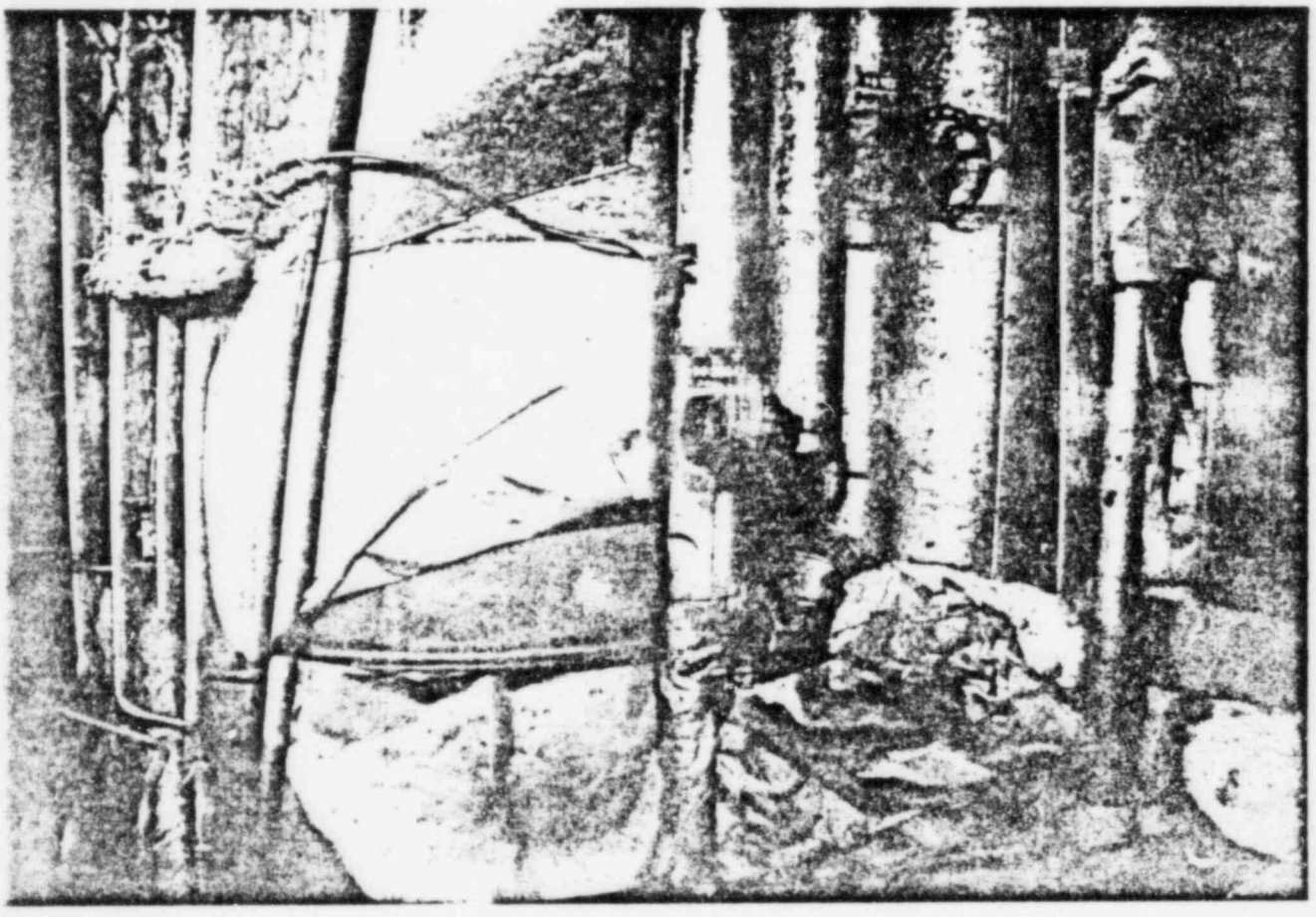

Figure C-8 Damage to jacketed fiberglass insulation located on the HDR blowdown test. Source: letter from G. Holman to A. Serkiz, NRC, "Photograpns of HDR blowdown damage," April 28, 1980.

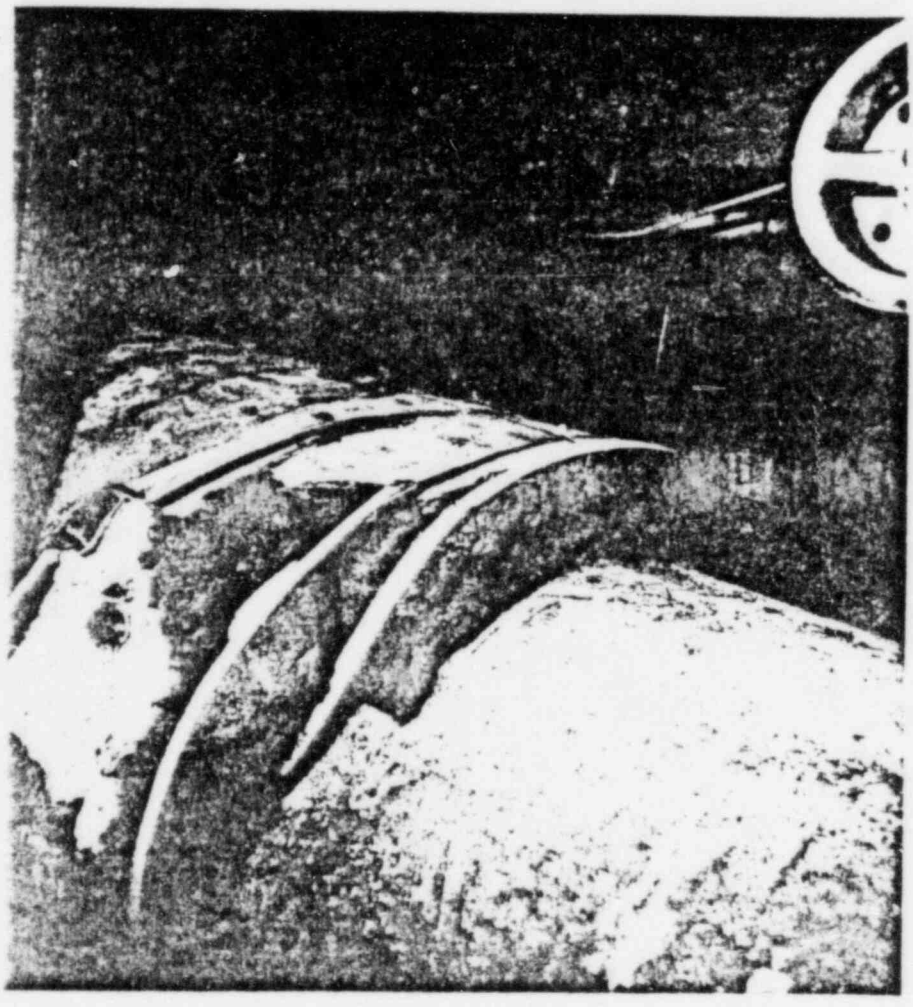

Figure C-9 Foam-glass insulation damage following a blowdown in the HDR. Foam-glass insulation withstood blowdown tests better than fiberglass. Source: letter from G. Holman to A. Serkiz, NRC, "Photographs of HDR Blowdown Damage," April 18, 1983.

Kernforschungszentrum Karlsruhe

Gesellschaft mit beschränkter Haftung

Kernforschungszentrum Karlsruhe GmbH · Postfach 3640 · D-7500 Karlsruhe 1

Mr. A.W. Serkiz
Task-Manager
Generic Issues Branch
Division of Safety
Technology
U.S. NRC
Mail Stop NL-5650

Washington, D.C. 20555
U.S.A.

Projekt HDR-Sicherheitsprogramm
Leiter: Dipl.-Ing. W. Müller-Dietsch

Datum: Aug. 02, 1983 - bo
Bearbeiter: Kl. Müller
Telefon: 07247/ 82 4343
Ihre Mitteilung:

Dear Mr. Serkiz:

I will send copies of our papers concerning equipment qualification next week to G.S. Holman (LLNL) for translation.

These papers conclude

- behavior of components during blowdown and in post blowdwon atmosphere
- distribution of isolation materials
- distribution of debries during blowdown in direction to the sump-area
- behavior of containment structures during blowdown.
- proposal of using HDR as a equipment qualification testbed.

Kernforschungszentrum Karlsruhe, Wissenschaftlich-Technische Einrichtungen und Verwaltung: 7514 Eggenstein-Leopoldshafen
Tel. (07247) 821, Telex: 7826484, Drahtwort: Reaktor Karlsruhe; Stadtbüro u. Postanschrift: D-7500 Karlsruhe 1, Weberstraße 5, Postfach 3640
Vorsitzender des Aufsichtsrats: Staatssekretär Hans Hilger Haunschild;
Vorstand: Prof. Dr. Rudolf Harde, Vorsitzender, Dr. Heilmut Wagner, Stellv. Vorsitzender, Prof. Dr. Horst Böhm, Dr. Hans Henning Hennies, Prof. Dr. Wolfgang Kliese
Handelsregister: Amtsgericht Karlsruhe HRB 302, Baden-Württembergische Bank AG, Karlsruhe, Kto Nr. 400 24713 00 (BLZ 660 200 20); Commerzbank AG, Karlsruhe, Kto Nr. 2 221 000 (BLZ 660 400 18); Deutsche Bank AG, Karlsruhe, Kto Nr. 0236 521 (BLZ 660 700 04); Dresdner Bank AG, Karlsruhe, Kto Nr. 5 634 398 (BLZ 660 800 52)

Mr. Wind of HDR-project will join the 11th WRS-Meeting end October 1983. Perhaps you can contact him together with G. Holman. He will answer additional questions and if needed from your side, he can illustrate component behavior and-damage by slides. In this case please contact me during September 1983 by phone or telex.

With best regards
Kernforschungszentrum Karlsruhe GmbH
Project HDR Safety Program

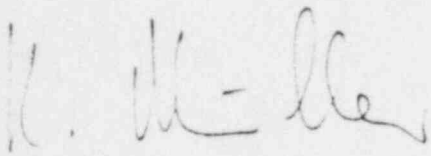

Project HDR Safety Program
Kl. Müller

Kernforschungszentrum Karlsruhe

Aug. 1, 1983 - bo

NOTA: INSULATION DAMAGE IN THE HDR BLOWDOWN EXPERIMENTS

1. Glas Fibre Insulation

HDR was equipped with this typ of insulation at the begin of the experiments. In the break compartment all glas fibre insulation was destroyed at 2 m around the break nozzle and distributed through the whole reactor in very fine particles on the walls and floor. The iron wrappers were thrown away from vessels within 4 m around the break nozzle, the glas fibre being untouched. With enforced shieldings (steel bandages) around the vessels nothing happened.

2. Glas Foam Insulation

Glas foam insulation around pipes up to 200 mm Ø withstood the blowdown impact even in a distance of about 2 m around the nozzle, except a small area where the mass flow touched the pipe. At these placed the insulation was cut out. The insulation of the pressure vessel was destroyed at great areas around the break nozzle caused by the first pressure wave cracking the material (short break nozzle RDB-E experiment).

Kernforschungszentrum Karlsruhe. Wissenschaftlich-Technische Einrichtungen und Verwaltung. 7514 Eggenstein-Leopoldshafen
Tel. (07247) 821. bei Durchwahl 82 . Telex: 7826484. Drahtwort: Reaktor Karlsruhe. Stadtbüro u. Postanschrift: D-7500 Karlsruhe 1. Weberstraße 5. Postfach 3640

The glas foam then was cracked into great pieces not leaving the break compartment and a great amount of fine particels following the blowdown pathes up to the sump inlet.

3. Glas Foam with Stainless Steel Shielding

This material withstood all impacts and retained intact even installed about 1 m around the break nozzle.

4. Insolating Matrazes

They consist of an special cloth outside eventually reinforced by steel wires filled with glass fibre or stone wool. This material withstood all impacts even good as material point 3. Nevertheless there were some corrosion effects on the cloth caused by demineralized water at high temperatures.

More detailed information you will get on request from Mr. Wind of K. Mueller.

Kernforschungszentrum Karlsruhe
Gesellschaft mit beschränkter Haftung

Kernforschungszentrum Karlsruhe GmbH Postfach 3640 D-7500 Karlsruhe 1

Mr. A.W. Serkiz
Task-Manager
Generic Issues Branch
Division of Safety Technology
U.S. NRC
Mail Stop NL 5650

Washington D.C. 20555
U.S.A.

Projekt HDR-Sicherheitsprogramm
Leiter: Dipl.-Ing. W. Müller-Dietsche

Datum: Sept. 12, 1983
Bearbeiter: K. Müller
Telefon: 07247/ 82 4343
Ihre Mitteilung:

Dear Mr. Serkiz,

I read the reports you send to me with great interest. There are some additional remarks concerning Nureg/CR-2982 coming from our experiments.

We found out; the jet forces are main cause for debris generation and distribution; pipe whip etc. are negligable.

Jet forces act only in a diameter of 2 - 5 m around the nozzle, depending on break diameter and break geometry.

We did these experiments with pure steam and pure water jet with nozzle diameters of 200 - 450 mm Ø.

First the pressure wave mainly destroys covers around fibre-glass and mineral wool and brittle insulation materials as glas foam. Than the impact of the fluid peels off the unprotected "wool layer" or cuts out the foam glas around pipes.

The jet and the following turbulences transport even heavy weight fragments to the next compartments. Here heavy parts are normaly fixed by drag force and only light wight particles will be transported further especially into the dome.

Kernforschungszentrum Karlsruhe, Wissenschaftlich-Technische Einrichtungen und Verwaltung: 7514 Eggenstein-Leopoldshafen
Tel. (07247) 821, Telex: 7826484, Drahtwort: Reaktor Karlsruhe, Stadtbüro u. Postanschrift: D-7500 Karlsruhe 1, Weberstraße 5, Postfach 3640
Vorsitzender des Aufsichtsrats: Staatssekretär Hans Hilger Haunschild
Vorstand: Prof. Dr. Rudolf Harde, Vorsitzender; Dr. Hellmut Wagner, Stellv. Vorsitzender; Prof. Dr. Horst Böhm, Dr. Hans Henning Hennies, Prof. Dr. Wolfgang Kliese
Handelsregister: Amtsgericht Karlsruhe HRB 302, Baden-Württembergische Bank AG., Karlsruhe, Kto. Nr. 400 24713 00 (BLZ 660 200 20); Commerzbank AG., Karlsruhe, Kto. Nr. 2 221 000 (BLZ 660 400 18); Deutsche Bank AG., Karlsruhe, Kto. Nr. 0236 521 (BLZ 660 700 04); Dresdner Bank AG., Karlsruhe, Kto. Nr. 5 634 398 (BLZ 660 800 52)

All grids and components within the building act as a screen for fixing these light wight particles, so in containments with a complicate interior most of the generated debris are fixed before reaching the sump area.

So only a break location with direct access to the sump area will block the screens in the way described in your papers.

In the post blowdown phase when the emergency cooling system is fed by the sump water there are only some "main water ways" left leading from the nozzle to the sump. These "main water ways" will not cause pump failure.

From my opinion you will get more debris collected and settled within the core barrel and other core internals than reactivated by the back flow of the water to the sump.

Even if activating the Containment spraysystem you will get more problems with the blockage of the injection nozzles of a water spray system by the debris than blocking the pump or sump inlet.

Yours sincerely,
Kernforschungszentrum Karlsruhe GmbH
Projekt HDR-Sicherheitsprogramm

Ø: G. Holman, LLNL
F. Wind, PHDR

APPENDIX D

DETERMINATION OF RECIRCULATION VELOCITIES

APPENDIX D

DETERMINATION OF RECIRCULATION VELOCITIES

1.0 General

During the recirculation mode of operating the ECCS, water on the reactor floor will drain to the sump, the source of water for pumps which provide long-term cooling of the reactor. This flow of water on the reactor floor may be at sufficient velocity such that insulation debris is transported with the flow, resulting in blockage of the sump screens and a pressure drop across the screens. Of major concern is the impact of this potential pressure drop on the pump flow and on the available pump NPSH compared to the required NPSH.

Various types of insulation materials have been tested to determine what flow velocities will initiate movement and transport of this debris. Of equal importance is the determination of what flow velocities will exist in a given plant during the recirculation mode, as it is the relative magnitude of the actual recirculation velocities to the experimentally determined transport velocities which determines the probability of insulation debris blocking the sump screens.

Due to the arrangement of plant walls, structures, and equipment, there will be only certain flow paths available from each postulated break location to the sump(s). Some plant layouts will result in a few obvious flow paths; in other plants, the flow paths may be numerous and not so easily defined. Those paths having the shortest length and offering the least resistance (losses) will produce the greatest velocities (i.e., have the most water surface slope). For a given velocity, the flow path with the largest cross-sectional area will carry the largest discharge. Local velocities will be considerably different from average velocities due to local flow contractions. Losses may be produced by surface friction, drag due to the flow past appurtenant structures, equipment, or pipes, expansion losses downstream from constricted

openings, bends of the flow path, and any other phenomena causing turbulent energy dissipation.

This appendix will review various means for determining the recirculation velocities, such that an assessment of debris transport can be made. If a preliminary analysis using simplified methods indicates recirculation velocities are within a factor of about two (2) compared to the experimentally derived transport velocity for the insulation type(s) under study, then more refined analyses are warranted. For example, if recirculation velocities are up to about 50% less than the predetermined debris transport velocities, transport may still actually occur since many approximations are inherent in the preliminary analyses. On the other hand, if the recirculation velocities are up to about twice the transport velocities, transport may be less severe than indicated for similar reasons. To be conservative, it should be assumed that all flow is returned by the safety injection system since this maximizes recirculation velocities on the containment floor.

2.0 Review of Network Resistance Method

A preliminary method of estimating recirculation velocities is to define a system of possible flow paths with varying resistance. This flow/resistance network is simplified by finding equivalent resistances to series and parallel paths, until one equivalent flow path remains. Since the total flow is known and the equivalent resistance may be estimated from coefficients of friction and losses available in handbooks, the total head drop from the break to the sump may be calculated. As all parallel flow paths are subject to this same total drop, the individual flows in all other paths may then be determined. Knowledge of flows per path allows local velocities to be determined from the known local cross-sectional areas. This preliminary analytic method is presented in NUREG/CR-2791, and is summarized below (using conventional hydraulic terms).

As an illustration, assume the simplified situation shown in Figure D-1 (taken from NUREG/CR-2791). Flow from the break may reach the sump in all combination of the paths illustrated, and this combination may be reduced to the flow/resistance diagram shown, where resistances R1 through R8 correspond to the similarly numbered flow paths. The resistance may be determined from the following set of equations, starting with the well known Darcy-Weisbach resistance formula (4, 8).

$$h_L = f \frac{L}{4R_H} \frac{V^2}{2g} \qquad \text{(D-1)}$$

where h_L = the drop in water level (piezometric head) (ft)

f = friction factor (dimensionless)

L = flow path length (ft)

R_H = hydraulic radius = flow area/wetted perimeter (ft)

V = average cross-section flow velocity (ft/sec)

g = acceleration due to gravity (ft/sec^2)

Values of f, which depend on the relative roughness of the flow path and the flow Reynolds number, are available from standard text and handbooks, such as (4, 8). Since

$$V = Q/A \qquad \text{(D-2)}$$

where

Q = flow rate (ft^3/sec)

A = cross sectional flow area (ft^2)

letting $C = 1/2g$

$$K = \frac{fL}{4R_H}$$

then

$$h_L = \frac{KC}{A^2} Q^2 \qquad \text{(D-3)}$$

By setting

$$R = KC/A^2$$

we obtain the usual system loss equation

$$h_L = RQ^2 \qquad \text{(D-4)}$$

indicating greater resistance (higher values for R) for paths having greater friction, longer lengths, and smaller cross-section areas, and vice versa.

Equivalent resistances may be found for combined flow paths by use of the above equations and continuity, noting that the loss for each parallel flow path equals the total loss. The result is that resistances in series add, and resistances in parallel follow a reciprocal law.

Therefore, the network in Figure D-1 may be simplified to

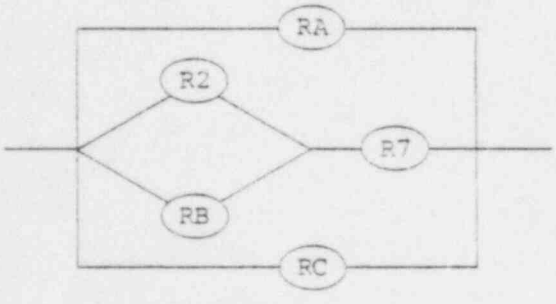

where RA = R1 + R8
RB = R3 + R6
RC = R4 + R5

Parallel resistances such as R2 and RB may be combined by finding an equivalent resistance

$$RD = \left[\frac{1}{\sqrt{\frac{1}{R2}} + \sqrt{\frac{1}{RB}}} \right]^2$$

such that the network is now simplified to

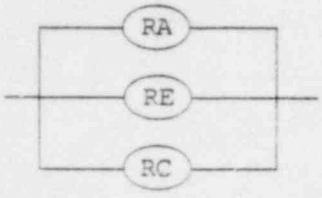

where RE = RD + R7

which in turn is reduced to one equivalent resistance RF by application of the reciprocal law for parallel resistances. Therefore

$$h_L = (RF)Q^2$$

and h_L may now be calculated, because RF is estimated from the individual branch resistances, and the total flow of the ECCS is known. Given the calculated h_L, which is the same for all parallel branches, flow in each branch may be calculated using the individual resistances for that branch. For example,

$$Q_1 = Q_8 = \sqrt{\frac{h_L}{R1 + R8}}$$

and the velocity at any section along flow path 1-8 may be determined by dividing the above determined flow rate by the cross-sectional area at the section of interest. It is important to consider local flow contractions to less than actual structural openings. A typical flow contraction can be as low as about 0.65 of the actual available opening, depending on the geometry involved.

The above summarized method appearing in NUREG/CR-2791, although sound in principle, includes many approximations. A basic problem is that values for f are available only for straight, prismatic channels, and that average values of f and R_H are used for the entire flow path. This may be overcome by using much shorter flow paths, each having the proper value of f and R_H, but this makes the calculation more laborious. It should also be recognized that most of the flow resistance is due to drag of various objects in the flow path, to bends, and due to flow expansions from contracted areas. Drag losses may be expressed as (4)

$$h_D = C_D \frac{V^2}{2g}$$

where C_D = a dimensionless drag coefficient.

A similar expression is used for losses due to bends

$$h_B = C_B \frac{V^2}{2g}$$

where C_B will vary with the bend radius.

Values for C_D and C_B are available for a variety of shapes in standard text and handbooks (4, 8). Head losses due to flow expansions are given by (1, 4 & 8)

$$h_E = \left[1 - \frac{a}{A} \right]^2 \frac{V_a^2}{2g} = C_E \frac{V_a^2}{2g}$$

where a = contracted flow area (ft^2)

A = downstream cross-sectional area (ft^2)

V_a = contracted area velocity (ft/sec)

The contracted velocity may be related by continuity to the average flow velocity of the branch, and C_E expressed in terms of V instead of V_a. The total head loss for a given flow path may thus be calculated from

$$h_L' = \left[f \frac{L}{4R_H} + C_D + C_B + C_E\right] \frac{V^2}{2g} = R'Q^2 \qquad \text{(D-5)}$$

where

$$R' = \left(\frac{fL}{4R_H} + C_D + C_B + C_E\right) \frac{1}{2gA^2} \qquad \text{(D-6)}$$

The above illustrated calculations will be improved by the addition of these terms, but numerous flow paths must be defined such that the available values of R_H, C_D, C_B, and C_E really apply to that section, as average or effective values of these coefficients for varying path characteristics cannot be determined.

Despite the possible refinements to this method, not all flow/resistance networks can be simplified to one equivalent resistance. Consider, for example, the following simple case.

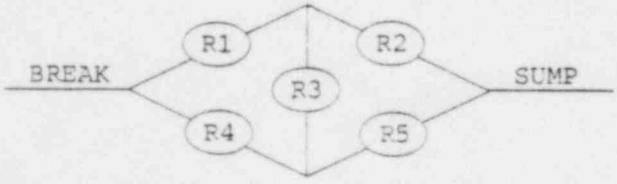

This problem may be overcome by using a different type of analyses, as illustrated below for a more complex flow network postulated for a given plant.

3.0 Complex Network Analysis

In the example illustrated in Figure D-2 there are 28 flow paths and 18 junctions, A to R. For each flow path Eq. (D-5) is applicable. For example, for the flow path 5,

$$H_C - H_B = R'_5 Q_5^2 \qquad \text{(D-7)}$$

where H = piezometric head at the junction identified by the sub-script (ft)

Q = flowrate along the flow path identified by the subscript (ft^3/sec)

R' = an overall resistance factor as defined in equation (D-6) for the flow path identified by the subscript (sec^2/ft^5)

Similar to Eq. (D-7), 28 equations corresponding to the 28 flow paths are available. Also, for each junction the continuity equation can be applied.

For example, in Figure D-2, for junction J, assuming inflow from flow paths 16 and 21

$$Q_{17} = Q_{16} + Q_{21} \qquad \text{(D-8)}$$

Combining Eq. (D-8) with head loss relationships similar to Eq. (D-7) gives

$$\left(\frac{H_J - H_A}{R'_{17}}\right)^{1/2} = \left(\frac{H_K - H_J}{R'_{16}}\right)^{1/2} + \left(\frac{H_I - H_J}{R'_{21}}\right)^{1/2} \qquad \text{(D-9)}$$

For each of the junctions, one could write an equation similar to Eq. (D-9). Hence, if flow directions are first assumed, 18 junction equations are obtained to form a system of nonlinear equations with the 18 unknown piezometric

heads at junctions. One of the most widely used method for solving such a system numerically is the Newton-Ralphson method (5) which iteratively solves the system of equations. Computer programs using the Newton-Ralphson method are readily available in many books on pipe network analysis (5, 10) or on numerical analysis of nonlinear equations (3). To use the Newton-Ralphson method, one assumes the flow directions and provides an initial estimate of the piezometric heads conforming to the assumed flow directions. Since the method is iterative, the acceptable error in final solution should also be indicated. The method usually converges very fast, although convergences may not be obtained if initial values are unreasonable and too far from actual values. The flow directions, if wrong, will be automatically corrected by the calculation procedure to conform to the values of the piezometric heads obtained after each iteration.

For the example considered, the piezometric head at the sump and the total flow into the sump Q_T would be known. Referring to Figure D-2, H_A, the piezometric head at junction A is known. If the piezometric heads at each of the junctions B to R are determined, one could calculate the flows using the flow path equations similar to Equation (D-7). There are 17 unknowns, namely H_B to H_R, and the required 17 equations can be obtained by writing the continuity equations at each of the junctions A to Q. For example at junction A,

$$\left(\frac{H_J - H_A}{R_{17}'}\right)^{1/2} + \left(\frac{H_Q - H_A}{R_2'}\right)^{1/2} + \left(\frac{H_B - H_A}{R_6'}\right)^{1/2}$$

$$+ \left(\frac{H_B - H_A}{R_7'}\right)^{1/2} + \left(\frac{H_B - H_A}{R_8'}\right)^{1/2} - Q_T = 0 \qquad \text{(D-10)}$$

The Newton-Ralphson method can be used to solve the 17 equations similar to (D-10) for the 17 unknowns H_B to H_R. The method is iterative and solves a linear matrix as explained below:

Let the 17 non-linear equations be,

$$F_1 = 0$$
$$F_2 = 0$$
$$- - - -$$
$$- - - -$$
$$- - - -$$
$$F_{17} = 0$$

A linear matrix is written as,

$$\begin{bmatrix} \frac{\partial F_1}{\partial H_B}, & \frac{\partial F_1}{\partial H_C}, & - - - - , & \frac{\partial F_1}{\partial H_R} \\ \frac{\partial F_2}{\partial H_B}, & \frac{\partial F_2}{\partial H_C}, & - - - - , & \frac{\partial F_2}{\partial H_R} \\ - - - - & - - - - & - - - - & - - - - \\ - - - - & - - - - & - - - - & - - - - \\ \frac{\partial F_{17}}{\partial H_B}, & \frac{\partial F_{17}}{\partial H_C}, & - - - - , & \frac{\partial F_{17}}{\partial H_R} \end{bmatrix} \begin{bmatrix} Z_B \\ Z_C \\ - \\ - \\ Z_R \end{bmatrix} = \begin{bmatrix} F_1 \\ F_2 \\ - \\ - \\ F_{17} \end{bmatrix} \qquad \text{(D-11)}$$

Using the initial guesses of H_B to H_R, the values of $\partial F_1/\partial H_B$, $\partial F_1/\partial H_C$ etc. and F_1, F_2 etc. are calculated first and the linear matrix (D-11) is solved to obtain, Z_B to Z_R, the corrections to initial guesses of H_B to H_R. Note that the values of F_1, F_2 etc might be non-zero, since the initial guesses are not actual values.

The corrected values of H_B to H_R are used for the next iteration, and the calculations are repeated until Z_B to Z_R are within stated acceptable error margins. After several iterations, the final corrected values of H_B to H_R will be considered as the actual values, and these are then used in the flow path equations similar to (D-7) to obtain the flows in each flow path.

Alternatively, a network analysis based on corrections to the flows in each loop could be performed. The flow system given in Figure D-2 could be transformed to an eight loop network as given in Figure D-3 by replacing parallel pipes with equivalent pipes. In this case, initial guesses of flows along each flow path should be made such that the continuity equation is satisfied at each junction. Referring to Figure D-3, there are 8 loops. For each loop the algebraic sum of the head losses around the loop would be zero. The positive direction of flow must be defined, such as clockwise around each loop. For example, referring to Figure D-3, for loop 6 with assumed flow directions let the initial guesses of flows be Q_{13}, Q_4, Q_{11}, and Q_{12} along the flow paths 13, 4, 11, and 12 respectively. Since the algebraic sum of the head losses around the loop would be zero, we get

$$F_6 = R'_{13} (Q_{13} + \Delta Q_6)^2 - R'_4 (Q_4 - \Delta Q_6 + \Delta Q_1)^2$$

$$- R'_{11} (Q_{11} - \Delta Q_6 + \Delta Q_5)^2 + R'_{12} (Q_{12} + \Delta Q_6 - \Delta Q_7)^2$$

$$= 0 \qquad \text{(D-12)}$$

where ΔQ_i is the correction to flows in the loop i required to convert initial estimates to actual values of flows. When a flow path is common to more than one loop, corrections from each of the loops have to be included to get the actual flow for that flow path.

Writing similar equations for each loop, we get

$$F_1 = 0$$
$$F_2 = 0$$
$$- - -$$
$$- - -$$
$$F_8 = 0$$

As a first iteration, the unknowns ΔQ_1 to ΔQ_8 are solved by Newton-Ralphson method for the assumed initial guess of the flows around each loop. Then the flows are corrected with the obtained values of ΔQ_1 to ΔQ_8 and the next iteration is carried out. The procedure is repeated until ΔQ_1 to ΔQ_8 become acceptably small.

This method is quicker in that a lesser number of unknowns (equal to number of flow loops) is involved. However, it is difficult to give initial estimates of flows satisfying continuity equation at each junction.

Instead of the Newton-Ralphson method, other iterative methods can be used, such as Hardy-Cross or linear methods, to solve the nonlinear system of equations (5).

Irrespective of the method of analysis for large networks, the time consuming part is providing the initial data of R' values for each flow path and the initial estimates of piezometric heads or flows. It must also be realized that many break locations must be considered, with each location requiring re-evaluation (perhaps redefinition) of the flow network. Therefore two other methods to predict flow patterns and local velocities are addressed below.

4.0 Two-Dimensional Analyses

Rather than pre-defining flow paths, another approach is to use a two-dimensional numerical model which, by its nature, accounts for the shape and size of the various flow paths and obstructions in the containment building. The flow to the sump being basically horizontal, the complete three-dimensional flow equations are integrated vertically over the water depth (depth averaged) and solved numerically using one of several techniques. The two basic classes of techniques are the finite differences and finite elements methods. In the former, a grid is defined covering the flow field, and the derivatives appearing in the differential equations are approximated based on the values of the variables at the nodes of the grid. The most

common type of finite differences grid is rectangular, with possibility of a variable resolution, but other grids are possible, particularly circular grids for problems with obvious circular characteristics.

In finite elements methods, the variations of the variables of interest are approximated continuously over elements through pre-defined "basis functions" (or interpolating functions) and nodal values. The most common type of element is triangular with nodes at the vertices. but there is no limitation on the shape of the elements that can be used (rectangular and curvilinear are common), and the number of nodes per element depends on the choice of basis function. One of the advantages of the finite elements method over the finite difference method is that the flow domain can be approximated more closely and that variations of resolution are more convenient with finite elements. As an example, a grid of triangular finite elements is shown in Figure D-4 for the previously discussed application. Finite elements solutions, however, tend to require larger computation times than finite differences solutions.

There are many other differences between available two-dimensional models. These other differences concern the details of the numerical technique used, such as the way in which the nonlinear terms are treated or handling of the advective terms (which tend to create numerical instabilities), or the way time integration is performed. Another important difference between available models is the way in which turbulence and the corresponding Reynolds stresses are simulated. A common approach is to use an eddy viscosity concept but flow separation is then difficult to reproduce, and the values of the eddy viscosity has a large effect on numerical stability, making the selection of this parameter all the more critical. The so-called κ-ε method of turbulence simulation has recently been shown to be very powerful, at the expense of an increased number of differential equations to be solved.

For such two-dimensional analyses, the break flow is simulated by a flow source term(s) at one or more nodes at the break location. The sump may be simulated either by sink terms for nodes around the sump, or specifying values

of normal velocity components at these locations. Various assumptions regarding the distribution of velocity or flow around the sump may be made. Losses due to friction and distributed drag from small pipes or structures are estimated and appropriate values of f selected. Losses due to flow eddies and large-scale turbulence may be simulated depending on the grid detail and on the analytic model. For practical grid sizes such as on Figure D-4, proper modeling of flow separation is doubtful. Initial values must be prescribed for velocities and water depths at all nodes, and zero velocities and a horizontal water surface are convenient initial conditions. At solid boundaries, zero normal (perpendicular) velocities must exist, although the tangential velocity component may be either zero or unprescribed.

Several two-dimensional models which are applicable to this problem are available, including those by Wang & Connor (9), Leendertse (7), Benque et al (2) and Launder and Spaulding (6). Application of any of these models to the calculation of recirculating flow patterns in containment buildings should, however, be subject to careful evaluation as a number of features exist in the proposed application for which the analytic models have not been fully tested. A notable feature to be checked is the flow separation that can be expected behind obstructions.

Results of two-dimensional models are flow velocities and water surface elevation at the node points versus time. For this application, transient effects would probably be negligible, but the computation time would remain large because of the fine grids required to account for the geometrical details of the domain. In spite of the relatively dense grid shown in Figure D-4, it is not possible to closely follow the actual bounding geometry in regions of small clearances and local contractions.

None of the analytic techniques described above includes consideration of the initial break flow momentum, nor do they closely simulate the complex geometry of the containment and appurtenant equipment, as either one- or two-dimensional approximations are made. Also, losses must be independently

estimated. If complex flow patterns have significant effects on the problem under consideration, it is accepted practice that a physical (hydraulic) model study may be necessary.

5.0 Hydraulic Model Studies

Depending on how close any analytically predicted recirculation velocities are to the experimentally determined debris transport velocities and the need to further refine the evaluation of potential debris transport to the sump, it may be advantageous to use a physical (hydraulic) model. Such a model would include all geometric features of the containment floor area which could affect flow patterns. A portion of the type of model which would be suitable is illustrated in Figure D-5. Although a full-scale simulation of the reactor floor and sump geometry may be considered, it is more efficient to use a reduced scale model (and there is no technical reason to the contrary). NUREG/CR-2760 reports on studies specifically designed to evaluate potential scale effects on sump hydraulics. These studies show no scale effects as long as model flow Reynolds numbers exceed certain limiting values, such as typically achieved at geometric scale ratios of about 1:4.

The advantages of using a hydraulic model are

(1) There is no need to make assumptions regarding loss and contraction coefficients as these are implicitly included.

(2) Flow paths are reproduced to their actual geometry rather than simulated by one- or two-dimensional techniques, allowing accurate spatial definition of velocity variations.

(3) The break flow momentum can be scaled, and numerous break locations can be evaluated without model reconstruction.

(4) Basic debris transport phenomena, such as relative volumes moved and downstream settling in lower velocity areas, can be demonstrated using simulated (scaled) debris.

5.1 Similitude Requirements

The main similitude requirement is based upon scaling the two dominant forces in free surface flow, gravity and inertia. These primary forces are embodied in the Froude number, F,

$$F = \frac{V}{\sqrt{gH}}$$

(where V, g, and H are as previously defined) and equality of Froude number between model and prototype leads to proper scaling of flow patterns from the break to the sump. The selected geometric scale ratio must be large enough, however, such that viscous forces involved with friction and drag are properly scaled. This will be true if the model Reynolds number is large enough such that loss coefficients are equal to those of the prototype. Alternately, adjustments in the size of components causing losses may be made to compensate for the lower model Reynolds number. The use of standard laboratory velocity meters may also influence the choice of the model scale ratio.

It should be noted that the actual reactor pressures and water temperature do not have to be scaled in the hydraulic model. The gas pressure over the water is constant in space and will have no effect on flow patterns. Water temperature affects the water viscosity and surface tension, but neither parameter influences flow patterns for sufficiently large geometric scale ratios and model Reynolds number.

Simulation of the insulation debris transport, if desired, is more complex. Since it may not be possible to directly scale all relevant parameters as is the case for other analogous hydraulic models simulating material transport,

test results are more qualitative than quantitative. One approach is to find a model material which is transported at the model velocity scaling the known actual transport velocity for that insulation material. Alternately, the actual insulation material may be used (at scaled size and volume) if the model flow and velocity is increased to actual (prototype) values, while maintaining the water depth. For a scale ratio of 1:4, this involves doubling the model flow and velocities from that given by normal Froude scaling. It should be demonstrated that such flow increases do not change the flow patterns as determined from running the model at Froude scaled flows.

REFERENCES

1. Baumeister, Theodore, editor, Marks' Standard Handbook for Mechanical Engineers, Chapter 3, Eighth Edition; McGraw-Hill Book Company, Inc., 1978.

2. Benque, J.P., J.A. Cunge, J. Feuillet, A. Hauguel, and F.M. Holly, "New Method for Tidal Current Computation," in Journal of the Waterways, Port, Coastal and Ocean Division, ASCE, Vol. 108, No. WW3, August 1982.

3. Conte, S.D., and C. DeBoor, Elementary Numerical Analysis, McGraw Hill, 1965.

4. Daily, J.W., and D.R.F. Harleman, Fluid Dynamics, Addison-Wesley Publishing Company, Inc., 1966.

5. Jeppson, R.W., Analysis of Flow in Pipe Networks, Ann Arbor Science, 1979.

6. Launder, B.E., and D.B. Spaulding, Lectures in Mathematical Models of Turbulence, Academic Press, New York, 1972.

7. Leendertse, J.J., "Aspect of a Computational Model for Long Period Water Wave Propagation," Rand Corporation, Memorandum RM-5294-PR, May 1967.

8. Streeter, V.L., Handbook of Fluid Dynamics, Section 3, First Edition; McGraw-Hill Book Company, Inc., 1961.

9. Wang, J.D., "Real Time Flow in Unstratified Shallow Water," in Journal of the Waterways, Port, Coastal and Ocean Division, ASCE, Vol. 104, No. WW1, February 1978.

10. Watters, G.Z., Modern Analysis and Control of Unsteady Flow in Pipelines, Ann Arbor Science, 1979.

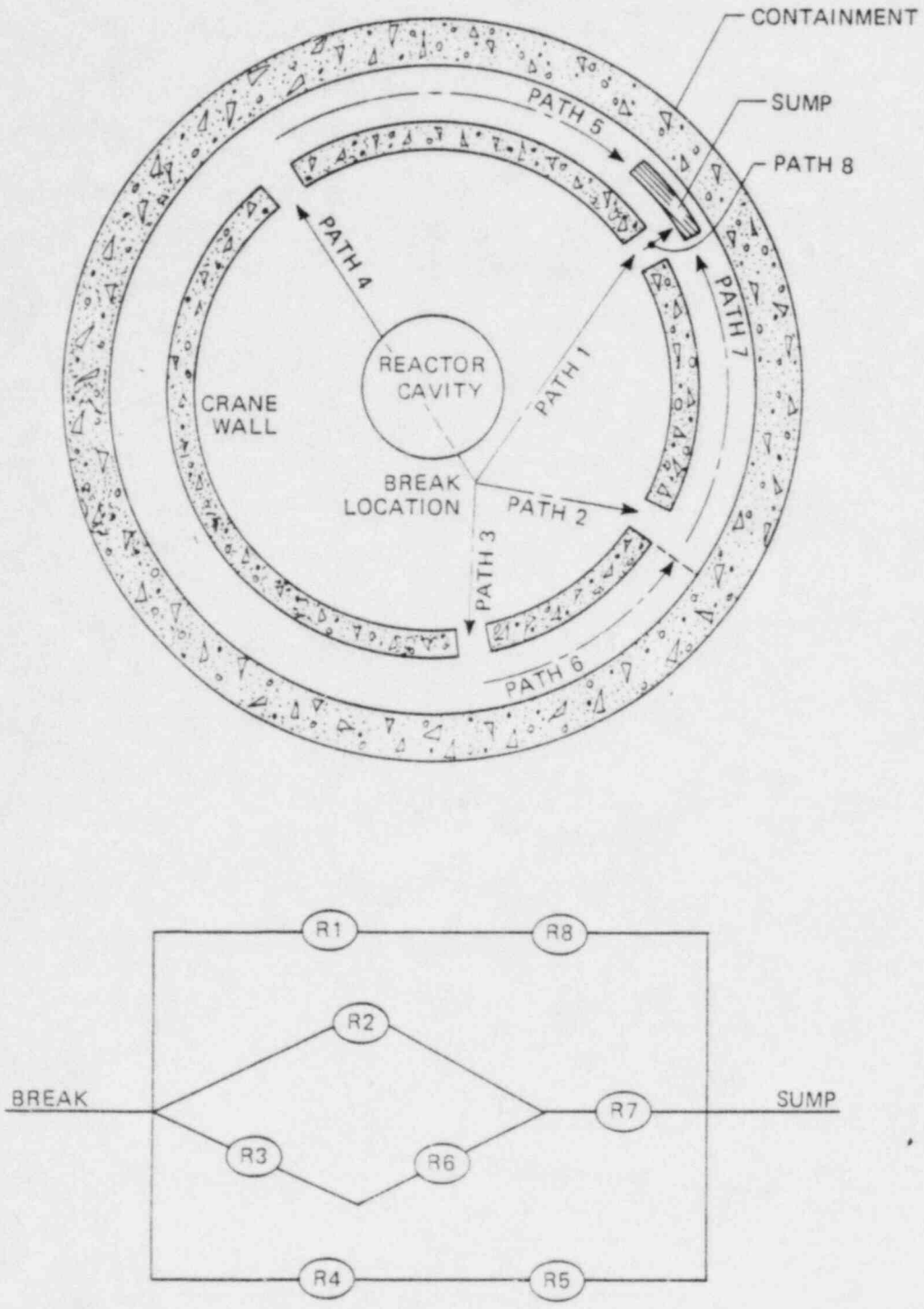

FIGURE D-1 SIMPLIFIED FLOW PATTERN WITHIN CONTAINMENT

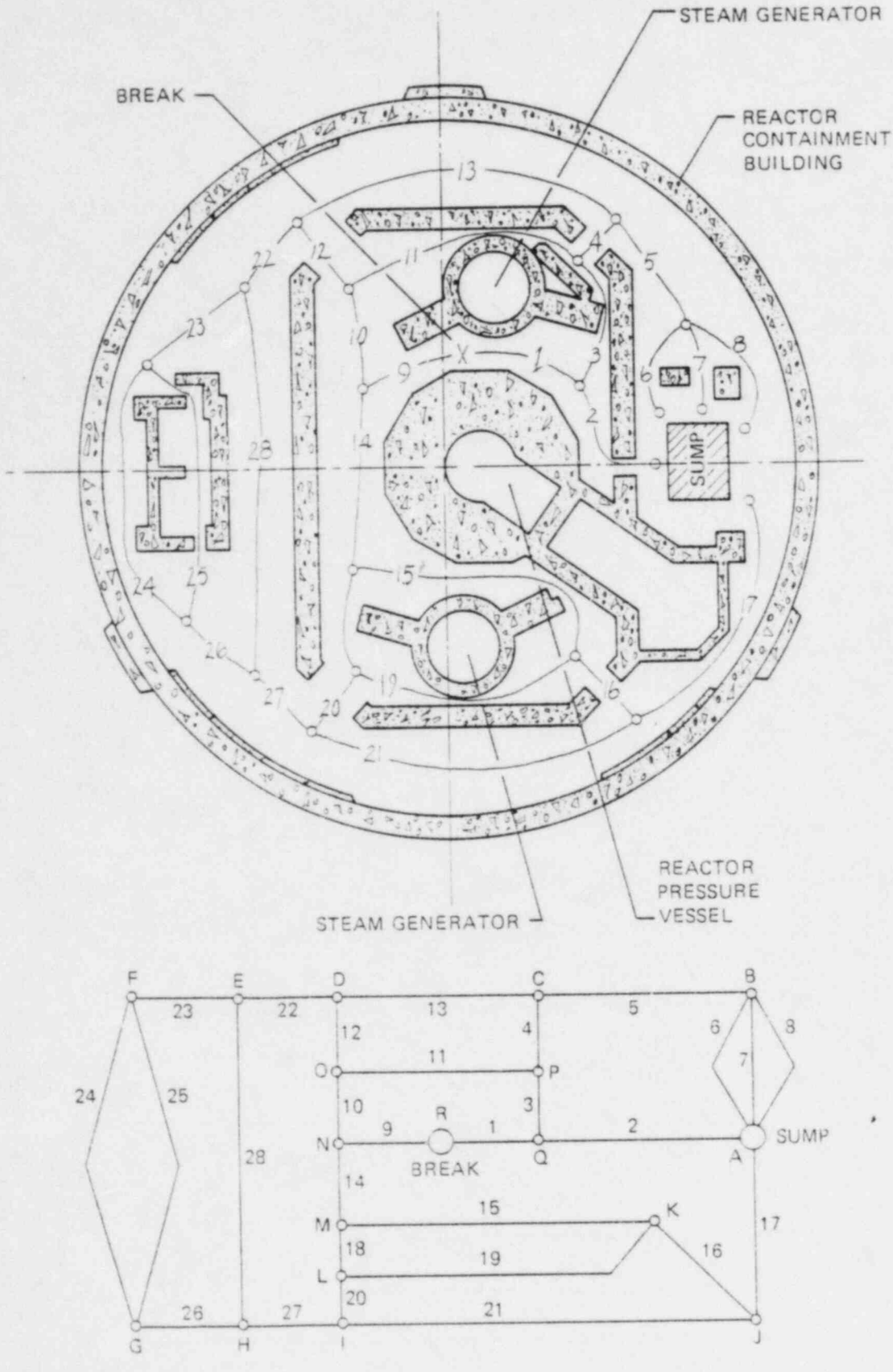

FIGURE D-2 COMPLEX FLOW NETWORK FOR CONTAINMENT

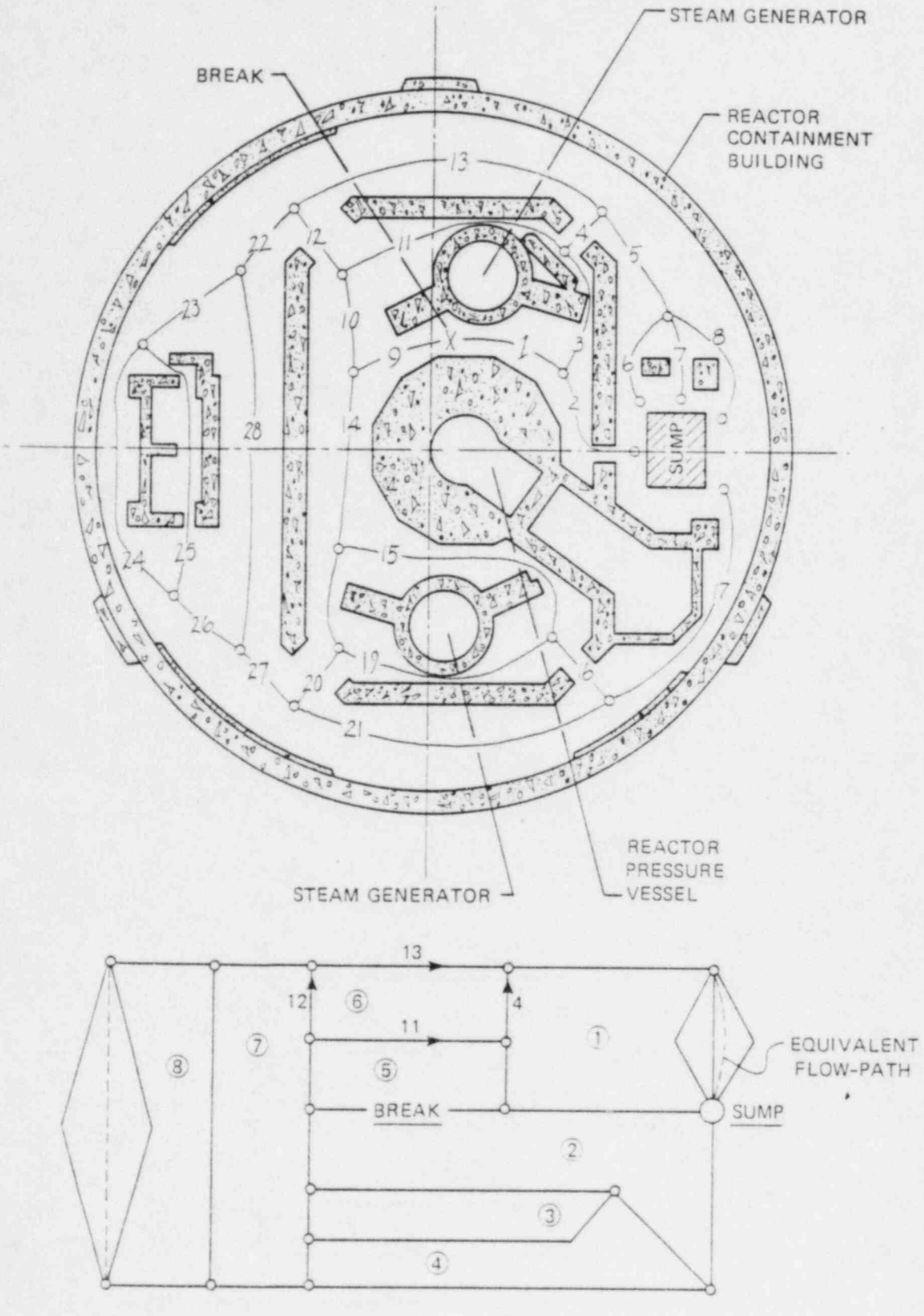

FIGURE D-3 COMPLEX NETWORK WITH FLOW LOOPS IDENTIFIED

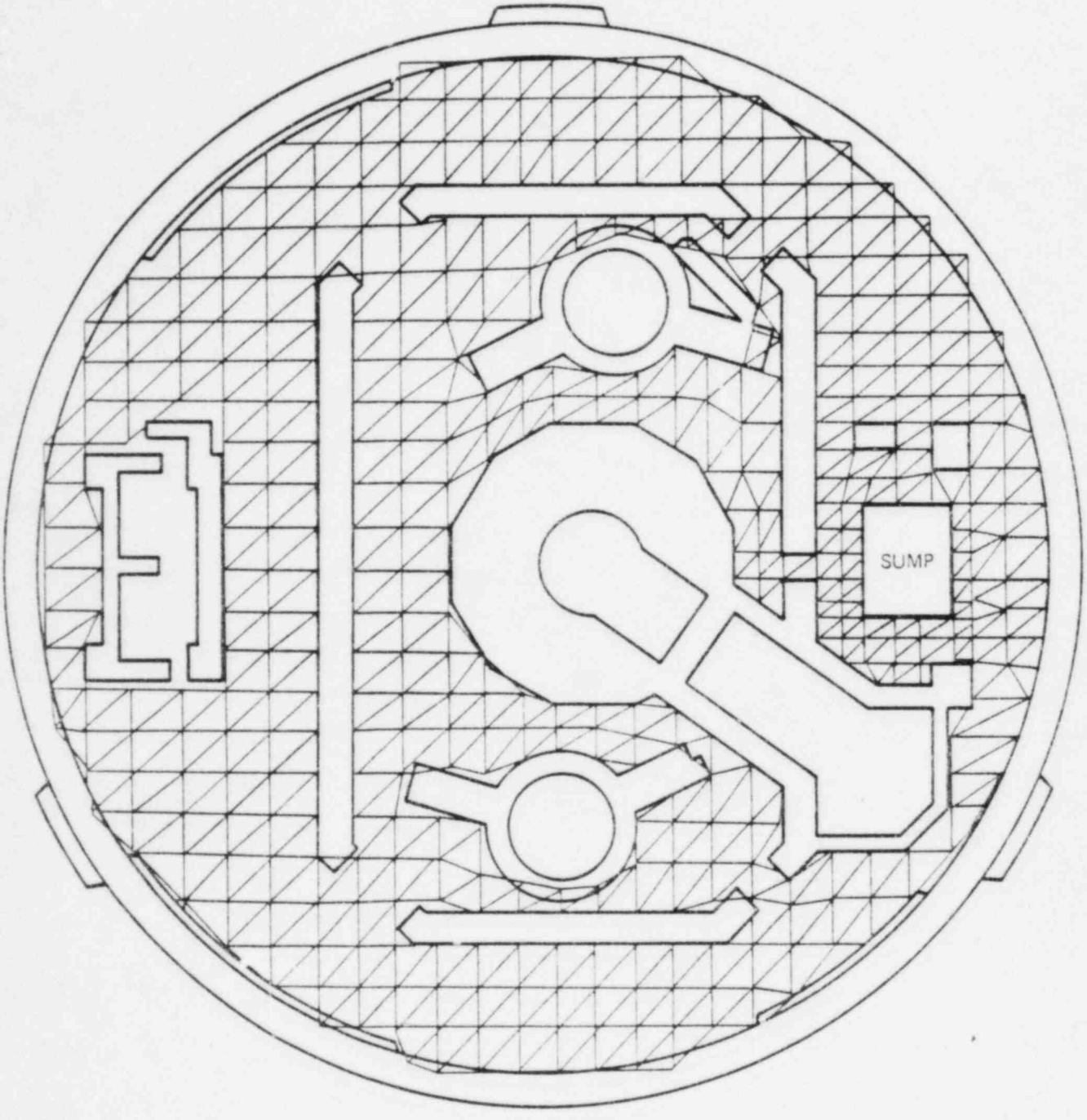

FIGURE D-4 TWO DIMENSIONAL REPRESENTATION OF CONTAINMENT RECIRCULATION FLOW

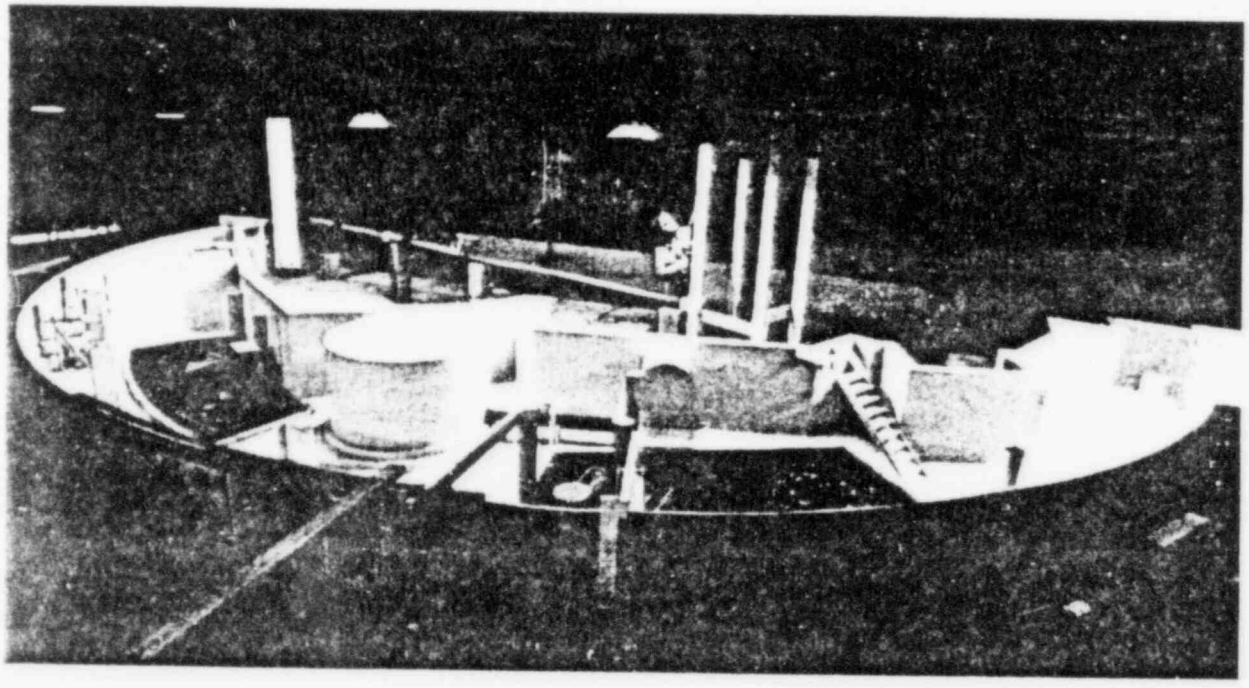

NOTE: PHOTO COURTESY OF ALDEN RESEARCH LABORATORY, WORCESTER POLYTECHNIC INSTITUTE

FIGURE D-5 HYDRAULIC MODEL OF CONTAINMENT FLOOR AREA

APPENDIX E

MIRROR® INSULATION PERFORMANCE DURING LOCA CONDITIONS

PROVIDED BY

DIAMOND POWER COMPANY

HDR TEST RESULT SUMMARY
MIRROR® INSULATION PERFORMANCE DURING LOCA CONDITIONS
DCN AE6609-111984-02

Prepared By:

K. T. Gilbert
Senior Engineer
Technical Support
Mirror Insulation

Reviewed By:

R. L. Patel
Senior Group Supervisor
Technical Support
Mirror Insulation

Approved By:

B. D. Ziels
Manager
Mirror Engineering

Introduction

Insulation reaction to LOCA jet forces ultimately relates to the Emergency Core Cooling System's ability to perform its intended function, since insulation debris has the potential to block sump screens and reduce the pump's ability to recirculate the cooling medium. Based on postulated damage thresholds and modes, testing has been performed to determine the transport potential and resulting screen blockage patterns for components of metallic reflective insulation (NUREG/CR-3616). The subject testing was designed to answer questions related to how reflective insulation reacts when exposed to LOCA magnitude jet forces:

- How is metallic reflective insulation damaged by jet forces?
- Will it be removed from the pipe or remain in place as installed?
- If the insulation is torn apart by the jet forces, what sizes and shapes of debris will be generated?

The test results summarized in the following pages provide valuable insight for understanding the fundamental questions of damage potential and mode, so that the most realistic assessment of screen blockage potential can be made. The test results summarized here are the only test results available that provide information on reflective insulation reaction to high pressure jet forces. For more details of the test program, please refer to Diamond Power Specialty Co. report #DCN AE6609-111984-01, "HDR TEST RESULTS, MIRROR® INSULATION PERFORMANCE DURING LOCA CONDITIONS."

Test Facility Description

A decommissioned nuclear reactor (100MW prototype BWR) has been refitted to allow full scale testing with conditions representative of commercial LWR operation. The "HDR" (paraphrased meaning "superheated steam reactor") is a real nuclear power plant which offers test capabilities relevant to modern commercial plants.

The initial thermal hydraulic state for this specific HDR blowdown test was 110 bar, 318°C (saturated steam), which reflects nominal PWR operating conditions. The reactor vessel design parameters include 10m height, 2.96m I.D., 75m^3 volume, 110 bar design pressure and 360°C design temperature. The design basis break was simulated by means of a set of rupture disks mounted in a 450mm I.D. nozzle. Approximately four feet from the nozzle end, a large deflection plate is located to guide the jet away from direct impact with the compartment walls.

Four specimens of MIRROR® metallic reflective insulation were provided for simultaneous testing. Each of the specimens was designed and manufactured using standard practice and materials. All materials used were 304 stainless steel and all fasteners (screws, buckles, pop rivets) were standard production components. The location of the test specimens relative to the test nozzle and deflection plate are shown in Figure 1.

- Origin = Center of nozzle discharge
- X Axis along axis of nozzle
- Dimensions to approximate center of installed specimen
- Coordinates are (X,Y,Z)

SPECIMEN NUMBER	DISTANCE FROM NOZZLE DISCHARGE (APPROXIMATE)
①	2.5 FT
②	22 FT
③	11 FT
④	10 FT

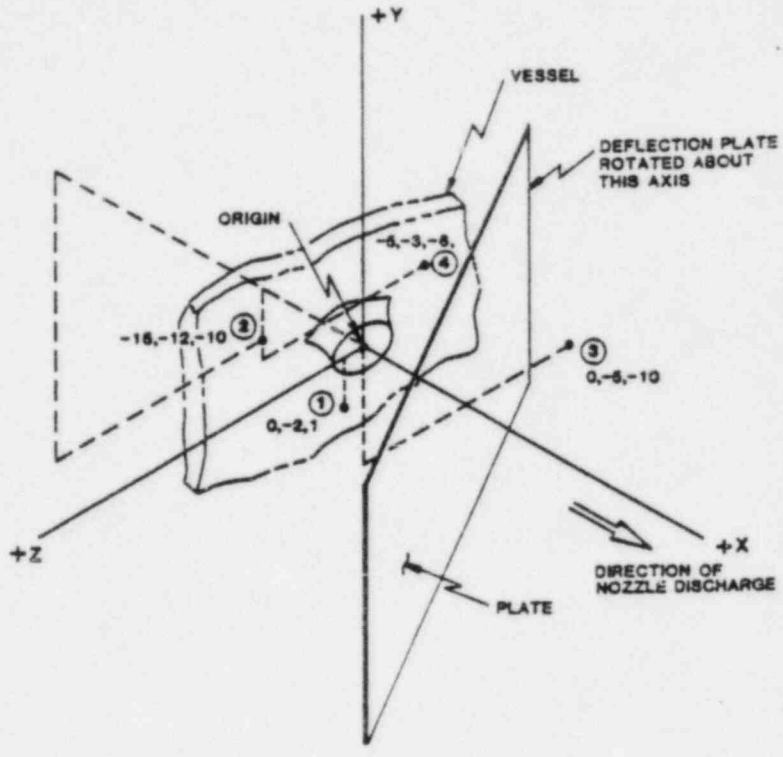

Isometric

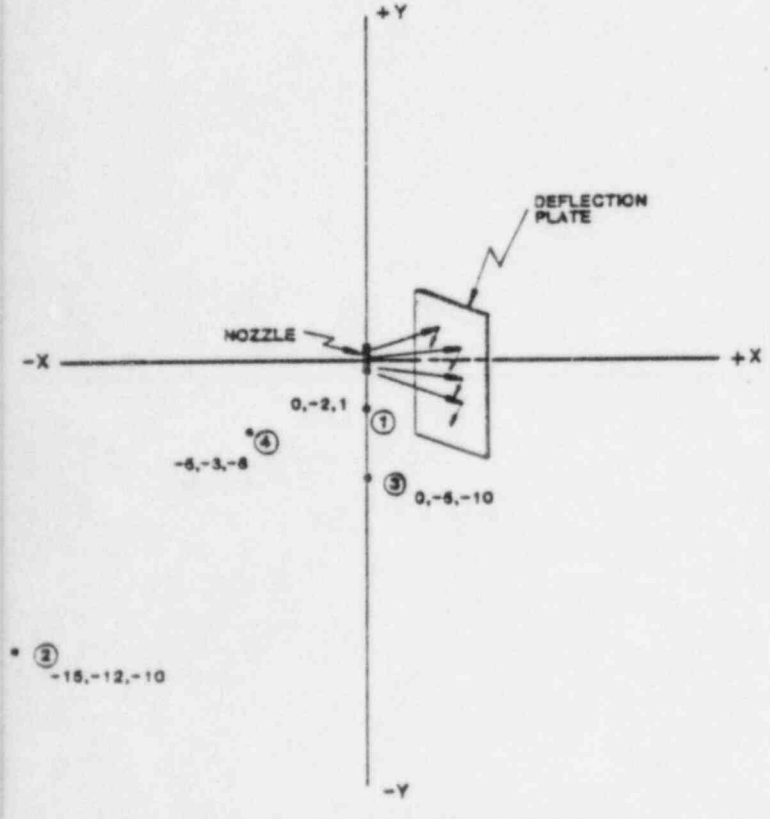

View From X-Y Plane or Elevation View

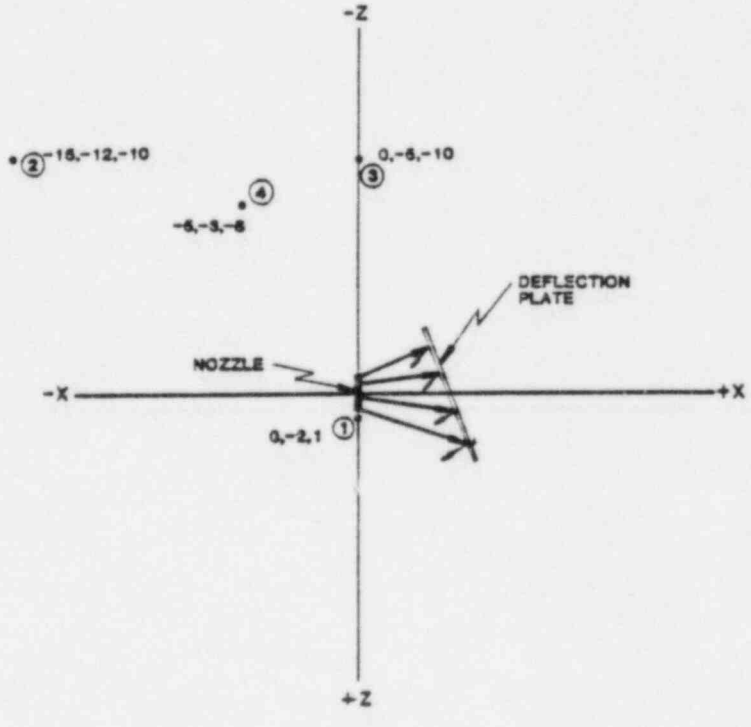

View From X-Z Plane or Plan View

FIGURE 1; ISOMETRIC LOCATION DRAWING

Test Results

"Before" and "after" photographs support the following general observations:

- o No large, flat pieces of sheet metal were released from insulation units.

- o Forces required to "tear apart" insulation units tear and deform thin gage liner material into many irregular shaped and/or small pieces.

- o Insulation installed farther than approximately 10 feet from the break location remained in its installed location and essentially undamaged.

- o Metallic components/debris did not affect test (measurement) instrumentation or plant instrumentation.

- o No insulation debris was transported outside the test compartment by either the blowdown jet forces or subsequent flow velocities.

Representative photographs are included on the following pages. The arrows superimposed on the "before test" photographs represent the best estimate of the steam jet directions relative to the insulation specimens.

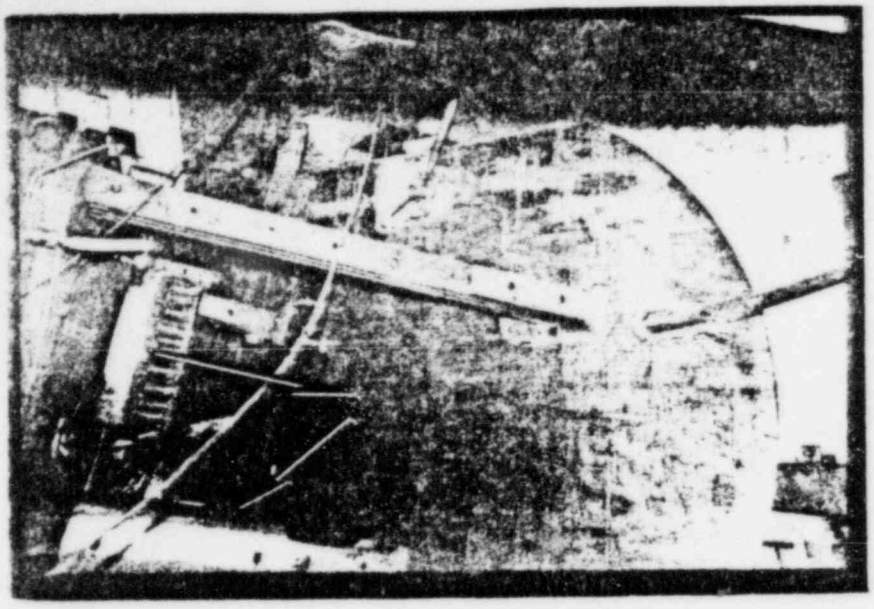

FIGURE 2, SPECIMEN 1
BEFORE TEST

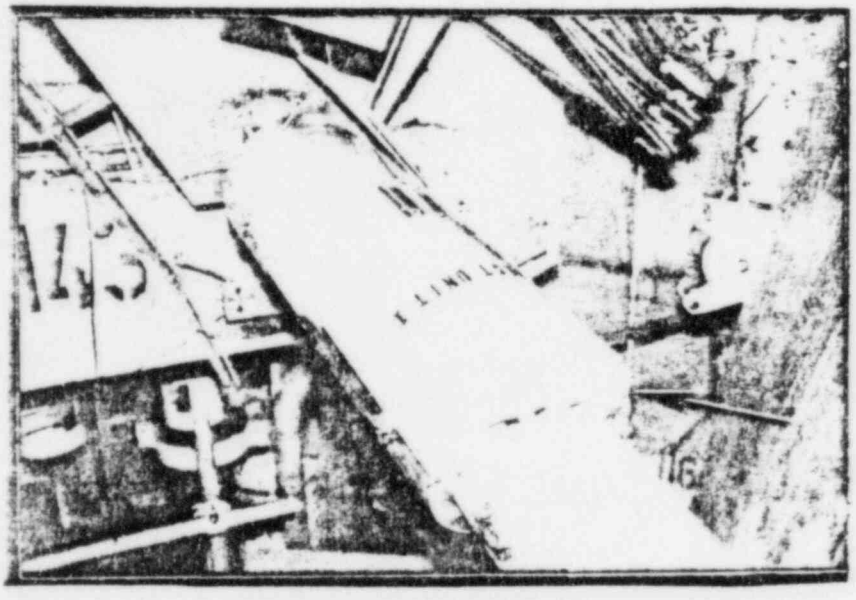

FIGURE 3, SPECIMEN 1
BEFORE TEST

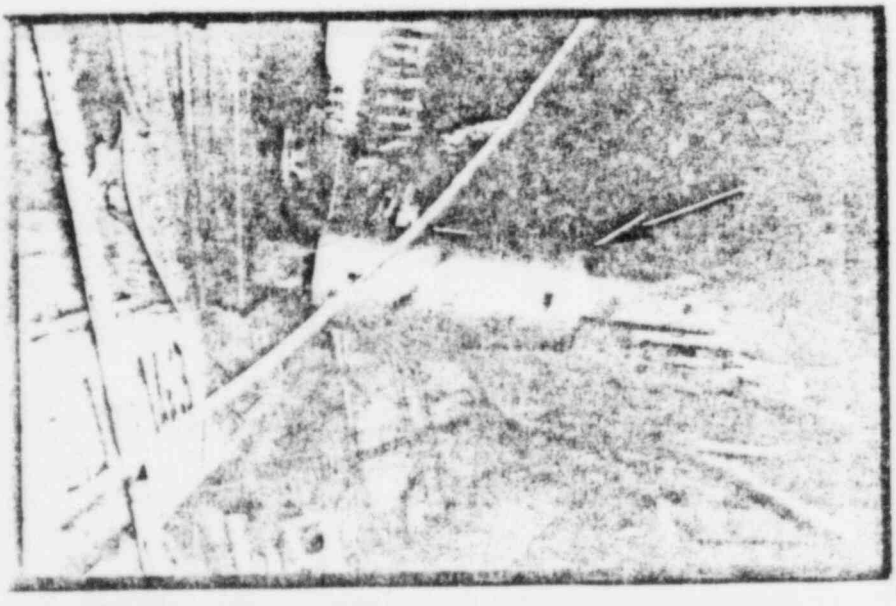

FIGURE 4, SPECIMEN 1
BEFORE TEST

SPECIMEN 1,
BEFORE TEST

Figure 2 shows the insulation (in the lower left corner) relative to the nozzle and the deflector plate. Figure 3 shows a closeup of the test unit with the strut connection to the deflector plate in the lower right hand corner. Figure 4 clearly shows the test specimen installed on the strut.

Details:

O.D. of insulation=12"
Length of Unit=30"
Thickness of insul=2.0"
Liner material=.0025"
Material=All 304 S.S.
Distance from
nozzle $\mathbb{C}$ = 2.5 ft.

FIGURE 5, SPECIMEN 1
AFTER TEST

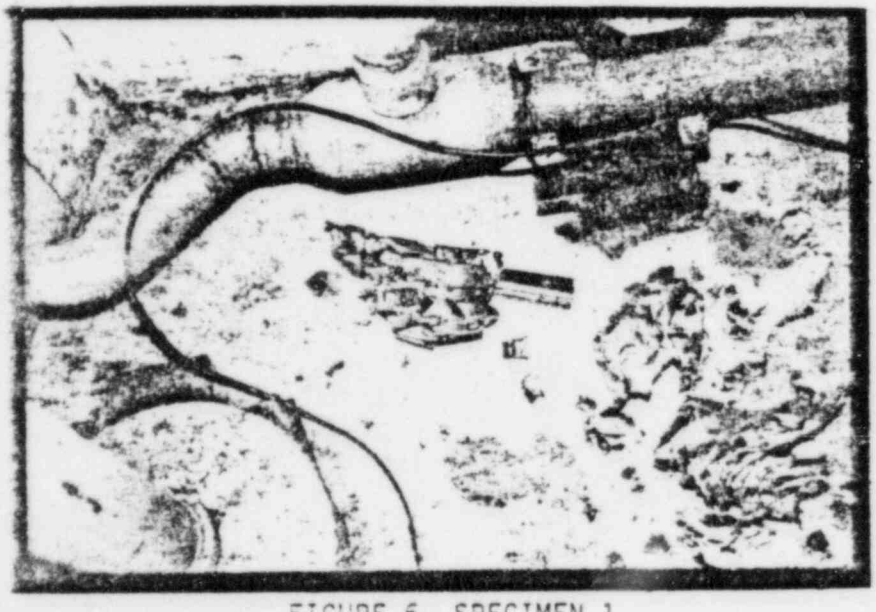

FIGURE 6, SPECIMEN 1
AFTER TEST

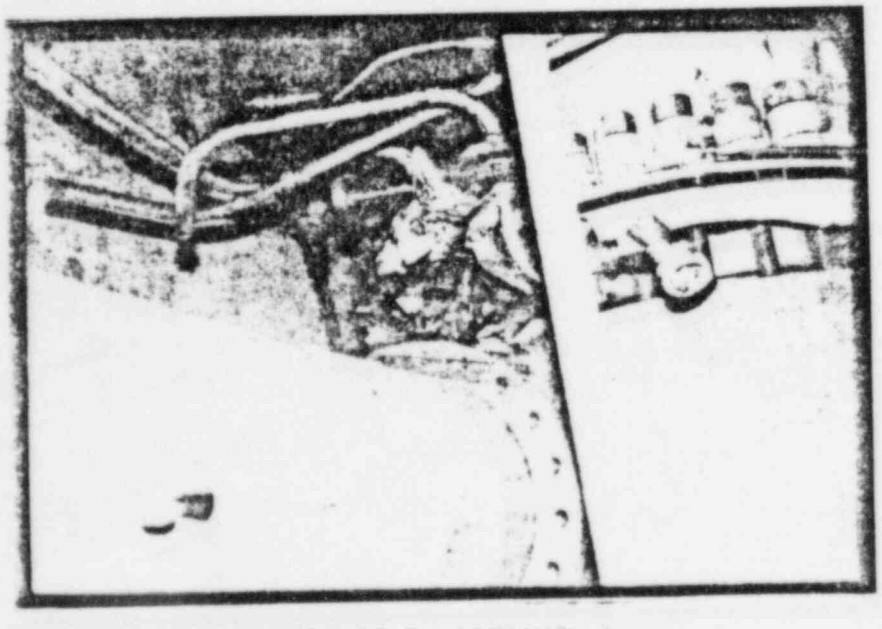

FIGURE 7, SPECIMEN 1
AFTER TEST

SPECIMEN 1
AFTER TEST

Figures 5 and 6 show debris from test specimen 1. These photos indicate that thin gauge liner material debris is torn and crumpled by forces required to tear apart the insulation section. Note that no evidence of large, flat sheets of liner material resulted from the test.

Figure 7 demonstrates the tendency of insulation sections to remain intact, even under severe destructive conditions. No components from this section were set loose, even though it is severely crushed and deformed.

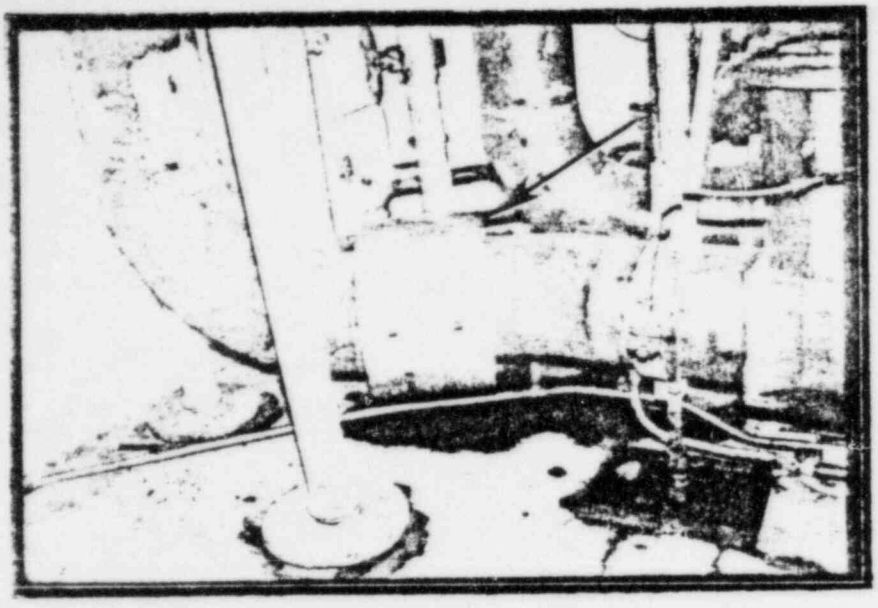

FIGURE 8, SPECIMEN 2
BEFORE TEST

FIGURE 9, SPECIMEN 2
AFTER TEST

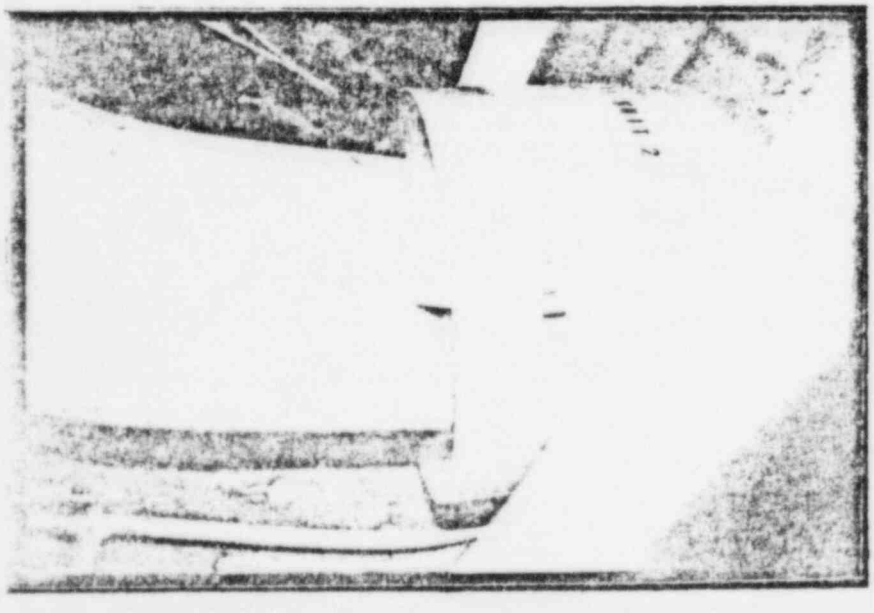

FIGURE 10, SPECIMEN 2
AFTER TEST

SPECIMEN 2

Figure 8 shows the insulation specimen installed on the pipe prior to the test.

Details:

O.D. of insulation=24"
Length of unit=15.75"
Thickness of insul=3.0"
Liner material = .0025"
Material = All 304 S.S.
Distance from
nozzle ℄ ≅ 22 ft.

Figures 9 and 10 show the test unit on the pipe following the test (photos from opposite side of pipe). Note that the test unit has been moved along the pipe and has sustained a small amount of deformation on one end disc due to the motion relative to very rough pipe surface.

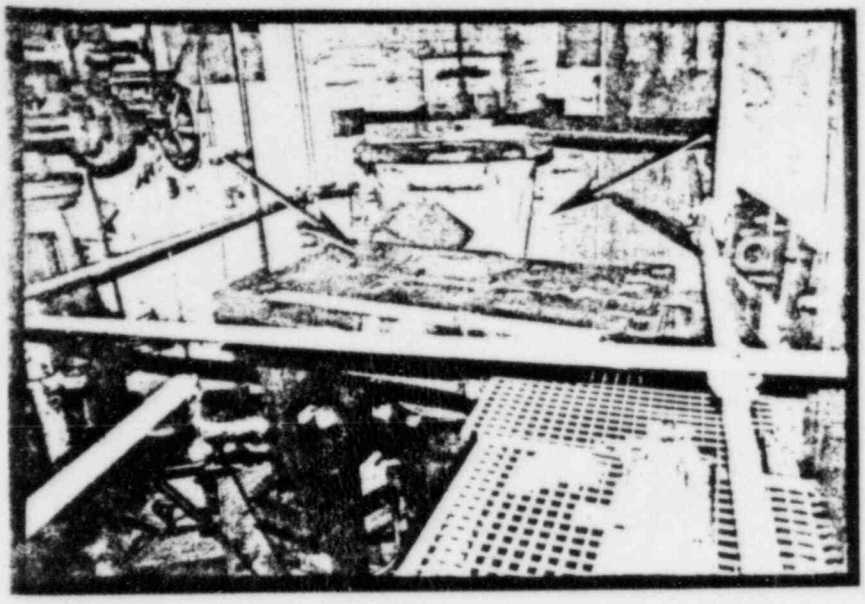

FIGURE 11, SPECIMEN 3
BEFORE TEST

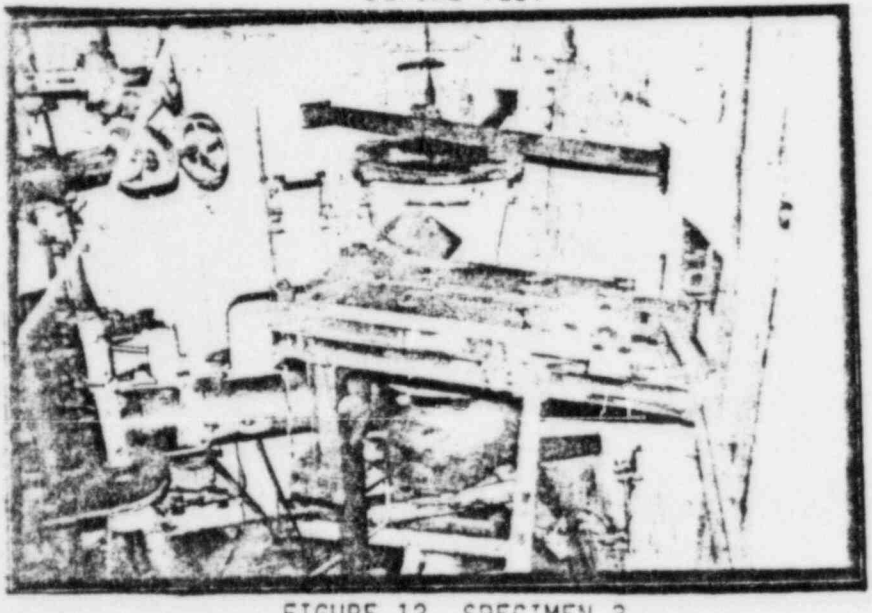

FIGURE 12, SPECIMEN 3
AFTER TEST

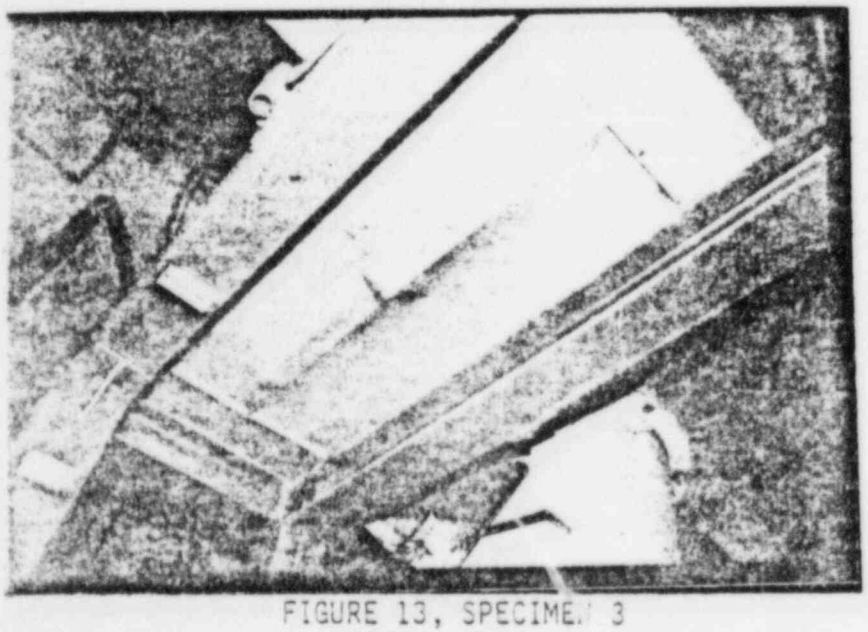

FIGURE 13, SPECIMEN 3
AFTER TEST

SPECIMEN 3

Figure 11 shows the insulation installed. The insulation is fastened together with buckles and screws and is supported on the edges on I-Beams.

Details:
Panel size: 11.7x46"
Thickness of insul=4.0"
Liner material=.0025"
Material=All 304 S.S.
Distance from
nozzle $\mathcal{L}$ ≅ 11 ft

Figures 12 and 13 show the insulation sections after the test was performed. No damage was apparent from above the insulation. The slight damage observed from below the specimen (Figure 13) must have been caused by impact from a foreign object, since no damage was observed from above.

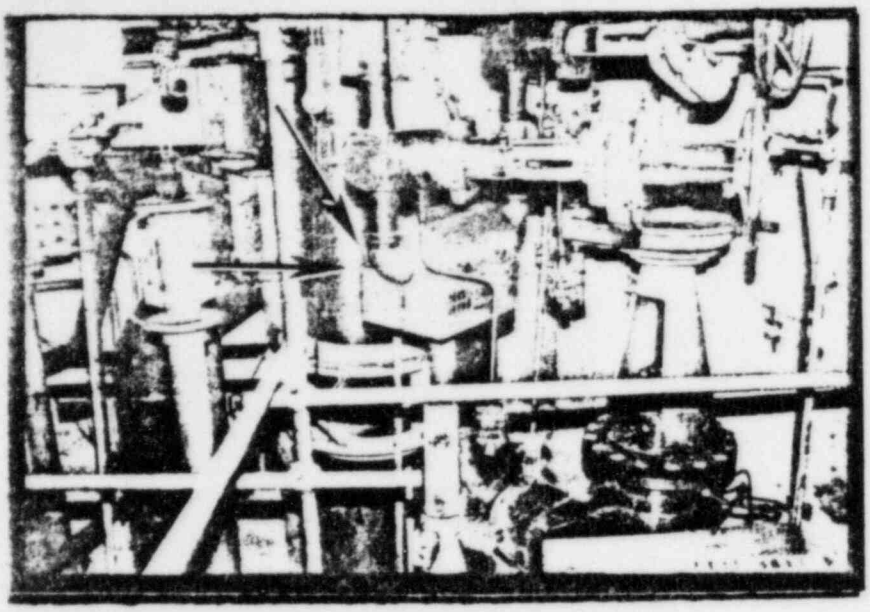

FIGURE 14, SPECIMEN 4
BEFORE TEST

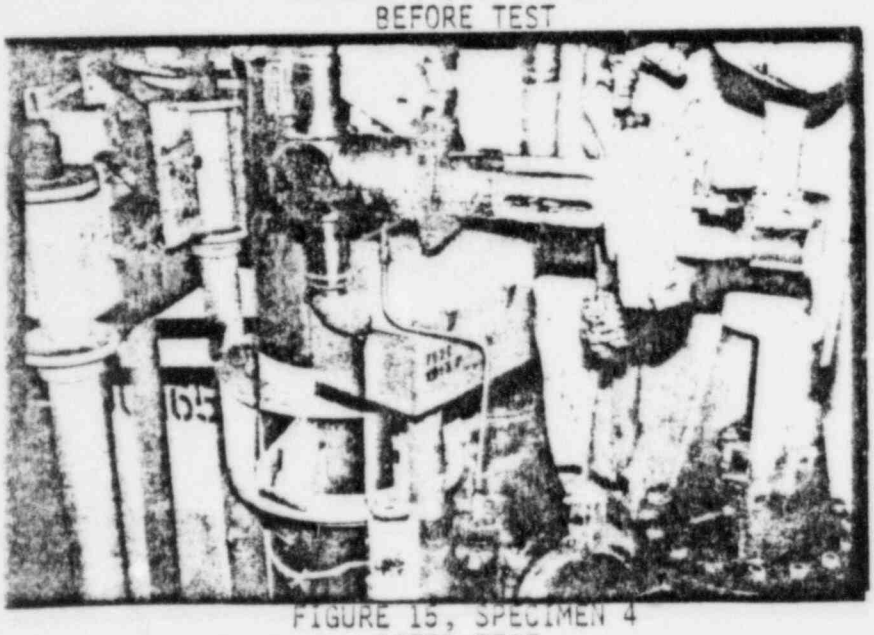

FIGURE 15, SPECIMEN 4
AFTER TEST

FIGURE 16, SPECIMEN 4
AFTER TEST

SPECIMEN 4

Figure 14 shows the U-shaped box insulation installed on a tee.

Details

Length of unit=16.0"
Thickness of insul=2.0"
Diameter of circular section = 12.0"
Liner material = All 304 S.S.
Distance from nozzle ℄ = 10 ft.

Figures 15 and 16 show the test unit after the test was performed. Damage was confined to local areas around the end disc (vertical surfaces). Damage shown in the lower photograph is believed due to impact from a foreign object.

APPENDIX F

HDR BLOWDOWN TESTS WITH NUKON INSULATION BLANKETS

PROVIDED BY

OWENS-CORNING FIBERGLAS CORPORATION

Test Report:

HDR Blowdown Tests

With NUKON Insulation Blankets

Gordon H. Hart

Insulation Technology Laboratory

Owens-Corning Fiberglas Corporation

Research and Development Division

Granville, Ohio

Revised: March 27, 1985

HDR Blowdown Tests
Owens-Corning Fiberglas
March 27, 1985

SUMMARY:

This report summarizes the results of the two tests conducted this past summer at the HDR facility in West Germany. For Owens-Corning, the objective of these tests was to determine the capability of the NUKON nuclear containment area insulation to withstand the impact of a high pressure steam-water blast and to determine the size distribution of the fibrous insulation debris resulting from the impacted blankets. The report summarizes the test procedure and the results; it contains, in addition, "before" and "after" photographs and weight tables of the various components.

In short, the tests demonstrated that unjacketed NUKON blankets, or NUKON blankets covered in a metal mesh, that are located within nine pipe diameters of the simulated pipe break, can be totally destroyed but may not be, depending on the orientation (i.e., over 90 percent of the wool insulation was reduced to fine fibers). However, NUKON blankets enclosed in the standard NUKON 22 gage stainless steel jackets withstood the blast to such an extent that less than 50 percent of the metal jacketed wool insulation was reduced to fine fibers (for pipe insulation within seven pipe diameters from the simulated pipe break). These test results are unique to NUKON insulation systems since they likely depend on type and thickness of stainless steel jackets, strength of jacket latches, type of insulation wool, type of fabric covers, strength of fabric to fabric seams, strength of the Velcro joints, and strength of the Velcro to fabric seams. Further, it should be emphasized that the success of the metal jacketed NUKON pipe insulation in resisting the blast constitutes only two data points. These should not be used as points of extrapolation to cover different materials or conditions. While it is reasonable to assume that a flat NUKON blanket, covered with 22 gage stainless steel jacketing, would also resist damage by a water-steam jet blast, no actual data for this configuration was obtained in these tests.

ANALYSIS OF THESE RESULTS:

A. Overview:

Attachments 1 and 7 show the layouts of the nozzle, the impingement plate, and the support strut for both Tests No. 1 and 2. The center of the impingement plate was positioned 1.5 m from the burst plate of the nozzle. The impingement plate was a 2.6 m diameter disk with its center positioned 2.0 m from the ceiling, or its upper edge 0.85 m from the ceiling (note that the plate and the ceiling are not perpendicular).

Set-up for Test No. 1 (conducted on June 15):

A single blanket of NUKON pipe insulation (measuring 870 mm long, 50 mm thick, and of adequate stretch-out to cover a 100 mm by 120 mm rectangular bar that was used to simulate a pipe) was placed on one of three rectangular steel struts. See Attachment 2 for positioning of the pipe blanket relative to the 450 mm inner diameter nozzle. This blanket was left unjacketed. The center of this blanket was located within a 350mm cone of the nozzle, representing 0.8 pipe diameters (0.8 D). However, as it was likely for this blanket to be hit by water reflected

from the impingement plate, the reflected distance was 1850mm, or 4.1 D (to the center of the blanket in both cases). Two flat blankets, each measuring 500 mm by 750 mm by 50 mm (thick), were attached to the ceiling, directly above the axis of the jet nozzle; see Attachments 1A and 1B. This plate was oriented perpendicular to the axis of the nozzle. See Attachment 3 for photographs of the flat blankets before the test. Attachments 1A and 1B show the position of the nozzle, the insulated bar, the impingement plate, and other support elements. The impingement plate was positioned 1.5 m from the burst plate of the nozzle with the insulated strut extending between the two and slightly below the center axis of the nozzle. The flat blankets were not located within a "90 degree cone" extending out from the center of the nozzle. Therefore, for the purposes of impact, their distance from the nozzle, was calculated to be 3320mm or 7.4 D pipe diameters, assuming that they would be impacted by water from the impingement plate. See the NRC report, "Methodology for Evaluation of Insulation Debris Effects", pp. 22-26, for an explanation of the 90-degree cone extending out from the nozzle. The blankets were attached to the ceiling with Velcro strips and pins with speed washers (with the pins imbedded into the concrete ceiling).

Results for Test No. 1:

Both types of unjacketed NUKON blankets were badly destroyed by the jet blast which originated from water-steam heated to 310 degrees C and 110 bar. The flat insulation was totally destroyed, with only pieces of cloth, which were caught on pipe supports, able to be retrieved. The pipe insulation was largely destroyed although 15 percent of the wool was left intact, enclosed in the fiberglass fabric. All pieces were located around the test room but none in original positions. See Attachments 4 and 5 for photographs of the resulting fabric material. These results are inconsistent since material located 7.4D from the nozzle was totally destroyed while other material, located 4.1D from the nozzle, was left 15 percent intact.

Set-up for Test No. 2: (Conducted on July 4)

For the second test, the impingement plate was angled about 30 degrees from the center line axis. With this orientation, a greater strut length was available for insulating. Therefore, two pieces of pipe insulation blankets, each of the same size as for Test No. 1, were able to be placed on the strut that was on the side impacted by water reflecting off the angled impingement plate. Each pipe blanket was covered with standard NUKON 22 gage stainless steel jacketing. These shall be referred to as Pipe Blankets A and B. See Attachments 7A, and 7B, and 8, lower photograph.

The flat blankets were positioned exactly as for Test No. 1. This time, however, they were covered with metal scrim jacketing. See Attachment 8, upper photograph. The test conditions for Test No. 2 were about the same as for Test No. 1: 310 degrees C, 110 bar.

Results for Test No. 2:

The flat blankets, located 7.4 D from the nozzle, were totally destroyed by the blast, as in Test No. 1. The fabric and the metal scrim were again strewn about and caught on components in the test chamber. Of the two pipe blankets, the one closest to the nozzle (Pipe Blanket A) was just slightly damaged, retaining 93 percent of its original weight of wool (the end of the blanket was slightly torn up). Its center was located 125mm, or 0.3D, from the nozzle itself, although it is likely that reflected water-steam had the greatest impact. For the reflected case, the distance was about 2830mm, or 6.3D. Blanket A remained in its original position. The one closest to the impingement plate (Pipe Blanket B) was partially damaged, retaining 25 percent of its original weight of wool. Its metal jacketing, badly deformed, remained on the bar as did the piece of blanket that contained the wool. This latter blanket had its center located 1350mm, or 3.0D from the nozzle, although for reflected water-steam, its distance was 1930mm, or 4.3D. See Attachments 9 and 10 for photographs of this pipe insulation after the blast.

Attachment 11 shows photographs of the metal jacketing for Pipe Blanket B. A more careful examination of this jacket leads to several conclusions. The majority of the jacket damage can be attributed to the water-steam pressure. The rivets for the latches all appear to be blown radially straight out by an internal pressure. Most cracks in the steel had been initiated from an internal pressure pushing out. The fracture shown in Attachment 11 occurred along the initial bend of the rectangular jacket; apparently, internal water pressure ripped the metal jacket where the added stress of the bend caused a weak spot. There was some question as to whether or not the burst plate damaged the steel jacketing. Two cracks in the jacket showed very clean edges and evidence of abrasion. It is quite possible that they were caused by the flying burst plate. Dents and cracks in Attachment 12 strengthen this conclusion.

B. Summary of the Tests:

Table 1 gives a summary of the weights of the blankets both before and after each test. The flat blankets are, of course, separated from the pipe blankets on this weight table. The Velcro, used to attach the pipe blankets and sewn onto the fabric, is treated as part of the fabric. The weights of the NUKON base wool are separated since the wool, not the fabric, is considered to pose the greater sump blockage potential and hence its fate was of most interest in this testing. In Table 1, what is of greatest significance is the difference between the results of Test No. 1 and Test No. 2. By metal jacketing the pipe insulation, the percentage of pipe wool reduced to debris was dropped from 85 percent to 41 percent. This is significant because it demonstrates the effectiveness of metal jacketing in protecting the blankets. It also demonstrates that a substantial portion of the wool insulation, that started within seven pipe diameters (7D) of the break, was not reduced to fine fibers. This contradicts the assumption made by the NRC that all fibrous insulation located within 7D of a break would be reduced to fine fibers by a blast.

On the other hand, the flat blankets, placed on the ceiling directly above the impingement plate and at 7.4D of the break, were totally reduced to fibrous debris. The addition of the metal mesh jacketing apparently had no effect whatever in protecting the blanket. On this basis, if calculations show there is a need to reduce the sump blockage potential, it is recommended that flat, or nearly flat, blankets placed on steam generators be covered by stainless steel jacketing, not by mesh. However, it would be advisable to obtain actual test data on flat, metal jacketed blankets subjected to a blast.

C. Previous Jet Impingement Tests:

The NRC assumption, that all blankets within 7D of a break will be reduced to loose fiber debris, is a rational one. It is based on "jet impingement" tests conducted in 1982 and 1983 at the Alden Research Laboratories (ARL). These tests demonstrated that, in the worst case, blankets made of fibrous insulation will be torn apart by dynamic water pressures of 20 psig or greater when located within a "90 degree cone". Using this pressure, the NRC backed out the "7D" assumption. On this basis, the assumption is rational.

However, the ARL tests were performed using cold water emerging from a two-inch diameter nozzle. In an actual two-phase blast, such as would occur in a pressurized water reactor containment area accident, the water-steam jet would have less momentum at 20 psig than a cold water jet, hence it would have less destructive potential. Also, because it could not constitute a defined jet, it would likely have less destructive potential. However, the NRC was justified in using the ARL data because it was the only data available at that time.

The two HDR tests, showing that metal jacketing can be used to protect fibrous insulation, really only constitutes a single data "point". That data point should not be extrapolated in other directions to predict the behavior of other types of wool, fabric, stitching, metal jacketing, latches, or insulation system designs. A variation in any of these variables could have had a profound effect on the results presented in the two OCF tests conducted at HDR.

D. Issue of Size Distribution of Fibrous Debris:

One of the original objectives of this testing was to obtain a size distribution of the fibrous debris. This distribution, it was reasoned, could then be used with ARL water transport data to calculate the quantity of debris that could reach a sump screen in a specific plant sump analysis. However, such a size distribution could not be obtained. The wool that was torn from the blankets was not able to be found and, hence, was assumed to be entirely reduced to loose fibers. All the wool retrieved was still enclosed in fiberglass fabric; hence, its size distribution was not an issue (i.e., enclosed in fabric, it would not transport to the sump screen as loose fibers). Therefore, the results of the test were binary: wool that remained enclosed in the fabric was not transportable, while wool that was torn from the fabric enclosure was reduced to loose fibers.

E. Conclusions and Recommendations:

From the HDR Blowdown Tests No. 1 and 2 on NUKON insulation blankets, several conclusions can be drawn:

1. Unjacketed blankets, and those jacketed in metal mesh, located about 7.4 pipe diameters from the jet nozzle, were reduced to shredded fabric and unretrievable loose insulation fibers. Most of the fabric generated by the tests was caught on protrusions in the area. The wool not retrieved was assumed to be reduced to loose fibers. On the other hand, unjacketed pipe insulation, located within 0.8D of the nozzle, was only 85 percent destroyed.

2. Some of the 22 gage metal pipe jacketing in Test No. 2 was badly bent by the blast; however, it was not torn away from its position around the strut it had covered. The suggestion is that the reflected jet, rather than the primary jet, inflicted the greatest damage.

3. The use of metal jacketing over pipe blankets was effective in reducing the level of wool destruction from 85 percent (Test No. 1) to 41 percent (Test No. 2), or 75 percent for Pipe Blanket B and 7 percent for Pipe Blanket A.

It is recommended that for sump analyses involving pipes insulated with metal jacketed NUKON blankets, Attachment 13 replace Figure 3.26 in the NRC report, NUREG-0897. The curves on these graphs have been redrawn by using data collected in these tests. It is also recommended that, if possible, further testing be conducted. This would include metal jacketed flat NUKON blankets and insulation samples placed at various other positions and orientations. Ideally, the impingement plate should be removed and insulation samples should be impacted by the primary jet, not only by reflected water.

Finally, it is recommeded that these results not be extended to insulation materials fabricated with different gage metal jacketing, matal latches, compressibility of insulation, etc. Variations could have a profound effect on the results. Also, caution should be urged on extrapolating these results to so-called "encapsulated" insulation since that is not a clearly defined type of insulation and since its behavior could be significantly different.

HDR Blowdown Tests
Owens-Corning Fiberglas
March 27, 1985

TEST #1

Original Weights (kg)*

Piece of NUKON	Cloth	Scrim	Velcro	Wool	Total
1. Pipe	1.03	0.09	0.025	1.50	2.66
2. Flat A	0.54	0.05	----	0.70	1.27
3. Flat B	0.54	0.05	----	0.70	1.29

Comparative Weights from Test #1 (kg)

Piece	Cloth & Velcro			Wool		
	Before*	After	% Lost	Before*	After	% Lost
1. Pipe	1.05	0.83	21%	1.50	0.22	85%
2. Flat A	0.54	0.51	12%	0.70	0	100%
3. Flat B	0.54	0.44	12%	0.70	0	100%

TEST #2

Original Weights (kg)*

NUKON Blanket	Cloth	Scrim	Velcro	Wool	Total
1. Pipe A	1.03	0.09	0.025	1.50	2.66
2. Pipe B	1.03	0.09	0.025	1.50	2.66
3. Flat A	0.54	0.05	----	0.70	1.30
4. Flat B	0.54	0.05	----	0.70	1.29

Comparative Weights from Test #2 (kg)

NUKON Blanket	Cloth & Velcro				Wool			
	Before*	After	% Lost		Before*	After	% Lost	
1. Pipe A	1.05	1.03	80%		1.50	1.39	7%	41%
2. Pipe B	1.05	0.64			1.50	0.38	75%	
3. Flat A	0.54	0.27	----		0.70	0	100%	
4. Flat B	0.54				0.70	0	100%	
5. Unidentifiable Fabric Scraps	----	0.49	----		----	----	----	
6. All Blankets	3.18	2.43	24%		----	----	----	

* Based on average values of the weights of the materials for six different blankets constructed for the tests.

ATTACHMENT 1A
(TEST #1)
A. END VIEW

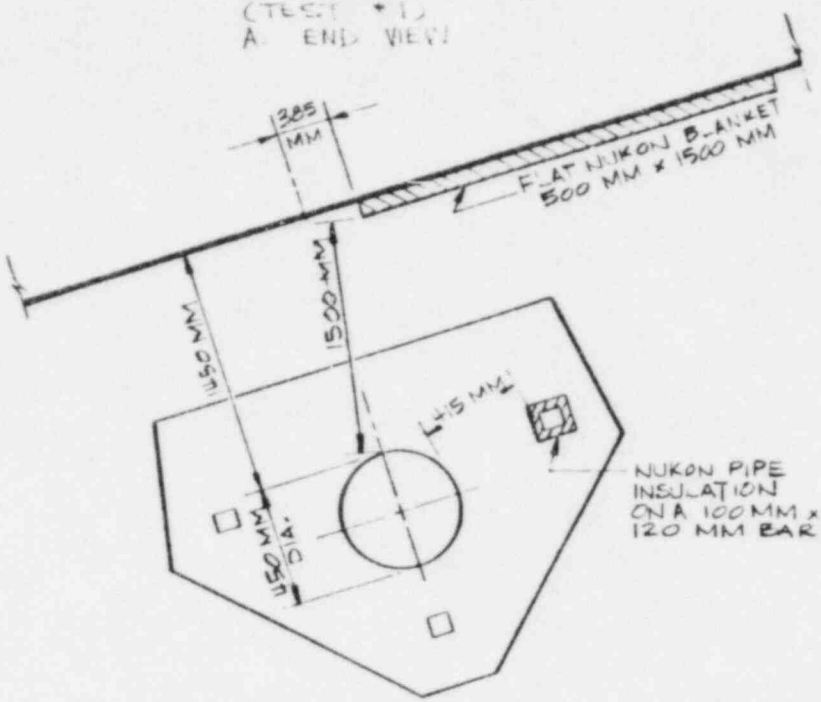

SECTION A-A

ATTACHMENT 1B
(TEST #1)
B. SIDE VIEW

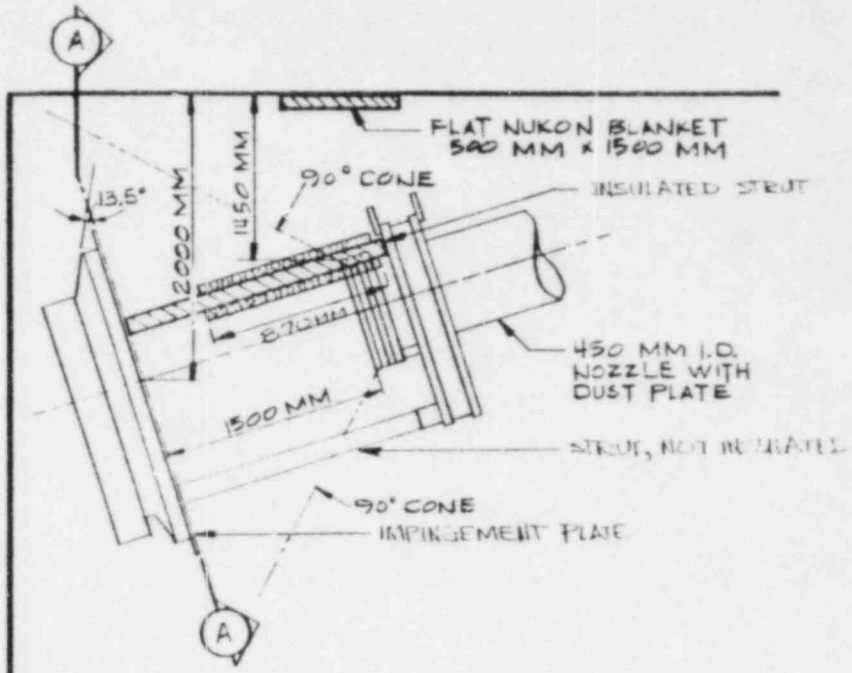

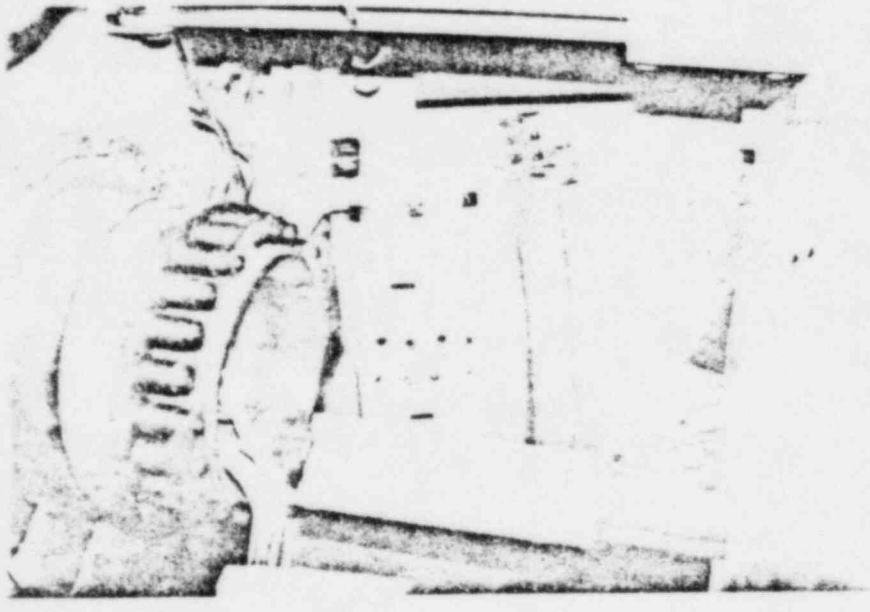

INSTALLED INSULATION BEFORE TEST 1

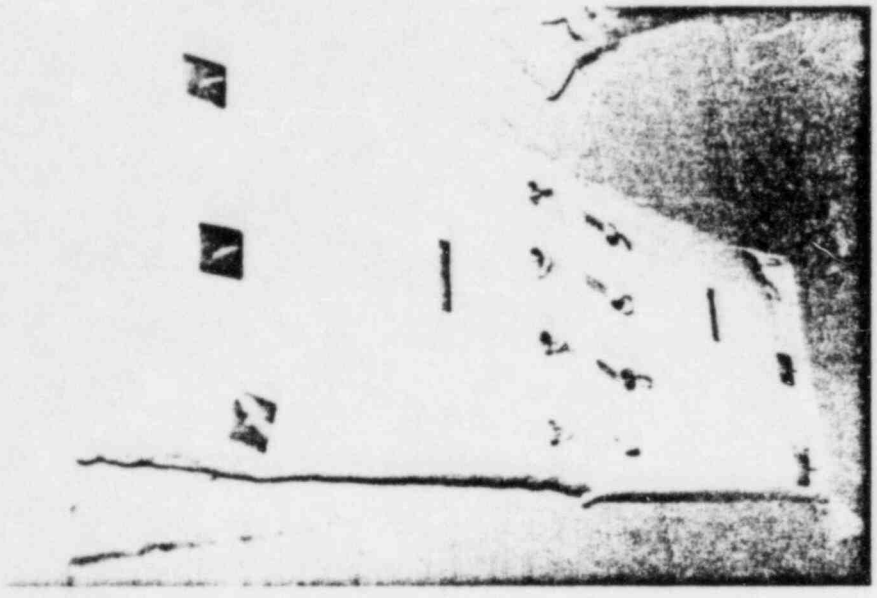

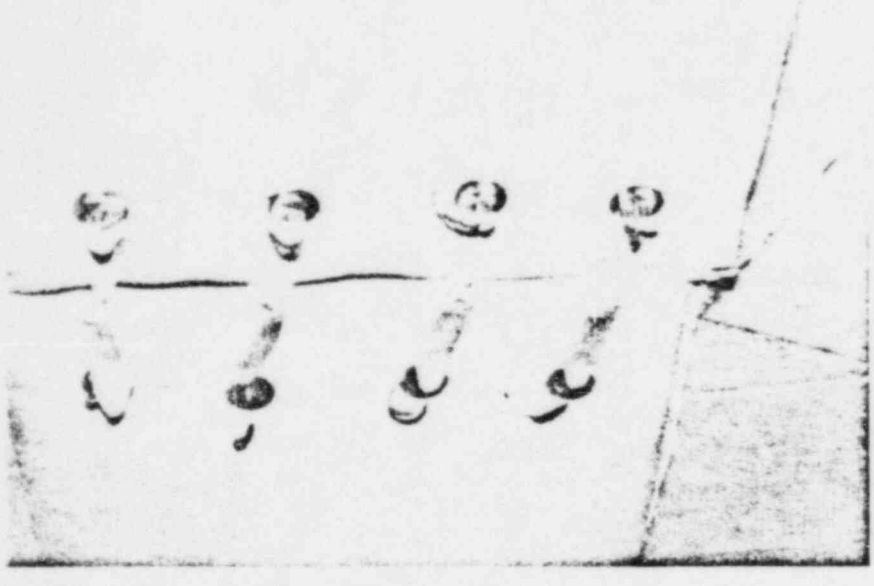

INSTALLATION OF FLAT BLANKETS BEFORE TEST 1

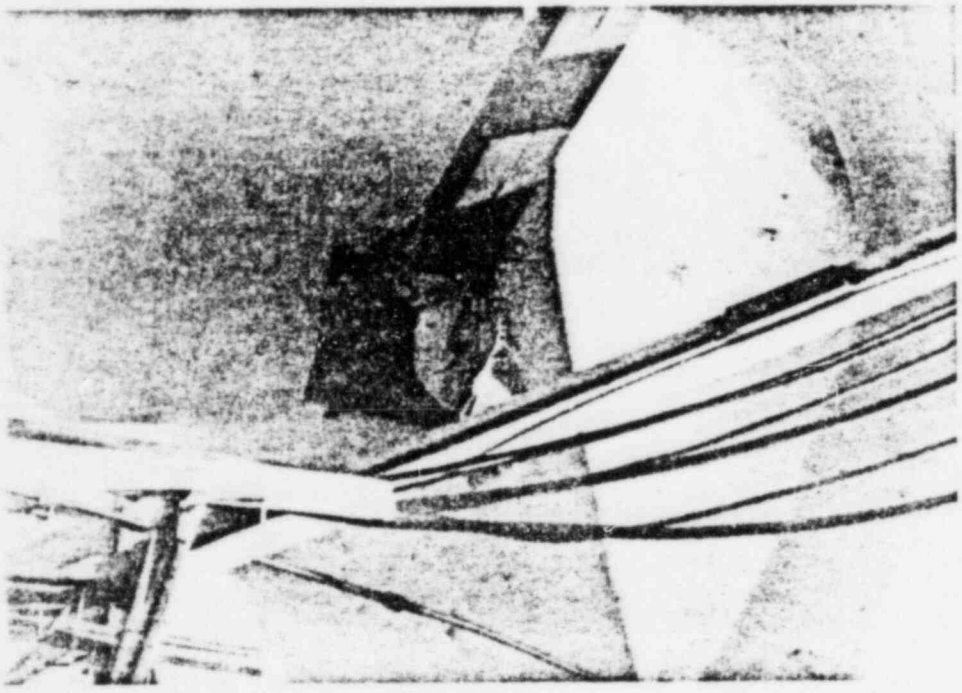

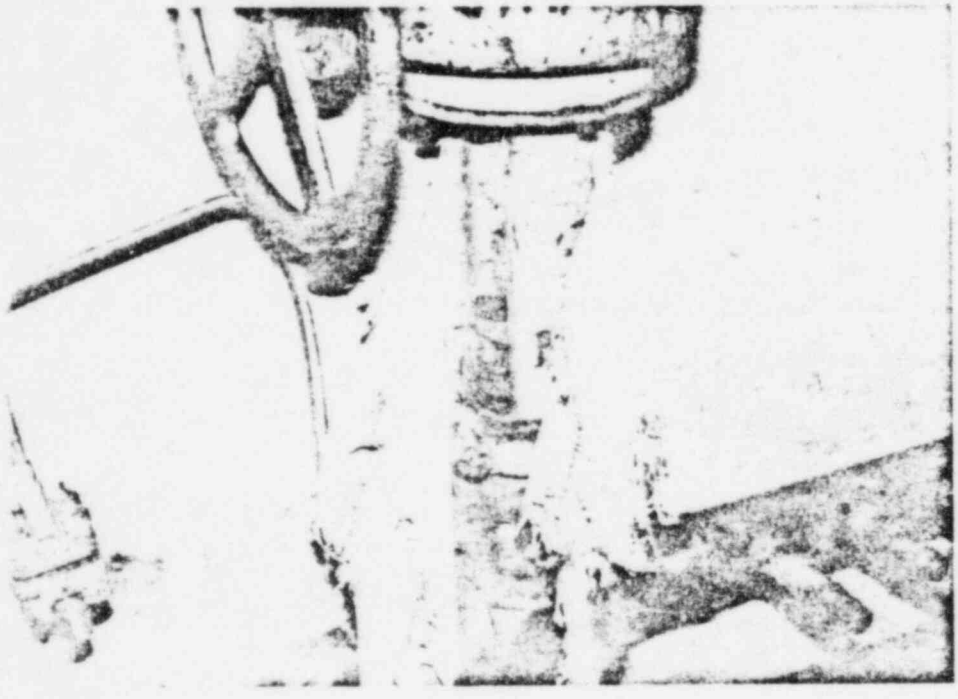

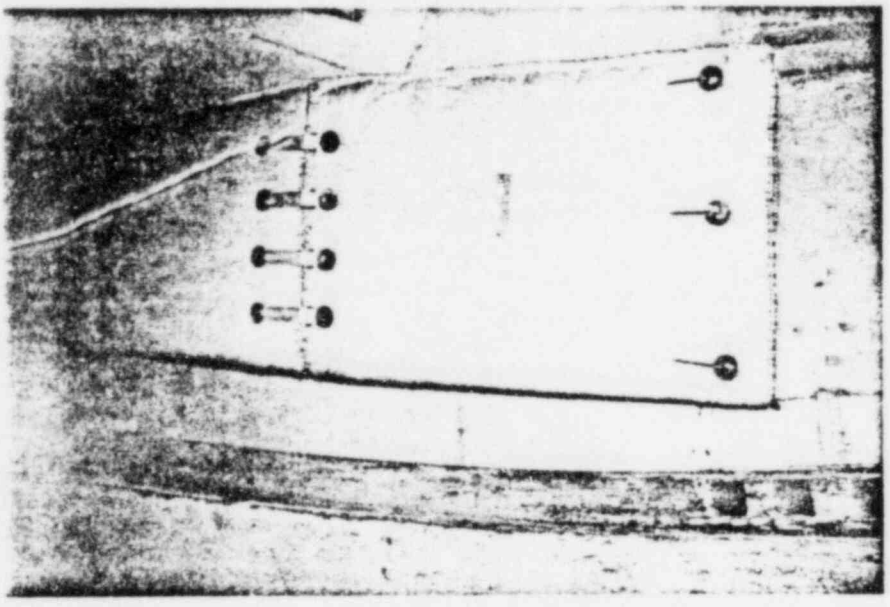

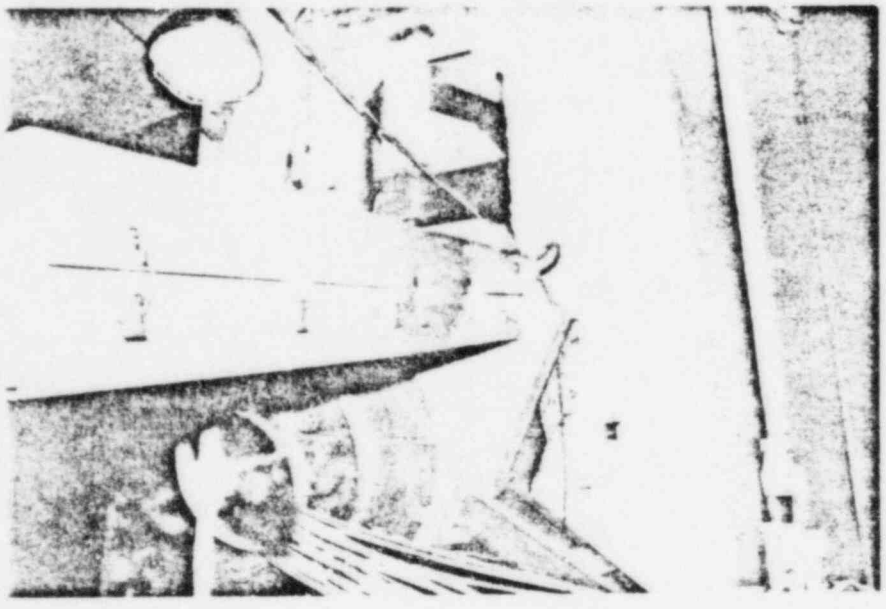

INSTALLED INSULATION BEFORE TEST 2

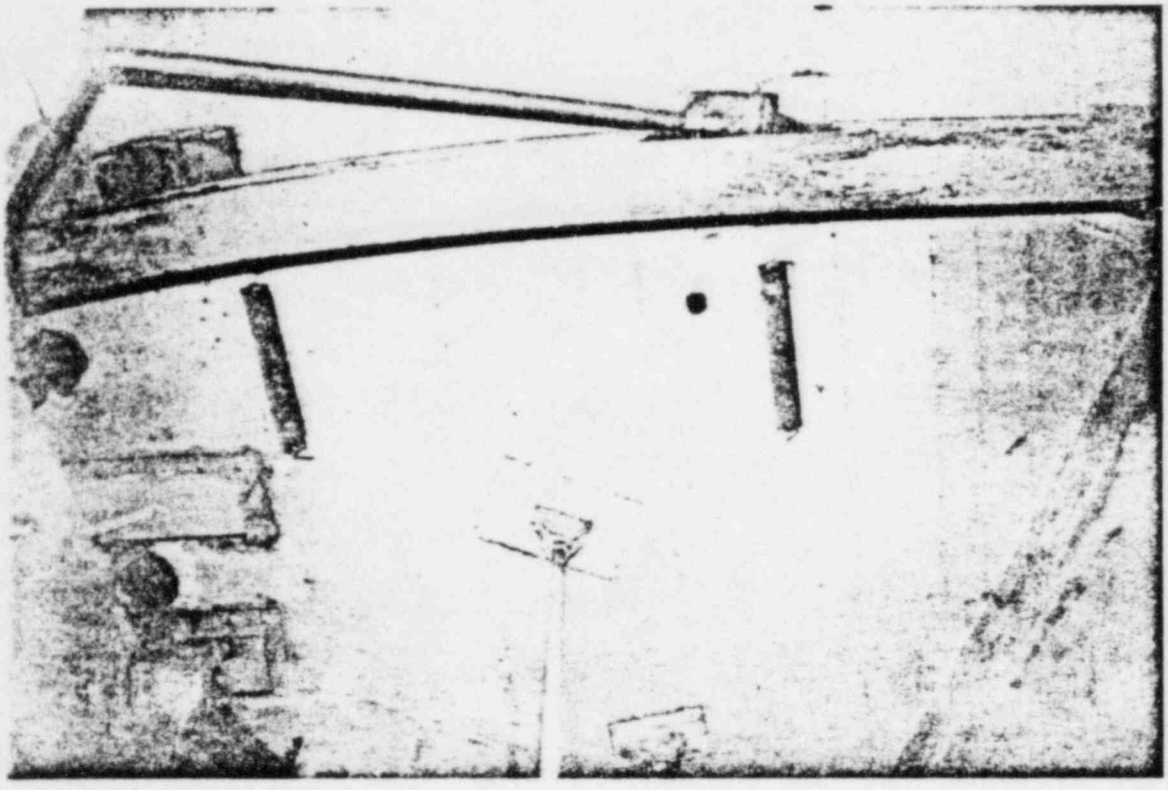

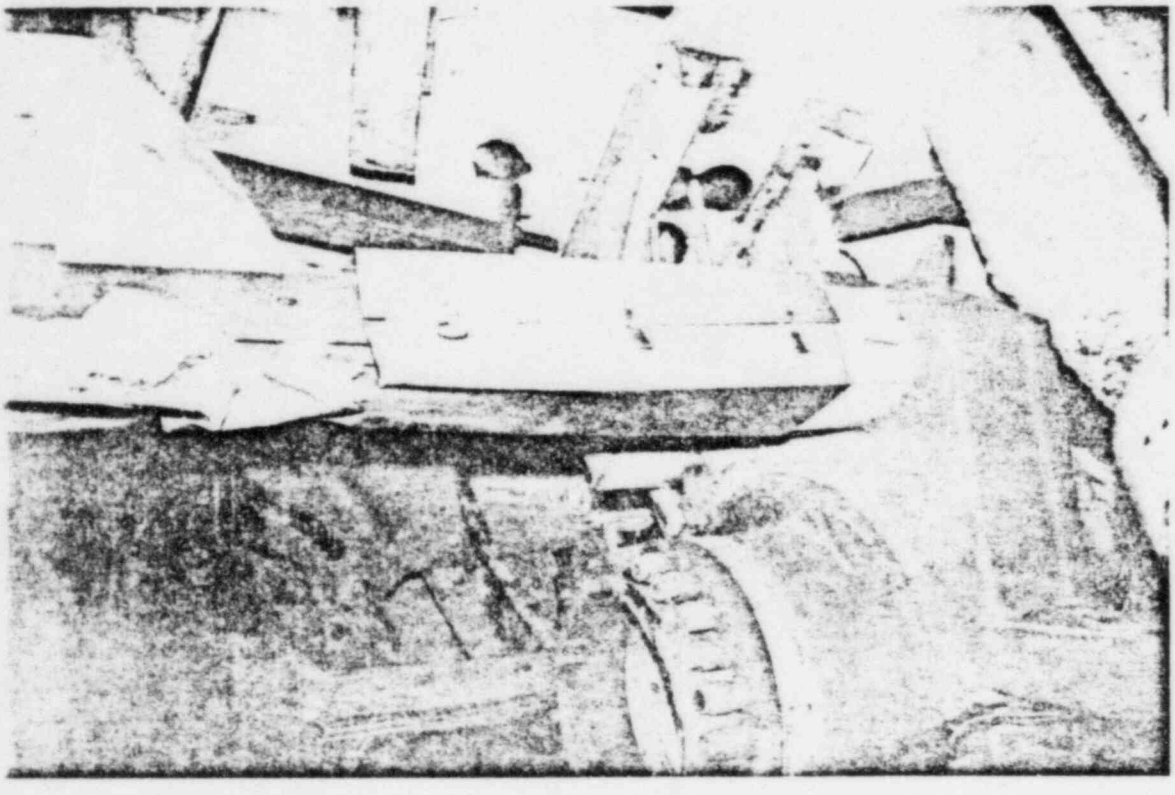

RESULTS OF TEST 2

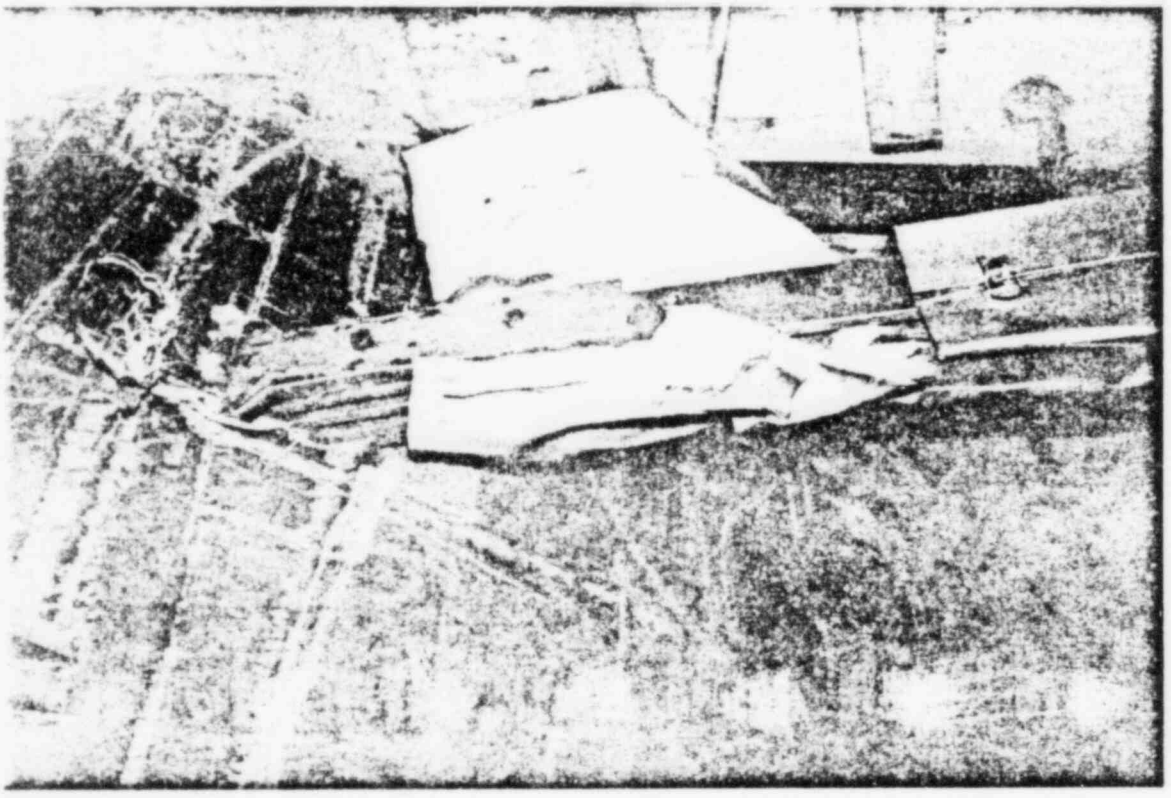

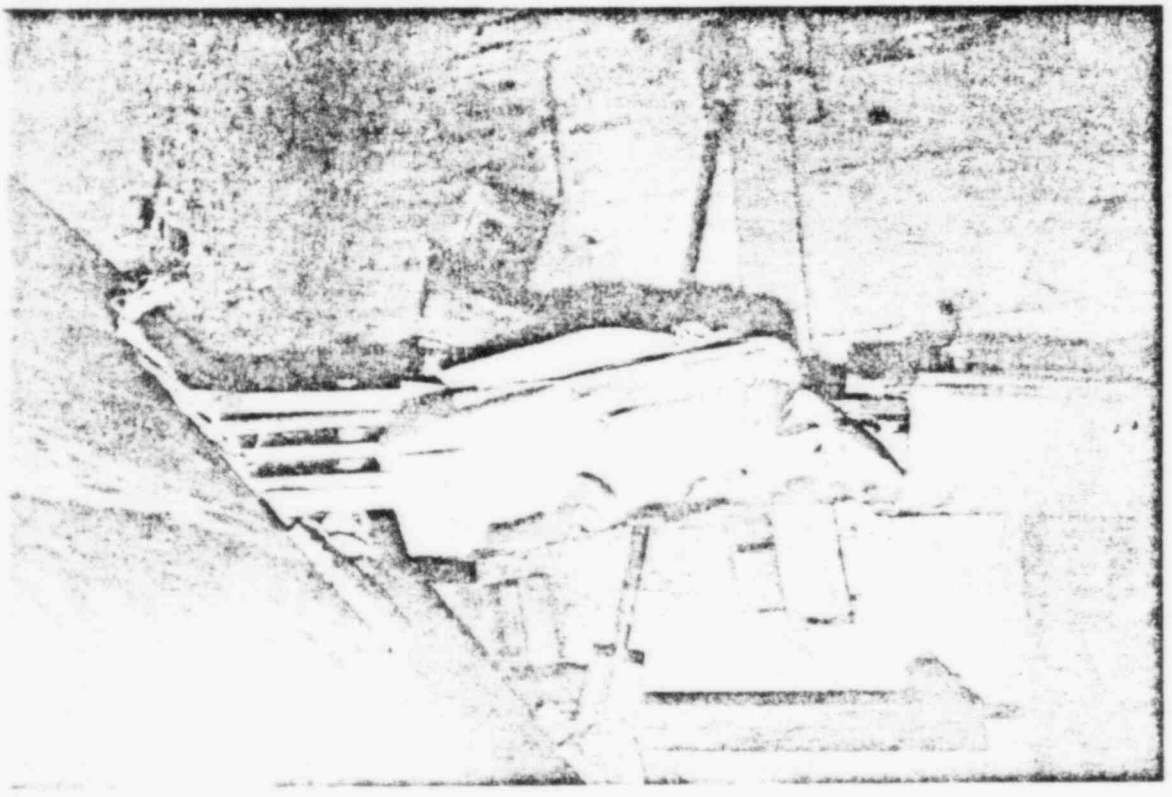

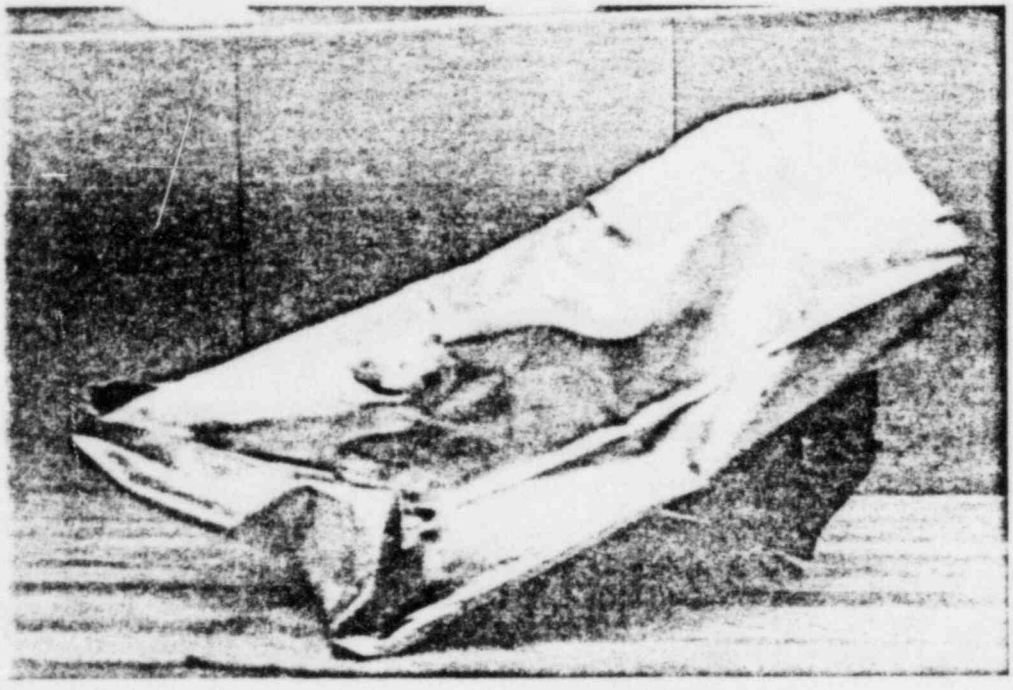

JACKET NEAREST THE IMPINGEMENT PLATE

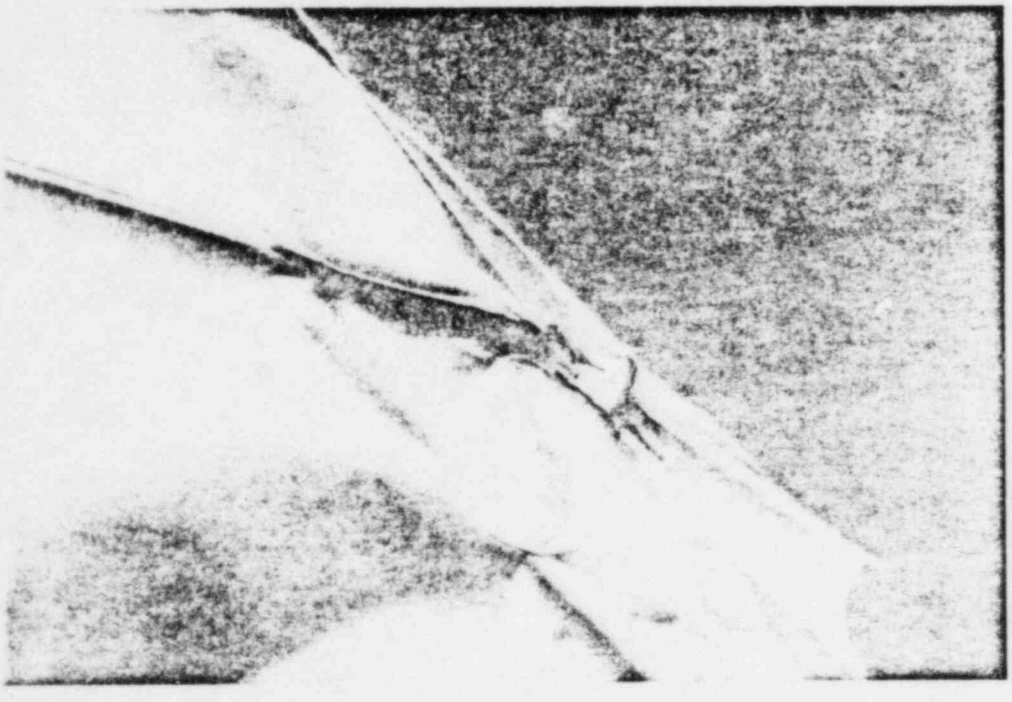

FRACTURE CAUSED BY WATER PRESSURE

STUDY OF STAINLESS STEEL JACKET FAILURE

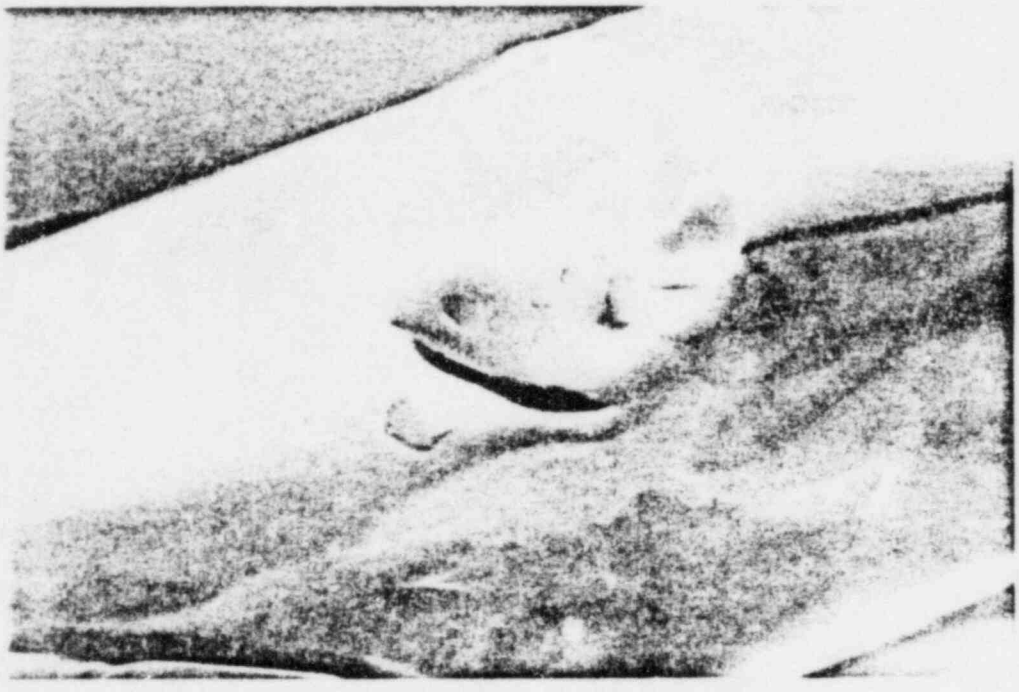

SUSPECTED BURST PLATE DAMAGE

INITIAL BURST PLATE DAMAGE PROPAGATED BY
INTERNAL WATER PRESSURE

STUDY OF STAINLESS STEEL JACKET FAILURE